

Guidelines for Determining Flood Flow Frequency

Bulletin 17C

Chapter 5 of
Section B, Surface Water
Book 4, Hydrologic Analysis and Interpretation



Techniques and Methods 4-B5
Version 1.1, May 2019

Cover. International bridge over the St. John River in Fort Kent, Maine, at U.S. Geological Survey gaging station 01014000, during flood of April 30, 2008. Photograph by M. Huard, USGS.

Guidelines for Determining Flood Flow Frequency

Bulletin 17C

By John F. England, Jr., U.S. Army Corps of Engineers

Timothy A. Cohn, U.S. Geological Survey (deceased)

Beth A. Faber, U.S. Army Corps of Engineers

Jery R. Stedinger, Cornell University

Wilbert O. Thomas, Jr., Michael Baker International

Andrea G. Veilleux, U.S. Geological Survey

Julie E. Kiang, U.S. Geological Survey

Robert R. Mason, Jr., U.S. Geological Survey

Chapter 5 of

Section B, Surface Water

Book 4, Hydrologic Analysis and Interpretation

Techniques and Methods 4–B5

Version 1.1, May 2019

U.S. Department of the Interior
DAVID BERNHARDT, Secretary

U.S. Geological Survey
James F. Reilly II, Director

U.S. Geological Survey, Reston, Virginia
First release: 2018, online and in print
Revised: May 2019 (ver. 1.1), online

For more information on the USGS—the Federal source for science about the Earth, its natural and living resources, natural hazards, and the environment—visit <https://www.usgs.gov> or call 1–888–ASK–USGS.

For an overview of USGS information products, including maps, imagery, and publications, visit <https://store.usgs.gov/>.

Any use of trade, product, or firm names in this publication is for descriptive purposes only and does not imply endorsement by the U.S. Government.

Although this information product, for the most part, is in the public domain, it also may contain copyrighted materials as noted in the text. Permission to reproduce copyrighted items must be secured from the copyright owner.

Suggested citation:
England, J.F., Jr., Cohn, T.A., Faber, B.A., Stedinger, J.R., Thomas, W.O., Jr., Veilleux, A.G., Kiang, J.E., and Mason, R.R., Jr., 2018, Guidelines for determining flood flow frequency—Bulletin 17C (ver. 1.1, May 2019): U.S. Geological Survey Techniques and Methods, book 4, chap. B5, 148 p., <https://doi.org/10.3133/tm4B5>.

ISSN 2328-7047 (print)
ISSN 2328-7055 (online)

ISBN 978-1-4113-4223-1

Preface

This series of manuals on Techniques and Methods (TM) describes approved scientific and data-collection procedures and standard methods for planning and executing studies and laboratory analyses. The material is grouped under major subject headings called “books” and further subdivided into sections and chapters. Book 4 is on hydrologic analysis and interpretation and section B is on surface water.

The unit of publication, the chapter, is limited to a narrow field of subject matter. These publications are subject to revision because of experience in use or because of advancement in knowledge, techniques, or equipment, and this format permits flexibility in revision and publication as the need arises. Chapter B5 of book 4 (TM 4–B5) deals with flood flow frequency analysis at gaged sites using the Expected Moments Algorithm. The use of extreme flood data represented by interval and censored data types, including historical, paleoflood, botanical evidence, is emphasized.

This revision is adopted with the knowledge and understanding that review of these procedures will be ongoing. Updated methods will be adopted when warranted by experience and by examination and testing of new techniques.

Acknowledgments

These revised Guidelines were written by a team assembled from the Hydrologic Frequency Analysis Workgroup (HFAWG), under the auspices of the Subcommittee on Hydrology (SOH) of the Advisory Committee on Water Information (ACWI). Input from other members of HFAWG and of the SOH is gratefully acknowledged. HFAWG and SOH Work Group Members and participants in this revision are listed in appendix 2. The authors would also like to acknowledge the contributions of the U.S. Geological Survey (USGS) colleague reviewers, whose comments and suggestions materially improved this report. We also appreciate the technical advice and assistance from Dr. William H. Asquith (USGS).

Lastly, our colleague and friend, Dr. Timothy A. Cohn, authored or coauthored many of the papers that form the foundation of this update to the flood frequency guidelines. He wrote software that was critical to implementing the concepts and shared it with others. He gave freely of his time in teaching and instructing others in flood frequency and statistics. Tim was also instrumental in building support amongst HFAWG, SOH, and many Federal agencies. He will be missed.

Timothy A. Cohn
February 26, 1957–February 20, 2017

This page intentionally left blank.

Contents

Abstract	1
Introduction	1
Background	2
Purpose and Scope	3
Risk Accumulates	4
Flood Flow Frequency Information	5
Use of Annual Maximum Series	5
Data Sources for a Site	6
Systematic Records	6
Historical Flood Information	6
Paleoflood and Botanical Information	9
Common Issues with At-Site Data Records	11
Broken, Incomplete, and Discontinued Records	11
Extraordinary Floods	12
Zero Flows and Potentially Influential Low Floods	14
Data Representation Using Flow Intervals and Perception Thresholds	15
Regional Information and Nearby Sites	18
Flood Estimates from Precipitation	18
Data Assumptions and Specific Concerns	20
Flow Measurement Errors	20
Randomness of Events	21
Mixed Populations	21
Watershed Changes	22
Climate Variability and Change	23
Determination of the Flood Flow Frequency Curve	23
Plotting Positions	23
Flood Distribution	24
Parameter Estimation—Simple Case	25
Moments and Parameters	25
Weighted Skew Coefficient Estimator	25
Zero Flows and Identifying Potentially Influential Low Floods	26
Expected Moments Algorithm	27
Record Extension with Nearby Sites	29
Confidence Intervals for Quantiles	30
Estimating Regional Skew	30
Comparisons of Frequency Curves	31
Comparisons with Similar Watersheds	32
Comparisons with Flood Estimates from Precipitation	33

Weighting of Independent Frequency Estimates	33
Frequency Curve Extrapolation	34
Software and Examples	34
Future Studies	35
Ungaged Sites	35
Regulated Flow Frequency	35
Urbanization and Watershed Change	36
Applicability of These Guidelines	36
References Cited	37
Glossary	53
Appendix 1. List of Symbols	59
Appendix 2. Subcommittee and Work Group Members	61
Appendix 3. Data Sources and Representation	63
Data Sources	63
Systematic Records	63
Historical Data	64
Paleoflood Data and Botanical Information	65
Regional Information	66
Precipitation and Climate Information	66
Data Representation	67
Appendix 4. Initial Data Analysis	71
Visual Inspection—Plot the Data	71
Autocorrelation	71
Trends and Shifts	71
Statistical Tests	72
Example—Skokie River near Highland Park, Illinois	72
Appendix 5. Threshold-Exceedance Plotting Positions	75
Appendix 6. Potentially Influential Low Floods	77
PILF Background and Philosophy	77
Computational Details for Identifying PILFs with MGBT	78
Appendix 7. Expected Moments Algorithm (EMA)	80
EMA Computational Details	80
The Generalized Expected Moments Algorithm	82
Uncertainty of EMA Moments	84
Confidence Intervals with EMA	86
Appendix 8. Record Extension with Nearby Sites	88
Record Augmentation of the Mean and Variance	88
Record Extension with MOVE	91
Summary of Procedure	92
MOVE Example—Suwanee Creek at Suwanee, Georgia	94

Appendix 9. Weighting of Independent Estimates	101
Weighting Method	101
Example	102
Appendix 10. Examples	103
Flood Frequency Steps and Examples	103
Systematic Record Example—Moose River at Victory, Vermont	105
EMA Representation of Peak Flow Data for Flood Frequency Analysis	105
Results from Flood Frequency Analysis	108
PILF Example—Orestimba Creek near Newman, California	111
EMA Representation of Peak Flow Data for Flood Frequency Analysis	113
Results from Flood Frequency Analysis	113
Broken Record Example—Back Creek near Jones Springs, West Virginia	117
EMA Representation of Peak Flow Data for Flood Frequency Analysis	117
Results from Flood Frequency Analysis	117
Historical Record Example—Arkansas River at Pueblo, Colorado	123
EMA Representation of Peak Flow Data for Flood Frequency Analysis	123
Results from Flood Frequency Analysis	127
Crest Stage Gage Example—Bear Creek at Ottumwa, Iowa	130
EMA Representation of Peak Flow Data for Flood Frequency Analysis	130
Results from Flood Frequency Analysis	134
Historical and PILF Example—Santa Cruz River near Lochiel, Arizona	136
EMA Representation of Peak Flow Data for Flood Frequency Analysis	138
Results from Flood Frequency Analysis	138
Paleoflood Record Example—American River at Fair Oaks, California	142
EMA Representation of Peak Flow Data for Flood Frequency Analysis	142
Results from Flood Frequency Analysis	146

Figures

1. Photograph of a streamflow-gaging station with crest-stage gage at U.S. Geological Survey station 01589238, Gwynns Falls Tributary at McDonogh, Maryland	6
2. Photograph of historic flood high-water marks and flood of March 13–15, 2010, Potomac River at Great Falls Park, Virginia	7
3. Graph showing an example peak-discharge time series with historical period and discharge perception threshold	8
4. Graph showing an example site with three large historical floods outside the gaging record, Big Sandy River at Bruceton, Tennessee	9
5. Graph showing an example site with an extraordinary flood peak that represents a longer time frame, Plum Creek near Louviers, Colorado	9
6. Graph showing an example site with historical/paleoflood nonexceedance information, North Platte River near Seminoe Reservoir, Wyoming	9

7.	Diagram of a section showing typical paleoflood features used as paleostage indicators	11
8.	Photograph of inclined western juniper trees with upright branches from the 1861–1862 flood, Crooked River near Prineville, Oregon	11
9.	Graph showing an example streamflow-gaging station with a broken record, U.S. Geological Survey station 01614000, Back Creek near Jones Springs, West Virginia	12
10.	Graph showing an example streamflow-gaging station with a discontinued record, U.S. Geological Survey station 07099500, Arkansas River near Pueblo, Colorado	13
11.	Graph showing an example empirical frequency distribution and potentially influential low floods at U.S. Geological Survey station 11274500, Orestimba Creek near Newman, California	15
12.	Graph showing an example peak-discharge time series with peak flows, interval and binomial-censored flood observations, flow intervals, and perception thresholds	17
3–1.	Graph showing typical flow intervals and perception thresholds for gaging stations	69
3–2.	Graph showing typical flow intervals and perception thresholds for crest-stage gages	69
3–3.	Graph showing typical flow intervals and perception thresholds for historical data	70
4–1.	Graph showing U.S. Geological Survey station 05535070 Skokie River near Highland Park, Illinois, time-series plot	73
4–2.	Graph showing U.S. Geological Survey station 05535070 Skokie River near Highland Park, Illinois, autocorrelation plot with thresholds for significant autocorrelation	74
8–1.	Map showing locations of Suwanee Creek at Suwanee, Georgia, U.S. Geological Survey station 02334885, and Etowah River at Canton, Georgia, U.S. Geological Survey station 02392000	94
8–2.	Graph showing annual peak flows for Suwanee Creek, U.S. Geological Survey station 02334885, the short record station	96
8–3.	Graph showing annual peak flows for the Etowah River, U.S. Geological Survey station 02392000, the long record station	97
8–4.	Graph of 20 concurrent years of record for Suwanee Creek and the Etowah River for the period 1985 to 2004 with the ordinary least squares regression line	98
10–1.	Graph showing U.S. Geological Survey station 01134500 Moose River at Victory, Vermont, annual peak-flow time series consisting of 68 peaks from 1947 to 2014	108
10–2.	Graph showing annual exceedance probability plot for U.S. Geological Survey station 01134500 Moose River at Victory, Vermont, based on flood frequency analysis using Expected Moments Algorithm with Multiple Grubbs-Beck Test and weighted skew	109
10–3.	Graph showing annual exceedance probability plot for U.S. Geological Survey station 01134500 Moose River at Victory, Vermont, based on flood frequency analysis using Expected Moments Algorithm with Multiple Grubbs-Beck Test and station skew	110
10–4.	Graph showing U.S. Geological Survey station 11274500 Orestimba Creek near Newman, California, annual peak-flow time series consisting of 82 peaks from 1932 to 2013	111
10–5.	Graph showing annual exceedance probability plot for U.S. Geological Survey station 11274500 Orestimba Creek based on flood frequency analysis using Expected Moments Algorithm with Multiple Grubbs-Beck Test	116
10–6.	Graph showing U.S. Geological Survey station 01614000 Back Creek near Jones Springs, West Virginia, annual peak-flow time series consisting of 56 peaks from 1929 to 2012	118

10–7.	Graph showing annual exceedance probability plot for U.S. Geological Survey station 01614000 Back Creek near Jones Springs, West Virginia, based on flood frequency analysis using Expected Moments Algorithm with Multiple Grubbs-Beck Test	122
10–8.	Graph showing peak discharge, historical and paleoflood estimates, Arkansas River at Pueblo State Park	125
10–9.	Graph showing the peak discharge frequency curve, Arkansas River at Pueblo State Park, including gage, historical, and paleoflood data	129
10–10.	Graph showing U.S. Geological Survey station 05489490 Bear Creek at Ottumwa, Iowa, annual peak-flow time series consisting of 49 peaks from 1965 to 2014	133
10–11.	Graph showing annual exceedance probability plot for U.S. Geological Survey station 05489490 Bear Creek at Ottumwa, Iowa, based on flood frequency analysis using Expected Moments Algorithm (EMA) with Multiple Grubbs-Beck Test	135
10–12.	Graph showing U.S. Geological Survey station 09480000 Santa Cruz River near Lochiel, Arizona, annual peak-flow time series consisting of 65 peaks from 1949 to 2013	136
10–13.	Graph showing annual exceedance probability plot for U.S. Geological Survey station 09480000 Santa Cruz River based on flood frequency analysis using Expected Moments Algorithm with Multiple Grubbs-Beck Test	141
10–14.	Graph showing approximate unregulated peak discharge and paleoflood estimates, with historical and paleoflood exceedance thresholds, American River at Fair Oaks	144
10–15.	Graph showing approximate unregulated peak discharge frequency curve, American River at Fair Oaks, including gage, historical, and paleoflood data	148

Tables

1.	Flow and year terms used in the Expected Moments Algorithm	29
1–1.	List of symbols used in this report	59
2–1.	Subcommittee on Hydrology members	62
2–2.	Hydrologic Frequency Analysis Work Group members	62
3–1.	Generalized data representation of peak-flow intervals and perception thresholds for each year	68
5–1.	Typical plotting position parameter a values and their motivation	76
7–1.	Expected Moments Algorithm censored-data threshold categories	85
8–1.	Summary of concurrent observed annual peak data for the Etowah River and Suwanee Creek	95
8–2.	MOVE extended record for 13 years (1972 to 1984) for Suwanee Creek at Suwanee, Georgia	99
8–3.	Flood records for 93 years for the Etowah River at Canton, Georgia	100
10–1.	Summary of flood frequency examples	104

10–2.	U.S. Geological Survey station 01134500 Moose River at Victory, Vermont, annual peak-flow record consisting of 68 peaks from 1947 to 2014	106
10–3.	U.S. Geological Survey station 01134500 Moose River at Victory, Vermont, Expected Moments Algorithm flow intervals for the systematic period from 1947 to 2014	107
10–4.	U.S. Geological Survey station 01134500 Moose River at Victory, Vermont, Expected Moments Algorithm perception thresholds from 1947 to 2014	108
10–5.	Peak-flow quantiles in cubic feet per second for U.S. Geological Survey station 01134500 Moose River at Victory, Vermont, based on flood frequency analysis using Expected Moments Algorithm with Multiple Grubbs-Beck Test	110
10–6.	U.S. Geological Survey station 11274500 Orestimba Creek near Newman, California, annual peak-flow record from 1932 to 2013	112
10–7.	U.S. Geological Survey station 11274500 Orestimba Creek Expected Moments Algorithm flow intervals from 1932 to 2013	114
10–8.	U.S. Geological Survey station 11274500 Orestimba Creek Expected Moments Algorithm perception thresholds for the period from 1932 to 2013	115
10–9.	Peak-flow quantiles for U.S. Geological Survey station 11274500 Orestimba Creek near Newman, California, based on flood frequency analysis using Expected Moments Algorithm with Multiple Grubbs-Beck Test	115
10–10.	U.S. Geological Survey station 01614000 Back Creek near Jones Springs, West Virginia, annual peak-flow record consisting of 56 peaks from 1929 to 2012	119
10–11.	U.S. Geological Survey station 01614000 Back Creek near Jones Springs, West Virginia, Expected Moments Algorithm flow intervals for the systematic period from 1929 to 2012	120
10–12.	U.S. Geological Survey station 01614000 Back Creek near Jones Springs, West Virginia, Expected Moments Algorithm perception thresholds for the systematic period from 1929 to 2012	121
10–13.	Peak-flow quantiles in cubic feet per second for U.S. Geological Survey station 01614000 Back Creek near Jones Springs, West Virginia, based on flood frequency analysis using Expected Moments Algorithm with Multiple Grubbs-Beck Test	121
10–14.	U.S. Geological Survey station 07099500 (and others) Arkansas River annual peak-flow record consisting of 85 peaks from 1864 to 1976	124
10–15.	Arkansas River at Pueblo EMA flow intervals for the period from 1864 to 1976	126
10–16.	U.S. Geological Survey station 07099500 (and others) Arkansas River Expected Moments Algorithm perception thresholds for the paleoflood, historical, and systematic period from 1165 to 2004	127
10–17.	Peak-flow quantiles for U.S. Geological Survey station 07099500 (and others) Arkansas River based on flood frequency analysis using Expected Moments Algorithm with Multiple Grubbs-Beck Test	128
10–18.	U.S. Geological Survey station 05489490 Bear Creek at Ottumwa, Iowa, annual peak-flow record consisting of 49 peaks from 1965 to 2014	131
10–19.	U.S. Geological Survey station 05489490 Bear Creek at Ottumwa, Iowa, Expected Moments Algorithm flow intervals for the systematic period from 1965 to 2014	132
10–20.	U.S. Geological Survey station 05489490 Bear Creek at Ottumwa, Iowa, Expected Moments Algorithm perception thresholds from 1965 to 2014	134

10–21. Peak-flow quantiles in cubic feet per second for U.S. Geological Survey station 05489490 Bear Creek at Ottumwa, Iowa, based on flood frequency analysis using Expected Moments Algorithm with Multiple Grubbs-Beck Test	134
10–22. U.S. Geological Survey station 09480000 Santa Cruz River near Lochiel, Arizona, peak-flow record consisting of 65 peaks from 1949 to 2013	137
10–23. U.S. Geological Survey station 09480000 Santa Cruz River near Lochiel, Arizona, Expected Moments Algorithm flow intervals for the systematic period from 1949 to 2013	139
10–24. U.S. Geological Survey station 09480000 Santa Cruz River near Lochiel, Arizona, Expected Moments Algorithm perception thresholds for the historical and systematic period from 1927 to 2013	140
10–25. Peak-flow quantiles for U.S. Geological Survey station 09480000 Santa Cruz River near Lochiel, Arizona, based on flood frequency analysis using Expected Moments Algorithm with Multiple Grubbs-Beck Test	140
10–26. U.S. Geological Survey station 11446500 American River at Fair Oaks annual peak-flow record with historical floods and paleofloods	143
10–27. U.S. Geological Survey station 11446500 American River at Fair Oaks Expected Moments Algorithm flow intervals for the historical and systematic period from 650 to 1997	145
10–28. U.S. Geological Survey station 11446500 American River at Fair Oaks Expected Moments Algorithm perception thresholds for the paleoflood, historical, and systematic period from 1 to 2000	146
10–29. U.S. Geological Survey station 11446500 American River at Fair Oaks Expected Moments Algorithm perception thresholds for the paleoflood, historical, and systematic period from 1 to 2000	147
10–30. Peak-flow quantiles in cubic feet per second for U.S. Geological Survey station 11446500 American River at Fair Oaks based on flood frequency analysis using Expected Moments Algorithm with Multiple Grubbs-Beck Test	147

Conversion Factors

U.S. customary units to International System of Units

Multiply	By	To obtain
foot (ft)	0.3048	meter (m)
mile (mi)	1.609	kilometer (km)
square mile (mi^2)	2.590	square kilometer (km^2)
cubic foot per second (ft^3/s)	0.02832	cubic meter per second (m^3/s)

Datum

Horizontal coordinate information is referenced to the North American Datum of 1983 (NAD 83).

Vertical coordinate information is referenced to the National Geodetic Vertical Datum of 1929 (NGVD 29).

Abbreviations

ACWI	Advisory Committee on Water Information
AEP	annual exceedance probability
AMS	annual maximum series
B-GLS	Bayesian generalized least squares
B-WLS	Bayesian weighted least squares
CDF	cumulative distribution function
CSG	crest-stage gage
EMA	Expected Moments Algorithm
ENSO	El Niño-Southern Oscillation
FEMA	Federal Emergency Management Agency
GB	Grubbs-Beck
GLS	generalized least squares
HFAWG	Hydrologic Frequency Analysis Work Group
HWM	high-water mark
LP-III	Log-Pearson Type III distribution
MGBT	Multiple Grubbs-Beck Test
MOVE	Maintenance of Variance Extension
MSE	mean square error
NOAA	National Oceanic and Atmospheric Administration
NRCS	Natural Resources Conservation Service
NWIS	USGS National Water Information System
NWS	National Weather Service
OLS	ordinary least squares
P-III	Pearson Type III distribution
PDS	partial-duration series
PILF	Potentially Influential Low Flood

PSI	paleostage indicator
Reclamation	Bureau of Reclamation
RFC	River Forecast Center (NWS)
SOH	Subcommittee on Hydrology
USACE	U.S. Army Corps of Engineers
USGS	U.S. Geological Survey
WLS	weighted least squares

This page intentionally left blank.

Guidelines for Determining Flood Flow Frequency

Bulletin 17C

By John F. England, Jr., Timothy A. Cohn, Beth A. Faber, Jery R. Stedinger, Wilbert O. Thomas, Jr., Andrea G. Veilleux, Julie E. Kiang, and Robert R. Mason, Jr.

Abstract

Accurate estimates of flood frequency and magnitude are a key component of any effective nationwide flood risk management and flood damage abatement program. In addition to accuracy, methods for estimating flood risk must be uniformly and consistently applied because management of the Nation's water and related land resources is a collaborative effort involving multiple actors, including most levels of government and the private sector.

Flood frequency guidelines have been published in the United States since 1967, and have undergone periodic revisions. In 1967, the U.S. Water Resources Council presented a coherent approach to flood frequency with Bulletin 15 ([USWRC, 1967](#)), "A Uniform Technique for Determining Flood Flow Frequencies." The method it recommended involved fitting the log-Pearson Type III distribution to annual peak flow data by the method of moments.

The first extension and update of Bulletin 15 was published in 1976 as Bulletin 17 ([USWRC, 1976](#)), "Guidelines for Determining Flood Flow Frequency" (Guidelines). It extended the Bulletin 15 procedures by introducing methods for dealing with outliers, historical flood information, and regional skew. Bulletin 17A was published the following year to clarify the computation of weighted skew. The next revision, Bulletin 17B by the Interagency Committee on Water Data ([IACWD, 1982](#)), provided a host of improvements and new techniques designed to address situations that often arise in practice, including better methods for estimating and using regional skew, weighting station and regional skew, detection of outliers, and use of the conditional

probability adjustment (CPA) ([Thomas, 1985; Griffis and Stedinger, 2007a](#)).

The current version of these Guidelines are presented in this document, denoted Bulletin 17C. It incorporates changes motivated by four of the items listed as "Future Work" in Bulletin 17B and 30 years of post-17B research on flood processes and statistical methods. The updates include: adoption of a generalized representation of flood data that allows for interval and censored data types; a new method, called the Expected Moments Algorithm ([Cohn and others, 1997, 2001](#)), which extends the method of moments so that it can accommodate interval data; a generalized approach to identification of low outliers in flood data ([Cohn and others, 2013](#)); and an improved method for computing confidence intervals.

Federal agencies are requested to use these Guidelines in all planning activities involving water and related land resources. State, local, and private organizations are encouraged to use these Guidelines to assure uniformity in the flood frequency estimates that all agencies concerned with flood risk should use for Federal planning decisions.

This revision is adopted with the knowledge and understanding that review of these procedures will be ongoing. Updated methods will be adopted when warranted by experience and by examination and testing of new techniques.

Introduction

These Guidelines describe the data and procedures for computing flood flow frequency where

2 Guidelines for Determining Flood Flow Frequency—Bulletin 17C

systematic streamgaging records of sufficient length (at least 10 years, with an informative regional skew and [or] record extension) to warrant statistical analysis are available. The procedures do not cover watersheds where flood flows are appreciably altered by reservoir regulation, watershed changes, or hydrologic nonstationarities, or where the possibility of unusual events, such as dam failures, must be considered.

Background

In December 1967, Bulletin No. 15, “A Uniform Technique for Determining Flood Flow Frequencies,” was issued by the Hydrology Committee of the Water Resources Council ([USWRC, 1967](#)). The report recommended use of the Pearson Type III distribution with log transformation of the data (log-Pearson Type III distribution) as a base method for flood flow frequency studies. As pointed out in that report, further studies were needed covering various aspects of flow frequency determinations.

In March 1976, Bulletin 17, “Guidelines for Determining Flood Flow Frequency” was issued by the Water Resources Council ([USWRC, 1976](#)). The guide was an extension and update of Bulletin 15. It provided a more complete guide for flood flow frequency analysis, incorporating currently accepted technical methods with sufficient detail to promote uniform application. It was limited to defining flood potentials in terms of peak discharge and exceedance probability at locations where a systematic record of peak flood flows is available. The recommended set of procedures was selected from those used or described in the literature prior to 1976, based on studies conducted for this purpose at the Center for Research in Water Resources of the University of Texas at Austin ([Beard, 1974](#)) that are summarized in [IACWD \(1982, appendix 14\)](#) and other studies by the Work Group on Flood Flow Frequency.

These Guidelines were revised and reissued in June 1977 as Bulletin 17A, which clarified the procedure for computing weighted skew. Bulletin 17B was the next effort to improve and expand upon the earlier publications. Bulletin 17B was issued in 1981, and reissued with minor corrections in 1982

([IACWD, 1982](#)). Bulletin 17B provided revised procedures for weighting station skew values with results from a generalized skew study, detecting and treating outliers, making two station comparisons, and computing confidence limits about a frequency curve. [Thomas \(1985\)](#) and [Griffis and Stedinger \(2007a\)](#) present additional details on the history of Bulletins 17, 17A, and 17B.

In 2005, the Hydrologic Frequency Analysis Work Group (HFAWG), under the Subcommittee on Hydrology (SOH), began discussing recent research on flood frequency and potential significant revisions to Bulletin 17B. The HFAWG submitted a plan to SOH in 2006 ([Hydrologic Frequency Analysis Work Group, 2006](#)) to conduct studies on flood frequency improvements. The focus was on evaluating a generalized method of moments approach ([Cohn and others, 1997](#)), with tests on gaging station peak-flow data and with Monte-Carlo simulation ([Cohn and others, in press](#)). New procedures were developed to deal with troublesome datasets, and new methods were extensively tested with selected datasets and in Monte Carlo studies ([Cohn and others, in press](#)). In 2013, the HFAWG made recommendations to SOH to revise Bulletin 17B ([Hydrologic Frequency Analysis Work Group, 2013](#)). Additional background on revision efforts is available on the HFAWG web page at <https://acwi.gov/hydrology/Frequency/minutes/index.html>.

This document is an update to the guidelines published earlier in Bulletins 17, 17A, and 17B. Revisions incorporated in this document address major limitations of Bulletin 17B. Most of these limitations were well known and are listed in Bulletin 17B ([IACWD, 1982](#)) on p. 27–28 as topics needing future study.

A particularly important innovation in these new guidelines is the elimination of the need, implicit in application of Bulletin 17B, that all annual peaks be either point-value flow estimates, or upper bounds on historical flows, or on low flows and zero flows. With new statistical and computational procedures, these Guidelines employ a new comprehensive data framework; flood data are now generalized as “interval estimates” that incorporate both standard point-value flood observations, as well as upper bound, lower

bounds, or simple interval estimates describing the value of the peak flood in each year.

These Guidelines take advantage of the new data framework by utilizing the Expected Moments Algorithm (EMA) to analyze available flood data in a single, uniform, and consistent framework that does not require the introduction of additional algorithms to adjust the flood frequency curve to incorporate or account for the presence in the dataset of historic information, zero flows, or low outliers, as is the case with Bulletin 17B. Thus, it avoids the need for arbitrary selection of a sequence of such adjustments described on pages 12–2 through 12–4 of Bulletin 17B.

These Guidelines improve on Bulletin 17B by introducing a standardized Multiple Grubbs-Beck test to identify potentially influential low flood observations (PILFs), which can be given special treatment to prevent their exerting excessive influence on the fitting of the flood frequency curve. This is a very important addition because the new procedure provides clear, reasonable, and objective steps for the identification of such PILFs.

In addition, these Guidelines improve on procedures for estimating regional skewness estimators and their precision, thus replacing the map provided in plate 1 of Bulletin 17B. The recommended procedure employs Bayesian generalized least squares (GLS) regionalization concepts to develop improved estimates of regional flood skew, reflecting the precision of available estimates, their cross correlation, and the precision of the regional model.

Finally, taking together the use of the interval-data framework, EMA, and Bayesian skew coefficient regionalization permits the development of a more accurate estimation of confidence intervals about the flood frequency curve than do procedures described in Bulletin 17B. Large differences in confidence intervals may be observed between intervals computed with Bulletin 17B and procedures in these Guidelines (Bulletin 17C) because the Bulletin 17B confidence intervals ignored the uncertainty in the estimated skewness coefficient and had no provision for recognizing the value of historical information.

Purpose and Scope

The present Guidelines incorporate updated flood frequency methods based on research summarized by Stedinger and Griffis (2008), concepts described by England and Cohn (2007, 2008), testing by Cohn and others (2019), and a substantial body of literature over the past 30 years cited throughout this document (see [References Cited](#)). These updated methods address some of the recommended research and limitations in Bulletin 17B. The important improvements include the following:

1. The ability to accommodate a generalized form of peak-flow data, specifically interval estimates of peak-discharge magnitudes;
2. A generalization of the method of moments that can accommodate interval, censored, and binomial-censored data called the Expected Moments Algorithm (EMA) (Cohn and others, 1997);
3. Accurate confidence interval formulas that can account for historical and paleoflood information as well as regional skew information (Cohn and others, 2001); and
4. A generalized low-outlier procedure, based on the existing Grubbs-Beck test, called the Multiple Grubbs-Beck Test (MGBT), which can identify multiple potentially influential low floods in the peak flow dataset (Cohn and others, 2013).

These Guidelines are divided into nine sections, which are summarized below.

Flood Flow Frequency Information—Flood data are recognized in the following categories: systematic records, historical data, paleoflood and botanical data, regional information, comparison with similar watersheds, and flood estimates from precipitation. Common data issues and representation of data using intervals and thresholds are presented. How each can be used to define the flood potential is briefly described.

Data Assumptions and Specific Concerns—A brief discussion of basic data assumptions is presented as a reminder to those developing flood flow

4 Guidelines for Determining Flood Flow Frequency—Bulletin 17C

frequency curves to be aware of potential data issues and concerns. Flow measurement error, randomness of events, trends, long-term persistence, mixed populations, watershed changes, and climate variability are briefly discussed.

Determination of the Flood Flow Frequency Curve—This section provides guidance for the determination of a frequency curve. The Pearson Type III distribution with log transformation of the flood data (log-Pearson Type III) is recommended as the basic distribution for defining the annual flood series ([USWRC, 1967](#); [IACWD, 1982](#); [Griffis and Stedinger, 2007b](#)). The method of moments with the EMA is used to estimate the parameters of the distribution from station data, including historical and paleoflood data, when available. Adjustments are made for potentially influential low floods. Regional information is used to estimate the skew coefficient. Optional record extension methods using nearby stations is presented. Statistical uncertainty in flood quantile estimates, including the construction of confidence interval, is described.

Estimating Regional Skew—The general procedure that is recommended to estimate a regional skew is described.

Comparisons of Frequency Curves—Some concepts are described for making comparisons of frequency curves estimated using the procedures in these Guidelines to those from similar watersheds and flood estimates from precipitation. In some situations, a weighted combination of frequency curves may provide an improved estimate.

Software and Examples—Software to estimate frequency curves and examples demonstrating the use of these procedures are described.

Future Studies—Recommended future studies are listed, including methods for ungaged sites and for regulated frequency and urbanization situations.

Applicability of These Guidelines—The applicability of these Guidelines and some limitations are discussed in this section.

Appendix—The appendixes provide information on data sources, procedures for initial data analysis, the methods and some computational details for the recommended procedures, flood frequency steps and examples that implement the

recommended procedures. Symbols are defined in [appendix 1](#). [Appendix 2](#) lists HFAWG and SOH members involved in the study and revision effort.

It is possible to standardize many elements of flood frequency analysis. These Guidelines describe each major element of the process of defining the flood potential at a specific location in terms of peak discharge and annual exceedance probability (AEP). Flood quantiles with AEP ranging from 0.10 to about 0.002 are estimated using annual maximum flood series and methods described here. These estimates depend on the data used in the analysis. When longer historical and paleoflood records are used (> 1,000 years), floods with AEPs < 0.002 can be estimated. Use is confined to stations where available records are adequate to allow reliable statistical analysis of the data. Special situations may require other approaches. In those cases where the procedures of these Guidelines are not followed, deviations must be supported by appropriate study and accompanied by a comparison of results using the recommended procedures.

Flood records are limited. As more years of record become available at each location, the determination of flood potential may change. Thus, an estimate may be outdated a few years after it is made. Additional flood data alone may be sufficient reason for a fresh assessment of the flood potential. When making a new assessment, the analyst should incorporate a review of earlier estimates in their study. Where differences appear, they should be acknowledged and explained.

Risk Accumulates

It is important to realize that the probabilities computed here correspond to the annual exceedance probability, or the probability in any year that a flood threshold is exceeded. However, when considering the chance that homes, stores, factories, and other public and private facilities are flooded, owners and occupants should consider the likelihood of flooding not just in a single year, but the chance over 10, 25, or even 100 years. Such permanent facilities are generally built with design lives (corresponding to a planning horizon) of 25 or more years.

As used in these Guidelines, risk is defined as the probability that one or more events will exceed a given flood magnitude within a specified period of years n . Assuming the flow frequency curve is accurate and that events from year to year are independent, the probability p_n that a damage threshold is exceeded at least once in an n -year period is (Yen, 1970; Kite, 1988), as shown in the following equation:

$$p_n = 1 - (1 - p)^n \quad (1)$$

where p is the annual exceedance probability (AEP) for each year.

Thus, given the probability that a threshold has an AEP of 0.01 (or 1 percent), over a 25-year period, there is a 22 percent chance of the threshold being exceeded; over a 50-year period, there is a 40 percent chance of the threshold being exceeded, and over a 100-year period, there is a 63 percent chance of the threshold being exceeded. Or viewed another way, a new home or business that is protected to have only a 1 percent chance of being flooded in a single year has a 26 percent probability of being flooded over the life of a 30-year mortgage. Thus, there is about a one-in-four chance the property will be flooded in that time period. Whereas the probability of flooding in a single year may seem small when the AEP is just 1 percent or less, the chance of flooding accumulates over time so that the probability of flooding over 25 or 50 years is substantial. A full risk analysis that includes uncertainty (National Research Council, 2000) is an addition that could be considered, but is beyond the scope of these Guidelines.

Flood Flow Frequency Information

When developing a flood flow frequency curve, the analyst should consider all available information. The general types of data and information that can be included in the flood flow frequency analysis are described in the following sections, as well as how to best characterize available data. Flood frequency analysis relies primarily on systematic records, which typically can be represented as point observations. Other types of data, such as historical and

paleoflood data, may be represented with intervals or thresholds, because the magnitudes of flood peaks might be known with less precision. The analyst also needs to consider the use of regional information and flood estimates from precipitation. Specific applications are discussed in subsequent sections of these Guidelines.

Use of Annual Maximum Series

Flood events can be analyzed using either annual maximum series (AMS) or partial-duration series (PDS). The annual maximum flood series is based on the instantaneous maximum flood peak for each year. Annual maximum mean daily discharge or annual maximum n -day flood volumes (U.S. Army Corps of Engineers, 1993; Lamontagne and others, 2012) may also be considered, depending on the intended use of the flood frequency relationship. A PDS is obtained by taking all flood peaks equal to or greater than a predefined base flood. Thus an n -year record can produce m peaks with $m > n$.

Flood frequency estimates using these Guidelines are appropriate for the 0.10 AEP or less flood ($Q_p > Q_{0.10}$), where the AEP $p \leq 0.1$, such as 0.01. The annual maximum flood series provides a satisfactory sample for this type of analysis. There is little difference in AEP estimates using AMS or PDS for these quantiles (Langbein, 1949). The AMS is also used because of widespread availability and extended length of AMS data. There are limited PDS records and challenges in defining PDS threshold(s) (Madsen and others, 1997).

If minor floods are of interest, with $Q_p \leq Q_{0.10}$ AEP, a PDS may be appropriate. The PDS base is selected to assure that all events of interest are evaluated. A major problem encountered when using a PDS is to define flood events to ensure that all events are independent. It is common practice to establish an empirical basis for separating flood events (Lang and others, 1999). The basis for separation will depend upon the investigator and the intended use. No specific guidelines are recommended for defining flood events to be included in a PDS.

Beard (1974) sought to determine if a consistent relationship existed between the annual and

6 Guidelines for Determining Flood Flow Frequency—Bulletin 17C

partial series, which could be used to convert from the annual to the PDS. Based on that work, it is recommended that the PDS be developed from observed data. An alternative but less desirable solution is to convert from the annual to the PDS using a factor.

The procedures described in these Guidelines apply to the annual maximum flood series. If minor flood estimates are needed ($Q_p \leq Q_{0.10}$), such as $Q_{0.95}$, a frequency analysis such as peaks over threshold (Stedinger and others, 1993; Coles, 2001) using partial-duration data may be appropriate. No specific guidelines are recommended herein for conducting a partial-duration frequency analysis.

Data Sources for a Site

The main data sources that are recommended for use in flood frequency include systematic records, historical flood information, and paleoflood and botanical information. These at-site flood data are briefly described; additional information on data sources is in appendix 3. Refer to the [Glossary](#) for data-related definitions and notation.

Systematic Records

Systematic flood data consist of annual peak discharge data collected at regular, prescribed intervals at a gaging station (Salas and others, 1994; Wahl and others, 1995). Systematic flood data involve the continuous monitoring of flood properties by hydrologists (Rantz and others, 1982a; Baker, 1987). In the United States, the USGS operates and maintains a nationwide gaging station network (Wahl and others, 1995), and is the primary source for systematic flood data. Stream gages are also operated by Federal agencies (for example, Bureau of Reclamation [Reclamation] and U.S. Army Corps of Engineers [USACE]), State agencies (for example, California, Colorado), local agencies, and private enterprises.

The data typically used for flood frequency analysis consist of annual peak discharge values or peak discharges above a base value (PDS). Most annual peak records are obtained either from a continuous trace of river stages or from periodic observations provided by a crest-stage gage (CSG, fig. 1). Crest-stage records may provide information only on peaks



Figure 1. Photograph of a streamflow-gaging station showing a water-stage recorder, sharp-crested weir, and crest-stage gage at U.S. Geological Survey station 01589238, Gwynns Falls Tributary at McDonogh, Maryland.

above some preselected base. The records are usually continuous, although missing data or zero flow years may be present. A statistical analysis of these data is the primary basis for the determination of the flow-frequency curve for each station. A major portion of these data are available in the USGS National Water Information System (NWIS) and other electronic files; additional information in published or unpublished form is available from many sources (appendix 3).

Historical Flood Information

At many locations, particularly where people have occupied the flood plain for an extended period, or where civil works projects have been constructed by Federal agencies or others, there is information about major floods that occurred either before or after the period of systematic data collection.



Figure 2. Photograph of historic flood high-water marks and flood of March 13–15, 2010, Potomac River at Great Falls Park, Virginia, upstream of U.S. Geological Survey streamflow-gaging station 01646500, Potomac River near Washington, D.C.

Similar information may be available at sites where the gage has been discontinued, or where records are broken or incomplete. Data for recent floods that occurred outside the systematic data collection period are also treated as historical floods. This historical flood information can often be used to make estimates of peak discharge. It also may define an extended period during which the largest floods, either recorded or historic, are known. In many cases, people make a physical mark, which represents the approximate high-water mark of a flood (Koenig and others, 2016), on a relatively permanent surface (fig. 2). The high-water mark elevation must be tied to a known datum in order to determine the peak discharge from a stage-discharge relation established after the flood.

Historical data are valuable information that are used in frequency analysis as follows: Let n_s denote the number of years in the systematic (gage) record, n_h be the number of years in the historical period and n be the total period of record, where $n_s + n_h = n$. Let T_h represent a discharge perception threshold that describes the knowledge that flood magnitudes exceeded this level, or were less than this level, during the historical period (fig. 3). The historical flood data are represented by the historic (e_h) peaks and the systematic (e_s) peaks that exceed the

threshold T_h during the total flood period n . There is also knowledge that during the historical period n_h , there are many years that no flood exceeded T_h (indicated with gray shading in fig. 3). The total number of floods that exceed the perception threshold is k , where $k = e_s + e_h$. The section [Data Representation Using Flow Intervals and Perception Thresholds](#) discusses the determination of the historical period n_h and estimation of perception threshold(s) T_h .

Historical data for flood frequency typically consists of the following three types that can extend the temporal information on flood magnitudes:

- Large flood estimates prior to (outside of) the gaging station record (fig. 4);
- An extraordinary large flood and knowledge that one (or more) floods within the gaging record are actually the largest in a longer time period n than that of the gaging station record n_s (fig. 5); and
- Knowledge that floods did not exceed some value T_h (nonexceedance information) over a longer time n_h (fig. 6).

An example is used to illustrate each situation.

In the first case, there are three historical floods that occurred prior to the establishment of the gaging station record. It is known that these floods exceeded a perception threshold of 18,000 cubic feet per second (ft^3/s). These three floods are the largest on record, extend the observational record by 35 years (1895–1929), and are the most important for estimating flood frequency (fig. 4). In the second case, there is one extraordinary flood that occurred in June 1965 (Matthai, 1969, p. B39). This extraordinary flood is the largest in the 48-year gaging record (1948–1989), and there is historical flood and paleoflood information that indicates this flood might be the largest in over 900 years (Osterkamp and Costa, 1987) (fig. 5), rather than the largest in 48 years. Additional discussion for this extraordinary flood situation is in the section [Extraordinary Floods](#). In the third case, one has information from a physical feature, such as a bridge or river terrace, where no floods have exceeded a perception threshold. From detailed investigation of river terraces along the North Platte

8 Guidelines for Determining Flood Flow Frequency—Bulletin 17C

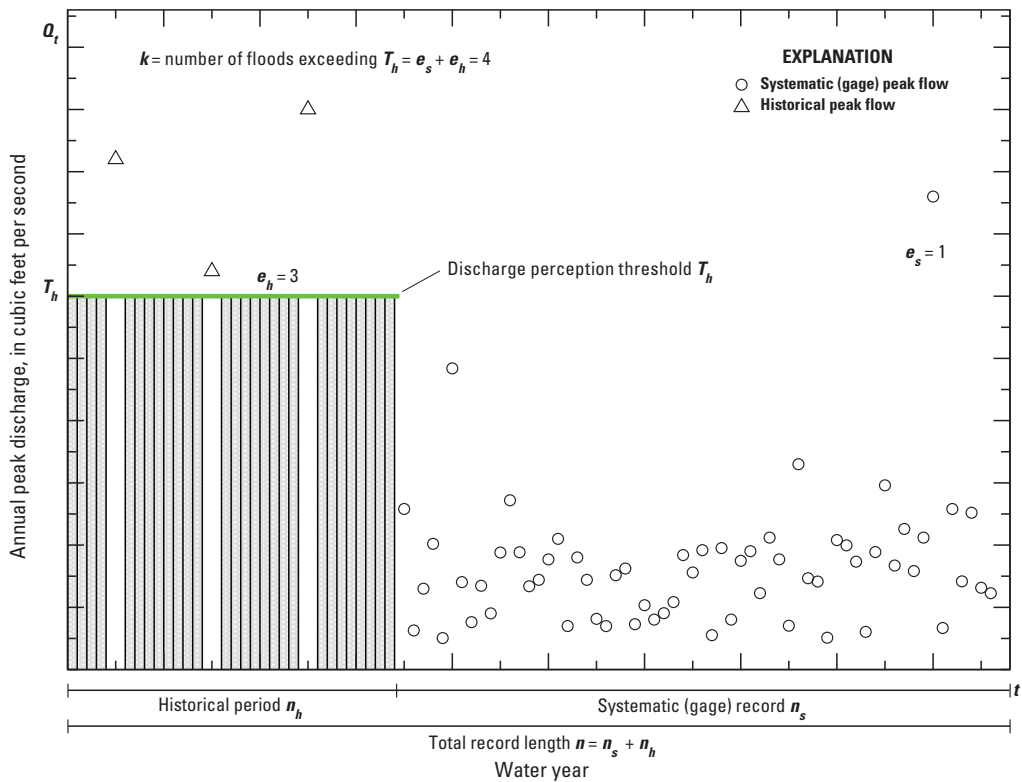


Figure 3. Graph showing an example peak-discharge time series with a historical period and a discharge perception threshold T_h . The gray shaded area represents floods of unknown magnitude less than T_h during the historical period n_h . Black vertical bars during the historical period represent flow intervals for each year for the unrecorded observations. Perception threshold T_h is shown as a green line. Historical floods that exceed the perception threshold (3 years) are shown as black triangles. Systematic (gage) peak flows are shown as black circles.

River near Seminoe dam, floods have not exceeded 45,000 ft³/s in the past 7,000 years (Levish, 2002; Levish and others, 2003) (fig. 6). Additional discussion for this situation is in the section [Paleoflood and Botanical Information](#).

The USGS includes some historical flood information in its published reports and online. Additional information may be obtained from the files of other agencies, extracted from newspaper files, or obtained by intensive inquiry and investigation near the site for which the flood frequency information is needed (Thomson and others, 1964). Reports prepared by Federal agencies (such as the U.S. Army Corps of Engineers and Reclamation) to Congress requesting funding for civil works projects often contain historical flood information that supports the need for the project. These reports are available

at many university and public libraries around the country. Data sources that could be used to identify the historical period n_h , perception threshold(s) T_h , and the largest floods outside the gaging record are described in appendix 3.

Over the past several decades, historical data and information have been shown to be extremely valuable in flood frequency analysis (Leese, 1973; Condie and Lee, 1982; Stedinger and Cohn, 1986, 1987; Cohn and others, 1997; England and others, 2003a). Dalrymple (1960) notes the following: “Historical floods provide probably the most effective data available on which to base flood frequency determinations, and where the data are reliable, this information should be given the greatest weight in constructing the flood frequency graph.” Historical flood information should be obtained and

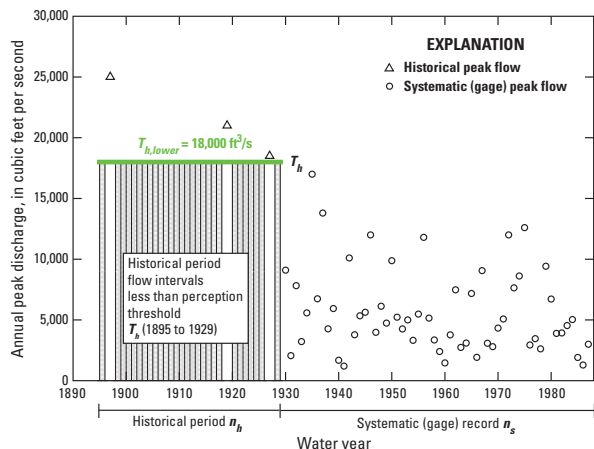


Figure 4. Graph showing an example site with three large historical floods outside the gaging record, Big Sandy River at Bruceton, Tennessee, U.S. Geological Survey streamflow-gaging station 03606500. Three historical floods are known to exceed the perception threshold T_h of 18,000 cubic feet per second (ft^3/s).

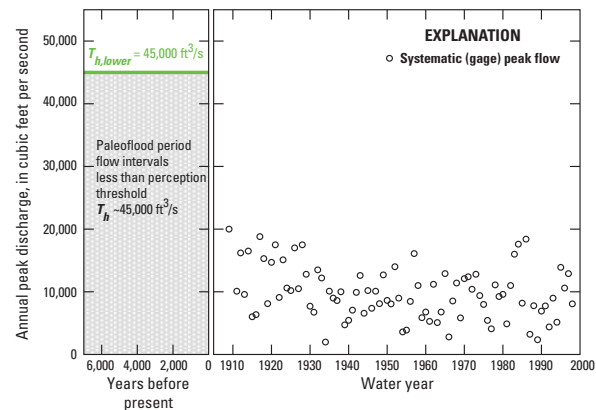


Figure 6. Graph showing an example site with historical/paleoflood nonexceedance information, North Platte River near Seminoe Reservoir, Wyoming (Levish and others, 2003). A scale break is used to separate the gaging station data from the longer historical/paleoflood period. Floods have not exceeded a perception threshold T_h of 45,000 cubic feet per second (ft^3/s) in the past 7,000 years along the river; the largest floods in the gage record are 20,000 ft^3/s .

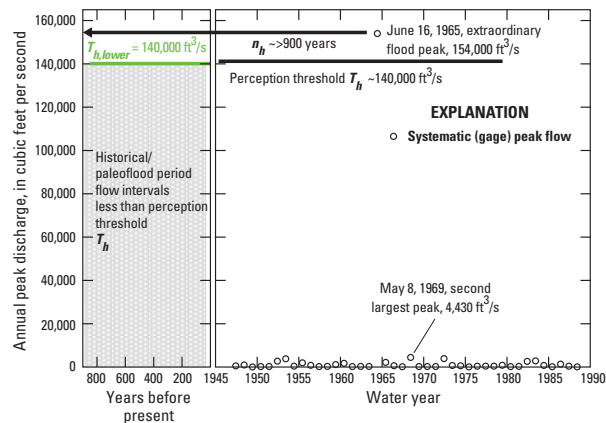


Figure 5. Graph showing an example site with an extraordinary flood peak that represents a longer time frame, Plum Creek near Louviers, Colorado, U.S. Geological Survey streamflow-gaging station 06709500. A scale break is used to separate the gaging station data from the longer historical/paleoflood period. Horizontal lines indicate the approximate historical period n_h and the perception threshold T_h .

documented whenever possible. Use of historical data assures that estimates fit community experience and improves the frequency determinations. This information is valuable in flood frequency analysis because it directly contributes extreme flood data on low annual-exceedance probability floods.

Paleoflood and Botanical Information

Over the past 40 years, there have been significant developments and advances in paleoflood hydrology (Costa, 1978, 1987; Baker and others, 1988; Jarrett, 1991; House and others, 2002a) and increased use of paleoflood data in flood frequency studies by Federal agencies and many others (Jarrett and Tomlinson, 2000; Levish and others, 2003; Sutley and others, 2008; Harden and others, 2011; O'Connor and others, 2014). Paleoflood hydrology primarily involves the study of floods that occurred before human record. Paleofloods are different from historical floods in that they are determined by geologic and physical evidence of past floods rather than records based on community memory or referenced by built infrastructure. Paleoflood hydrology focuses on direct evidence of large, rare floods or the absence of such records. This is critical information for estimating the frequency of such floods (Baker, 1987; Baker and others, 2002).

Extraordinarily large floods often create geomorphologically significant changes to flood plains

10 Guidelines for Determining Flood Flow Frequency—Bulletin 17C

and terraces, and leave evidence of flood stages in the geologic record that are long-lasting in time. Paleoflood data that are relevant for flood frequency typically consist of the following: paleostage indicators (PSIs) (discrete evidence of maximum flood stages) and nonexceedance bound information (time intervals during which particular discharges have not been exceeded) (Levish, 2002) (see [Glossary](#) for complete definitions). Paleoflood features that are typically used as PSIs for flood frequency are shown in figure 7 (Jarrett and England, 2002) and consist of slackwater deposits (SWDs) (Kite and others, 2002; House and others, 2002b); cobble and gravel flood bars (FBs) (Jarrett and England, 2002); tree scars (Yanosky and Jarrett, 2002); erosional scars and scour lines (Jarrett and Malde, 1987); and silt lines (O'Connor and others, 1986; Koenig and others, 2016). Geomorphic surfaces (primarily terraces) adjacent to rivers are used to place limits on flood discharges to estimate nonexceedance bounds (Levish, 2002).

Paleoflood data-collection methods and applications, including comprehensive overviews and current state of knowledge, are described in Baker and others (1988) and House and others (2002a). In many cases, paleoflood evidence persists for hundreds to thousands of years. This allows flood hydrologists and geologists to obtain a great deal of relevant data and information about the largest floods that have occurred during an extended time period. Applied paleoflood and flood frequency studies (England and others, 2006; Harden and others, 2011) have shown that such evidence can greatly increase the precision of flood frequency estimates at a relatively low cost. In addition, these data are available **now**; one does not have to wait decades to obtain a substantially longer record.

Paleoflood data are treated in the same way as historical flood data for flood flow frequency analysis using these Guidelines. Discharge perception thresholds for individual paleoflood magnitudes and nonexceedance bounds are used with age ranges for various paleoflood periods. In some cases, a single perception threshold, shown in figure 3, is generalized to multiple thresholds for more complex paleoflood datasets (see [Data Representation Using Flow Inter-](#)

[vals and Perception Thresholds](#) section). Paleoflood information should be obtained and documented whenever possible, particularly where the systematic record is relatively short and (or) the AEPs of interest are small (≤ 0.01). Some sources for paleoflood data, including regional approaches, are listed in appendix 3.

Botanical information consists of vegetation that records evidence of a flood (or several floods) and (or) indicates stability of a geomorphic surface for some time period. The types of botanical evidence utilized in paleohydrology studies consist primarily of age investigations, placement, distribution, and damage to trees. The four major types of botanical evidence of floods are (Hupp, 1987) corrosion scars, adventitious sprouts, tree age, and tree ring anomalies. Scars are the most easily observed damage feature, although outward evidence may disappear after a few years.

Sprouts generally occur from broken or inclined tree stems, sometimes called “clipper ships” (fig. 8). Tree age may be utilized to date a particular flood or a geomorphic surface that has been inundated by a flood or may indicate the relative stability of a surface. Vegetation ages in both cases represent a minimum age since the surface was created. In some cases, tree trunks may be partially buried by flood-transported sediments; tree ages in this case are older than the geomorphic surface. Different tree ring patterns (eccentric, shifts, vessel changes, and so forth) occur because of floods. Currently, the most reliable and accurate method of tree-ring-determined dates of flooding is the analysis of increment cores or cross sections through scars (Hupp, 1988). Annual formation of rings permits flood dating to within a year, and sometimes to within several weeks (Yanosky and Jarrett, 2002). Detailed descriptions of each type of evidence are presented in Sigafoos (1964); Yanosky (1983); Hupp (1987, 1988); and Yanosky and Jarrett (2002). Hupp and Osterkamp (1996) review the role of vegetation in fluvial geomorphic processes, including extreme floods. In flood frequency analysis, it is common to describe botanical information as binomial-censored observations corresponding to exceedances of a perception threshold. Some sources for botanical data are listed in appendix 3.

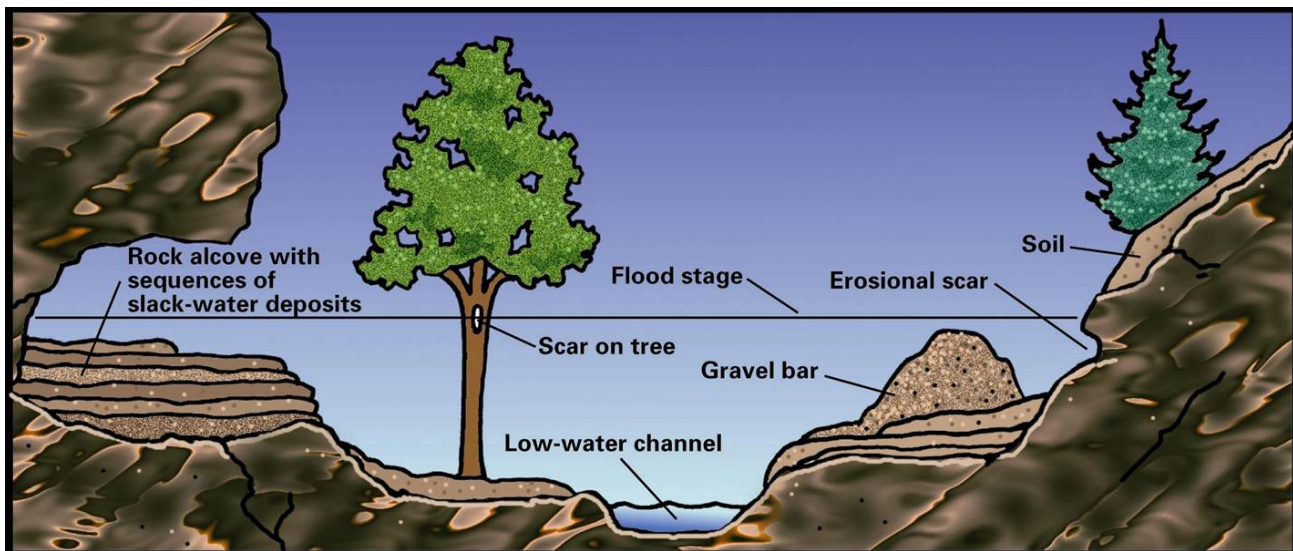


Figure 7. Diagram of a section showing typical paleoflood features used as paleostage indicators (from Jarrett and England, 2002).



Figure 8. Photograph of inclined western juniper trees with upright branches from the 1861–1862 flood, Crooked River near Prineville, Oregon.

Common Issues with At-Site Data Records

There are several common issues associated with streamflow data records from gaging stations that may require investigation and treatment by the analyst. These issues include handling of incomplete records, extraordinary floods, and potentially influential low floods (PILFs).

Broken, Incomplete, and Discontinued Records

Annual peaks for certain years may be missing because of conditions not related to flood magnitude, such as gage removal. These records are considered “broken;” a typical example is shown in figure 9. In this case, the analyst needs to determine if the records are equivalent, and if there is additional information such as historical or paleoflood information that can place the largest floods in a longer time context (Paretti and others, 2014a, fig. 4). The different record segments can be analyzed as a continuous record with length equal to the sum of both records if the gage is reestablished in a nearby location, unless there is some physical change in the watershed between segments, which may make the total record nonhomogeneous. Data from an upstream or downstream gage may provide additional information to estimate a perception threshold on the magnitude of floods that occurred during the missing or broken period.

An “incomplete” record refers to a streamflow record in which some peak flows are missing because they were too low or too high to record, or the gage was out of operation for a short period because of flooding. Missing high and low data require different

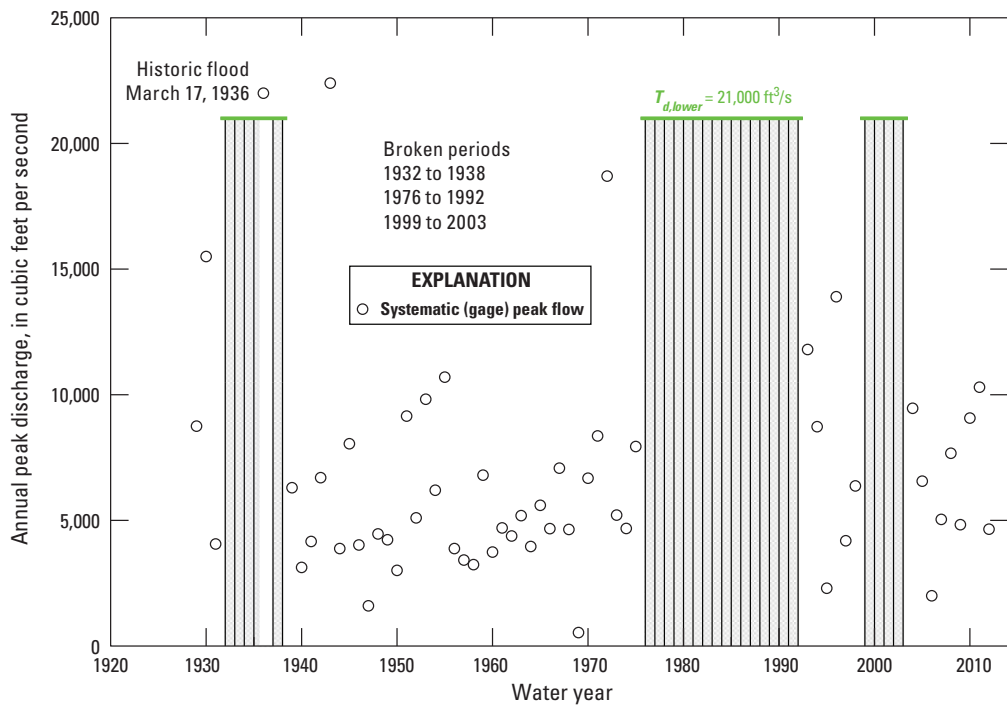


Figure 9. Graph showing an example streamflow-gaging station with a broken record, U.S. Geological Survey station 01614000, Back Creek near Jones Springs, West Virginia. The gray shaded areas represent floods of unknown magnitude less than a perception threshold T_d in cubic feet per second (ft^3/s) during the systematic record n_s when the gage was discontinued. Black vertical bars during the systematic record represent flow intervals for each year for the unrecorded observations, with the perception threshold T_d based on the March 1936 flood.

treatment. When one or more high annual peaks during the period of systematic record have not been recorded, there is usually information available from which the peak discharge can be estimated, or a flow interval estimate can be made.

A perception threshold is used to describe the knowledge that floods are not measured above a certain stage. For example, the NWIS provides a code “8” that indicates a discharge was greater than an indicated value. This and other NWIS codes are described in [Asquith and others \(2017, appendix 1\)](#).

At some crest gage sites, the bottom of the gage is not reached in some years. The NWIS provides a code “4” that a discharge was less than an indicated value. For this situation, a perception threshold is set to properly represent the incomplete observations less than some value. In most instances, the data-collecting agency provides information to estimate

peak discharges, flow intervals, and (or) perception thresholds. Estimates that are made as part of the flood frequency analysis should be documented.

Streamflow-gaging data are available at many locations where records are no longer being collected. These stations and records are considered “discontinued,” are extremely valuable, and should be used for frequency analysis. Streamflow records in many watersheds have been discontinued because of watershed development, including construction of dams and reservoirs. These discontinued records can be extended with the use of reservoir records (appendix 3) and a perception threshold (fig. 10).

Extraordinary Floods

Extraordinary floods are those floods that are the largest magnitude at a gaging station or miscellaneous site and that substantially exceed the other

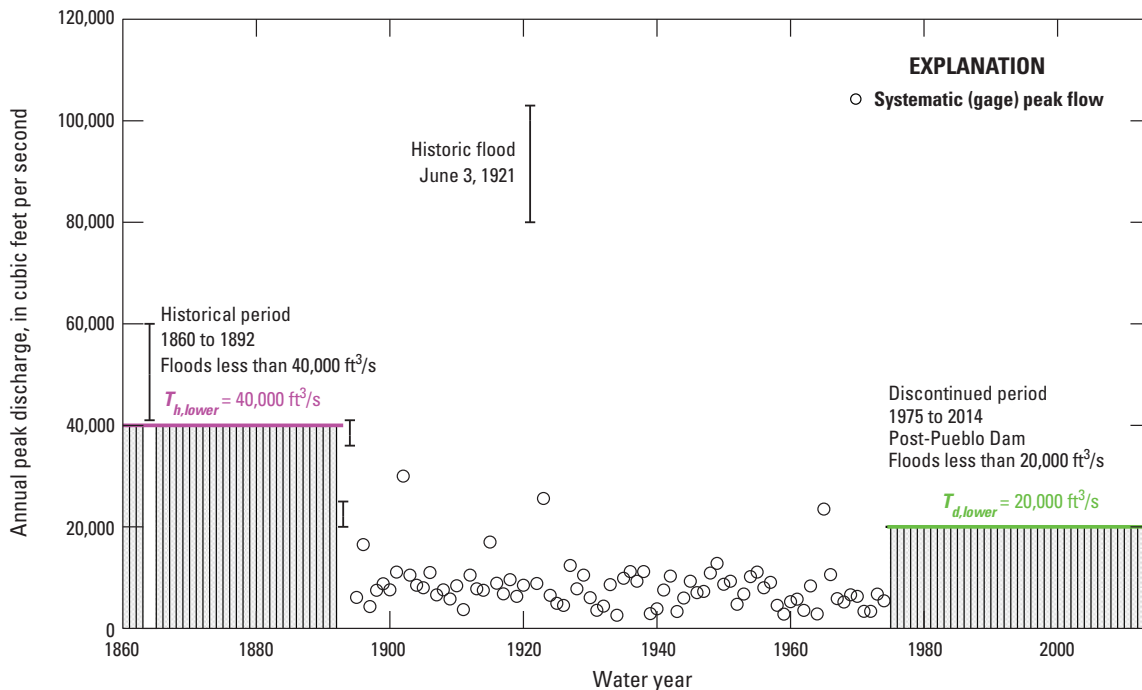


Figure 10. Graph showing an example streamflow-gaging station with a discontinued record that is extended with a perception threshold from reservoir records, U.S. Geological Survey station 07099500, Arkansas River near Pueblo, Colorado. The gage was discontinued in 1975; floods since then have not exceeded a 20,000 cubic feet per second (ft^3/s) perception threshold T_d , shown as a green line. Large floods that occurred in 1864, 1893, 1894 (Follansbee and Sawyer, 1948), and the June 1921 extraordinary flood are described as interval observations and are shown as vertical bars with caps that represent lower and upper flow estimates. A perception threshold T_h for the historical period is shown as a magenta line.

flood observations (Costa and Jarrett, 2008). Extraordinary floods may be from gaging station records, indirect measurements at miscellaneous sites or from historical flood, paleoflood, or botanical information, as described in the sections [Historical Flood Information](#) and [Paleoflood and Botanical Information](#). These floods typically exceed the second largest observation at a gaging station by a factor of two or greater, and in some cases, can be 35 times larger (fig. 5). There are many examples of extraordinary floods throughout the United States, such as the June 1921 flood on the Arkansas River in Colorado (Hazen, 1930) (fig. 10); the record 1954 flood on the Pecos River in Texas (Kochel and others, 1982; Lane, 1987); the 1976 Big Thompson River

flash flood in Colorado (Costa, 1978; Jarrett and Costa, 1988); and the June 2008 Cedar River, Iowa flood (Eash, 2010). Costa and Baker (1981) describe some extraordinary floods that represent substantially longer time frames than the gaging record length n_s at each site. Costa and Jarrett (2008) discuss the physical process recognition and indirect discharge issues in estimating extraordinary flood magnitudes, and note that the uncertainty of these estimates is large.

These extraordinary floods are of critical importance because these estimates have a direct and large influence on the fitting of the flood frequency distribution, and are the events of interest to estimate flood magnitude and frequency. Extraordinary floods

14 Guidelines for Determining Flood Flow Frequency—Bulletin 17C

should be identified by using flood-peak ratios, time-series plots, and regional flood-peak envelope curves (Crippen and Bue, 1977; Asquith and Slade, 1995; O'Connor and Costa, 2004). The method used to estimate the extraordinary flood magnitude and relevant documentation should be reviewed to examine for potential errors, gather additional information about the flood, and to estimate uncertainty (Costa and Jarrett, 2008).

All extraordinary flood observations are to be retained and used in frequency analysis. These record floods represent a longer timeframe than that of the gaging record length n_s . Historical flood, paleoflood, and botanical information should be collected within the watershed and region of interest, in order to estimate perception thresholds T_h and expand the record length n_h for the extraordinary flood(s). The recommended procedures described in the section [Determination of the Flood Flow Frequency Curve](#) are appropriate for analyzing extraordinary floods at gaging stations. The use of other frequency distributions, estimation procedures, or more complex models for extraordinary floods is not warranted, unless there is a need to estimate extreme flood quantiles less than 0.01 AEP as described in the section [Frequency Curve Extrapolation](#). It is recommended to closely examine the fit of the flood frequency curve to the largest observations, and understand the influence of any extraordinary observations on the fitted frequency curve. Confidence intervals should be used to estimate the range of AEPs for the flood. Examination of and comparison with regional flood information is also warranted. Regional flood-peak envelope probabilities (Vogel and others, 2007) can be considered in order to assess frequency estimates.

Zero Flows and Potentially Influential Low Floods

Many rivers and streams in arid and semi-arid regions within the Western United States, such as in California (Lamontagne and others, 2012) and Arizona (Paretti and others, 2014a), have zero or very small flows for the entire year. The annual flood series for these streams will have one or more

low-magnitude or zero flood values (fig. 11). Such observations merit special attention. In particular, the logarithm of zero is negative infinity, and the logarithm of unusually small values can also be anomalous. Moreover, small flood values can have a large influence on the fitting of the flood frequency distribution and the estimation of the magnitude of rare flood flows. These small observations are called potentially influential low floods (PILFs) (Cohn and others, 2013).

In these watersheds, the processes that create very large floods (that is, the floods of interest) may be different from the processes that cause the low (or zero) value annual peaks. Many low values can occur because of the influence of basin characteristics, such as channel-infiltration losses or evapotranspiration exceeding annual rainfall (Paretti and others, 2014a). The result is that the series of annual peaks appears to be generated from a mixed distribution. For example, peak flows in the range of 5,000 to 15,000 ft³/s are of interest on Orestimba Creek (fig. 11), rather than the numerous zero values and small flows less than about 1,000 ft³/s at this site. Consequently, the magnitudes of small annual peaks typically do not reveal much about the upper right-hand tail of the frequency distribution, and, thus, should not have a highly influential role when estimating the probabilities of large floods (Cohn and others, 2013). These low (or zero) flows are, thus, not relevant to estimating the probabilities of the largest flood events (Klemeš, 1986, 2000).

These Guidelines recommend the use of robust estimation procedures (Kuczera, 1982; Lamontagne and others, 2013) and a focus on the largest floods—the upper tail of the flood frequency distribution (National Research Council, 1988)—to eliminate PILFs. Robust estimation procedures are reasonably efficient when the assumed characteristics of the flood distribution are true, while not doing poorly when those assumptions are violated (Stedinger and others, 1993; Cohn and others, 2013). A focus on the most extreme events (upper tail) is based on the observation that hydrometeorological and watershed processes during extreme events are likely to be quite different from those same processes during more common events (National Research Council,

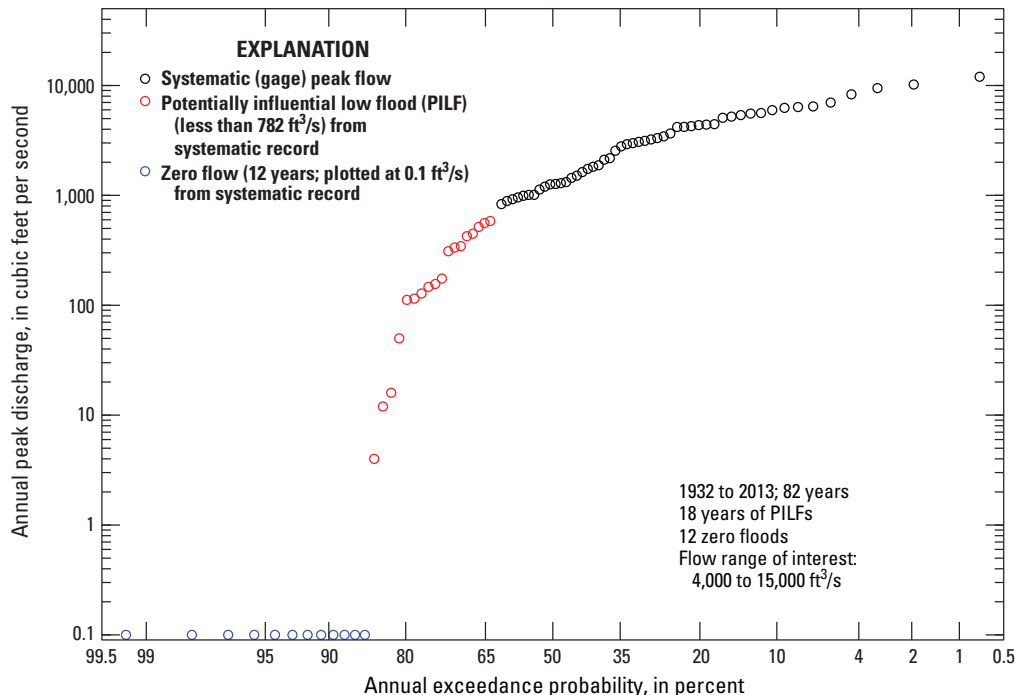


Figure 11. Graph showing an example empirical frequency distribution and potentially influential low floods (PILFs) at U.S. Geological Survey station 11274500, Orestimba Creek near Newman, California.

1988, p. 7). The statistical procedure presented in the section [Zero Flows and Identifying Potentially Influential Low Floods](#) is used to detect PILFs.

Data Representation Using Flow Intervals and Perception Thresholds

Traditionally, flood flow frequency determination focused on the analysis of flood observations Q recorded in every year Y at continuous-record stream gages, which could be represented as point data Q_Y . The description of flood and streamflow data for frequency analysis, and knowledge of the statistical characteristics of the data, have changed over the past 30 years. Valuable flood data that cannot usually be represented as point values include those from crest-stage gages, historical information, and paleoflood and botanical information. A generalized representation is used to capture what is known about annual peak flows in a given year Y , or over a range of years n . This includes information about specific annual floods that are known to be within a range of values, or above or below an estimated perception threshold. Also, there may be information

over a range of years in which it is known that no flood occurred above a known perception threshold. There may be sites where multiple perception thresholds are needed to represent different segments of the sample data across the historical period.

Representations of peak-flow observations are now generalized to include concepts such as flow intervals, exceedances, nonexceedances, and multiple perception thresholds. These concepts are described in this section to provide a generalized data representation for flood frequency. Selected definitions and symbols for these concepts are presented in the [Glossary](#). The recommended procedures in these Guidelines, described in the section [Determination of the Flood Flow Frequency Curve](#), can readily incorporate these new types of information, and can use the data properly in frequency analysis of large floods. This allows use of all types of information in multiple combinations as necessary to best utilize the flood data available at a site. In these Guidelines, all flood data are represented by flow intervals and perception thresholds (fig. 12).

For each year Y , the magnitude of Q_Y is characterized as a flow interval ($Q_{Y,lower}$, $Q_{Y,upper}$).

16 Guidelines for Determining Flood Flow Frequency—Bulletin 17C

A lower estimate $Q_{Y,lower}$ and upper estimate $Q_{Y,upper}$ (an interval) are made based on observations, written records, or physical evidence. For the majority of floods, such as those from a gaging station, the discharge is nearly “exactly” known (for all practical purposes), and $Q_{Y,lower} = Q_{Y,upper} = Q_Y$. Floods that are described by intervals or ranges currently address the following two situations (fig. 12): (1) a flood that is known to exceed some level, with no upper estimate (binomial-censored data); and (2) floods that are known to fall within a large range (interval data). In the binomial case, one only knows the lower estimate $Q_{Y,lower}$; the upper estimate $Q_{Y,upper} \cong +\infty$ is represented by a dashed line (fig. 12). Flow intervals are used to describe, in some cases, the largest flood magnitudes that are estimated from historical and paleoflood records, and sometimes indirect measurements or field estimates at a gage, which have large uncertainty (> 25 percent). Flow intervals ($Q_{Y,lower}, Q_{Y,upper}$) are not used to provide ranges on gaged flows and reflect measurement uncertainties that are within 5–25 percent. The interval observations are shown in figure 12 with bars for the lower and upper estimates. For unobserved historical floods whose magnitudes are only known to be less than some perception threshold (T_h), the lower estimate $Q_{Y,lower} = 0$, and the upper estimate $Q_{Y,upper}$ corresponds to the perception threshold for that year, such as $T_{h1,lower}$ or $T_{h2,lower}$ (fig. 12). For crest-stage gages, flow intervals are determined with consideration of equipment recording limits of stage. There is usually a base (minimum) discharge Q_b established; this may vary each year.

Perception thresholds ($T_{Y,lower}, T_{Y,upper}$) are used to describe the knowledge in each year Y within the flood record, for which the value of Q_Y would have been observed or recorded. The lower bound ($T_{Y,lower}$) represents the smallest peak flow that would result in a recorded flow; the upper bound ($T_{Y,upper}$) represents the largest peak flow that could be observed or recorded. The interval ($T_{Y,lower}, T_{Y,upper}$) defines the range of “perceptible values”—the range of potentially measurable flood discharges. These perception thresholds reflect the range of flows whose magnitude would have been recorded had they occurred, and are a

function of the type of data collected at or near a gaging station and the physical characteristics of the river. In other words, the perception thresholds represent the “observable range” of floods. It is important to note that the perception thresholds T_Y do not depend on the actual peak discharges Q_Y that have occurred.

Lower and upper perception thresholds T_Y need to be estimated for each and every year of the record. The lower bound $T_{Y,lower}$ represents the smallest annual peak flow that would result in a permanent record. For systematic (gaging) records, this is typically represented by the “gage-base discharge,” which is typically 0 (zero). At crest-stage gages, $Q_b > 0$, and may vary. For historical floods, $T_{Y,lower}$ is typically estimated to be equal to a historical flood discharge threshold T_h (fig. 12). For most sites with a systematic, continuous gaging record, $T_{Y,upper}$ is assumed to be infinite; larger floods typically get recorded. At crest-stage gages and for historical and paleoflood periods, $T_{Y,upper}$ needs to be estimated based on the CSG recording range, historical information (such as markers, bridges or buildings), or from geologic or botanical evidence. For periods where the gage has been discontinued (broken record) or ceased operation, the observation thresholds are both set to infinity if there is no other information such as a gage base or historical information. By setting $T_{Y,lower} = T_{Y,upper} = \infty$, this means that there is no information about that particular year. If there is historical information that is used for record extension of the largest floods during broken record periods, $T_{Y,lower}$ can be set to a historical flood discharge threshold T_h . Some examples of flow intervals and perception thresholds are provided in appendix 3.

In some situations, flood datasets need to be represented by multiple perception thresholds. This means more than one perception threshold is required to describe the data at hand. Two example perception thresholds are shown during the historical period in figure 12. The period 1890–1909 represents very limited observations prior to the establishment of a permanent settlement in a river canyon, where high stages and high-water marks (HWMs) that exceed $T_{h2,upper}$ are not preserved or documented.

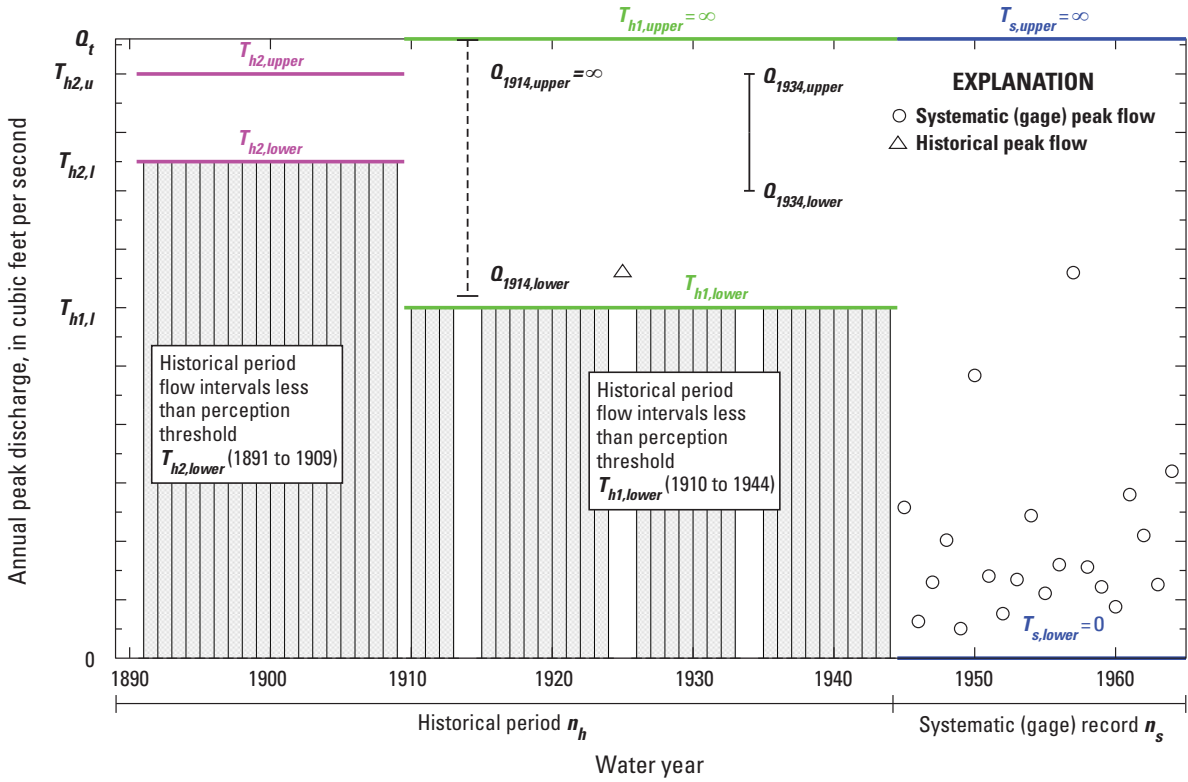


Figure 12. Graph showing an example peak-discharge time series with peak flows, interval and binomial-censored flood observations, flow intervals, and perception thresholds. Systematic (gage) peak flows are shown as black circles, where $Q_{Y,lower} = Q_{Y,upper}$. During the historical period, there are the following three floods: a “binomial” observation in 1914; one flood with known magnitude in 1925; and an interval observation in 1934. The 1925 peak flow is shown as a black triangle, where the magnitude is exactly known ($Q_{1925,lower} = Q_{1925,upper}$). The 1914 flood is described as a binomial observation and shown with a dashed line; it is known that this flood exceeded $Q_{1914,lower}$ but the upper estimate is unknown. The flood in 1934 is known to fall within a certain range described with an interval ($Q_{1934,lower} < Q_{1934,upper}$). Flood intervals are shown as black vertical bars with caps that represent lower and upper flow estimates. The gray-shaded areas represent floods of unknown magnitude less than the perception thresholds $T_{h1,lower}$ and $T_{h2,lower}$ during the historical period. The green lines represent the range in which floods would have been measured or recorded for the period 1910–1945, with lower and upper perception thresholds $T_{h1,lower}$ and $T_{h1,upper}$. The magenta lines are the perception thresholds $T_{h2,lower}$ and $T_{h2,upper}$ for the period 1891–1909. The perceptible range for the systematic (gage) period (1945–1965) $T_{s,lower}, T_{s,upper} (0, \infty)$ is shown as blue lines.

The period 1910–1944 represents increasing observations and awareness of all high river stages that exceed $T_{h1,lower}$ (with no upper limit), prior to the establishment of a gaging station in 1945.

It is appropriate to utilize multiple perception thresholds, particularly with longer historical records and paleoflood data, to properly represent the data and information at hand. In this situation, the two

perception thresholds shown in figure 12 would be extended with additional perception thresholds that are larger in magnitude than $T_{h2,lower}$ and represent longer timeframes.

It is critical to collect historical data and determine the historical period n_h for flood frequency. The beginning of the historical period may be based on, for example, the earliest known

18 Guidelines for Determining Flood Flow Frequency—Bulletin 17C

historical settlement dates (such as 1860) along a river (fig. 10), from archaeological information, or from paleoflood information and dating of river terraces and nonexceedance bounds (figs. 5 and 6). The historical period does not begin at the earliest (first) observed flood, which is a biased estimate of n_h , as it is a lower bound on the true historical period (Hirsch and Stedinger, 1987).

The lower perception threshold $T_{Y,lower}$ is particularly important to estimate. It represents our best judgment, for any given year, of the smallest size flood that would have left evidence that the investigator would know about today. The historical or paleoflood information needs to persist so that hydrologists and geologists can obtain the data from written records, historical investigations, or paleoflood studies. For example, for every year during the period 1891–1909, no evidence was found to indicate peak flows Q_Y had exceeded $T_{h2,lower}$ (fig. 12). The investigator should recognize that the lower limit of the perception threshold may be a rough approximation, and that it usually changes (increases in magnitude) as one moves backwards in time. In some cases, only the most catastrophic events would have been recorded and the threshold is high (fig. 5); these are the events that are of interest.

Regional Information and Nearby Sites

Flood information from within a region surrounding the gage site or watershed of interest is useful to improve flood frequency estimates, particularly when streamflow-gaging records are short (less than 30 years) (Stedinger and others, 1993). For these and other modest-length records, it is known that the station skew coefficient is sensitive to extreme events (Griffis and Stedinger, 2007a, 2009). Since Bulletin 17 (Beard, 1974), regional skew information G has been used to stabilize the station skew coefficient ($\hat{\gamma}$), which defines the shape of the fitted frequency distribution, through the use of a “weighted” skew coefficient \tilde{G} . The techniques for estimating regional skew have evolved over the past 30 years (Tasker and Stedinger, 1986; Griffis and Stedinger, 2007c; Parrett and others, 2011), with the result that estimates are now much more accurate and their

statistical properties are better understood than at the time Bulletin 17B was written. It is recommended that regional skew information G is considered and weighted appropriately when estimating flood frequency curves. Some sources of regional skew information are listed in appendix 3. Additional guidance is provided in the sections [Estimating Regional Skew](#) and [Weighted Skew Coefficient Estimator](#).

Other types of regional information that may be valuable for flood frequency can be considered, in addition to regional skew information. Griffis and Stedinger (2007a) describe several flood frequency estimators and show that regional estimates of the mean and standard deviation can be valuable. In arid and semiarid regions, regional mean and standard deviation estimates from peak flows can be used to improve at-site flood frequency estimates, such as the desert region in California (Gotvald and others, 2012). Physiographic characteristics within a watershed or region, such as mean basin elevation, drainage area, mean annual precipitation, and other physical factors, are useful in estimating regional parameters and in conducting regional flood frequency studies. Such studies usually employ generalized least squares regression techniques (Tasker and Stedinger, 1989) to provide regional flood quantile estimates and quantile variances. These estimates are available for many States (Gotvald and others, 2012; Eash and others, 2013) and may be valuable for record extension and weighting of independent estimates. Additional guidance is provided in the sections [Record Extension with Nearby Sites](#) and [Weighting of Independent Frequency Estimates](#).

Flood Estimates from Precipitation

Flood discharges estimated from climatic data (rainfall and [or] snowmelt) can be a useful addition to direct streamflow measurements. Estimates may be available from several cases, such as: (1) flood estimates from individual extreme events that are based on observed rainfall; (2) synthetic flood events and frequency curves from rainfall frequency estimates; and (3) continuous streamflow

estimates and frequency curves from precipitation and climate information.

Such estimates require at least adequate climatic data and a valid watershed model for converting precipitation to discharge. In some situations, existing watershed models may be available that are already calibrated to the watershed of interest. For example, the National Weather Service (NWS) has calibrated watershed models for flood forecasting on major river basins through their River Forecast Centers (RFCs). Other Federal agencies (U.S. Army Corps of Engineers, Reclamation, and Natural Resources Conservation Service) may have calibrated flood watershed models for flood control, levee design, and other projects within their jurisdiction. As part of flood-plain management studies for the Federal Emergency Management Agency (FEMA), State agencies, counties, and local watershed protection districts may have calibrated watershed models for large floods that may be used to supplement streamflow-gaging station records.

Individual extreme floods or flood frequency curves can be estimated from event-based or continuous rainfall-runoff models ([National Research Council, 1988](#); [Singh, 1995](#); [U.S. Bureau of Reclamation and Utah State University, 1999](#); [Beven, 2001](#); [FEMA, 2009](#)) using observed watershed precipitation, precipitation observed at nearby stations in a meteorologically homogeneous region, or from stochastically generated precipitation. The rainfall-runoff model needs to be calibrated to extreme flood observations, using procedures such as those presented in [Duan and others \(2003\)](#), in order to be useful for flood frequency estimation and prediction. It is recommended that an uncertainty analysis be conducted ([Kjeldsen and others, 2014](#)), including prediction uncertainty ([Beven, 2001](#), chapter 7), to reflect the range of variability associated with the estimated flood frequency curve from the rainfall-runoff model. The variance of flood quantile estimates from rainfall-runoff models is also needed for potential weighting of the estimate, as described in the section [Weighting of Independent Frequency Estimates](#).

Flood frequency estimates from rainfall-runoff models can be biased low ([Thomas, 1982](#)) or high

and exhibit a loss of variance ([Lichty and Liscum, 1978](#); [Thomas, 1987](#)) when model and other errors are not properly accounted for in uncertainty analysis. The inclusion of variability in precipitation and temperature inputs ([Clark and others, 2004](#)) helps in this situation. In some cases, rainfall-runoff models are calibrated to or parameters are adjusted to better match flood frequency curves based on peak-flow statistics ([Reed, 1999](#); [Swain and others, 2006](#); [MGS Engineering Consultants, 2009](#)). Frequency curves from rainfall-runoff models need to be independent of the frequency curve estimated using the recommended procedures in these Guidelines if curves are to be weighted and combined.

Analysts making use of such procedures should clearly document the rainfall-runoff method used for computing the floods and evaluate its performance based upon flood and storm experience in a hydrologically and meteorologically homogeneous region, including calibration and uncertainty analysis. Whether or not such studies are useful will depend upon the availability of the information, the adequacy of the existing flood records, and the purpose for which the watershed model was developed and calibrated. The magnitude and AEP of the precipitation or flood event are the most important factors to consider when including these estimates. The largest or most extreme flood events, with AEPs < 0.02 are very useful, especially for ungaged sites or in situations where gaging stations have been destroyed.

In addition to flood estimates from precipitation, hydroclimatological information ([Maddox and others, 1980](#); [Hirschboeck, 1991](#)) is very useful and provides a broad perspective on data and flood processes for frequency analysis. Atmospheric circulation patterns ([Hirschboeck, 1987a](#)) and climate indices such as the El Niño-Southern Oscillation (ENSO) ([Webb and Betancourt, 1992](#)) can be coupled with streamflow records to gain insight to the types of flood-causing mechanisms and flood variability ([National Research Council, 1999](#)). [Redmond and others \(2002\)](#) describe important connections between climate mechanisms, paleofloods, and flood variability. Some sources for precipitation and climate information are listed in appendix 3.

Data Assumptions and Specific Concerns

The conventional assumptions for a statistical analysis are that the array of flood information is reliable and it is a representative time sample of random, homogeneous events. Assessment of the adequacy and applicability of flood records is, therefore, a necessary first step in flood frequency analysis. This section discusses flow measurement errors, randomness of events, mixed populations, watershed changes, and climate variability and change considerations for flood frequency analysis.

Flow Measurement Errors

Peak-flow measurement errors exist in streamflow records, as in all other measured values. [Sauer and Meyer \(1992\)](#) describe sources of error in streamflow measurement. Absolute errors in flow estimates are generally greatest during maximum flood flows. Peak-flow estimates of the largest floods from systematic (gage) records, historical floods, paleofloods, or from other sources, can be substantially in error because of the uncertainty in both stage and stage-discharge relationships, and because the flows may be estimated from rating-curve extensions or indirect methods, rather than by direct measurement. Many improvements have been made in direct measurements of streamflow by the USGS over the past several decades ([Turnipseed and Sauer, 2010](#)), with “good” (5 percent) accuracy of most discharge measurements. However, the largest flows are generally not directly measured because of problems with debris, inaccessibility issues, and safety considerations ([Costa and Jarrett, 2008](#)). Other sources of potential error in large discharges include undocumented and unmetered breakout flows from the main river channel and ice effects ([Rantz and others, 1982b](#)). The largest floods are usually estimated by rating-curve extensions or indirect methods, with estimation errors that can exceed 25 percent in many cases, to over 100 percent in high-gradient streams ([Jarrett, 1987](#)). Measurement errors can seriously degrade flood quantile estimates in some situations

([Potter and Walker, 1985](#)); therefore, estimation errors in the largest floods should be investigated.

In many instances, annual peak discharges are estimated from rating-curve extensions. Significant errors in discharge estimation may occur from rating-curve extensions ([Cook, 1987; Kuczera, 1996](#)), especially if the discharge value is more than twice the greatest measurement by current meter. Unfortunately, high outliers or significant flood peaks are usually never measured directly and are many times greater than twice the measured value ([Klemeš, 1987](#)). [Kuczera \(1996\)](#) indicates that rating-curve extensions, in the presence of correlated errors, can significantly affect quantile estimates from such extrapolations.

Indirect methods are utilized to measure peak discharges after flood periods ([Benson and Dalrymple, 1967; Rantz and others, 1982a](#)), using HWMs or PSIs ([Koenig and others, 2016](#)). The slope-area method ([Dalrymple and Benson, 1967](#)) is most commonly used by the USGS; other indirect methods are presented by [Cook \(1987\)](#) and [Webb and Jarrett \(2002\)](#). Slope-area methods have documented sources of uncertainty ([Bathurst, 1986; Jarrett, 1987; Kirby, 1987; McCuen and Knight, 2006](#)). Significant errors in indirect discharge estimates have been noted in mountain areas; the measurements typically are overestimated ([Jarrett, 1987](#)). Neglecting channel scour or fill is the most significant factor that may introduce large errors in indirect discharge estimates ([Kirby, 1987](#)). [Quick \(1991\)](#) presents sources of errors in the slope-area method and indicates that the method has a strong upward bias. [Webb and Jarrett \(2002\)](#) describe assumptions in estimating historical and paleoflood peak discharges; they also outline information needed to support discharge estimates.

At times errors will be apparent or suspected. Substantial efforts should be made to understand sources of flow measurement errors, and to quantify the uncertainty associated with such errors. If substantial, the errors should be brought to the attention of the data collecting agency, with supporting evidence and a request for a corrected value.

Randomness of Events

In general, a time series of annual peak-flow estimates may be considered to be a random sample of independent, identically distributed random variables. The peak-flow time series is assumed to be a representative sample of the population of future floods. This assumption is contingent upon conducting exploratory data analysis (appendix 4) and further physical knowledge of the system. In essence, the stochastic process that generates floods is assumed to be stationary or invariant in time. Stationarity is a property of an underlying stochastic process and not of observed data. Realizations from stationary processes can exhibit excursions and trends that persist for decades or centuries (Cohn and Lins, 2005). Nonstationary processes are difficult to detect in peak-flow series (Villarini and others, 2009a) and may be challenging to determine (Koutsoyiannis, 2011). In some situations, long-term persistence concepts (Lins and Cohn, 2011) or shifting mean models (Salas and Boes, 1980; Sveinsson and others, 2003) could be considered.

Before conducting flood frequency analysis, these Guidelines recommend that analysts perform an initial analysis of the data. Helsel and Hirsch (2002) and Hirsch and others (1993) provide overviews and details on conducting exploratory data analysis. The recommended procedures for initial data analysis include plotting the series, estimating serial correlation, examining for trends and abrupt shifts (changepoints), and are presented in appendix 4.

In certain locations, flood records may indicate apparent nonrandomness and exhibit strong multidecadal trends or wet and dry cycles that are not explained by land use change, water management, or climate change. Such records are particularly challenging and this is one of the most vexing problems in flood frequency analysis. The Work Group did not evaluate methods to account for nonrandomness and (or) multidecadal trends in flood frequency. Additional work in this area is warranted, as it is a seriously unresolved problem. If multidecadal trends of this sort are identified through appropriate statistical tests and data analysis, it is recommended

that the underlying physical mechanisms be investigated to gain hydrological understanding (Lins and Cohn, 2011). How to adjust such a record for flood frequency is an unresolved problem.

Even when statistical tests of the serial correlation coefficients indicate a significant deviation from the independence assumption, the annual peak data may define an unbiased estimation of future flood activity if other assumptions are attained. The non-randomness of the peak series will, however, result in error in the estimated uncertainty associated with the fitted frequency curve (Tasker, 1983). Effective record-length concepts (Tasker, 1983; Vogel and Kroll, 1991) should be used to correct uncertainty estimates in the presence of serial correlation.

Mixed Populations

Flooding in some watersheds is caused by different types of meteorological events associated with distinct physical processes. For example, flooding at some locations may arise from snowmelt, rainstorms, or by combinations of both snowmelt and rainstorms (Jarrett and Costa, 1988). Such a record may not be homogeneous and may require special treatment. This mixed population results in flood frequency curves with abnormally large skew coefficients reflected by abnormal slope changes when plotted on logarithmic normal probability paper. In some situations, the frequency curve of annual events can best be described by computing separate curves for each type of event and then combining the results.

One example of mixed population is rainfall-runoff mixed with snowmelt. In the Sierra Nevada region of California, hydrologic factors and relationships operating during general winter rain floods are usually quite different from those operating during spring snowmelt floods or during local summer cloudburst floods. In this region, peak flows are primarily caused by winter rainfall at lower elevations, whereas at higher elevations, peak flows are generally caused by spring snowmelt or rain-on-snow events (Parrett and others, 2011). Frequency studies in the Sierra Nevada have been made separately for rain floods, which occur principally during

22 Guidelines for Determining Flood Flow Frequency—Bulletin 17C

the months of November through March, and for snowmelt floods, which occur during the months of April through July. Peak flows were segregated by cause—those predominately caused by snowmelt and those predominately caused by rain (Crippen, 1978). Likewise, in the Colorado Front Range, peak flows are caused by both rainfall and snowmelt during the spring and summer (Elliott and others, 1982), especially in the lower elevation of the foothills zone (Jarrett and Costa, 1988).

Flooding in the eastern United States is caused by a mixture of flood-generating mechanisms, with tropical cyclones and extratropical systems playing a central role (Smith and others, 2011). Along the Atlantic and Gulf Coasts, in some instances, floods from hurricane and nonhurricane events have been separated, thereby improving frequency estimates (Murphy, 2001). Ice-jam floods that occur in northern regions (Murphy, 2001) are another mixed-population example.

Hydroclimatological data, including the use of synoptic weather patterns (Hirschboeck, 1987b), is particularly useful to provide independent, physically based information on climate-induced flood processes and to separate flood series by type. Additional data, such as paleohydrologic and paleoclimate data, may also be considered (Redmond and others, 2002). The flood types and particular causative mechanisms may also be explored using a watershed perspective and considering variables such as storm rainfall and duration, flood seasonality, timing, and runoff response (Merz and Blöschl, 2003).

When it can be shown that there are two or more distinct and generally independent causes of floods, it may be more reliable to segregate the flood data by cause, analyzing and computing separate curves for each type of event and then combining the curves into an overall analysis of the flood frequency at the site. Procedures such as those described in Crippen (1978), U.S. Army Corps of Engineers (1982), Jarrett and Costa (1988), and Murphy (2001) may be considered. For ice-jam flow situations, one may consider using the same mixed-population approach (Murphy, 2001), or a method that focuses on maximum elevation (Vogel and Stedinger, 1984). An example of combining frequency

curves was performed for the Black Hills region as part of the peak-flow frequency estimates for South Dakota (Sando and others, 2008). Alila and Mtiraoui (2002) describe other examples. In some situations, there may not be sufficient data to perform a mixed-population analysis, or the results may not be as reliable (Gotvald and others, 2012). The Work Group did not conduct an evaluation of these procedures. Additional efforts are needed to provide guidance on the identification and treatment of mixed distributions.

Separation by calendar periods in lieu of separation by events is not considered hydrologically reasonable, unless the events in the separate periods are clearly caused by different hydrometeorological conditions. The fitting procedures in these Guidelines can be used to fit each flood series separately, with the exception that regional skew coefficients cannot be used unless developed for the specific types of events being examined. If the flood events that are believed to comprise two or more populations cannot be identified and separated by an objective and hydrologically meaningful criterion, the record shall be treated as coming from one population.

Watershed Changes

It is becoming increasingly difficult to find watersheds in which the flow regime has not been altered by modifications to the river channel, to the river flood plain, creation or destruction of reservoirs and levees, or modifications to the characteristics of the watershed at large (for example, urbanization, wildfires, change of cropping practices, erosion control, land drainage, or deforestation). Developments that can change flow conditions include urbanization, channelization, agricultural drainage, levees, and the construction of reservoirs, diversions, and alteration of land cover conditions (Sauer and others, 1983). Impervious areas within the watershed and their effects on runoff are also important considerations (Moglen, 2009).

Watershed history and flood records should be carefully examined to assure that no major watershed changes have occurred during the period of record. Documents that accompany flood records often list

such changes that occurred at discrete times. However, the effects of urbanization or the construction of numerous small reservoirs over a period of several years will likely not be documented. Such incremental changes may not noticeably alter the flow regime from year to year but the cumulative effect can be significant.

Special effort should be made to identify those records that are not homogeneous. The data analysis tools described in appendix 4 may be used to assess records for potential gradual trends or shifts that might be associated with watershed changes. Spatial and temporal estimates of land use data within watersheds should be obtained where they are available. These data are particularly useful in quantifying urbanization impacts on flood frequency ([Moglen and Beighley, 2002](#); [McCuen, 2003](#)).

Only records that represent relatively constant watershed conditions should be used for frequency analysis ([Konrad, 2003](#); [Moglen and Shivers, 2006](#)). In some situations, flow records may be adjusted to account for watershed change so that they represent current watershed conditions, where physical evidence of watershed change exists in a significant portion of the watershed ([McCuen, 2003](#)). The Work Group did not evaluate methods to account for watershed changes and makes no particular recommendations, as additional work is needed in this area.

Climate Variability and Change

There is much concern about changes in flood risk associated with climate variability and long-term climate change. Time invariance was assumed in the development of these Guidelines. In those situations where there is sufficient scientific evidence to facilitate quantification of the impact of climate variability or change in flood risk, this knowledge should be incorporated in flood frequency analysis by employing time-varying parameters or other appropriate techniques. All such methods employed need to be thoroughly documented and justified.

The Work Group did not evaluate methods to account for climate variability in flood frequency. Additional work in this area is warranted. Some information and background on nonstationarity is

presented in [Olsen and others \(2010\)](#) and [Kiang and others \(2011\)](#). In the interim, analysts might consider the following:

- Data on synoptic weather patterns ([Hirschboeck, 1987b](#));
- Paleoclimate information ([Redmond and others, 2002](#));
- Climate variability and climate projection information ([Brekke and others, 2009](#));
- Interannual and interdecadal variations in climate ([Jain and Lall, 2001](#)); and
- Time-varying distribution parameters ([Stedinger and Griffis, 2011](#); [Salas and Obeysekera, 2014](#)).

Determination of the Flood Flow Frequency Curve

This section presents the recommended procedures for determining a flood flow frequency curve. The procedures include the following: approaches for plotting positions; the flood distribution; parameter estimation; methods to handle zero flows and identifying PILFs; the EMA; record extension; and confidence intervals for quantiles. Computer programs are required in order to make these calculations; see the section [Software and Examples](#) for available products.

Plotting Positions

Empirical frequency distributions are a “non-parametric” or distribution-free method to infer the probability distribution function (mathematical model) that describes flood risk. They are used to assess distribution function (for example, LP-III) fits the data. Probability estimates are made using plotting positions. A basic plotting position formula is ([Stedinger and others, 1993](#), p. 18.24)

$$p_i = \frac{i - a}{n + 1 - 2a} \quad (2)$$

24 Guidelines for Determining Flood Flow Frequency—Bulletin 17C

where p_i is the exceedance probability of flood observations Q_i ranked from largest ($i = 1$) to smallest ($i = n$), and a is a plotting position parameter ($0 \leq a \leq 0.5$) (see table 5–1 in appendix 5).

Historical flood peaks reflect the frequency of large floods and, thus, should be incorporated into flood frequency analysis. They can also be used to judge the adequacy of estimated flood frequency relationships. For this latter purpose, appropriate plotting positions or estimates of the average exceedance probabilities associated with the historical peaks and the remainder of the data are desired. [Hirsch and Stedinger \(1987\)](#) and [Hirsch \(1987\)](#) provide an algorithm for assigning plotting positions to censored data, such as historical floods. They emphasized the correct interpretation of the information conveyed by historical flood data, the recognition of the limited precision of estimates of the exceedance probabilities of historical floods, and showed that all estimators were relatively imprecise ([Hirsch and Stedinger, 1987](#)). The threshold-exceedance plotting-position formula is given in appendix 5. It is applicable for potentially influential low flood cases, in addition to historical data, as the censored-data principles are the same.

Flood Distribution

Flood records describe a succession of natural events that do not fit any one specific known statistical distribution. To make the problem of defining flood probabilities tractable, it is convenient to select a reasonable mathematical distribution. These Guidelines recommend the use of the log-Pearson Type III (LP-III) distribution. This distribution has been in use by Federal agencies since 1967 ([USWRC, 1967](#); [Benson, 1968](#)).

Several studies have been conducted over the years to investigate which of many possible distributions and alternative parameter estimation procedures would best meet the purposes of these Guidelines. [Beard \(1974\)](#), summarized in [IACWD \(1982\)](#), found that the LP-III distribution with a regional skew coefficient performed well. [Griffis and Stedinger \(2007b\)](#) explored the characteristics of the LP-III distribution and showed that it is flexible and encompasses

a wide range of reasonable models for log-space skews, such as $|\gamma| \leq 1.414$. The method of moments parameter estimation procedure works well with reasonable constraints on parameters ([Griffis and Stedinger, 2007d](#)) and an informative regional skew ([Griffis and Stedinger, 2009](#)). The Work Group concluded from these studies, many applications over the past 40 years, and testing ([Cohn and others, in press](#)) that the Pearson Type III distribution with log transformation of the data (log-Pearson Type III distribution) with a regional skew coefficient is the base method for analysis of annual peak-flow data. The LP-III distribution also performs well and is appropriate for applications with historical and paleoflood data ([England, 1998](#); [Bureau of Reclamation, 2002](#); [Blainey and others, 2002](#); [England and others, 2003a, 2010](#); [Harden and others, 2011](#)).

The base-10 logarithms X_1, \dots, X_n of peak flows Q_1, \dots, Q_n are assumed to follow a Pearson Type III (P-III) distribution; this probability density function $f(x)$ is

$$f(x|\tau, \alpha, \beta) = \frac{\left(\frac{x-\tau}{\beta}\right)^{\alpha-1} \exp\left(-\frac{x-\tau}{\beta}\right)}{|\beta|\Gamma(\alpha)}, \quad (3)$$

with $\left(\frac{x-\tau}{\beta}\right) \geq 0$ and distribution parameters τ , α , and β , where τ is the location parameter, α is the shape parameter, β is the scale parameter, and $\Gamma(\alpha)$ is the gamma function defined as

$$\Gamma(\alpha) = \int_0^\infty t^{\alpha-1} \exp(-t) dt. \quad (4)$$

The shape parameter α is limited to positive values, and the scale parameter β may be positive or negative. When $\beta > 0$, the P-III distribution has a lower bound τ and is positive skewed; the distribution is negative skewed when $\beta < 0$ (τ is an upper bound). This behavior may also be described using the skewness coefficient, rather than parameters. When the skewness coefficient γ is greater than zero $\gamma > 0$ ($\beta > 0$), the distribution has a positive skew and floods are unbounded. When $\gamma < 0$ ($\beta < 0$), the distribution of the logarithm of floods has a negative skew and an upper bound. In this situation, the log-space skew is constrained to $\gamma \geq -1.41$. [Griffis](#)

and Stedinger (2007b) present additional properties of the P-III distribution, including plots of the P-III probability density function.

Parameter Estimation—Simple Case

These Guidelines recommend the method of moments using the logarithms of flood flows to estimate the parameters of the P-III distribution. The first three sample moments are used to estimate the P-III parameters. These include the mean ($\hat{\mu}$), standard deviation ($\hat{\sigma}$), and skewness coefficient ($\hat{\gamma}$).

Moments and Parameters

In the case where only systematic data are available, with no historical information or PILFs, the mean, standard deviation, and skewness coefficient of station data may be computed using the following equations:

$$\hat{\mu} = \left(\frac{1}{n} \right) \sum_{i=1}^n X_i, \quad (5)$$

$$\hat{\sigma} = \sqrt{\left(\frac{1}{n-1} \right) \sum_{i=1}^n (X_i - \hat{\mu})^2}, \text{ and} \quad (6)$$

$$\hat{\gamma} = \left(\frac{n}{\hat{\sigma}^3(n-1)(n-2)} \right) \sum_{i=1}^n (X_i - \hat{\mu})^3 \quad (7)$$

where n is the number of flood observations and (^) represents a sample estimate. The standard deviation ($\hat{\sigma}$) and skewness coefficient ($\hat{\gamma}$) include bias correction factors $(n-1)$ and $(n-1)(n-2)$ for small samples.

The parameters are estimated from the sample moments as

$$\hat{\alpha} = \frac{4}{\hat{\gamma}^2}, \quad (8)$$

$$\hat{\beta} = \text{sign}(\hat{\gamma}) \left(\frac{\hat{\sigma}^2}{\hat{\alpha}} \right)^{1/2}, \quad (9)$$

and

$$\hat{\tau} = \hat{\mu} - \hat{\alpha}\hat{\beta}. \quad (10)$$

Flood quantiles \hat{Q}_q for the P-III distribution can be estimated by

$$\hat{X}_q = \hat{\tau} + \hat{\beta}P^{-1}(\hat{\alpha}, q) \quad (11)$$

where $P^{-1}(\hat{\alpha}, q)$ is the inverse of the incomplete gamma function (Abramowitz and Stegun, 1964) and

$$\hat{Q}_q = 10^{\hat{X}_q} \quad (12)$$

where q is the cumulative probability of interest (for example, $q = 0.99$, and $q = 1 - p$). Flood quantiles can also be estimated with the use of a frequency factor $K_{\hat{\gamma},p}$ that is a function of the skew coefficient $\hat{\gamma}$ and exceedance probability p , as shown by the following equation

$$\hat{X}_p = \hat{\mu} + \hat{\sigma}K_{\hat{\gamma},p}, \quad (13)$$

and $K_{\hat{\gamma},p}$ can be estimated from available algorithms (Kirby, 1972; Stedinger and others, 1993).

Weighted Skew Coefficient Estimator

There is relatively large uncertainty in the at-site sample skewness coefficient (third moment) $\hat{\gamma}$ because it is sensitive to extreme events in modest-length records (Griffis and Stedinger, 2007a). The station skew coefficient $\hat{\gamma}$ and regional skew coefficient G can be combined to form a better estimate of skew \tilde{G} for a given watershed, as illustrated by the concepts in Tasker (1978). Under the assumption that the regional skew coefficient G is unbiased and independent of the station skew $\hat{\gamma}$, the mean square errors (MSEs) of the the station skew $\text{MSE}_{\hat{\gamma}}$ and the regional skew MSE_G can be used to estimate a weighted skew coefficient, as described in appendix 7. The MSE of the station skew is computed directly by EMA. The MSE of the regional skew is usually estimated through the procedures described in the section [Estimating Regional Skew](#).

If the regional and station skews differ by more than 0.5, a careful examination of the data and the

flood-producing characteristics of the watershed should be made. Possibly greater weight may be given to the station skew, depending on record length, the largest floods within the gaging record and watershed, and watershed characteristics. Large deviations between the regional skew and station skew may indicate that the flood frequency characteristics of the watershed of interest are different from those used to develop the regional skew estimate. It is thought that station skew is a function of rainfall skew, channel storage, and basin storage ([McCuen and Smith, 2008](#)). There is considerable variability of response among different basins with similar observable characteristics, in addition to the random sampling variability in estimating skew from a short record. It is considered reasonable to give greater weight to the station skew, after due consideration of the data and flood-producing characteristics of the basin.

Zero Flows and Identifying Potentially Influential Low Floods

Potentially influential points (“outliers”) are data points that depart significantly from the trend of the remaining data. In the case of annual peak flows, low outliers may be floods caused by different processes than the larger floods in the annual peak series, as defined in the section [Zero Flows and Potentially Influential Low Floods](#). Because inclusion of these zero flow values and “outliers” can significantly affect the statistical parameters computed from the data, especially for small samples, the presence of PILFs in the dataset will bias parameter estimates.

The purpose of flood flow frequency estimation is to describe the relationship between discharge and exceedance probability at the high end of the frequency distribution where AEPs are values such as 0.05, 0.02, 0.01, and smaller. There are cases where observed values of some of the smaller annual floods can have a strong effect on the shape of the estimated frequency distribution at the high-discharge end. The purpose of the procedures described here is to eliminate the influence of low floods so that these small floods have little or no impact on the frequency estimates at high discharges. The ultimate goal is to

obtain a good agreement between the high end of the observed frequency distribution and the high end of the estimated frequency distribution. This may result in a poor fit at the low end of the frequency distribution; however, there is generally no negative practical consequences to a lack of fit at the low end.

The smallest observations in the dataset do not convey meaningful or valid information about the magnitude of significant flooding ([appendix 6](#)), although they do convey valid information about the frequency of significant flooding. Therefore, if the upper tail of the frequency curve is sensitive to the numerical values of the smallest observations, then that sensitivity is a spurious artifact based on the mathematical form of the assumed, but in fact unknown, flood distribution, and has no hydrologic validity. Any procedure for treating outliers ultimately requires judgment involving both mathematical and hydrologic considerations. The analyst must use hydrological knowledge while applying a consistent and mathematically appropriate procedure.

These Guidelines recommend the use of the Multiple Grubbs-Beck Test (MGBT) for the detection of PILFs. Statistical procedures for identifying outliers have been extensively studied, including methods for addressing the case of multiple low outliers considered here, as described in [Cohn and others \(2013\)](#), [Lamontagne and others \(2013\)](#), [Lamontagne and others \(2016\)](#), and citations therein. The new Multiple Grubbs-Beck test was developed as an improvement to the Grubbs-Beck (GB) test ([Grubbs and Beck, 1972](#)) used in Bulletin 17B. The GB test is easily defeated by the occurrence of multiple low outliers, which exert a large distorting influence on the fitted frequency curve but also increase the standard deviation, thereby making the standardized distances between observations too small to trigger the GB test.

The MGBT is a statistically appropriate generalization of the GB test, and is sensitive to the possibility that **several** of the smallest observations are “unusual,” or are potentially influential. The MGBT also correctly evaluates cases where one or more observations are zero, or are below a recording threshold (partial record sites). Thus, it provides a consistent, objective, and statistically defensible

algorithm that considers whether a range of the smallest observations should be classified as outliers (or PILFs) for a much wider range of situations.

The MGBT follows the same reasoning as Rosner's R-statistic procedure (Rosner, 1983). Population mean and variance are computed from sample points that cannot be outliers under either the null or alternative hypotheses. The MGBT is a one-sided application of this procedure where only low outliers are believed to exist. In flood flow frequency analysis, high values are not treated as outliers. Low outliers are of concern because by using the logarithms of the flood peaks to fit a distribution, one or more unusual low-flow values can substantially distort the entire fitted frequency distribution. Therefore, the detection of such values is important. In addition, fitted distributions should be compared graphically with the data to check for problems.

The MGBT is applied to the systematic data of annual peaks from the station record. Let $\{X_1, \dots, X_n\}$ be a series of logarithms of the annual peak floods. Consider the sorted dataset, $\{X_{[1:n]}, X_{[2:n]}, \dots, X_{[n:n]}\}$, where $X_{[1:n]}$ is the smallest observation in the sample of size n . The null hypothesis is that all observations $\{X_1, \dots, X_n\}$ are drawn from the same population of independent and identically distributed normal variates. The alternative hypothesis is that the k -th smallest observation in the dataset, $X_{[k:n]}$, is unusually small compared to that population. If $X_{[k:n]}$ is declared a PILF, then all observations less than $X_{[k:n]}$ are also PILFs.

Annual peaks in the dataset that are detected as potentially influential are then recoded as less than a threshold discharge T_{PILF} and treated as interval data in the EMA, as discussed below. Zero flow values, if observed in the peak-flow dataset, are defined as PILFs. Computational details of the MGBT algorithm and p-values used for determining PILFs are described in appendix 6. For the case of a single low outlier, the Multiple Grubbs-Beck test is identical to the Grubbs-Beck test (Grubbs and Beck, 1972) that was used in IACWD (1982). Where appropriate, if the MGBT does not adequately identify PILFs, the analyst may define a low outlier threshold based on hydrological considerations, knowledge of the watershed, and site characteristics. The justification for a

PILF threshold T_{PILF} should be thoroughly documented.

Expected Moments Algorithm

The Expected Moments Algorithm (EMA) is a generalized method of moments procedure to estimate the P-III distribution parameters. The EMA provides a direct fit of the P-III distribution using the entire dataset, simultaneously employing regional skew information and a wide range of historical flood and threshold-exceedance information, while adjusting for any potentially influential low floods, missing values from an incomplete record, or zero flood years (Stedinger and Griffis, 2008). The EMA utilizes multiple types of at-site flood information, including Systematic Records, Historical Flood Information, and Paleoflood and Botanical Information. It also includes information about the magnitudes of historical floods and paleofloods, flow intervals, changing base discharges from CSGs, and knowledge of the number of years in the historical period when no large flood occurred, as described in the section Data Representation Using Flow Intervals and Perception Thresholds. The EMA also directly uses regional flood information (section Regional Information and Nearby Sites) in the form of a regional skew coefficient G . For the simple data situation that consists of a systematic record, no historical information, and no PILFs, the EMA returns the standard method of moments estimates presented in the section Parameter Estimation—Simple Case.

The EMA is the reasonable extension of the Bulletin 17B LP-III method of moments approach to deal in a consistent statistical framework with all of the sources of information that are likely to be available. There have been numerous studies that document some weaknesses and potential improvements to the moments estimation methods in Bulletin 17B, including historical data, handling of low outliers, use of regional skew, and confidence intervals. Stedinger and Cohn (1986) and Lane (1987) recognized that there are historical and paleoflood data that are not efficiently used by Bulletin 17B. The EMA was first developed as an alternative to Bulletin 17B (Lane, 1995; Lane and Cohn, 1996; Cohn and others,

28 Guidelines for Determining Flood Flow Frequency—Bulletin 17C

1997) in order to fully use historical and paleoflood information (England and others, 2003b,a).

The EMA was then extended to consistently handle low outlier adjustments and regional skew information (Griffis and others, 2004; Griffis, 2008), in addition to historical information. Confidence intervals with EMA have been developed (Cohn and others, 2001), as described in the section [Confidence Intervals for Quantiles](#); thus, there is a consistent statistical framework for flood frequency. For simple cases with only a systematic record and a regional skew (see section [Parameter Estimation—Simple Case](#)), the EMA reverts to the method of moments as recommended in IACWD (1982). Additional history, background, and perspectives are presented in Griffis and Stedinger (2007a) and Stedinger and Griffis (2008).

The EMA employs the peak-flow intervals $Q_{Y,lower}$ and $Q_{Y,upper}$ to estimate the moments of the LP-III distribution. The EMA requires the corresponding perception thresholds $T_{Y,lower}$ and $T_{Y,upper}$ to estimate the confidence intervals and other measures of uncertainty in frequency estimates. It is, therefore, important to estimate the flow intervals and thresholds accurately, based on all the data and information available that is presented in the section [Flood Flow Frequency Information](#). As described in the section [Data Representation Using Flow Intervals and Perception Thresholds](#), peak-flow intervals and perception thresholds are defined for each data type and for each year.

For the general case of a historical perception threshold T_h and a PILF threshold T_{PILF} , the inputs to EMA are determined by counting the floods greater than ($>$) (exceedances) and floods less than ($<$) (censored) for each year, relative to each perception threshold. Recall that $X = \log_{10}(Q)$, and that X_h and X_{PILF} are the base-10 logarithms of T_h and T_{PILF} , respectively (see also the [Glossary](#) for notation and definitions). The logarithms of flood magnitudes are expressed as a union of four sets (Cohn and others, 1997):

$$\{X\} = \{X_s^>\} \cup \{X_h^>\} \cup \{X_s^<\} \cup \{X_h^<\}, \quad (14)$$

and where PILFs are identified, the systematic period

is divided into floods above and below a PILF threshold X_l (Griffis, 2008):

$$\{X_s^<\} = \{X_l^>\} \cup \{X_l^<\} \quad (15)$$

with terms defined in table 1.

The EMA for the general situation with a historical flood perception threshold X_h and a PILF threshold X_l includes the following steps:

1. Perception thresholds for the historical period X_h and PILFs X_l within the systematic period are defined;
2. Using the values that exceeded the thresholds $\{X_h^>\}$ and $\{X_l^>\}$, initial estimates of the sample moments $\{\hat{\mu}_1, \hat{\sigma}_1, \hat{\gamma}_1\}$ are computed as if one had a complete sample;
3. For iteration $i = 1, 2, \dots$, the parameters of the P-III distribution $\{\hat{\alpha}_{i+1}, \hat{\beta}_{i+1}, \hat{\tau}_{i+1}\}$ are estimated using the previously computed sample moments, as shown in the following equations:

$$\hat{\alpha}_{i+1} = 4/\hat{\gamma}_i, \quad (16)$$

$$\hat{\beta}_{i+1} = \left(\frac{1}{2}\right) \hat{\sigma}_i \hat{\gamma}_i, \text{ and} \quad (17)$$

$$\hat{\tau}_{i+1} = \hat{\mu}_i - \hat{\alpha}_{i+1} \hat{\beta}_{i+1}; \quad (18)$$

4. New sample moments $\{\hat{\mu}_{i+1}, \hat{\sigma}_{i+1}, \hat{\gamma}_{i+1}\}$ are estimated using expected moments; and
5. Convergence test—iterate EMA steps 3 and 4 until parameter estimates converge.

For example, using the mean, as shown in equation 5, the iteration $i + 1$ is

$$\hat{\mu}_{i+1} = \left(\frac{1}{n}\right) \sum_{i=1}^n \tilde{X}_i \quad (19)$$

where

$$\tilde{X}_i = \begin{cases} X_i & \text{if } X_i \text{ is measured} \\ & \text{or "exact"} \\ E[X|X_{lower} < X_i < X_{upper}] & \text{if } X_{lower} < X_i < X_{upper} \end{cases} \quad (20)$$

and $E[X|X_{lower} < X_i < X_{upper}]$ is the expected value of an observation known to lie within a range. The equations and computation details for EMA are presented in appendix 7. The EMA confidence intervals are described in the section [Confidence Intervals for Quantiles](#).

Record Extension with Nearby Sites

The minimum record length recommended for frequency analysis in Bulletin 17C is 10 years of annual maximum peak flows. Even with the use of an informative regional skew, historical data, and adjustment for low floods, 10 years of record may not be an adequate sample for estimating the more extreme floods like the 0.01 annual exceedance probability flood. Extending records in time is a way of achieving a more representative sample. The following are a number of reasons why a short record station may not be representative of long-term conditions:

- The short record may represent a wet period where one or more major floods occurred in a short period of time;
- The short record may represent a drought period where no major floods occurred; and
- It may be known that large historical floods occurred prior to or after systematic data collection at the short record station and estimates of these floods need to be incorporated into the frequency analysis.

Record extension involves estimating additional years of record at the short-term station utilizing data at a nearby long-term station. The estimated annual peak flows are then analyzed along with the observed data in a Bulletin 17C frequency analysis. The recommended approach for record extension

Table 1. Flow and year terms used in the Expected Moments Algorithm.

Flow or year	Definition
$\{X_s^>\}$	Logarithms of floods that occurred in the systematic record with magnitudes that are greater than the historical threshold X_h .
$\{X_h^>\}$	Logarithms of historical floods or paleofloods with magnitudes greater than X_h that occurred during the historical period.
$\{X_l^>\}$	Logarithms of floods that occurred in the systematic record with magnitudes that are greater than the Potentially Influential Low Flood (PILF) threshold X_l and less than X_h .
$\{X_h^<\}$	Logarithms of unmeasured historical floods or paleofloods less than X_h , because their magnitudes did not exceed X_h .
$\{X_l^<\}$	Logarithms of floods in the systematic record that are less than the PILF threshold X_l .
$\{n_s^<\}$	Number of floods in the systematic record with magnitudes that are less than X_h .
$\{n_h^<\}$	Number of unmeasured floods in the historical period with magnitudes that are less than X_h .
$\{n_l^<\}$	Number of floods in the systematic record with magnitudes that are less than X_l .

is based on the Maintenance of Variance Extension (MOVE) techniques ([Hirsch, 1982](#)) with subsequent improvements ([Vogel and Stedinger, 1985](#)). The MOVE equations, with an example application, are presented in appendix 8. A reasonable approach to implement MOVE is to use concurrent data at a nearby long-term station that has similar watershed characteristics as the site of interest. There should be at least 10 years of overlapping data for the short record and long record stations and the correlation coefficient needs to exceed a critical value as defined in appendix 8. It is recommended that MOVE be considered when the short record site is less than 20 years, with a minimum length of 10 years.

Confidence Intervals for Quantiles

The user of frequency curves should be aware that the curve is only an estimate of the population curve; it is not an exact representation. A streamflow record is only a sample. How well this sample will predict the flood experience (population) depends upon the sample size, its representativeness, and whether or not the underlying distribution is known or chosen wisely.

The record of annual peak flows at a site is a random sample of the underlying population of annual peaks and can be used to estimate the frequency curve of that population. If the same size random sample could be selected from a different period of time, a different estimate of the underlying population frequency curve probably would result.

Thus, an estimated flood frequency curve can only be an approximation to the true frequency curve of the underlying population of annual flood peaks. To gauge the accuracy of this approximation, one may construct an interval or range of hypothetical frequency curves that, with a high degree of confidence, contains the population frequency curve. Such intervals are called confidence intervals and their end points are called confidence limits.

Confidence intervals provide either a measure of the uncertainty of the estimated exceedance probability of a selected discharge or a measure of the uncertainty of the discharge at a selected exceedance probability. Confidence intervals on the discharge

for the P-III distribution can be estimated using the method described in appendix 7. The EMA with all available data, including historical floods, PILFs, interval data, and regional skew, is used. Uncertainty in the at-site and regional estimates of the skewness coefficients is also included.

Application of confidence intervals in reaching water-resource planning decisions depends upon the needs of the user. This discussion is presented to emphasize that the frequency curve developed using these Guidelines is only today's best estimate of the flood frequency distribution. As more data become available, the estimate will normally be improved and the confidence intervals narrowed.

Estimating Regional Skew

As described in the section [Weighted Skew Coefficient Estimator](#), it is recommended that the skew coefficient used be a weighted average of the station skew and a regional skew ([Griffis and Stedinger, 2007a](#)). A recommended procedure for estimating regional skew is using the Bayesian weighted least squares/Bayesian generalized least squares (B-WLS/B-GLS) method ([Veilleux and others, 2011](#)).

[Tasker and Stedinger \(1986\)](#) developed a weighted least squares (WLS) procedure for estimating regional skewness coefficients based on sample skewness coefficients for the logarithms of annual peak-discharge data. Their method of regional analysis of skewness estimators accounts for the precision of the skewness estimator for each station, which depends on the length of record for each station and the accuracy of an ordinary least squares (OLS) regional mean skewness.

More recently, [Reis and others \(2005\)](#), [Gruber and others \(2007\)](#), and [Gruber and Stedinger \(2008\)](#) developed a Bayesian generalized least squares (B-GLS) regression model for regional skewness analyses. Use of a generalized least squares (GLS) model allows the incorporation of the cross correlation of skewness estimators. Cross correlation arises as skewness estimators are dependent upon concurrent cross correlation flood records. The Bayesian

method allows for the computation of a posterior distribution of both the regression parameters and the model error variance. As shown in [Reis and others \(2005\)](#), for cases in which the model error variance is small compared to the sampling error of the at-site estimates, the Bayesian posterior distribution provides a more reasonable description of the model error variance than both the GLS method of moments and maximum likelihood point estimates ([Veilleux, 2011](#)).

Whereas WLS regression accounts for the precision of the regional model and the effect of the record length on the variance of skewness coefficient estimators, GLS regression also considers the cross correlations among the skewness coefficient estimators. The B-GLS regression procedures extend the GLS regression framework by also providing a description of the precision of the estimated model error variance, a pseudo analysis of variance, and enhanced diagnostic statistics; see also [Griffis and Stedinger \(2009\)](#).

Because of complexities introduced by the use of the EMA ([Cohn and others, 1997](#)) and large cross correlations between annual peak discharges at some pairs of gages sites ([Parrett and others, 2011](#)), the B-WLS/B-GLS regression procedure was developed to provide both stable and defensible results for regional skewness coefficient models ([Veilleux, 2011; Veilleux and others, 2011](#)). The B-WLS/B-GLS procedure uses an OLS analysis to fit an initial regional skewness model; that OLS model is then used to generate a stable regional skewness coefficient estimate for each site. That stable regional estimate is the basis for computing the variance of each at-site skewness coefficient estimator employed in the WLS analysis. Then, Bayesian WLS is used to generate estimators of the regional skewness coefficient model parameters. Finally, B-GLS is used to estimate the precision of those B-WLS parameter estimators, to estimate the model error variance and the precision of that variance estimator, and to compute various diagnostic statistics, including Bayesian plausibility values, pseudo adjusted R-squared, pseudo analysis of variance table, two diagnostic error variance ratios, as well as leverage and influence metrics. This method has been successfully

used to generate regional skew estimates around the Nation.

It is recommended that regional skew coefficient G estimates and mean square error MSE_G estimates be obtained from studies completed by the USGS that use the B-WLS/B-GLS regression procedure. Current (2017) estimates are available for many States; others are being revised by the USGS. Appendix 3 contains information regarding recent regional skew studies. Additional information on skew studies, available reports, and contact information is available at <https://acwi.gov/hydrology/Frequency/b17c/>. In lieu of current published estimates, it is recommended that users consult with the USGS to determine the availability of regional skew estimates that have been prepared using the current methods that are described in this section. The regional skew estimates published in [IACWD \(1982, plate 1\)](#) are not recommended for use in flood frequency studies.

Comparisons of Frequency Curves

Major problems in flood frequency analysis at gaged locations are encountered when making flood estimates for probabilities more rare than defined by the available record. The accuracy of flood probability estimates based upon statistical analysis of flood data deteriorates for probabilities more rare than those directly defined by the at-site flood period of record that may include systematic, historical, and paleoflood data. This is due to several major factors, including the sampling error of the statistics from the station data, because the basic underlying distribution of flood data is not exactly known and the physical flood processes may change at larger magnitudes.

Although other procedures for estimating floods on a watershed and flood data from adjoining watersheds can sometimes be used for evaluating flood levels at high flows and rare exceedance probabilities, procedures for doing so cannot be standardized to the same extent as the procedures discussed thus far. For these situations, these Guidelines describe the information to incorporate in the analysis but allow considerable latitude in application.

Frequency curves that are estimated using the recommended procedures in the section [Determination of the Flood Flow Frequency Curve](#) can be compared with those from similar watersheds using regional frequency methods, or with frequency curves from precipitation using rainfall-runoff models. Independent estimates can in some cases be weighted and combined for an improved estimate as described in the section [Weighting of Independent Frequency Estimates](#). Prior to making comparisons, analysts should ensure that all data at the location of interest and within the region, as described in the section [Flood Flow Frequency Information](#) and appendix 3, have been adequately considered and incorporated into the frequency analysis. In this way, the flood frequency curve may reflect (as appropriate) the following: temporal information such as historical and paleoflood data; spatial information such as regional skew and watershed characteristics; and causal information such as hydroclimate information and mixed-population data. [Merz and Blöschl \(2008a,b\)](#) describe ways to include and combine various sources of flood frequency information.

The purpose for which the flood frequency information is needed will determine the amount of time and effort that can justifiably be spent to obtain additional data, make comparisons with other watersheds, utilize flood estimates from precipitation, and weight the independent estimates. All types of analyses should be incorporated when estimating flood magnitudes for exceedance probabilities less than 0.01 AEP, including comparisons with similar watersheds and comparisons with flood estimates from precipitation.

The following sections describe the use of additional information to compare and potentially refine the flood frequency analysis using quantile weighting. Recommendations of specific procedures for regional comparisons or for appraising the accuracy of such estimates are beyond the scope of these Guidelines.

Comparisons with Similar Watersheds

Comparisons and potential adjustment of a frequency curve based upon flood experience and flood

statistics in nearby hydrologically similar watersheds can improve most flood frequency determinations. Use of the weighted skew coefficient recommended by these Guidelines is one form of transferring regional information to the site at hand. Additional comparisons may be helpful and are described in the following paragraphs.

A comparison between flood and extreme storm records, such as those in [U.S. Army Corps of Engineers \(1973\)](#) (and others) and flood flow frequency analyses at nearby hydrologically similar watersheds, will often aid in evaluating and interpreting both unusual flood experience and the flood frequency analysis of a given watershed. The shorter the flood record and the more unusual a given flood event, the greater will be the need for such comparisons.

When flood frequency curves are available for similar watersheds within a region, comparisons can be made with flood quantiles for selected exceedance probabilities or with the moments of the distribution. Flood quantile estimates from regional quantile regression models that use basin characteristics and physiographic factors, such as [Paretti and others \(2014b\)](#), are usually available and are recommended for use in comparisons with at-site frequency curves.

Regional flood quantile methods have a long history of use ([Benson, 1964, 1962](#); [Feaster and others, 2009](#)) and have been shown to perform well against alternatives ([Griffis and Stedinger, 2007a](#)). Comparisons of quantiles and frequency curve shapes can be made using the index flood method ([Dalrymple, 1960](#); [Hosking and Wallis, 1997](#)), which may illustrate similarities or differences in flood runoff mechanisms ([Bureau of Reclamation, 2002](#); [England and others, 2010](#)). Comparing regional moment estimates of the mean and standard deviation with at-site estimates is also informative ([Griffis and Stedinger, 2007a](#)); regional models of these moments can also be constructed ([Gotvald and others, 2012](#)). Simple drainage-area plots and peak-flow envelope curve comparisons can be useful, with an appropriate examination of flood processes and moments within a region ([Blöschl and Sivapalan, 1997](#)). If these estimates are independent of the station analysis, a weighted average of the two estimates will be more accurate than either alone. In many situations, the

at-site estimate is used in a regional estimate; thus, the two estimates are correlated ([Moss and Thomas, 1982](#)).

Comparisons with Flood Estimates from Precipitation

Floods and frequency curves developed from precipitation estimates can be used for comparison and to potentially adjust flood frequency curves, including extrapolation beyond experienced values. As described in the section [Flood Estimates from Precipitation](#), flood estimates from precipitation may be available based on reconstruction of specific flood events, synthetic flood events, or continuous streamflow estimates.

When a flood frequency curve is available from a calibrated rainfall-runoff model for the watershed of interest, comparisons can be made to estimates from the recommended procedures in the section [Determination of the Flood Flow Frequency Curve](#). Plotting of the flood estimates for a range of exceedance probabilities provides a guide for potentially combining and extrapolating the frequency curve. Quantile variance estimates from the rainfall-runoff model are needed in order to potentially combine estimates.

Any potential weighting or combination of frequency curves must recognize the relative accuracy of the flood estimates and the other flood data used in the rainfall-runoff model. Whether or not such effort is warranted depends upon the procedures and data available and on the use to be made of the flood frequency estimates.

Because of the wide variety of rainfall-runoff models, parameters, and inputs, no specific procedures are recommended. Appraisal of the techniques to use flood estimates from rainfall-runoff models is currently outside the scope of these Guidelines. Alternative procedures for making such studies or criteria for deciding when available flood records should be combined or extended by such procedures have not been evaluated.

Weighting of Independent Frequency Estimates

When flood frequency estimates are available from similar watersheds or from rainfall-runoff models and they are independent of the at-site estimates made using the procedures described in the section [Determination of the Flood Flow Frequency Curve](#), these flood quantile estimates \hat{Q}_q may be weighted and combined. The weights are based on quantile variance and are assumed to be unbiased and independent. The weight given to each estimate is inversely proportional to its variance. Appendix 9 describes the recommended weighting method and provides an example.

It is recommended that weighting be done when reliable estimates of flood quantiles and the variances of quantiles are available. Prior to weighting and combining estimates, the quantiles and variances of the estimates need to be evaluated. Flood quantile estimates may be substantially different for a variety of reasons ([Rogger and others, 2012](#)). In some situations, highly variable estimates (for example, from rainfall-runoff models) may be unreliable and should not be weighted, as they would degrade the at-site estimate.

[Griffis and Stedinger \(2007a\)](#) evaluated several weighting methods, including quantile weighting and moment weighting with two and three parameters, among other alternatives. As described in the section [Regional Information and Nearby Sites](#), regional mean and standard deviation estimates may be available. These moments could be considered in weighting frequency curves. The computational study by [Griffis and Stedinger \(2007a\)](#) demonstrates that the simple weighting of at-site and regional regression quantile estimates performs nearly as well as more complex alternatives, and for short records, it provides a substantial improvement in quantile accuracy. Weighting is particularly useful when the at-site record is short (10 years). Quantile weighting, described in appendix 9, is the recommended approach.

Analysts are encouraged to include flood frequency information from all sources, as appropriate. In some cases, information from numerous sources

can be combined (Viglione and others, 2013). Other than the procedure recommended in appendix 9, these methods have not been fully evaluated.

Frequency Curve Extrapolation

In some situations, there is a need to estimate extreme floods with AEPs less than 0.01, such as $Q_{0.002}$, or other extraordinary floods. The need for these estimates may be because of an engineering design requirement, flood-plain analysis, and management or other infrastructure assessment. As described in the section [Comparisons of Frequency Curves](#), all types of analyses should be incorporated when estimating flood magnitudes for exceedance probabilities less than 0.01 AEP.

For these situations, the recommended approach described in the section [Determination of the Flood Flow Frequency Curve](#) is appropriate, with inclusion of additional information as follows. First, expand the flood data in time for the location of interest and at sites within a region, to include historical information, paleoflood and botanical data, and extraordinary floods as described in the sections [Historical Flood Information](#), [Paleoflood and Botanical Information](#), and [Extraordinary Floods](#). Additional flood data collection in the field is warranted. Second, expand and improve regional skew models using the procedures described in the section [Estimating Regional Skew](#) to include these longer records. Third, expand with regional independent information such as extreme flood rainfall-runoff models within the watershed, regional extreme flood information (frequency estimates, envelope curves, and so forth), or other physical and causal estimates as described in the section [Comparisons of Frequency Curves](#). In all extrapolation situations, a careful examination of PILFs and their effects on the at-site skew coefficient, regional skew coefficient, and upper tail of the frequency curve, is warranted. Finally, quantify uncertainty of the quantile estimates with confidence intervals.

The amount of extrapolation depends on the quantity and quality of flood information at the site of interest, data and information within the larger region, the designs and decisions to be made, and

tolerance for uncertainty in the extrapolated results. It is not simply based on the at-site data record length; there are variations in quantity and quality of flood information, as well as in the purposes of the designs and decisions to be made using the flood frequency estimates. A flexible approach using multiple lines of flood evidence for extrapolation is appropriate. [Swain and others \(2006\)](#) and [Nathan and Weinmann \(2016\)](#) contain additional information on extrapolation of frequency curves.

Software and Examples

Specialized software has been developed by various agencies that implements the recommended flood frequency procedures in these Guidelines. This includes estimating the log-Pearson Type III distribution parameters using the EMA with available historical and paleoflood data, PILFs, and regional skew information. Confidence intervals and plotting positions are also estimated. The software includes the methods and computations presented in the section [Determination of the Flood Flow Frequency Curve](#), PILFs described in appendix 6, and the EMA described in appendix 7. A list of recommended software packages is provided on the HFAWG web page at <https://acwi.gov/hydrology/Frequency/b17c/>.

The initial data analysis (appendix 4) and record extension techniques (appendix 8) can be performed without the need for specialized software. Available ancillary materials and examples are provided on the HFAWG web page.

Some representative flood frequency examples that illustrate the recommended methods described in the section [Determination of the Flood Flow Frequency Curve](#) are presented in appendix 10. The main emphasis is on the data, flow intervals, and threshold inputs to the EMA. The seven examples include the following: a systematic record; potentially influential low floods record; a broken record; a historical record; a crest-stage record; a historical and PILF record; and a paleoflood record. Each example includes a detailed description of the data, a time-series plot, and a flood frequency curve. Input and output files from software used to create the

examples are also available on the HFAWG web page at <https://acwi.gov/hydrology/Frequency/b17c/>. These examples are meant to illustrate the main concepts presented in these Guidelines, and are not meant to be all inclusive.

Future Studies

These Guidelines are designed to meet a current, ever-pressing demand that the Federal Government develop a coherent set of procedures for accurately defining flood potentials as needed in programs of flood damage abatement. Much additional study and data are required before the twin goals of accuracy and consistency will be obtained. It is hoped that these Guidelines contribute to this effort by defining the essential elements of a coherent set of procedures for flood frequency determination. Although selection of the analytical procedures to be used in each step or element of the analysis has been carefully made based upon a review of the literature, the considerable practical experience of Work Group members, and special studies conducted to aid in the selection process, there is a need for additional studies.

The following is a list of some additional needed topics of study identified by the Work Group:

1. The identification and treatment of mixed distributions, including those based on hydrometeorological or hydrological conditions;
2. Guides for defining flood potentials for ungaged watersheds and watersheds with limited gaging records, as described below;
3. Methods to include watershed hydrological processes and physical considerations into the analysis that can influence the frequency curve;
4. Procedures for improving flood frequency analysis using precipitation data, rainfall-runoff models, and associated uncertainty analysis;
5. Guides for defining flood potentials for watersheds altered by urbanization, wildfires, deforestation, and by reservoirs, as described below;

6. Guides for estimating dynamic flood frequency curves that vary with time, incorporating climate indices, changing basin characteristics, and addressing potential nonstationary climate conditions;
7. Frequency estimation in cases where long-term trends are evident in the data but are not readily explainable by the history of land use, land use practices, or engineering modifications of the river or flood plain; and
8. An examination and redefinition of risk, reliability, and return periods under nonstationary conditions.

There is a need to develop guidance in the following three important areas: ungaged sites, regulated flow frequency, and urbanization. Some existing practices are listed below for each area. Whereas important work has been done on these topics by researchers around the world, those efforts have not yet been evaluated for broad and systematic application as contemplated in these Guidelines.

Ungaged Sites

Many of the stream sites of interest do not have gages with sufficient records or are ungaged. One area of future work needed is to develop national guidance on methods for estimating flood flow frequency curves at ungaged sites. The following two common methods are used to estimate frequency curves for ungaged watersheds ([Thomas and others, 2001](#)): (1) regional flood quantile regression equations based on generalized least squares ([Tasker and Stedinger, 1989](#)); and (2) rainfall-runoff models ([Pilgrim and Cordery, 1993](#); [McCuen, 2004](#)). Regional regression equations are available through the USGS StreamStats software ([Ries and others, 2008](#)). A limited comparison of these two methods is in [Thomas and others \(2001\)](#).

Regulated Flow Frequency

A large portion of the stream sites of interest has flows that are altered to some degree by regulating structures such as dams, reservoirs, and

diversions, or flows are affected by levees. One area of future work needed is to develop national guidance on methods for estimating flood flow frequency curves at stream locations affected by varying degrees of regulation. Some common regulated flood frequency methods include estimating unregulated flows using empirical relationships or synthetic floods ([U.S. Army Corps of Engineers, 1993](#)), graphical frequency analysis, or by applying total probability concepts ([Kubik, 1990; Sanders and others, 1990](#)). [Durrans \(2002\)](#) summarizes these approaches and describes other methods that could be considered, and [Asquith \(2001\)](#) regionalizes the effects of cumulative flood storage per unit area on statistics of annual peaks.

Urbanization and Watershed Change

At many stream sites of interest, flood frequency relationships may be changing because of alterations within watershed and the stream corridor over time. This may be because of urbanization ([Konrad, 2003](#)), land development, and other factors described in the section [Watershed Changes](#). National guidance for estimating flood flow frequency curves in watersheds experiencing urbanization and (or) watershed change is an area needing further work. One option is to develop flood frequency regression equations that include urbanization factors ([Sauer and others, 1983](#)). Other approaches for estimating flood frequency for watersheds undergoing land use change are in [McCuen \(2003\)](#) and [Villarini and others \(2009b\)](#).

Applicability of These Guidelines

Bulletin 17C goes a long way towards addressing known concerns with Bulletin 17B. However, many concerns remain, such as the best methods of addressing regulated flows and mixed distributions, methods for addressing urbanizing areas and other land use changes, better ways to use information provided by rainfall records and rainfall-frequency analyses, and better use of physiographic watershed characteristics to define the flood flow frequency relationship. How to handle climate change and climate

variability will continue to be issues of concern as science comes to better understand the likely impact of such atmospheric phenomena on hydrologic processes. Development of flood flow frequency relationships between gaged and ungaged sites is an important topic not addressed here.

Whereas many improvements have been made, there are important limitations that apply to use of procedures included in these Guidelines. First and foremost, these Guidelines are predicated on the availability of flood data that constitute a reliable, representative, and homogeneous sample of expected future floods. Flood data that represent unique occurrences such as dam failures, ice jams, or importation or diversion of flood waters should not be used to characterize flood potential unless they are properly adjusted to represent prevailing (natural) watershed conditions. There are currently many concerns about potential changes in the distribution of floods because of watershed changes and anthropogenic climate change; such concerns may require special procedures as discussed in the section [Data Assumptions and Specific Concerns](#).

These Guidelines assume the use of the annual-maximum flood series and generally apply only to portions of the flood frequency curve for AEPs less than 0.10. Flood frequencies for larger, more common AEPs may be more appropriately determined from use of the PDS data, which allow for more than one large flood per year rather than the annual-maximum flood series. Some procedures for these analyses are mentioned in the section [Flood Flow Frequency Information](#).

These Guidelines apply only to those situations for which there are sufficient data for carrying out the necessary computations. In general, flood frequency computations are not reliable with records composed of less than 10 annual flood observations. Accurate determination of floods for small AEPs (<0.01) generally requires more data; estimations of floods for AEPs smaller than 0.005 generally require augmentation of the systematically observed flood records with general regional information, insight from precipitation records, or paleoflood information, as available (section [Flood Flow Frequency Information](#)).

These Guidelines permit augmentation of flood records by incorporation of community experience such as the documentation of floods in news reports, community accounts, or paleoflood indicators (see the sections [Historical Flood Information](#) and [Paleoflood and Botanical Information](#) and appendix 3). However, these conditions must be properly described by specification of accurate observation intervals and thresholds based upon consideration of the physical flood indicators and hydraulic conditions. These considerations must be well documented by a qualified analyst, together with the necessary computations.

These Guidelines may be used to estimate flood frequencies for urban conditions where there are flood observation datasets of sufficient length that represent stable development or that can be adjusted to account for changes in urban infrastructure and routing parameters ([Sauer and others, 1983](#); [McCuen, 2003](#)). Similarly, any regional skewness estimator should be derived from flood records representing urban conditions.

These Guidelines describe the set of procedures recommended for defining flood potential as expressed by a flood flow frequency curve. Special situations may require other approaches, perhaps defining the frequency relationship for flood volumes or river stages. In those cases where the procedures of these Guidelines are not followed, deviations must be supported by appropriate study, including a comparison of the results obtained with those obtained using these Guidelines.

There is much concern about changes in flood risk associated with climate variability and long-term climate change. Time invariance was assumed in the development of these Guidelines. In those situations where there is sufficient scientific evidence to facilitate quantification of the impact of climate variability or change in flood risk, this knowledge should be incorporated in flood frequency analysis by employing time-varying parameters or other appropriate techniques. All such methods employed need to be thoroughly documented and justified.

It is not anticipated that many special situations warranting other approaches will occur at sites that have reasonable flood flow records. These

procedures should be followed, unless there are compelling technical reasons for departing from these Guidelines. These deviations are to be documented and supported by appropriate study, including the comparison of results. The Subcommittee on Hydrology requests that these situations be called to its attention for consideration in future modifications of these Guidelines.

References Cited

- Abramowitz, M., and Stegun, I.A., 1964, Handbook of mathematical functions: Washington, D.C., National Bureau of Standards, 1046 p.
- Aldridge, B.N., and Eychaner, J.H., 1984, Floods of October 1977 in southern Arizona and March 1978 in central Arizona: U.S. Geological Survey Water-Supply Paper 2223, 143 p., accessed October 30, 2017, at <https://pubs.er.usgs.gov/publication/wsp2223>.
- Aldridge, B.N., and Hales, T.A., 1984, Floods of November 1978 to March 1979 in Arizona and west-central New Mexico: U.S. Geological Survey Water-Supply Paper 2241, 149 p., accessed October 30, 2017, at <https://pubs.er.usgs.gov/publication/wsp2241>.
- Alila, Younes, and Mtiraoui, Ahmed, 2002, Implications of heterogeneous flood-frequency distributions on traditional stream-discharge prediction techniques: *Hydrological Processes*, v. 16, no. 5, p. 1065–1084, accessed August 29, 2017, at <https://doi.org/10.1002/hyp.346>.
- Asquith, W.H., 2001, Effects of regulation on L-moments of annual peak streamflow in Texas: U.S. Geological Survey Water-Resources Investigations Report 01-4243, 66 p., accessed November 30, 2017, at <https://pubs.usgs.gov/wri/wri014243/>.
- Asquith, W.H., Kiang, J.E., and Cohn, T.A., 2017, Application of at-site peak-streamflow frequency analyses for very low annual exceedance probabilities: U.S. Geological Survey Scientific Investigations Report 2017-5038, 93 p., accessed November 30, 2017, at <https://pubs.er.usgs.gov/publication/sir20175038>.

38 Guidelines for Determining Flood Flow Frequency—Bulletin 17C

- Asquith, W.H., and Slade, R.M., 1995, Documented and potential extreme peak discharges and relation between potential extreme peak discharges and probable maximum flood peak discharges in Texas: U.S. Geological Survey Water-Resources Investigations Report 95-4249, 58 p., accessed October 30, 2017, at <https://pubs.er.usgs.gov/publication/wri954249>.
- Baker, V.R., 1987, Paleoflood hydrology and extraordinary flood events: *Journal of Hydrology*, v. 96, nos. 1–4, p. 79–99.
- Baker, V.R., 2008, Paleoflood hydrology; Origin, progress, prospects: *Geomorphology*, v. 101, nos. 1–2, p. 1–13.
- Baker, V.R., 2013, Global Late Quaternary fluvial paleohydrology, with special emphasis on paleofloods and megafloods, in Shroder, J.F., and Wohl, E., eds., v. 9.26, Treatise on geomorphology: San Diego, Academic Press, p. 511–527, accessed August 29, 2017, at <https://doi.org/10.1016/B978-0-12-374739-6.00252-9>.
- Baker, V.R., Kochel, R.C., and Patton, P.C., 1988, Flood geomorphology: New York, John Wiley and Sons, 503 p.
- Baker, V.R., Webb, R.H., and House, P.K., 2002, The scientific and societal value of paleoflood hydrology, in House, P.K., Webb, R.H., Baker, V.R., and Levish, D.R., eds., Water Science and Application Series, v. 5, Ancient floods, modern hazards: Washington, D.C., American Geophysical Union, p. 1–19, accessed August 29, 2017, at <https://doi.org/10.1029/WS005p0001>.
- Bathurst, J., 1986, Slope-area discharge gaging in mountain rivers: *Journal of Hydraulic Engineering*, v. 112, no. 5, p. 376–391, accessed August 27, 2017, at [https://doi.org/10.1061/\(ASCE\)0733-9429\(1986\)112:5\(376\)](https://doi.org/10.1061/(ASCE)0733-9429(1986)112:5(376)).
- Beard, L.R., 1974, Flood flow frequency techniques: Center for Research in Water Resources, CRWR-119, University of Texas.
- Benito, G., and O'Connor, J.E., 2013, Quantitative paleoflood hydrology, in Shroder, J.F., and Wohl, E., eds., v. 9.24, Treatise on geomorphology: San Diego, Academic Press, p. 459–474, accessed June 27, 2017, at <https://doi.org/10.1016/B978-0-12-374739-6.00250-5>.
- Benson, M.A., 1962, Factors influencing the occurrence of floods in a humid region of diverse terrain: U.S. Geological Survey Water-Supply Paper 1580-B, 64 p., accessed October 30, 2017, at <https://pubs.er.usgs.gov/publication/wsp1580B>.
- Benson, M.A., 1964, Factors affecting the occurrence of floods in the southwest: U.S. Geological Survey Water-Supply Paper 1580-D, 72 p., accessed October 30, 2017, at <https://pubs.er.usgs.gov/publication/wsp1580D>.
- Benson, M.A., 1968, Uniform flood-frequency estimating methods for federal agencies: *Water Resources Research*, v. 4, no. 5, p. 891–908, accessed August 29, 2017, at <https://doi.org/10.1029/WR004i005p00891>.
- Benson, M.A., and Dalrymple, Tate, 1967, General field and office procedures for indirect discharge measurements: U.S. Geological Survey Techniques of Water-Resources Investigations, book 3, chap. A1, 30 p., accessed October 30, 2017, at <https://pubs.er.usgs.gov/publication/twri03A1>.
- Beven, K.J., 2001, Rainfall-runoff modeling, the primer: Chichester, United Kingdom, John Wiley and Sons, 360 p.
- Blainey, J., Webb, R., Moss, M., and Baker, V., 2002, Bias and information content of paleoflood data in flood-frequency analysis, in House, P.K., Webb, R.H., Baker, V.R., and Levish, D.R., eds., Water Science and Application Series, v. 5, Ancient floods, modern hazards: American Geophysical Union, p. 161–174, accessed October 30, 2017, at <https://doi.org/10.1029/WS005p0161>.
- Blöschl, Günter, and Sivapalan, Murugesu, 1997, Process controls on regional flood frequency; coefficient of variation and basin scale: *Water Resources Research*, v. 33, no. 12, p. 2967–2980, accessed August 29, 2017, at <https://doi.org/10.1029/97WR00568>.
- Brekke, L.D., Kiang, J.E., Olsen, J.R., Pulwarty, R.S., Raff, D.A., Turnipseed, D.P., Webb, R.S., and White, K.D., 2009, Climate change and water resources management—A Federal perspective:

- U.S. Geological Survey Circular 1331, 65 p., accessed October 30, 2017, at <https://pubs.usgs.gov/circ/1331/>.
- Bureau of Reclamation, 2002, Flood hazard analysis—Folsom dam, Central Valley Project, California: U.S. Department of Interior, Bureau of Reclamation, Denver, Colo., 128 p.
- Clark, Martyn, Gangopadhyay, Subhrendu, Hay, Lauren, Rajagopalan, Balaji, and Wilby, Robert, 2004, The Schaake shuffle; A method for reconstructing space-time variability in forecasted precipitation and temperature fields: *Journal of Hydrometeorology*, v. 5, no. 1, p. 243–262, accessed August 29, 2017, at [https://doi.org/10.1175/1525-7541\(2004\)005<0243:TSSAMF>2.0.CO;2](https://doi.org/10.1175/1525-7541(2004)005<0243:TSSAMF>2.0.CO;2).
- Cohen, A.C., 1991, Truncated and censored samples—theory and application: New York, Marcel-Dekker, 312 p.
- Cohn, T.A., Barth, N.A., England, J.F., Faber, B., Mason, R.R., and Stedinger, J.R., 2019, Evaluation of recommended revisions to Bulletin 17B: U.S. Geological Survey Open-File Report 2017–1064.
- Cohn, T.A., England, J.F., Berenbrock, C.E., Mason, R.R., Stedinger, J.R., and Lamontagne, J.R., 2013, A generalized Grubbs-Beck test statistic for detecting multiple potentially influential low outliers in flood series: *Water Resources Research*, v. 49, no. 8, p. 5047–5058, accessed June 27, 2017, at <https://doi.org/10.1002/wrcr.20392>.
- Cohn, T.A., Lane, W.L., and Baier, W.G., 1997, An algorithm for computing moments-based flood quantile estimates when historical flood information is available: *Water Resources Research*, v. 33, no. 9, p. 2089–2096.
- Cohn, T.A., Lane, W.L., and Stedinger, J.R., 2001, Confidence intervals for Expected Moments Algorithm flood quantile estimates: *Water Resources Research*, v. 37, no. 6, p. 1695–1706.
- Cohn, T.A., and Lins, H.F., 2005, Nature's style; naturally trendy: *Geophysical Research Letters*, v. 32, no. 23, accessed August 30, 2017, at <https://doi.org/10.1029/2005GL024476>.
- Coles, Stuart, 2001, An introduction to statistical modeling of extreme values: London, Springer, 208 p., accessed August 28, 2017, at <https://doi.org/10.1007/978-1-4471-3675-0>.
- Condie, R., and Lee, K.A., 1982, Flood frequency analysis with historic information: *Journal of Hydrology*, v. 58, p. 47–61.
- Cook, J.L., 1987, Quantifying peak discharges for historical floods: *Journal of Hydrology*, v. 96, nos. 1–4, p. 29–40, accessed August 30, 2017, at [https://doi.org/10.1016/0022-1694\(87\)90141-7](https://doi.org/10.1016/0022-1694(87)90141-7).
- Costa, J.E., 1978, Holocene stratigraphy in flood frequency analysis: *Water Resources Research*, v. 14, no. 4, p. 626–632, accessed August 30, 2017, at <https://doi.org/10.1029/WR014i004p00626>.
- Costa, J.E., 1986, A history of paleoflood hydrology in the United States, 1800–1970: *EOS, Transactions of the American Geophysical Union*, v. 67, no. 17, p. 425, 428–430.
- Costa, J.E., 1987, A history of paleoflood hydrology in the United States, 1800–1970, in Gillmor, C.S., Landa, E.R., Ince, Simon, and Back, William, eds., v. 3, History of geophysics: American Geophysical Union, p. 49–53, accessed August 30, 2017, at <https://doi.org/10.1029/HG003p0049>.
- Costa, J.E., and Baker, V.R., 1981, Surficial geology; Building with the Earth: New York, Wiley, 498 p.
- Costa, J.E., and Jarrett, R.D., 2008, An evaluation of selected extraordinary floods in the United States reported by the U.S. Geological Survey and implications for future advancement of flood science: U.S. Geological Survey Scientific Investigations Report 2008–5164, 232 p., accessed October 30, 2017, at <https://pubs.er.usgs.gov/publication/sir20085164>.
- Crippen, J.R., 1978, Composite log-type III frequency-magnitude curve of annual floods: U.S. Geological Survey Open-File Report 78–352, 5 p.
- Crippen, J.R., and Bue, C.D., 1977, Maximum floodflows in the conterminous United States: U.S. Geological Survey Water-Supply Paper 1887, 52 p., accessed October 30, 2017, at <https://pubs.er.usgs.gov/publication/wsp1887>.

40 Guidelines for Determining Flood Flow Frequency—Bulletin 17C

- Crowfoot, R.M., Paillett, A.V., Ritz, G.F., Smith, M.E., Jenkins, R.A., and O'Neill, G.B., 1997, Water resources data, Colorado, water year 1996, Volume 2, Colorado River Basin: U.S. Geological Survey Water-Data Report CO-96-2, 551 p., accessed October 30, 2017, at <https://pubs.usgs.gov/wdr/WDR-CO-96-2/>.
- Dalrymple, Tate, 1960, Flood-frequency analyses, Manual of hydrology; Part 3. Flood flow techniques: U.S. Geological Survey Water-Supply Paper 1543-A, 80 p., accessed October 30, 2017, at <https://pubs.er.usgs.gov/publication/wsp1543A>.
- Dalrymple, Tate, and Benson, M.A., 1967, Measurement of peak discharge by the slope-area method: U.S. Geological Survey Techniques of Water-Resources Investigations, book 3, chap. A2, 12 p., accessed October 30, 2017, at <https://pubs.er.usgs.gov/publication/twri03A2>.
- David, H.A., 1981, Order statistics: New York, Wiley, 360 p.
- Duan, Qingyun, Gupta, H.V., Sorooshian, Soroosh, Rousseau, A.N., and Turcotte, Richard, 2003, Calibration of watershed models: American Geophysical Union, 345 p., accessed August 30, 2017, at <https://doi.org/10.1029/WS006>.
- Durlin, R.R., and Schaffstall, W.P., 2002, Water resources data, Pennsylvania, water year 2002, volume 2, Susquehanna and Potomac River Basins: U.S. Geological Survey Water-Data Report PA-02-2, 536 p., accessed October 30, 2017, at <https://pubs.water.usgs.gov/WDRPA22>.
- Durrans, S.R., 2002, Regulated flood frequency methods: Hydrologic Frequency Analysis Work Group, Hydrology Subcommittee, Interagency Advisory Committee on Water Data.
- Eash, D.A., 2010, Estimating flood frequency, in Mutel, C.F., ed., A watershed year; Anatomy of the Iowa floods of 2008: Iowa City, University of Iowa Press, p. 61–70.
- Eash, D.A., Barnes, K.K., and Veilleux, A.G., 2013, Methods for estimating annual exceedance-probability discharges for streams in Iowa, based on data through water year 2010: U.S. Geological Survey Scientific Investigations Report 2013-5086, 63 p., accessed October 30, 2017, at <https://pubs.usgs.gov/sir/2013/5086/>.
- Elliott, J.G., Jarrett, R.D., and Ebling, J.L., 1982, Annual snowmelt and rainfall peak-flow data on selected foothills region streams, South Platte River, Arkansas River, and Colorado River Basins, Colorado: U.S. Geological Survey Open-File Report 82-426, 86 p., accessed October 30, 2017, at <https://pubs.er.usgs.gov/publication/ofr82426>.
- England, J.F., 1998, Assessment of historical and paleohydrologic information in flood frequency analysis: M.S. thesis, Colorado State University, Fort Collins, Colo., 292 p.
- England, J.F., and Cohn, T.A., 2007, Scientific and practical considerations related to revising Bulletin 17B; The case for improved treatment of historical information and low outliers, in Kabbes, K.C., ed., Proceedings of the World Environmental and Water Resources Congress 2007, May 15–19, 2007: Tampa, Fla., American Society of Civil Engineers Environmental and Water Resources Institute.
- England, J.F., and Cohn, T.A., 2008, Bulletin 17B flood frequency revisions; Practical software and test comparison results, in Babcock, R.W., Jr., and Walton, Raymond, eds., Proceedings of the World Environmental and Water Resources Congress 2008 Ahupua'a, May 12–16, 2008: Honolulu, Hawaii, American Society of Civil Engineers Environmental and Water Resources Institute, p. 1–11.
- England, J.F., Godaire, J.E., Klinger, R.E., Bauer, T.R., and Julien, P.Y., 2010, Paleohydrologic bounds and extreme flood frequency of the Upper Arkansas River, Colorado, USA: Geomorphology, v. 124, no. 1, p. 1–16, accessed October 30, 2017, at <https://dx.doi.org/10.1016/j.geomorph.2010.07.021>.
- England, J.F., Jarrett, R.D., and Salas, J.D., 2003a, Data-based comparisons of moments estimators using historical and paleoflood data: Journal of Hydrology, v. 278, no. 1, p. 172–196, accessed October 30, 2017, at [https://doi.org/10.1016/S0022-1694\(03\)00141-0](https://doi.org/10.1016/S0022-1694(03)00141-0).

- England, J.F., Klawon, J.E., Klinger, R.E., and Bauer, T.R., 2006, Flood hazard analysis for Pueblo dam, Colorado, final report: U.S. Department of Interior, Bureau of Reclamation, Denver, Colo., 160 p.
- England, J.F., Salas, J.D., and Jarrett, R.D., 2003b, Comparisons of two moments-based estimators that utilize historical and paleoflood data for the log Pearson type III distribution: Water Resources Research, v. 39, no. 9, p. 1243, accessed October 30, 2017, at <https://dx.doi.org/10.1029/2002WR001791>.
- Feaster, T.D., Gotvald, A.J., and Weaver, J.C., 2009, Magnitude and frequency of rural floods in the Southeastern United States, 2006: v. 3, South Carolina: U.S. Geological Survey Scientific Investigations Report 2009–5156, 226 p., accessed October 30, 2017, at <https://pubs.usgs.gov/sir/2009/5156/>.
- Federal Emergency Management Agency, 2009, Guidelines and specifications for flood hazard mapping partners. Appendix C; Guidance for riverine flooding analyses and mapping: Federal Emergency Management Agency, 77 p.
- Follansbee, R., and Jones, E.E., 1922, The Arkansas River floods of June 3–5, 1921: U.S. Geological Survey Water-Supply Paper 487, 44 p., accessed October 30, 2017, at <https://pubs.er.usgs.gov/publication/wsp487>.
- Follansbee, R., and Sawyer, L.R., 1948, Floods in Colorado: U.S. Geological Survey Water-Supply Paper 997, 151 p., accessed October 30, 2017, at <https://pubs.er.usgs.gov/publication/wsp997>.
- Gerard, R., and Karpuk, E.W., 1979, Probability analysis of historical flood data: Journal of Hydraulic Engineering, v. 105, no. HY9, p. 1153–1165.
- Godaire, J.E., and Bauer, T.R., 2012, Paleoflood study, North Fork Red River basin near Altus dam, Oklahoma: U.S. Department of Interior, Bureau of Reclamation, Denver, Colo., 55 p.
- Godaire, J.E., and Bauer, T.R., 2013, Paleoflood study on the Rio Chama near El Vado dam, New Mexico: U.S. Department of Interior, Bureau of Reclamation, Denver, Colo., 58 p.
- Godaire, J.E., Bauer, T.R., and Klinger, R.E., 2012, Paleoflood study, San Joaquin River near Friant dam, California: U.S. Department of Interior, Bureau of Reclamation, Denver, Colo., 60 p.
- Gotvald, A.J., Barth, N.A., Veilleux, A.G., and Parrett, Charles, 2012, Methods for determining magnitude and frequency of floods in California, based on data through water year 2006: U.S. Geological Survey Scientific Investigations Report 2012–5113, 38 p., accessed October 30, 2017, at <https://pubs.usgs.gov/sir/2012/5113/>.
- Gotvald, A.J., Feaster, T.D., and Weaver, J.C., 2009, Magnitude and frequency of rural floods in the Southeastern United States, 2006; v. 1, Georgia: U.S. Geological Survey Scientific Investigations Report 2009–5043, 120 p., accessed October 30, 2017, at <https://pubs.usgs.gov/sir/2009/5043/>.
- Griffis, V.W., 2008, EMA with historical information, low outliers, and regional skew, in Babcock, R.W., Jr., and Walton, Raymond, eds., Proceedings of the World Environmental and Water Resources Congress 2008 Ahupua'a, May 12–16, 2008: Honolulu, Hawaii, American Society of Civil Engineers Environmental and Water Resources Institute.
- Griffis, V.W., and Stedinger, J.R., 2007a, Evolution of flood frequency analysis with Bulletin 17: Journal of Hydrologic Engineering, v. 12, no. 3, p. 283–297.
- Griffis, V.W., and Stedinger, J.R., 2007b, Log-Pearson type 3 distribution and its application in flood frequency analysis. I: Distribution characteristics: Journal of Hydrologic Engineering, v. 12, no. 5, p. 482–491.
- Griffis, V.W., and Stedinger, J.R., 2007c, The use of GLS regression in regional hydrologic analyses: Journal of Hydrology, v. 344, no. 1–2, p. 82–95.
- Griffis, V.W., and Stedinger, J.R., 2007d, Log-Pearson type 3 distribution and its application in flood frequency analysis. II: Parameter estimation methods: Journal of Hydrologic Engineering, v. 12, no. 5, p. 492–500, accessed August 30, 2017, at [https://doi.org/10.1061/\(ASCE\)1084-0699\(2007\)12:5\(492\)](https://doi.org/10.1061/(ASCE)1084-0699(2007)12:5(492).).

42 Guidelines for Determining Flood Flow Frequency—Bulletin 17C

- Griffis, V.W., and Stedinger, J.R., 2009, Log-Pearson type 3 distribution and its application in flood frequency analysis. III: Sample skew and weighted skew estimators: *Journal of Hydrologic Engineering*, v. 14, no. 2, p. 121–130, accessed August 30, 2017, at [https://doi.org/10.1061/\(ASCE\)1084-0699\(2009\)14:2\(121\)](https://doi.org/10.1061/(ASCE)1084-0699(2009)14:2(121)).
- Griffis, V.W., Stedinger, J.R., and Cohn, T.A., 2004, Log Pearson type 3 quantile estimators with regional skew information and low outlier adjustments: *Water Resources Research*, v. 40, no. 7.
- Grover, N.C., 1937, The floods of March 1936, Part 3, Potomac, James, and upper Ohio Rivers: U.S. Geological Survey Water-Supply Paper 800, 351 p., accessed October 30, 2017, at <https://pubs.er.usgs.gov/publication/wsp800>.
- Grover, N.C., and Harrington, A.W., 1943, Stream flow: New York, John Wiley and Sons, 363 p.
- Grubbs, F.E., and Beck, G., 1972, Extension of sample sizes and percentage points for significance tests of outlying observations: *Technometrics*, v. 14, no. 4, p. 847–854.
- Gruber, A.M., Reis, D.S., and Stedinger, J.R., 2007, Models of regional skew based on Bayesian GLS regression, in Kabbes, K.C., ed., *Proceedings of the World Environmental and Water Resources Congress 2007*, May 15–19, 2007: Tampa, Fla., American Society of Civil Engineers Environmental and Water Resources Institute.
- Gruber, A.M., and Stedinger, J.R., 2008, Models of LP3 regional skew, data selection, and Bayesian GLS regression, in Babcock, R.W., Jr., and Walton, Raymond, eds., *Proceedings of the World Environmental and Water Resources Congress 2008 Ahupua'a*, May 12–16, 2008: Honolulu, Hawaii, American Society of Civil Engineers Environmental and Water Resources Institute.
- Harden, T.M., O'Connor, J.E., Driscoll, D.G., and Stamm, J.F., 2011, Flood-frequency analyses from paleoflood investigations for Spring, Rapid, Boxelder, and Elk Creeks, Black Hills, Western South Dakota: U.S. Geological Survey Scientific Investigations Report 2011–5131, 136 p., accessed October 30, 2017, at <https://pubs.usgs.gov/sir/2011/5131/>.
- Hazen, Allen, 1930, Flood flows: New York, John Wiley and Sons, 199 p.
- Helsel, D.R., and Hirsch, R.M., 2002, Statistical methods in water resources: U.S. Geological Survey Techniques of Water-Resources Investigations, book 4, chap. A3, 522 p., accessed October 30, 2017, at <https://pubs.usgs.gov/twri/twri4a3/>.
- Hirsch, R.M., 1982, A comparison of four streamflow record extension techniques: *Water Resources Research*, v. 18, no. 4, p. 1081–1088.
- Hirsch, R.M., 1987, Probability plotting position formulas for flood records with historical information: *Journal of Hydrology*, v. 96, nos. 1–4, p. 185–199.
- Hirsch, R.M., and De Cicco, L.A., 2015, User guide to exploration and graphics for RivEr trends (EGRET) and dataRetrieval; R packages for hydrologic data: U.S. Geological Survey Techniques and Methods, book 4, chap. A10, 93 p., accessed October 30, 2017, at <https://dx.doi.org/10.3133/tm4A10>.
- Hirsch, R.M., Helsel, D.R., Cohn, T.A., and Gilroy, E.J., 1993, Statistical analysis of hydrologic data, in Maidment, D.R., ed., *Handbook of Hydrology*, McGraw Hill, Inc., p. 17.1–17.55.
- Hirsch, R.M., and Stedinger, J.R., 1987, Plotting positions for historical floods and their precision: *Water Resources Research*, v. 23, no. 4, p. 715–727.
- Hirschboeck, K.K., 1987a, Catastrophic flooding and atmospheric circulation anomalies, in Mayer, L., and Nash, D., eds., *Catastrophic flooding*: Boston, Allen and Unwin, p. 23–56.
- Hirschboeck, K.K., 1987b, Hydroclimatically-defined mixed distributions in partial duration flood series, in Singh, V.P., ed., *Hydrologic frequency modeling*: Louisiana State University, Baton Rouge, D. Reidel Publishing Company, p. 199–212.
- Hirschboeck, K.K., 1991, Climate and floods, in Paulson, R.W., Chase, E.B., Roberts, R.S., and Moody, D.W., eds., *National water summary 1988–89—Hydrologic events and floods and droughts: U.S. Geological Survey Water-Supply Paper 2375*, p. 67–88.

- Hosking, J. R.M., and Wallis, J.R., 1997, Regional frequency analysis—An approach based on L-Moments: Cambridge University Press, 224 p.
- House, P.K., and Baker, V.R., 2001, Paleohydrology of flash floods in small desert watersheds in western Arizona: Water Resources Research, v. 37, no. 6, p. 1825–1839.
- House, P.K., Pearthree, P.A., and Klawon, J.E., 2002b, Historical flood and paleoflood chronology of the lower Verde River, Arizona: Stratigraphic evidence and related uncertainties, in House, P.K., Webb, R.H., Baker, V.R., and Levish, D.R., eds., Water Science and Application Series, v. 5, Ancient floods, modern hazards: American Geophysical Union, p. 267–293, accessed August 30, 2017, at <https://doi.org/10.1029/WS005p0267>.
- House, P.K., Webb, R.H., Baker, V.R., and Levish, D.R., 2002a, Ancient floods, modern hazards, v. 5: American Geophysical Union, 385 p., accessed August 30, 2017, at <https://doi.org/10.1029/WS005>.
- Hupp, C.R., 1987, Botanical evidence of floods and paleoflood history, in Singh, V.P., ed., Regional flood frequency analysis: D. Reidel Publishing Company, p. 355–369.
- Hupp, C.R., 1988, Plant ecological aspects of flood geomorphology and paleoflood history, in Baker, V.R., Kochel, R.C., and Patton, P.C., eds., Flood geomorphology: John Wiley and Sons, p. 335–356.
- Hupp, C.R., and Osterkamp, W.R., 1996, Riparian vegetation and fluvial geomorphic processes: Geomorphology, v. 14, no. 4, p. 277–295.
- Hydrologic Frequency Analysis Work Group, 2006, Flood frequency research needs: Memorandum to Subcommittee on Hydrology, accessed August 30, 2017, at https://acwi.gov/hydrology/Frequency_minutes/HFAWG_for_revising_Bulletin17B_4.pdf.
- Hydrologic Frequency Analysis Work Group, 2013, Recommendations memorandum to the Subcommittee on Hydrology: Hydrologic Frequency Analysis Work Group meeting minutes, accessed August 30, 2017, at https://acwi.gov/hydrology/Frequency/minutes/HFAWG_mins_june12-13_2013_meeting_revised_071213.pdf.
- Interagency Committee on Water Data, 1982, Guidelines for determining flood flow frequency, Bulletin 17B: Interagency Committee on Water Data, Hydrology Subcommittee, Technical Report.
- Jain, Shaleen, and Lall, Upmanu, 2001, Floods in a changing climate; Does the past represent the future?: Water Resources Research, v. 37, no. 12, p. 3193–3205, accessed August 30, 2017, at <https://doi.org/10.1029/2001WR000495>.
- Jarrett, R.D., 1987, Errors in slope-area computations of peak discharges in mountain streams: Journal of Hydrology, v. 96, nos. 1–4, p. 53–67, accessed August 30, 2017, at [https://doi.org/10.1016/0022-1694\(87\)90143-0](https://doi.org/10.1016/0022-1694(87)90143-0).
- Jarrett, R.D., 1991, Paleohydrology and its value in analyzing floods and droughts, in Paulson, R.W., Chase, E.B., Roberts, R.S., and Moody, D.W., eds., National water summary 1988–89—Hydrologic events and floods and droughts: U.S. Geological Survey Water-Supply Paper 2375, p. 105–116.
- Jarrett, R.D., and Costa, J.E., 1988, Evaluation of the flood hydrology in the Colorado Front Range using precipitation, streamflow, and paleoflood data for the Big Thompson River Basin: U.S. Geological Survey Water-Resources Investigations Report 87-4117, 37 p., accessed October 30, 2017, at <https://pubs.er.usgs.gov/publication/wri874117>.
- Jarrett, R.D., and England, J.F., 2002, Reliability of paleostage indicators for paleoflood studies, in House, P.K., Webb, R.H., Baker, V.R., and Levish, D.R., eds., Water Science and Application Series, v. 5, Ancient floods, modern hazards: American Geophysical Union, p. 91–109, accessed August 30, 2017, at <https://doi.org/10.1029/WS005p0091>.
- Jarrett, R.D., and Malde, H.E., 1987, Paleodischarge of the late Pleistocene Bonneville flood, Snake River, Idaho, computed from new evidence: Geological Society of America Bulletin, v. 99, p. 127–134.
- Jarrett, R.D., and Tomlinson, E.M., 2000, Regional interdisciplinary paleoflood approach to assess extreme flood potential: Water Resources Research, v. 36, no. 10, p. 2957–2984.

44 Guidelines for Determining Flood Flow Frequency—Bulletin 17C

- Kiang, J.E., Olsen, J.R., and Waskom, R.M., 2011, Introduction to the featured collection on “nonstationarity, hydrologic frequency analysis, and water management”: Journal of the American Water Resources Association, v. 47, no. 3, p. 433–435, accessed August 30, 2017, at <https://doi.org/10.1111/j.1752-1688.2011.00551.x>.
- Kirby, W., 1972, Computer-oriented Wilson-Hilferty transformation that preserves the first three moments and the lower bound of the Pearson type 3 distribution: Water Resources Research, v. 8, no. 5, p. 1251–1254, accessed August 30, 2017, at <https://doi.org/10.1029/WR008i005p01251>.
- Kirby, W.H., 1987, Linear error analysis of slope-area discharge determinations: Journal of Hydrology, v. 96, nos. 1–4, p. 125–138, accessed August 30, 2017, at [https://doi.org/10.1016/0022-1694\(87\)90148-X](https://doi.org/10.1016/0022-1694(87)90148-X).
- Kite, G.W., 1988, Frequency and risk analyses in hydrology: Littleton, Colorado, Water Resources Publications, 258 p.
- Kite, J.S., Gebhardt, T.W., and Springer, G.S., 2002, Slackwater deposits as paleostage indicators in canyon reaches of the Central Appalachians; reevaluation after the 1996 Cheat River flood, in House, P.K., Webb, R.H., Baker, V.R., and Levish, D.R., eds., Water Science and Application Series, v. 5, Ancient floods, modern hazards: American Geophysical Union, p. 257–266, accessed August 30, 2017, at <https://doi.org/10.1029/WS005p0257>.
- Kjeldsen, T.R., Lamb, Rob, and Blazkova, S.D., 2014, Uncertainty in flood frequency analysis, in Beven, Keith, and Hall, Jim, eds., Applied uncertainty analysis for flood risk management: Imperial College Press, p. 153–197, accessed August 30, 2017, at https://doi.org/10.1142/9781848162716_0008.
- Klemeš, V., 1986, Dilettantism in hydrology; Transition or destiny?: Water Resources Research, v. 22, no. 9, p. 177S–188S.
- Klemeš, V., 1987, Hydrological and engineering relevance of flood frequency analysis, in Singh, V.P., ed., Hydrologic frequency modeling: Louisiana State University, Baton Rouge, D. Reidel Publishing Company, p. 1–18.
- Klemeš, V., 2000, Tall tales about tails of hydrological distributions. I: Journal of Hydrologic Engineering, v. 5, no. 3, p. 227–231, accessed August 30, 2017, at [https://doi.org/10.1061/\(ASCE\)1084-0699\(2000\)5:3\(227\)](https://doi.org/10.1061/(ASCE)1084-0699(2000)5:3(227)).
- Klinger, R.E., and Bauer, T.R., 2010, Paleoflood study on the South Fork of the Boise River for Anderson Ranch dam, Idaho: U.S. Department of Interior, Bureau of Reclamation, Denver, Colo., 30 p.
- Klinger, R.E., and Godaire, J.E., 2002, Development of a paleoflood database for rivers in the western U.S.: U.S. Department of Interior, Bureau of Reclamation, Denver, Colo., 38 p.
- Kochel, R.C., Baker, V.R., and Patton, P.C., 1982, Paleo hydrology of southwestern Texas: Water Resources Research, v. 18, no. 4, p. 1165–1183.
- Koenig, T.A., Bruce, J.L., O'Connor, J.E., McGee, B.D., Holmes, R.R., Hollins, Ryan, Forbes, B.T., Kohn, M.S., Schellekens, M.F., Martin, Z.W., and Peppler, M.C., 2016, Identifying and preserving high-water mark data: U.S. Geological Survey Techniques and Methods, book 3, chap. A24, 47 p., accessed October 30, 2017, at <https://dx.doi.org/10.3133/tm3A24>.
- Kohn, M.S., Jarrett, R.D., Krammes, G.S., and Mommandi, Amanullah, 2013, Web-based flood database for Colorado, water years 1867 through 2011: U.S. Geological Survey Open-File Report 2012-1225, 26 p., accessed October 30, 2017, at <https://pubs.er.usgs.gov/publication/ofr20121225>.
- Konrad, C.P., 2003, Effects of urban development on floods: U.S. Geological Survey Fact Sheet 076-03, 4 p., accessed October 30, 2017, at <https://pubs.usgs.gov/fs/fs07603/>.
- Koutsoyiannis, Demetris, 2011, Hurst-Kolmogorov dynamics and uncertainty: Journal of the American Water Resources Association, v. 47, no. 3, p. 481–495, accessed August 30, 2017, at <https://doi.org/10.1111/j.1752-1688.2011.00543.x>.
- Kubik, H.E., 1990, Computation of regulated frequency curves by application of the total probability theorem: U.S. Army Corps of Engineers, Hydrologic Engineering Center, 17 p.

- Kuczera, G., 1982, Robust flood frequency models: Water Resources Research, v. 18, no. 2, p. 315–324, accessed August 30, 2017, at <https://doi.org/10.1029/WR018i002p00315>.
- Kuczera, G., 1996, Correlated rating curve error in flood frequency inference: Water Resources Research, v. 32, no. 7, p. 2119–2127.
- Kuichling, E., 1917, Discussion of flood flows by W.E. Fuller: Transactions, American Society of Civil Engineers, v. 77, no. 1293, p. 643–663.
- Lamontagne, J.R., Stedinger, J.R., Berenbrock, Charles, Veilleux, A.G., Ferris, J.C., and Knifong, D.L., 2012, Development of regional skews for selected flood durations for the Central Valley Region, California, based on data through water year 2008: U.S. Geological Survey Scientific Investigations Report 2012–5130, 60 p., accessed October 30, 2017, at <https://pubs.usgs.gov/sir/2012/5130/>.
- Lamontagne, J.R., Stedinger, J.R., Cohn, T.A., and Barth, N.A., 2013, Robust national flood frequency guidelines; what is an outlier?: in Showcasing the future, American Society of Civil Engineers, p. 2454–2466, accessed August 30, 2017, at <https://doi.org/10.1061/9780784412947.242>.
- Lamontagne, J.R., Stedinger, J.R., Yu, Xin, Wheaton, C.A., and Xu, Ziyao, 2016, Robust flood frequency analysis; Performance of EMA with multiple Grubbs-Beck outlier tests: Water Resources Research, v. 52, no. 4, p. 3068–3084, accessed August 30, 2017, at <https://doi.org/10.1002/2015WR018093>.
- Lane, W.L., 1987, Paleohydrologic data and flood frequency estimation, in Singh, V.P., ed., Application of frequency and risk in water resources: D. Reidel Publishing Company, p. 287–298.
- Lane, W.L., 1995, Method of moments approach to historical data: Bulletin 17B Working Group, Hydrology Subcommittee, Interagency Advisory Committee on Water Data.
- Lane, W.L., and Cohn, T.A., 1996, Expected moments algorithms for flood frequency analysis, in North American Water and Environment Congress & Destructive Water: American Society of Civil Engineers, p. 2185–2190.
- Lang, M., Ouarda, T.B.M.J., and Bobée, B., 1999, Towards operational guidelines for over-threshold modeling: Journal of Hydrology, v. 225, nos. 3–4, p. 103–117, accessed August 30, 2017, at [https://doi.org/10.1016/S0022-1694\(99\)00167-5](https://doi.org/10.1016/S0022-1694(99)00167-5).
- Langbein, W.B., 1949, Annual floods and the partial-duration flood series: Transactions of the American Geophysical Union, v. 30, no. 6, p. 879–881.
- Langbein, W.B., and Iseri, K.T., 1960, General introduction and hydrologic definitions. Manual of hydrology: Part 1. General surface water techniques: U.S. Geological Survey Water-Supply Paper 1541–A, 29 p., accessed October 30, 2017, at <https://pubs.er.usgs.gov/publication/wsp1541A>.
- Leese, M.N., 1973, Use of censored data in the estimation of Gumbel distribution parameters for annual maximum flood series: Water Resources Research, v. 9, no. 6, p. 1534–1542.
- Levish, D.R., 2002, Non-exceedance information for flood hazard assessment, in House, P.K., Webb, R.H., Baker, V.R., and Levish, D.R., eds., Water Science and Application Series, v. 5, Ancient floods, modern hazards: American Geophysical Union, p. 91–109, accessed August 30, 2017, at <https://doi.org/10.1029/WS005p0175>.
- Levish, D.R., England, J.F., Klawon, J.E., and O'Connell, D.R.H., 2003, Flood hazard analysis for Seminoe and Glendo dams, Kendrick and North Platte projects, Wyoming, final report: U.S. Department of Interior, Bureau of Reclamation, Denver, Colo., 126 p.
- Lichty, R.W., and Liscum, Fred, 1978, A rainfall-runoff modeling procedure for improving estimates of T-year (annual) floods for small drainage basins: U.S. Geological Survey Water-Resources Investigations Report 78-7, 44 p., accessed October 30, 2017, at <https://pubs.er.usgs.gov/publication/wri787>.
- Lins, H.F., and Cohn, T.A., 2011, Stationarity; Wanted dead or alive?: Journal of the American Water Resources Association, v. 47, no. 3, p. 475–480, accessed August 30, 2017, at <https://doi.org/10.1111/j.1752-1688.2011.00542.x>.

46 Guidelines for Determining Flood Flow Frequency—Bulletin 17C

- Lombard, F., 1987, Rank tests for changepoint problems: *Biometrika*, v. 74, no. 3, p. 615–624, accessed August 30, 2017, at <https://doi.org/10.1093/biomet/74.3.615>.
- Maddox, R.A., Canova, F., and Hoxit, L.R., 1980, Meteorological characteristics of flash flood events over the Western United States: *Monthly Weather Review*, v. 108, no. 11, p. 1866–1877.
- Madsen, Henrik, Rasmussen, P.F., and Rosbjerg, Dan, 1997, Comparison of annual maximum series and partial duration series methods for modeling extreme hydrologic events: 1. At-site modeling: *Water Resources Research*, v. 33, no. 4, p. 747–757, accessed August 30, 2017, at <https://doi.org/10.1029/96WR03848>.
- Mallakpour, Iman, and Villarini, Gabriele, 2016, A simulation study to examine the sensitivity of the Pettitt test to detect abrupt changes in mean: *Hydrological Sciences Journal*, v. 61, no. 2, p. 245–254, accessed August 30, 2017, at <https://doi.org/10.1080/02626667.2015.1008482>.
- Mastin, M.C., 2007, Re-evaluation of the 1921 peak discharge at Skagit River near Concrete, Washington: U.S. Geological Survey Scientific Investigations Report 2007–5159, 12 p., accessed October 30, 2017, at <https://pubs.usgs.gov/sir/2007/5159/>.
- Matalas, N.C., and Jacobs, B., 1964, A correlation procedure for augmenting hydrologic data: U.S. Geological Survey Professional Paper 434–E, 7 p., accessed October 30, 2017, at <https://pubs.er.usgs.gov/publication/pp434E>.
- Matthai, H.F., 1969, Floods of June 1965 in South Platte River basin, Colorado: U.S. Geological Survey Water-Supply Paper 1850–B, 64 p., accessed October 30, 2017, at <https://pubs.er.usgs.gov/publication/wsp1850B>.
- May, J.E., Gorman, J.G., Goodrich, R.D., Bobier, M.W., and Miller, V.E., 1996, Water resources data, Iowa, water year 1995: U.S. Geological Survey Water-Data Report IA–95–1, 387 p., accessed October 30, 2017, at <https://pubs.usgs.gov/wdr/1995/ia-95-1/report.pdf>.
- McCabe, G.J., and Wolock, D.M., 2002, A step increase in streamflow in the conterminous United States: *Geophysical Research Letters*, v. 29, no. 24, p. 38–1–38–4, accessed August 30, 2017, at <https://doi.org/10.1029/2002GL015999>.
- McCord, V. A.S., 1990, Augmenting flood frequency estimates using flood-scarred trees: Ph.D. dissertation, University of Arizona, 182 p.
- McCuen, R.H., 2003, Modeling hydrologic change; Statistical methods: Boca Raton, Fla., Lewis Publishers, 433 p.
- McCuen, R.H., 2004, Hydrologic analysis and design: Upper Saddle River, NJ, Prentice Hall, 888 p.
- McCuen, R.H., and Knight, Z., 2006, Fuzzy analysis of slope-area discharge estimates: *Journal of Irrigation and Drainage Engineering*, v. 132, no. 1, p. 64–69, accessed August 30, 2017, at [https://doi.org/10.1061/\(ASCE\)0733-9437\(2006\)132:1\(64\)](https://doi.org/10.1061/(ASCE)0733-9437(2006)132:1(64)).
- McCuen, R.H., and Smith, Eric, 2008, Origin of flood skew: *Journal of Hydrologic Engineering*, v. 13, no. 9, p. 771–775, accessed August 30, 2017, at [https://doi.org/10.1061/\(ASCE\)1084-0699\(2008\)13:9\(771\)](https://doi.org/10.1061/(ASCE)1084-0699(2008)13:9(771)).
- McGlashan, H.D., and Briggs, R.C., 1939, Floods of December 1937 in Northern California: U.S. Geological Survey Water-Supply Paper 843, 497 p., accessed October 30, 2017, at <https://pubs.er.usgs.gov/publication/wsp843>.
- Merz, R., and Blöschl, G., 2003, A process typology of regional floods: *Water Resources Research*, v. 39, no. 12, p. SWC 5–1 through SWC 5–20, accessed August 30, 2017, at <https://doi.org/10.1029/2002WR001952>.
- Merz, R., and Blöschl, G., 2008a, Flood frequency hydrology: 1. Temporal, spatial, and causal expansion of information: *Water Resources Research*, v. 44, no. 8, accessed August 30, 2017, at <https://doi.org/10.1029/2007WR006744>.
- Merz, R., and Blöschl, G., 2008b, Flood frequency hydrology: 2. Combining data evidence: *Water Resources Research*, v. 44, no. 8, accessed August 30, 2017, at <https://doi.org/10.1029/2007WR006745>.
- MGS Engineering Consultants, 2009, General storm stochastic event flood model (SEFM); Technical

- support manual: Bureau of Reclamation, Denver, Colo.
- Moglen, G.E., 2009, Hydrology and impervious areas: *Journal of Hydrologic Engineering*, v. 14, no. 4, p. 303–304, accessed August 30, 2017, at [https://doi.org/10.1061/\(ASCE\)1084-0699\(2009\)14:4\(303\)](https://doi.org/10.1061/(ASCE)1084-0699(2009)14:4(303)).
- Moglen, G.E., and Beighley, R.E., 2002, Spatially explicit hydrologic modeling of land use change: *Journal of the American Water Resources Association*, v. 38, no. 1, p. 241–252, accessed August 30, 2017, at <https://doi.org/10.1111/j.1752-1688.2002.tb01548.x>.
- Moglen, G.E., and Shivers, D.E., 2006, Methods for adjusting U.S. Geological Survey rural regression peak discharges in an urban setting: U.S. Geological Survey Scientific Investigations Report 2006–5270, 55 p., accessed October 30, 2017, at <https://pubs.usgs.gov/sir/2006/5270/>.
- Moran, M.A., 1974, On estimators obtained from a sample augmented by multiple regression: *Water Resources Research*, v. 10, no. 1, p. 81–85.
- Moss, M.E., and Thomas, W.O., 1982, Discussion of “WRC standard flood frequency guidelines” by D.R. Jackson: *Journal of Water Resources Planning and Management*, v. 108, no. 1, p. 166–168.
- Munn, J., and Savage, J.L., 1922, The Flood of June 1921 in the Arkansas River, at Pueblo, Colorado: *Transactions, American Society of Civil Engineers*, v. 85, no. 1480, p. 1–65.
- Murphy, P., 2001, Evaluation of mixed-population flood-frequency analysis: *Journal of Hydrologic Engineering*, v. 6, no. 1, p. 62–70, accessed August 30, 2017, at [https://doi.org/10.1061/\(ASCE\)1084-0699\(2001\)6:1\(62\).](https://doi.org/10.1061/(ASCE)1084-0699(2001)6:1(62).)
- Nathan, R.J., and Weinmann, E., 2016, Estimation of very rare to extreme floods: Engineers Australia, accessed August 30, 2017, at <https://arr.ga.gov.au/>.
- National Research Council, 1988, Estimating probabilities of extreme floods—Methods and recommended research: National Academy Press, 141 p.
- National Research Council, 1995, Flood risk management and the American River basin; An evaluation: National Academy Press, 256 p.
- National Research Council, 1999, Improving American River flood frequency analyses: National Academy Press, 123 p.
- National Research Council, 2000, Risk analysis and uncertainty in flood damage reduction studies: National Academy Press, 202 p.
- Nayak, M.A., and Villarini, Gabriele, 2016, Evaluation of the capability of the Lombard test in detecting abrupt changes in variance: *Journal of Hydrology*, v. 534, p. 451–465, accessed August 30, 2017, at <https://doi.org/10.1016/j.jhydrol.2016.01.016>.
- O'Connor, J.E., Atwater, B.F., Cohn, T.A., Cronin, T.M., Keith, M.K., Smith, C.G., and Mason, R.R., 2014, Assessing inundation hazards to nuclear powerplant sites using geologically extended histories of riverine floods, tsunamis, and storm surges: U.S. Geological Survey Scientific Investigations Report 2014–5207, 65 p., accessed October 30, 2017, at <https://pubs.usgs.gov/sir/2014/5207/>.
- O'Connor, J.E., and Costa, J.E., 2004, Spatial distribution of the largest rainfall-runoff floods from basins between 2.6 and 26,000 km² in the United States and Puerto Rico: *Water Resources Research*, v. 40, no. 1, accessed August 30, 2017, at <https://doi.org/10.1029/2003WR002247>.
- O'Connor, J.E., Webb, R.H., and Baker, V.R., 1986, Paleohydrology of pool-and-riffle pattern development; Boulder Creek, Utah: Geological Society of America Bulletin, v. 97, no. 4, p. 410–420, accessed August 30, 2017, at [https://doi.org/10.1130/0016-7606\(1986\)97<410:POPPDB>2.0.CO;2](https://doi.org/10.1130/0016-7606(1986)97<410:POPPDB>2.0.CO;2).
- Olsen, J.R., Kiang, Julie, and Waskom, Reagan, 2010, Workshop on nonstationarity, hydrologic frequency analysis, and water management: Colorado Water Institute, Colorado State University, Fort Collins, Colo., 304 p.
- Olson, S.A., and Veilleux, A.G., 2014, Estimation of flood discharges at selected annual exceedance probabilities for unregulated, rural streams in Vermont, *with a section on Vermont regional skew regression*: U.S. Geological Survey Scientific

48 Guidelines for Determining Flood Flow Frequency—Bulletin 17C

- Investigations Report 2014–5078, 27 p., accessed October 30, 2017, at <https://dx.doi.org/10.3133/sir20145078>.
- Osterkamp, W.R., and Costa, J.E., 1987, Changes accompanying an extraordinary flood on a sand-bed stream, *in* Mayer, L., and Nash, D., eds., *Catastrophic flooding*: Boston, Allen and Unwin, p. 201–224.
- Over, T.M., Saito, R.J., and Soong, D.T., 2016, Adjusting annual maximum peak discharges at selected stations in northeastern Illinois for changes in land-use conditions: U.S. Geological Survey Scientific Investigations Report 2016–5049, 33 p., accessed October 30, 2017, at <https://dx.doi.org/10.3133/sir20165049>.
- Paretti, N.V., Kennedy, J.R., and Cohn, T.A., 2014a, Evaluation of the expected moments algorithm and a multiple low-outlier test for flood frequency analysis at streamgaging stations in Arizona: U.S. Geological Survey Scientific Investigations Report 2014–5026, 61 p., accessed October 30, 2017, at <https://pubs.er.usgs.gov/publication/sir20145026>.
- Paretti, N.V., Kennedy, J.R., Turney, L.A., and Veilleux, A.G., 2014b, Methods for estimating magnitude and frequency of floods in Arizona, developed with unregulated and rural peak-flow data through water year 2010: U.S. Geological Survey Scientific Investigations Report 2014–5211, 61 p., accessed October 30, 2017, at <https://dx.doi.org/10.3133/sir20145211>.
- Parrett, Charles, Veilleux, Andrea, Stedinger, J.R., Barth, N.A., Knifong, D.L., and Ferris, J.C., 2011, Regional skew for California, and flood frequency for selected sites in the Sacramento–San Joaquin River basin, based on data through water year 2006: U.S. Geological Survey Scientific Investigations Report 2010–5260, 94 p., accessed October 30, 2017, at <https://pubs.usgs.gov/sir/2010/5260/>.
- Pettitt, A.N., 1979, A non-parametric approach to the change-point problem: *Journal of the Royal Statistical Society. Series C (Applied Statistics)*, v. 28, no. 2, p. 126–135, accessed August 30, 2017, at <https://www.jstor.org/stable/2346729>.
- Pilgrim, D.H., and Cordery, I., 1993, Flood runoff, *in* Maidment, D.R., ed., *Handbook of hydrology*: McGraw Hill, Inc., p. 9.1–9.72.
- Potter, K.W., and Walker, J.F., 1985, An empirical study of flood measurement error: *Water Resources Research*, v. 21, no. 3, p. 403–406.
- Prior, J.C., 1991, *Landforms of Iowa*: University of Iowa Press, 154 p.
- Quessy, J.-F., Favre, A.-C., Said, Meriem, and Champagne, Maryse, 2011, Statistical inference in Lombard's smooth-change model: *Environmetrics*, v. 22, no. 7, p. 882–893, accessed August 30, 2017, at <https://doi.org/10.1002/env.1108>.
- Quick, M.C., 1991, Reliability of flood discharge estimates: *Canadian Journal of Civil Engineering*, v. 18, p. 624–630.
- Rantz, S.E., and others, 1982a, Measurement and computation of streamflow; v. 1, *Measurement of stage and discharge*: U.S. Geological Survey Water-Supply Paper 2175, 284 p., accessed October 30, 2017, at <https://pubs.usgs.gov/wsp/wsp2175>.
- Rantz, S.E., and others, 1982b, *Measurement and computation of streamflow*; v. 2, *Computation of discharge*: U.S. Geological Survey Water-Supply Paper 2175, 631 p., <https://pubs.usgs.gov/wsp/wsp2175>.
- Redmond, K.T., Enzel, Yehouda, House, P.K., and Biondi, Franco, 2002, Climate variability and flood frequency at decadal to millennial time scales, *in* House, P.K., Webb, R.H., Baker, V.R., and Levish, D.R., eds., *Water Science and Application Series*, v. 5, *Ancient floods, modern hazards*: American Geophysical Union, p. 21–45, accessed August 30, 2017, at <https://doi.org/10.1029/WS005p0021>.
- Reed, Duncan, 1999, *Flood estimation handbook*, v. 1; overview: Institute of Hydrology, Wallingford, Oxfordshire, UK, 108 p.
- Reis, D.S., Stedinger, J.R., and Martins, E.S., 2005, Bayesian GLS regression with application to LP3 regional skew estimation: *Water Resources Research*, v. 41, p. 1–14.

- Ries, K.G., Guthrie, J.G., Rea, A.H., Steeves, P.A., and Stewart, D.W., 2008, StreamStats: A water resources web application: U.S. Geological Survey Fact Sheet 2008–3067, 6 p., accessed October 30, 2017, at <https://pubs.usgs.gov/fs/2008/3067/>.
- Rogger, M., Kohl, B., Pirkl, H., Viglione, A., Komma, J., Kirnbauer, R., Merz, R., and Blöschl, G., 2012, Runoff models and flood frequency statistics for design flood estimation in Austria—Do they tell a consistent story?: *Journal of Hydrology*, v. 456–457, p. 30–43, accessed August 30, 2017, at <https://doi.org/10.1016/j.jhydrol.2012.05.068>.
- Rosner, B., 1983, Percentage points for a generalized ESD many outlier procedure: *Technometrics*, v. 25, no. 2, p. 165–172.
- Russell, S.O., 1982, Flood probability estimation: *Journal of Hydraulic Engineering*, v. 108, no. HY1, p. 63–73.
- Salas, J.D., 1993, Analysis and modeling of hydrologic time series, in Maidment, D.R., ed., *Handbook of hydrology*: McGraw Hill, Inc., p. 19.1–19.72.
- Salas, J.D., and Boes, D.C., 1980, Shifting level modelling of hydrologic series: *Advances in Water Resources*, v. 3, no. 2, p. 59–63, accessed August 30, 2017, at [https://doi.org/10.1016/0309-1708\(80\)90028-7](https://doi.org/10.1016/0309-1708(80)90028-7).
- Salas, J.D., and Obeysekera, J., 2014, Revisiting the concepts of return period and risk for non-stationary hydrologic extreme events: *Journal of Hydrologic Engineering*, v. 19, no. 3, p. 554–568, accessed August 30, 2017, at [https://doi.org/10.1061/\(ASCE\)HE.1943-5584.0000820](https://doi.org/10.1061/(ASCE)HE.1943-5584.0000820).
- Salas, J.D., Wohl, E.E., and Jarrett, R.D., 1994, Determination of flood characteristics using systematic, historical and paleoflood data, in Rossi, G., Harmancioglu, N., and Yevjevich, Y., eds., *Coping with floods: The Netherlands*, Kluwer Academic Publishers, p. 111–134.
- Sanders, C.L., Kubik, H.E., Hoke, J.T., and Kirby, W.H., 1990, Flood frequency of the Savannah River at Augusta, Georgia: U.S. Geological Survey Water-Resources Investigations Report 90-4024, 87 p., accessed October 30, 2017, at <https://pubs.er.usgs.gov/publication/wri904024>.
- Sando, S.K., Driscoll, D.G., and Parrett, Charles, 2008, Peak-flow frequency estimates based on data through water year 2001 for selected streamflow-gaging stations in South Dakota: U.S. Geological Survey Scientific Investigations Report 2008–5104, 367 p., accessed October 30, 2017, at <https://pubs.usgs.gov/sir/2008/5104/>.
- Sauer, V.B., and Meyer, R.W., 1992, Determination of error in individual discharge measurements: U.S. Geological Survey Open-File Report 92–144, 21 p., accessed October 30, 2017, at <https://pubs.usgs.gov/of/1992/ofr92-144/>.
- Sauer, V.B., Thomas, W.O., Stricker, V.A., and Wilson, K.V., 1983, Flood characteristics of urban watersheds in the United States: U.S. Geological Survey Water-Supply Paper 2207, 63 p., accessed October 30, 2017, at <https://pubs.er.usgs.gov/publication/wsp2207>.
- Sauer, V.B., and Turnipseed, D.P., 2010, Stage measurement at gaging stations: U.S. Geological Survey Techniques and Methods, book 3, chap. A7, 45 p., <https://pubs.usgs.gov/tm/tm3-a7/>.
- Sigafoos, R.S., 1964, Botanical evidence of floods and flood-plain deposition: U.S. Geological Survey Professional Paper 485–A, 35 p., accessed October 30, 2017, at <https://pubs.er.usgs.gov/publication/pp485A>.
- Singh, V.P., 1995, Computer models of watershed hydrology: Highlands Ranch, Colo., Water Resources Publications, 1,130 p.
- Smith, J.A., Villarini, Gabriele, and Baeck, M.L., 2011, Mixture distributions and the hydroclimatology of extreme rainfall and flooding in the Eastern United States: *Journal of Hydrometeorology*, v. 12, p. 294–309, accessed August 30, 2017, at <https://doi.org/10.1175/2010JHM1242.1>.
- Southard, R.E., and Veilleux, A.G., 2014, Methods for estimating annual exceedance-probability discharges and largest recorded floods for unregulated streams in rural Missouri: U.S. Geological Survey Scientific Investigations Report 2014–5165, 39 p., accessed October 30, 2017, at <https://dx.doi.org/10.3133/sir20145165>.

50 Guidelines for Determining Flood Flow Frequency—Bulletin 17C

- Stedinger, J.R., and Cohn, T.A., 1986, Flood frequency analysis with historical and paleoflood information: *Water Resources Research*, v. 22, no. 5, p. 785–793.
- Stedinger, J.R., and Cohn, T.A., 1987, Historical flood-frequency data: Its value and use, *in* Singh, V.P., ed., *Regional flood frequency analysis*: D. Reidel Publishing Company, p. 273–286.
- Stedinger, J.R., and Griffis, V.W., 2008, Flood frequency analysis in the United States; Time to update: *Journal of Hydrologic Engineering*, v. 13, no. 4, p. 199–204.
- Stedinger, J.R., and Griffis, V.W., 2011, Getting from here to where? Flood frequency analysis and climate: *Journal of the American Water Resources Association*, v. 47, no. 3, p. 506–513, accessed August 30, 2017, at <https://doi.org/10.1111/j.1752-1688.2011.00545.x>.
- Stedinger, J.R., Surani, R., and Therivel, R., 1988, Max user's guide; A program for flood frequency analysis using systematic-record, historical, botanical, physical paleohydrologic and regional hydrologic information using maximum likelihood techniques: Cornell University, 111 p.
- Stedinger, J.R., Vogel, R.M., and Foufoula-Georgiou, Efi, 1993, Frequency analysis of extreme events, *in* Maidment, D.R., ed., *Handbook of hydrology*: McGraw Hill, Inc., p. 18.1–18.66.
- Stewart, J.E., and Bodhaine, G.L., 1961, Floods in the Skagit River Basin, Washington: U.S. Geological Survey Water-Supply Paper 1527, 66 p., accessed October 30, 2017, at <https://pubs.er.usgs.gov/publication/wsp1527>.
- Sutley, D.E., Klinger, R.E., Bauer, T.R., and Godaire, J.E., 2008, Trinity dam detailed hydrologic hazard analysis using the Stochastic Event Flood Model: U.S. Department of Interior, Bureau of Reclamation, Denver, Colo., 84 p.
- Suttie, R.H., 1928, Report on the water resources of Connecticut: Hartford, Conn., Connecticut Geological and Natural History Survey, 168 p.
- Sveinsson, O. G.B., Salas, J.D., Boes, D.C., and Pielke Sr., R.A., 2003, Modeling the dynamics of long-term variability of hydroclimatic processes: *Journal of Hydrometeorology*, v. 4, p. 489–505, accessed August 30, 2017, at [https://doi.org/10.1175/1525-7541\(2003\)004<0489:MTDOLV>2.0.CO;2](https://doi.org/10.1175/1525-7541(2003)004<0489:MTDOLV>2.0.CO;2).
- Swain, R.E., England Jr., J.F., Bullard, K.L., and Raff, D.A., 2006, Guidelines for evaluating hydrologic hazards: U.S. Bureau of Reclamation, Denver, Colo., 83 p.
- Tasker, G.D., 1978, Flood frequency analysis with a generalized skew coefficient: *Water Resources Research*, v. 14, no. 2, p. 373–376.
- Tasker, G.D., 1983, Effective record length for the T-year event: *Journal of Hydrology*, v. 64, p. 39–47.
- Tasker, G.D., and Stedinger, J.R., 1986, Regional skew with weighted LS regression: *Journal of Water Resources Planning and Management*, v. 112, no. 2, p. 225–237.
- Tasker, G.D., and Stedinger, J.R., 1989, An operational GLS model for hydrologic regression: *Journal of Hydrology*, v. 111, no. 4, p. 361–375.
- Thomas, W.O., 1982, An evaluation of flood frequency estimates based on rainfall/runoff modeling: *Journal of the American Water Resources Association*, v. 18, no. 2, p. 221–229, accessed August 30, 2017, at <https://doi.org/10.1111/j.1752-1688.1982.tb03964.x>.
- Thomas, W.O., 1985, A uniform technique for flood frequency analysis: *Journal of Water Resources Planning and Management*, v. 111, no. 3, p. 321–337.
- Thomas, W.O., 1987, Comparison of flood-frequency estimates based on observed and model-generated peak flows, *in* Singh, V.P., ed., *Hydrologic frequency modeling*: Louisiana State University, Baton Rouge, D. Reidel Publishing Company, p. 149–161.
- Thomas, W.O., Grimm, M.M., and McCuen, R.H., 2001, Evaluation of flood frequency estimates for ungaged watersheds: *Hydrologic Frequency Work Group*, Subcommittee on Hydrology, 12 p.
- Thomson, M.T., Gannon, W.B., Thomas, M.P., and Hayes, G.S., 1964, Historical floods in New England: U.S. Geological Survey Water-Supply Paper 1779-M, 105 p., accessed October 30, 2017, at <https://pubs.er.usgs.gov/publication/wsp1779M>.

- Turnipseed, D.P., and Sauer, V.B., 2010, Discharge measurement at gaging stations: U.S. Geological Survey Techniques and Methods, book 3, chap. A8, 87 p., accessed October 30, 2017, at <https://pubs.usgs.gov/tm/tm3-a8/>.
- U.S. Army Corps of Engineers, 1973, Storm rainfall in the United States, 1945–1973: U.S. Army Corps of Engineers, Washington, D.C.
- U.S. Army Corps of Engineers, 1982, Mixed-population frequency analysis: U.S. Army Corps of Engineers, Hydrologic Engineering Center, 43 p.
- U.S. Army Corps of Engineers, 1993, Hydrologic frequency analysis: U.S. Army Corps of Engineers, Washington, D.C.
- U.S. Army Corps of Engineers, 2008, Orestimba Creek hydrology; A reevaluation based on updated peak and volume frequency curves: U.S. Army Corps of Engineers, Water Management Section, Sacramento District.
- U.S. Bureau of Reclamation and Utah State University, 1999, A framework for characterizing extreme floods for dam safety risk assessment: U.S. Bureau of Reclamation, 67 p.
- U.S. Water Resources Council, 1967, A uniform technique for determining flood flow frequencies, Bulletin No. 15: U.S. Water Resources Council, Subcommittee on Hydrology, Washington, D.C.
- U.S. Water Resources Council, 1976, Guidelines for determining flood flow frequency, Bulletin No. 17: U.S. Water Resources Council, Subcommittee on Hydrology, Washington, D.C.
- Veilleux, Andrea, 2011, Bayesian GLS regression for regionalization of hydrologic statistics, floods, and Bulletin 17 skew: Ph.D. dissertation, Cornell University.
- Veilleux, A.G., Stedinger, J.R., and Lamontagne, J.R., 2011, Bayesian WLS/GLS regression for regional skewness analysis for regions with large cross-correlations among flood flows, in World Environmental and Water Resources Congress 2011 Bearing Knowledge for Sustainability, American Society of Civil Engineers Environmental and Water Resources Institute.
- Viglione, A., Merz, R., Salinas, J.L., and Blöschl, G., 2013, Flood frequency hydrology; 3. A Bayesian analysis: Water Resources Research, v. 49, no. 2, p. 675–692, accessed August 30, 2017, at <https://doi.org/10.1029/2011WR010782>.
- Villarini, Gabriele, Serinaldi, Francesco, Smith, J.A., and Krajewski, W.F., 2009a, On the stationarity of annual flood peaks in the continental United States during the 20th century: Water Resources Research, v. 45, no. 8, accessed August 30, 2017, at <https://doi.org/10.1029/2008WR007645>.
- Villarini, Gabriele, Smith, J.A., Serinaldi, Francesco, Bales, Jerad, Bates, P.D., and Krajewski, W.F., 2009b, Flood frequency analysis for nonstationary annual peak records in an urban drainage basin: Advances in Water Resources, v. 32, no. 8, p. 1255–1266, accessed August 30, 2017, at <https://doi.org/10.1016/j.advwatres.2009.05.003>.
- Vogel, R.M., and Kroll, C.N., 1991, The value of streamflow record augmentation procedures in low-flow and flood-flow frequency analysis: Journal of Hydrology, v. 125, no. 3–4, p. 259–276, accessed August 30, 2017, at [https://doi.org/10.1016/0022-1694\(91\)90032-D](https://doi.org/10.1016/0022-1694(91)90032-D).
- Vogel, R.M., Matalas, N.C., England, J.F., and Castellarin, Attilio, 2007, An assessment of exceedance probabilities of envelope curves: Water Resources Research, v. 43, no. 7, accessed August 30, 2017, at <https://doi.org/10.1029/2006WR005586>, w07403.
- Vogel, R.M., and Stedinger, J.R., 1984, Flood-plain delineation in ice jam prone regions: Journal of Water Resources Planning and Management, v. 110, no. 2, p. 206–219.
- Vogel, R.M., and Stedinger, J.R., 1985, Minimum variance streamflow record augmentation procedures: Water Resources Research, v. 21, no. 5, p. 715–723.
- Wahl, K.L., Thomas, W.O., and Hirsch, R.M., 1995, The stream-gaging program of the U.S. Geological Survey: U.S. Geological Survey Circular 1123, 22 p., accessed October 30, 2017, at <https://pubs.er.usgs.gov/publication/cir1123>.

52 Guidelines for Determining Flood Flow Frequency—Bulletin 17C

- Weaver, J.C., Feaster, T.D., and Gotvald, A.J., 2009, Magnitude and frequency of rural floods in the Southeastern United States, 2006; v. 2, North Carolina: U.S. Geological Survey Scientific Investigations Report 2009–5158, 111 p., accessed October 30, 2017, at <https://pubs.usgs.gov/sir/2009/5158/>.
- Webb, R.H., and Betancourt, J.L., 1992, Climatic variability and flood frequency of the Santa Cruz River, Pima County, Arizona: U.S. Geological Survey Water-Supply Paper 2379, 40 p., accessed October 30, 2017, at <https://pubs.er.usgs.gov/publication/wsp2379>.
- Webb, R.H., and Jarrett, R.D., 2002, One-dimensional estimation techniques for discharges of paleofloods and historical floods, *in* House, P.K., Webb, R.H., Baker, V.R., and Levish, D.R., eds., Water Science and Application Series, v. 5, Ancient Floods, Modern Hazards: American Geophysical Union, p. 111–125, accessed August 29, 2017, at <https://doi.org/10.1029/WS005p0111>.
- Wiley, J.B., and Atkins, Jr., J.T., 2010, Estimation of flood-frequency discharges for rural, unregulated streams in West Virginia: U.S. Geological Survey Scientific Investigations Report 2010–5033, 78 p., accessed October 30, 2017, at <https://pubs.usgs.gov/sir/2010/5033/>.
- Wohl, E.E., and Enzel, Y., 1995, Data for palaeohydrology, *in* Gregory, K.J., Starkel, L., and Baker, V.R., eds., Global continental palaeohydrology: John Wiley & Sons, Ltd., p. 24–59.
- Yanosky, T.M., 1983, Evidence of floods on the Potomac River from anatomical abnormalities in the wood of flood-plain trees: U.S. Geological Survey Professional Paper 1296, 42 p., accessed October 30, 2017, at <https://pubs.er.usgs.gov/publication/pp1296>.
- Yanosky, T.M., and Jarrett, R.D., 2002, Dendrochronologic evidence for the frequency and magnitude of paleofloods, *in* House, P.K., Webb, R.H., Baker, V.R., and Levish, D.R., eds., Water Science and Application Series, v. 5, Ancient floods, modern hazards: American Geophysical Union, p. 77–89, accessed August 29, 2017, at <https://doi.org/10.1029/WS005p0077>.
- Yen, B.C., 1970, Risks in hydrologic design of engineering projects: Journal of the Hydraulics Division, American Society of Civil Engineers, v. 96, no. HY4, p. 959–966.

Glossary

annual exceedance probability (AEP) The probability that flooding will occur in any given year considering the full range of possible annual floods.

annual flood The highest instantaneous peak discharge in each year of record. Practically, this is the highest value observed in the record of 15 minute or 60 minute values, depending on the recording interval of the device. Sometimes the maximum mean daily discharge is used on larger rivers.

annual flood series A list of annual maximum floods.

annual series A general term for a set of any kind of data in which each item is the maximum or minimum in a year.

autocorrelation The presence of autocorrelation indicates that the data in the time series are not random. Rather, future values are correlated with past values. Autocorrelation is calculated as the correlation between the values in a time series and the values in that same time series lagged by one or more time steps (that is, the correlation between X_i and X_{i+k} where i is the time step and k is the lag). Also known as serial correlation.

base discharge (for peak discharge) A discharge value, determined for selected stations, above which peak discharge data are published. The base discharge at each station is selected so that an average of about three peak flows per year will be published ([Langbein and Iseri, 1960](#)).

binomial censored data Floods that exceeded a threshold, where one knows only that a flood was larger than some level, but does not know the magnitude of the flood ([Russell, 1982](#); [Stedinger and Cohn, 1986](#)).

broken record A systematic record that is divided into separate continuous segments because of deliberate discontinuation of recording for significant periods of time. This typically occurs when a gage is shut off because of funding, prioritization, or other hydrological or management reasons, then reestablished at a later time (several years, rather than weeks or months) at the same location. *See also discontinued record.*

censored data In a sample size of n , a known number of observations is missing at either end or at both ends ([David, 1981](#); [Cohen, 1991](#)).

coefficient of skewness A numerical measure or index of the lack of symmetry in a frequency distribution. Function of the third moment of magnitudes about their mean, a measure of asymmetry. Also known as coefficient of skew or **skew coefficient**.

confidence limits Computed values on both sides of an estimate of a parameter or quantile that show for a specified probability the range in which the true value of the parameter or quantile lies.

crest-stage gage (CSG) A simple, economical, reliable, and easily installed device for obtaining the elevation of the flood crest of streams ([Sauer and Turnipseed, 2010](#)). These gages are nonrecording and consist of a partial streamflow record. Flow intervals and perception thresholds are needed to describe each year of the flood record.

54 Guidelines for Determining Flood Flow Frequency—Bulletin 17C

cross correlation A measure of similarity, interdependence, or relationship between two time series of observations in space at the same point or lagged points in time.

discontinued record A systematic record where streamflow data collection and measurements have ceased. This typically occurs when a gage is shut off because of funding, prioritization, other hydrological or management reasons, and not reestablished. *See also broken record.*

exceedance Knowledge that the magnitude (discharge or stage) of a flood was larger than some level or threshold. For example, the flood exceeded the bridge deck.

exceedance frequency The percentage of values that exceed a specified magnitude, 100 times exceedance probability.

exceedance probability Probability that a random event will exceed a specified magnitude in a given time period, usually one year unless otherwise indicated.

Expected Moments Algorithm (EMA) A generalized method of moments procedure to estimate the P-III distribution parameters using the entire dataset, simultaneously employing regional skew information and a wide range of historical flood and threshold-exceedance information, while adjusting for any potentially influential low floods, missing values from an incomplete record, or zero flood years.

extraordinary flood Those floods that are the largest magnitude at a gaging station or miscellaneous site and that substantially exceed the other flood observations ([Costa and Jarrett, 2008](#)).

gage base The minimum stage or discharge level at a gaging station, below which observations are not recorded or published. Also called **base discharge**.

gaging record Streamflow data collected at streamflow-gaging stations. A gaging record can consist of systematic data and historical flood data.

gaging station A selected site on a stream equipped and operated to furnish basic data from which continuous, systematic records of stage and discharge may be obtained ([Grover and Harrington, 1943](#); [Rantz and others, 1982a](#)).

generalized skew coefficient *See regional skew coefficient.*

high-water mark (HWM) Typically recent (hours to weeks) physical evidence of the (approximate) maximum flood stage ([Jarrett and England, 2002](#)). The physical evidence generally is of three types: (1) deposits along channel margins and in vegetation that consist of very light, floatable material such as pine needles, seeds, small twigs, grasses, and very fine sediments; (2) damage to vegetation such as bent or matted grasses, twigs, and branches, stripped leaves or bark; and (3) small erosional features such as scour lines. [Benson and Dalrymple \(1967\)](#) and [Koenig and others \(2016\)](#) discuss identification, preservation, and rating of high-water marks. The HWM evidence is typically short-lived (weeks), but woody debris may last from several years to several decades in arid and semi-arid climates ([Baker, 1987](#)), and geomorphic evidence can be preserved for millennia. Physical evidence, such as marks on buildings and other structures, is also long lived. This stage may represent a maximum discharge when a single-valued relationship exists between stage and discharge; [Costa and Jarrett \(2008\)](#) describe other hydraulic situations. *See also paleostage indicator.*

historical data Broad category of data collected by humans prior to establishing systematic protocols; it generally consists of diaries, written accounts of settlements, folklore, and descriptions that may document periods when and where extreme weather and (or) floods have occurred. It may also be used to infer times when there have been no large floods. These accounts were recorded in a manner that was preserved well enough that we know about it today.

historical floods Flood events which were directly observed by humans, generally in a nonsystematic manner by nonhydrologists (Baker, 1987). These events usually occurred and were described in some qualitative and (or) quantitative fashion prior to the systematic record. Information about the floods was recorded and preserved well enough so that we know about it today.

homogeneity Records from the same populations. Floods may be from different populations because they occurred before the building of a dam and after the building of a dam, or before the watershed was urbanized and after it became urbanized, or because some are generated by summer storms and others by snowmelt, or because some were generated in El Niño years and some were in other years. It may be difficult in some cases to definitively say if the flood record is homogeneous.

incomplete record A streamflow record in which some peak flows are missing because they were too low or high to record or the gage was out of operation for a short period because of flooding.

interval data Floods whose magnitude are not known exactly, but are known to fall within a range or interval (Stedinger and others, 1988; Cohn and others, 1997).

level of significance The probability of rejecting a hypothesis when it is in fact true. At a “10-percent” level of significance, the probability is 1/10.

low outlier See **outlier**.

mean square error (MSE) Sum of the squared differences between the true and estimated values of a quantity divided by the number of observations. It can also be defined as the bias squared plus the variance of the quantity (Stedinger and others, 1993).

method of moments A standard statistical computation for estimating the parameters of a distribution from the moments of the sample data.

Multiple Grubbs-Beck Test (MGBT) A statistical test used to identify multiple potentially influential low flood observations (PILFs) in an annual maximum time series.

nonexceedance Knowledge that the magnitude (discharge or stage) of a flood was less than some level or threshold.

outlier Outliers (extreme events) are observations that are exceedingly low or high compared to the distributional properties of the vast majority of the data. When plotted, along with a reasonably fitted cumulative distribution function (CDF) to the data, the outlier values plot far from the fitted line at the low or high ends of the distribution. A CDF, such as the LP-III, may not fit datasets with outliers, and the fitted curve usually fails to fit the bulk of the data as well as the outliers. Low outliers are outliers at the low end of the dataset, near zero, at least in comparison with the rest of the data. On a log-probability plot, the low outliers impart a strong downward curvature and a downward-drooping lower tail to the frequency curve. In comparison with the lower tail, the upper tail of the low-outlier-affected curve may appear relatively flat.

paleoflood data Physical evidence of past floods and their ages as observed from the geologic record or from botanical evidence. Paleoflood data typically consist of observations on individual past floods such as those derived from slackwater deposits, boulder bars, silt lines, or botanical information, that are collected as part of a paleoflood hydrology study (Benito and O'Connor, 2013). It can also consist of periods of landscape stability that can be used to place limits on flood magnitude over time, such as paleohydrologic bounds (Levish, 2002). Paleoflood data are distinguished from historical flood data, as a separate line of evidence, by the use of applied field geology techniques to examine and describe the geomorphic and stratigraphic context of extreme floods. In some cases, there is overlap between historical and paleoflood data, as historical and cultural artifacts such as barbed wire, beer cans (House and Baker, 2001), or pottery may be observed and used in dating and estimation of floods.

paleoflood hydrology The study of past or ancient floods that occurred prior to the time of human observation or direct measurement by modern hydrologic procedures (Baker, 1987). Paleoflood hydrology has also been defined as “the study of the movements of water and sediment in channels before the time of continuous hydrologic records or direct measurements” (Costa, 1986).

paleohydrologic bound A time interval during which a given discharge has not been exceeded (Levish, 2002). The term is sometimes shortened to “bound.” The paleohydrologic bound represents stages and discharges that have not been exceeded since the geomorphic surface stabilized. Bounds are appropriate for paleohydrologic information and are not dependent on human observation of a particular event, but on the physical setting (hydraulic and geomorphic). Also known as “paleoflood bound.”

paleostage indicator (PSI) An erosional or depositional feature that recorded the near peak stage of an individual flood (Jarrett and England, 2002) prior to human observation. Indirect evidence of the stage of past floods includes botanical evidence and sedimentological deposits (Jarrett, 1991). Large floods, especially in high-gradient channels, can transport and deposit coarse material (gravel, boulders, and woody debris, and so forth) that may be interpreted as HWMs. The primary differences between PSIs and HWMs are: (1) HWMs represent events that occurred “more recent” in time because of their relatively short preservation length as compared to PSIs; and (2) some PSIs may not represent the exact peak stage.

Partial-Duration Series (PDS) A list of all flows (such as flood peaks) that exceed a chosen base stage or discharge, regardless of the number of peaks occurring in a year. Also called basic-stage flood series, or floods above a base (Langbein and Iseri, 1960).

percent chance A probability multiplied by 100.

perception threshold The stage or flow above which it is estimated a source would provide information on the flood peak in any given year. Perception thresholds ($T_{Y,lower}$, $T_{Y,upper}$) reflect the range of flows that would have been measured or recorded had they occurred. If an event magnitude had occurred in a specific year, there is information that would indicate it would have been “recorded” in a manner that we could perceive it today. Perception thresholds describe the range of measurable potential discharges and are independent of the actual peak discharges that have occurred. They are used to provide a rank and record length for each reported flood peak (Gerard and Karpuk, 1979). Perception thresholds are used for historical data, when the information provided is based on human observation. They are also used to describe a paleoflood period and paleoflood data. In addition, perception thresholds are used to properly accommodate unrecorded floods below a “gage base.” A perception threshold is allocated to each information source for each year Y of the flood record. Perception thresholds may involve a significant amount of judgment on the part of the scientist and (or) historian regarding, for any given year, what is

the smallest event that would have been recorded (in a physical or textural manner) such that we would actually know about it today. Also known as **threshold**.

population The entire (usually infinite) number of data from which a sample is taken or collected. The total number of past, present, and future floods at a location on a river is the population of floods for that location, even if the floods are not measured or recorded.

potentially influential low flood (PILF) In an annual maximum flood series, small-magnitude flows (including zeros) that do not represent the physical processes that cause the largest flood observations. PILFs can exert high leverage and influence on the flood frequency distribution.

quantile Estimate of the flood magnitude for an annual exceedance probability from a fitted distribution.

record augmentation A procedure to improve the accuracy of the moments (mean and variance) of a short-record flood series by using information from longer records at nearby locations with high cross correlation ([Matalas and Jacobs, 1964](#); [Stedinger and others, 1993](#)).

record extension The creation of a longer flood-flow record (individual floods) at a site with a short record, by using flood observations at a long-record site with high cross correlation. The technique can also be used to fill in missing observations ([Hirsch and others, 1993](#); [Stedinger and others, 1993](#)).

regional skew coefficient A skew coefficient derived by a procedure that integrates values obtained at many locations.

robustness In flood frequency, a property of a statistical procedure that is reasonably efficient when the assumed characteristics of the flood distribution are true, while not doing poorly when those assumptions are violated ([Kuczera, 1982](#); [Cohn and others, 2013](#)).

sample An element, part, or fragment of a “population.” Every hydrologic record is a sample of a much longer record.

serial correlation *See autocorrelation.*

skew coefficient *See coefficient of skewness.*

standard deviation A measure of the dispersion or precision, of a series of statistical values such as precipitation or streamflow. It is the square root of the sum of squares of the deviations from the arithmetic mean divided by the number of values or events in the series. It is standard practice to divide by the number of values minus one in order to get an unbiased estimate of the variance from the sample data.

standard error An estimate of the standard deviation of a statistic. Often calculated from a single set of observations. Calculated like the standard deviation but differing from it in meaning.

systematic data Data that are collected at regular, prescribed intervals under a defined protocol. In the context of streamflow, systematic data consist of discharge and stage data collected at regular, prescribed intervals, typically at streamflow-gaging stations. Synonymous with systematic record.

threshold *See perception threshold.*

variance A measure of the amount of spread or dispersion of a set of values around their mean, obtained by calculating the mean value of the squares of the deviations from the mean, and, hence, equal to the square of the standard deviation.

58 Guidelines for Determining Flood Flow Frequency—Bulletin 17C

weighted means A value obtained by multiplying each of a series of values by its assigned weight and dividing the sum of those products by the sum of the weights.

Appendix 1. List of Symbols

The following is a list of symbols that are used in this report.

Table 1–1. List of symbols used in this report.

Symbol	Description
a	Plotting position parameter that is dependent on an assumed distribution ($0 \leq a \leq 0.5$); $a = 0 \equiv$ Weibull; $a = 0.5 \equiv$ Hazen (eq. 2)
e_s	Number of floods/records that exceed a censoring level, such as a historical threshold T_h or low-outlier threshold T_{PILF} , during the systematic record n_s ; ($e_s \leq k$; $e_s < n_s$)
e_h	Number of floods/records that exceed the historical threshold T_h during the historical/paleoflood period n_h ; ($e_h \leq k$; $e_h < n_h$)
g	Total number of known flood (observations) during the entire period of observation record n ; ($g = n_s + k - e_s = n_s + e_h$)
$\hat{\gamma}$	At-site (station) sample skew coefficient (in log space)
G	Regional sample skew coefficient (in log space)
\tilde{G}	Weighted skew coefficient
k	Total number of floods/records that exceed a censoring level, such as a historical threshold T_h or low-outlier threshold T_{PILF} , during the entire period of observation record n ; ($k = e_s + e_h$)
$\hat{\mu}$	At-site (station) sample mean (in log space)
$\hat{\sigma}$	At-site (station) sample standard deviation (in log space)
n	Total peak-flow period of record (years), including systematic n_s and historical n_h periods, as available, where $n = n_s + n_h$
n_h	Length of the historical and (or) paleoflood period (years) ($n_h < n$)
n_s	Length of the peak-flow systematic (gaging) record (years) ($n_s \leq n$)
p	Annual exceedance probability (AEP), $p = 1 - q$
q	Cumulative probability, $q = 1 - p$
Q	Flood discharge
Q_b	Base discharge, can be a constant, or vary with each year at a gaging station or CSG
Q_p	Discharge quantile for annual exceedance probability p
Q_q	Discharge quantile for cumulative probability q , equivalent to Q_p
Q_Y	Flood discharge estimate in year Y
$Q_{Y,lower}$	Discharge lower bound for year Y in EMA
$Q_{Y,upper}$	Discharge upper bound for year Y in EMA

60 Guidelines for Determining Flood Flow Frequency—Bulletin 17C

Table 1–1. List of symbols used in this report—Continued.

Symbol	Description
T_d	Perception threshold for a discontinued (broken) record at a gaging station with systematic period n_s
T_h	Perception threshold for a historical period n_h
T_{PILF}	PILF censoring threshold from the MGBT
$T_{Y,lower}$	Perception threshold lower bound for year Y in EMA; represents the smallest peak flow that would result in a recorded flow
$T_{Y,upper}$	Perception threshold upper bound for year Y in EMA; represents the largest peak flow that would result in a recorded flow
X_h	Base-10 logarithm of a perception threshold for a historical period n_h
X_l	Base-10 logarithm of the PILF censoring threshold from the MGBT
$X_{Y,lower}$	Base-10 logarithm of discharge lower bound $Q_{Y,lower}$ for year Y in EMA
$X_{Y,upper}$	Base-10 logarithm of discharge upper bound $Q_{Y,upper}$ for year Y in EMA
Y	Year

Appendix 2. Subcommittee and Work Group Members

The Subcommittee on Hydrology (SOH) is a subgroup under the Advisory Committee on Water Information (ACWI). The purpose of the SOH is to improve the availability and reliability of surface-water quantity information needed for hazard mitigation, water supply and demand management, and environmental protection. The SOH coordinates and oversees technical working groups, including the Hydrologic Frequency Analysis Work Group (HFAWG). The SOH sponsored this HFAWG work effort to prepare the update to these Guidelines. Current (2017) SOH membership is listed in table 2–1. Further details about SOH and its activities are available at <https://acwi.gov/hydrology/index.html>.

The overall goal of the Hydrologic Frequency Analysis Work Group is to recommend procedures to increase the usefulness of the current guidelines for Hydrologic Frequency Analysis computations (for example, Bulletin 17B) and to evaluate other procedures for frequency analysis of hydrologic phenomena. The work group forwards draft papers and recommendations to the Subcommittee on Hydrology of ACWI for appropriate action. As part of these activities, the HFAWG oversaw this revision. Current (2017) HFAWG membership is listed in table 2–2. Further details about HFAWG and its activities are available at <https://acwi.gov/hydrology/Frequency/index.html>.

62 Guidelines for Determining Flood Flow Frequency—Bulletin 17C

Table 2-1. Subcommittee on Hydrology members.

Member Organization	Representative
Association of State Floodplain Managers	Wilbert O. Thomas, Jr.
BECKER	Martin Becker
DOI/Bureau of Land Management	Robert Boyd
DOI/Bureau of Reclamation	Dr. Ian Ferguson
DOI/Office of Surface Mining	vacant
DOI/U.S. Geological Survey	Robert Mason (Chair)
Federal Energy Regulatory Commission	Dr. S. Samuel Lin
Federal Highway Administration	Brian Beucler
Global Ecosystems Center	Don Woodward
NASA/Goddard Space Flight Center	Sujay Kumar
National Hydrologic Warning Council	Ben Pratt
National Science Foundation	Dr. Thomas Torgersen
NOAA/National Weather Service	Victor Hom
U.S. Army Corps of Engineers	Dr. Chandra Pathak
USDA/Agricultural Research Service (ARS)	Dr. David C. Goodrich
USDA/Natural Resources Conservation Service (NRCS)	Claudia Hoeft
USDA/U.S. Forest Service	Michael Eberle
U.S. Environmental Protection Agency	Pravin Rana
USDHS/Federal Emergency Management Agency (FEMA)	Dr. Siamak Esfandiary (Vice Chair)
U.S. Nuclear Regulatory Commission (NRC)	Thomas J. Nicholson

Table 2-2. Hydrologic Frequency Analysis Work Group members.

Member Name	Organization	Location
Wilbert O. Thomas, Jr. (Chair)	Michael Baker International	Manassas, VA
Dr. Siamak Esfandiary	Federal Emergency Management Agency	Crystal City, VA
Don Woodward	Global Ecosystems Center	Derwood, MD
Martin Becker	BECKER	Atlanta, GA
Dr. Timothy Cohn	U.S. Geological Survey	Reston, VA
Dr. Beth Faber	U.S. Army Corps of Engineers	Davis, CA
Dr. John England	U.S. Army Corps of Engineers	Lakewood, CO
Prof. Jerry Stedinger	Cornell University	Ithaca, NY
Dr. Zhida Song-James	Consulting Hydrologist	Fairfax, VA
Dr. Jerry Coffey	Mathematical Statistician	Middletown, VA
Joe Krolak	Federal Highway Administration	Washington, D.C.
William Merkel	Natural Resources Conservation Service	Beltsville, MD
Dr. Sanja Perica	National Weather Service	Silver Spring, MD
Thomas Nicholson	U.S. Nuclear Regulatory Commission	Rockville, MD
Dr. S. Samuel Lin	Federal Energy Regulatory Commission	Washington, D.C.
Mike Eiffe (through Sept. 2014)	Tennessee Valley Authority	Knoxville, TN
Curt Jawdy	Tennessee Valley Authority	Knoxville, TN

Appendix 3. Data Sources and Representation

Data Sources

This appendix provides some representative data sources for flood frequency. Systematic records, historical data, paleoflood data and botanical information, regional information, and precipitation and climate information are briefly described. These sources are intended to be used as references and starting points for data collection, and are not all inclusive. Available sources and some websites for these data can be found at <https://acwi.gov/hydrology/Frequency/b17c/>.

Systematic Records

Systematic records that may be useful for estimating flood frequency include the following: peak flows, daily flows, reservoir inflows and elevations, hydrograph data, and streamflow measurements. Annual maximum instantaneous peak streamflow and gage height data can be obtained from the USGS National Water Information System (NWIS) at <https://nwis.waterdata.usgs.gov/usa/nwis/peak>. Users need to be familiar with the NWIS qualification codes for peak streamflow and peak gage height at <https://nwis.waterdata.usgs.gov/nwis/peak?help>. Daily streamflow data can be obtained from various sources. The main data source is the USGS NWIS at https://nwis.waterdata.usgs.gov/nwis/dv/?referred_module=sw. These data can be readily retrieved with software packages such as Hirsch and De Cicco (2015).

Other Federal agencies provide daily streamflow and extensive reservoir-related data, including elevations, inflows, and outflows. These data can be of direct use for extending discontinued streamflow gages and estimating unregulated flows.

Reclamation at <https://www.usbr.gov/> provides data through its five regions in the 17 Western States for numerous river locations and over 350 reservoirs. The Reclamation Hydromet databases provide data for the Great Plains Region and Pacific Northwest Region. Data within the Upper Colorado Region is obtained through reservoir operations at <https://www.usbr.gov/uc/>. Data within the Lower Colorado Region is obtained through river operations at <https://www.usbr.gov/lc/>. Reclamation's Mid-Pacific region provides data for many locations, including the Central Valley, through the California Data Exchange Center.

The U.S. Army Corps of Engineers provides streamflow and reservoir information, within the conterminous United States, through seven divisions. A map with links to each division is at <https://www.usace.army.mil>. Streamflow and reservoir data can be provided for specific projects or river basins, within each division. For example, the Northwestern Division provides data for the Missouri River basin through their reservoir control center.

Individual State agencies provide streamflow information, typically through their Division of Water Resources or Division of Natural Resources. Some examples of streamflow databases by States are the following: California, Colorado, Oregon, and Minnesota. Local flood-control districts and organizations may also have relevant streamflow data.

Instantaneous data (15-minute data, unit values, and complete hydrographs), from 2007 to present for active streamgages, can be obtained from the USGS NWIS at https://nwis.waterdata.usgs.gov/nwis/uv/?referred_module=sw. Hydrograph data from about the mid-1980s to 2007 can be obtained from the instantaneous data archive at <https://ida.water.usgs.gov/ida/>.

Data on manual measurements of streamflow and gage height, including indirect measurements, can be obtained from the USGS at <https://waterdata.usgs.gov/nwis/measurements>. These measurements are used to

supplement and (or) verify the accuracy of the automatically recorded observations, as well as to compute streamflow based on gage height. They are valuable for flood frequency studies to aid hydrologists in understanding how the largest flood estimates are made (such as a slope-area indirect measurement), and in estimating uncertainty.

Historical Data

Historical flood data sources can be obtained from a variety of locations. This section describes some of those data sources useful for flood frequency, and is an excerpt from [England \(1998, chapter 4\)](#), updated with additional recent studies. A literature search is performed, followed by field studies and historical data collection efforts in the watershed and community of interest ([Thomson and others, 1964](#); [Aldridge and Hales, 1984](#)).

One typically obtains USGS records as a first step in the search for historical data. Information on observed floods, occurring after about 1900 and that typically cause flooding of populated areas, damage, and sometimes deaths, are described in various USGS publications, such as Water-Supply Papers, Professional Papers, and Scientific Investigations Reports. The information generally consists of basin rainfall estimates, types of discharge or indirect measurements made, damage estimates, pictures of damaged structures, and erosion and deposition in channels and flood plains. In some cases, past historical flood dates, stages, and peak discharge estimates in the region are described in each report. For example, the report on the Arkansas River flood of June 3–5, 1921 ([Follansbee and Jones, 1922](#)) lists previous floods back to about 1844, based primarily on Denver and Rio Grande railroad records. [Stewart and Bodhaine \(1961\)](#) describe recent floods and present a historical flood chronology back to 1815 for the Skagit River Basin in Washington. In some cases, historic flood estimates are revised, such as the Skagit River near Concrete ([Mastin, 2007](#)). Many other Water-Supply Papers present historical flood information when documenting large regional floods, although in many cases the river stages and discharges are unknown ([McGlashan and Briggs, 1939](#)). In some cases, electronic databases of historical flood estimates are available, such as in Colorado, by [Kohn and others \(2013\)](#).

The USGS Water Resources Data Reports, which have been published for each State (1962–2005), contain some limited historical flood descriptions and information that can be extremely valuable for frequency analysis. The information is provided on the site information sheet for individual gaging stations. Since 2006 and if the gaging station is currently in operation, this same information can be obtained for each individual gage. Three types of data are typically presented in the reports and site information summaries: (1) dates, stages, and sometimes discharges of observed floods prior to the gaging station period of record, for example, [Durlin and Schaffstall \(2002, p. 210\)](#); (2) a large flood during the period of record that is known to be the maximum stage and discharge **since at least** some historic date, for example, [Crowfoot and others \(1997, p. 413\)](#); and (3) a large flood during the period of record that is known to be the maximum stage and discharge **since** some historic date, for example, [May and others \(1996, p. 193\)](#). The information provided in (2) and (3) sometimes only refers to either stage or discharge, depending on the observation or estimate made. In addition, there is a subtle difference between the information provided in (2) and (3). Data provided as (2) indicate one does not have information on any flood discharges or stages prior to the date stated. One does have knowledge of a flood in the historical year stated in (3). The information for cases (1) and (3) is typically stored in electronic format in the USGS NWIS database. The data are generally summarized in the following two columns: discharge codes ([Asquith and others, 2017, appendix 1](#)), where a “7” indicates that the discharge is a historic peak, and a “highest since” column, where the historic year is listed. These data need to be evaluated on an individual basis to properly estimate n_h and T_h .

State reports and publications are another major source of historical flood information. These publications can contain information on record floods, stages, historical periods, and impacts to infrastructure. For

example, [Suttie \(1928\)](#) states “there are three great storms affecting Connecticut that are worthy of particular mention: 1869, 1897, and 1927;” this information suggests that rainfall amounts and flood discharges are less than values estimated in the intervening time between these three events. For the 1869 flood, [Suttie \(1928, p. 120\)](#) states “the Connecticut River gage at Hartford registered 26.3 feet. This is the highest stage in over a century caused by rain alone;” this information can be utilized to estimate the historical period h one may use for the 1869 stage. Many other State reports contain relevant examples such as this one.

Journals and other Federal agency reports are invaluable sources for historical flood information. The primary historical journal references are the Journal of the Boston Society of Civil Engineers and Transactions of the American Society of Civil Engineers. For example, [Kuichling \(1917, p. 650–663\)](#) provides a table of maximum unit discharges for large floods in the United States to at least 1786; he also includes a reference list that includes many journals, USGS and State geological surveys reports. The U.S. Army Corps of Engineers retains flood files at District offices. Community flood information and experiences are usually included in Federal Emergency Management Agency (FEMA) Flood Insurance Studies. A detailed example of historical flood data collection is provided in [Thomson and others \(1964\)](#); they present a flood chronology in New England from 1620–1955.

Paleoflood Data and Botanical Information

Paleoflood data and botanical information for river basins and specific locations can be obtained from existing, previously published sources and institutions that have obtained the data, or by field data collection at the site of interest. The main sources of existing, previously published paleoflood and botanical data are various institutions that have collected the data, such as Federal agencies, State agencies, and academic institutions. These data are routinely documented in journal articles, technical reports and databases, books, and some electronic databases. Over the past 20 years, the University of Arizona, Reclamation, USGS, and other agencies and institutions have embarked on numerous field campaigns to obtain paleoflood data relevant for flood frequency. Similar to historical information, paleoflood and botanical data are obtained by initially searching for relevant documents and contacting institutions that have interests and facilities within the watershed of interest. After a literature search, paleoflood and botanical data can be obtained within the watershed by conducting comprehensive field studies and data collection efforts.

Several journal articles and books are key references in obtaining previously published paleoflood and botanical information, and are indispensable guides for data collection efforts. [Wohl and Enzel \(1995\)](#) provide a useful introduction and overview of available paleoflood data. [Baker and others \(1988\)](#) and [House and others \(2002a\)](#) are key references that describe data for numerous case studies and locations, present methods for paleoflood data collection, and contains numerous citations to other relevant works and data. [Baker \(2008, table 2\)](#) summarizes many paleoflood studies and data collection completed in the United States. [Benito and O'Connor \(2013\)](#) and [Baker \(2013\)](#) provide current summaries on paleoflood and paleohydrology data and methods. Paleoflood data are readily used with EMA; for example [England and others \(2003a\)](#) summarized paleoflood data and demonstrated its use in flood frequency with EMA for a number of sites in the United States.

Paleoflood data for many locations within the Western United States have been collected by Reclamation for dam safety analyses. These data are typically available for many rivers and locations adjacent to Reclamation dams and other Department of Interior facilities, in order to document the most extreme floods and nonexceedance information in the Holocene. Reclamation staff typically collect paleoflood data at one of three levels: reconnaissance, intermediate, or detailed. As the level of study increases, more stratigraphic and soil-age data are obtained, and hydraulic models used to estimate discharge increase in complexity. These data are available in numerous Reclamation reports for specific projects and (or) watersheds, and in databases ([Klinger](#)

66 Guidelines for Determining Flood Flow Frequency—Bulletin 17C

and Godaire, 2002). Some representative studies include the following: the American River and adjacent basins near Sacramento, California (Bureau of Reclamation, 2002); the North Platte River near Rawlins and Glendo, Wyoming (Levish and others, 2003); the Arkansas River near Pueblo, Colorado (England and others, 2006); the South Fork Boise River, Idaho (Klinger and Bauer, 2010); the North Fork Red River near Altus, Oklahoma (Godaire and Bauer, 2012); the San Joaquin River near Fresno, California (Godaire and others, 2012); and the Rio Chama near El Vado Dam, New Mexico (Godaire and Bauer, 2013). Peak-flow frequency estimates have been made at these sites using EMA. The USGS has also conducted numerous paleoflood studies using reconnaissance or regional approaches (Jarrett and Tomlinson, 2000) and detailed methods for flood hazard assessments at specific locations (Harden and others, 2011). Some paleoflood data are available in electronic databases, such as Kohn and others (2013).

Botanical information and data, such as tree scars and tree rings, are available in publications and some electronic databases. Some essential publications on methods and data are Hupp (1987, 1988), and Yanosky and Jarrett (2002); these contain numerous citations to other relevant works and data. McCord (1990) provides tree-scar data at select sites in Arizona, Utah, New Mexico, and Colorado. Additional resources include the Laboratory of Tree-Ring Research at the University of Arizona and the International Tree-Ring Data Bank.

Regional Information

Regional information that can be considered for flood frequency typically consists of regional estimates of flow statistics. Regional skew coefficient G estimates and mean-square error MSE_G estimates can be obtained for many locations in current USGS flood frequency reports for regions or individual States. For example, regional skew estimates are available for the Southeastern United States (Gotvald and others, 2009; Feaster and others, 2009; Weaver and others, 2009), California (Parrett and others, 2011; Gotvald and others, 2012), Iowa (Eash and others, 2013), Arizona (Paretti and others, 2014b), Missouri (Southard and Veilleux, 2014), and Vermont (Olson and Veilleux, 2014). The USGS is in the process of updating regional skew estimates for many other States. Regional flood quantile estimates Q_i and their variances $V_{regi,i}$ are also available in these reports, and are useful in record extension (appendix 8) and in weighting of independent estimates (appendix 9). These flood frequency reports and additional information on regional skew and regional quantile estimates for many locations are available from the USGS and the HFAWG at <https://acwi.gov/hydrology/Frequency/b17c/>.

In lieu of published estimates using B-GLS, it is recommended that users consult with the USGS to determine the availability of regional skew estimates that have been prepared using current methods, described in the section [Estimating Regional Skew](#). The regional skew estimates published in IACWD (1982, plate 1) are not recommended for use in flood frequency studies. When no other regional skew information is available, it is recommended that new estimates be developed for the region of interest.

Precipitation and Climate Information

Precipitation information that is potentially useful for flood rainfall-runoff modeling and flood frequency analysis is generally available from various Federal and State agencies. Point precipitation data and radar rainfall products are available from the National Oceanic and Atmospheric Administration (NOAA) and the NOAA National Centers for Environmental Information. National Weather Service River Forecast Centers also provide multisensor precipitation (combined radar and precipitation gage) estimates across the United States. Precipitation frequency estimates and time series are available from the National Weather Service (NWS) Hydrometeorological Design Studies Center. Precipitation data for many of the largest historical rainfall events and floods can be obtained from extreme storm catalogs at the U.S. Army Corps of Engineers, Reclamation, and through the Extreme Storm Events Working Group at <https://acwi.gov/hydrology/>

[extreme-storm/index.html](#). Precipitation and temperature data important for rainfall-runoff modeling of extreme floods can be obtained from the National Resources Conservation Service (NRCS) snow telemetry and snow course data. The NWS National Operational Hydrologic Remote Sensing Center snow data assimilation system, available through the National Snow and Ice Data Center, is another valuable dataset for snow cover and associated variables.

Climate information that is useful for a hydroclimatological perspective on floods is available from the NOAA Earth System Research Laboratory; other sources may be found through NOAA and at <https://acwi.gov/hydrology/Frequency/b17c/>. Information on climate models, downscaling information, and climate change, that is potentially relevant for floods, is under rapid development and has not been comprehensively evaluated for use in flood frequency studies. An overview is presented in Brekke and others (2009). Downscaled climate information and tools for climate change assessment studies are available from various sources, such as the Bureau of Reclamation at <https://www.usbr.gov/climate>, the USGS at <https://cida.usgs.gov/gdp/>, and the USACE at <https://www.corpsclimate.us/index.cfm>. Additional resources may be found at <https://acwi.gov/hydrology/Frequency/b17c/>.

Data Representation

As described in the section [Data Representation Using Flow Intervals and Perception Thresholds](#), a generalized representation of peak-flow data is used in flood frequency analysis to describe what is known about annual peak flows in a given year Y , over a range of years n . Typical peak-flow intervals and thresholds for systematic (gage) records, crest-stage gages, historical data, and potentially influential low floods (PILFs) are summarized in table 3–1.

At gaging stations (systematic record site), typical data consist of flow intervals and perception intervals that are shown in figure 3–1. Flows each year are typically known as and are considered “point” estimates. Because there is a gaging station and continuous observations, one can observe or measure a flow of any magnitude. Perception thresholds are typically 0 to ∞ . On occasion, there may be flows best described with interval observations, where one knows flows exceeded some lower estimate $Q_{Y,lower} = Q_Y$. In the case of a broken record, where the gage is discontinued or temporarily stopped for a period, one has no information or knowledge. For such broken record years, flows and perception thresholds are set equal to ∞ , unless one has additional information from a historical period or large flood, as shown in figure 9. A systematic record example is shown in figure 10–1.

The flow intervals and perception thresholds for a crest-stage gage are shown in figure 3–2. In this situation, flows are recorded only if they exceed a gage-base discharge Q_b . This is represented by a perception threshold T_b . Perception thresholds are typically T_b to ∞ . On occasion, there may be flows best described with interval observations, where one knows flows exceeded some lower estimate $Q_{Y,lower} = Q_Y$. A crest-stage gage example is shown in figure 10–10.

The typical flow intervals and perception thresholds for historical data are shown in figure 3–3. In this situation, flows are recorded only if they exceed a historical perception threshold T_h . There may be more than one perception threshold to describe historical and (or) paleoflood periods, as shown in figure 12 in the section [Data Representation Using Flow Intervals and Perception Thresholds](#). Perception thresholds are typically T_h to ∞ . Upper perception thresholds may be less than infinity where high-water marks from very high stages may not be preserved, especially in canyon environments. Within the historical period, there may be extreme floods that are best described with intervals or binomial observations, where one knows flows exceeded some lower estimate $Q_{Y,lower} = Q_Y$. Historical data examples are shown in figures 10–8 and 10–12, and with historical and paleoflood data (figure 10–14). It is important to estimate the historical periods and perception thresholds, as described in the section [Data Representation Using Flow Intervals and Perception Thresholds](#).

Table 3–1. Generalized data representation of peak-flow intervals and perception thresholds for each year (typical values).

[PILF, potentially influential low flood]

Data source	Data type	Flow interval	Perception threshold
Gage	Point	$Q_{Y,lower} = Q_Y$	$T_{Y,lower} = 0$
		$Q_{Y,upper} = Q_Y$	$T_{Y,upper} = \infty$
Gage	Interval	$Q_{Y,lower}$	$T_{Y,lower} = 0$
		$Q_{Y,upper}$	$T_{Y,upper} = \infty$
Gage	Broken record	$Q_{Y,lower} = \infty$	$T_{Y,lower} = \infty$
		$Q_{Y,upper} = \infty$	$T_{Y,upper} = \infty$
Crest stage	Point	$Q_{Y,lower} = Q_Y$	$T_{Y,lower} = Q_b$
		$Q_{Y,upper} = Q_Y$	$T_{Y,upper} = \infty$
Crest stage	Interval	$Q_{Y,lower} > Q_b$	$T_{Y,lower} = Q_b$
		$Q_{Y,upper}$	$T_{Y,upper} = \infty$
Historical	Point	$Q_{Y,lower} = Q_Y$	$T_{Y,lower} = Q_h$
		$Q_{Y,upper} = Q_Y$	$T_{Y,upper} = \infty$
Historical	Interval	$Q_{Y,lower} > Q_h$	$T_{Y,lower} = Q_h$
		$Q_{Y,upper}$	$T_{Y,upper} = \infty$
Historical	Binomial	$Q_{Y,lower} \geq Q_h$	$T_{Y,lower} = Q_h$
		$Q_{Y,upper} = \infty$	$T_{Y,upper} = \infty$
Historical	Censored	$Q_{Y,lower} = 0$	$T_{Y,lower} = Q_h$
		$Q_{Y,upper} = Q_h$	$T_{Y,upper} = \infty$
PILF	Censored	$Q_{Y,lower} = 0$	$T_{Y,lower} = Q_l$
		$Q_{Y,upper} = Q_l$	$T_{Y,upper} = \infty$

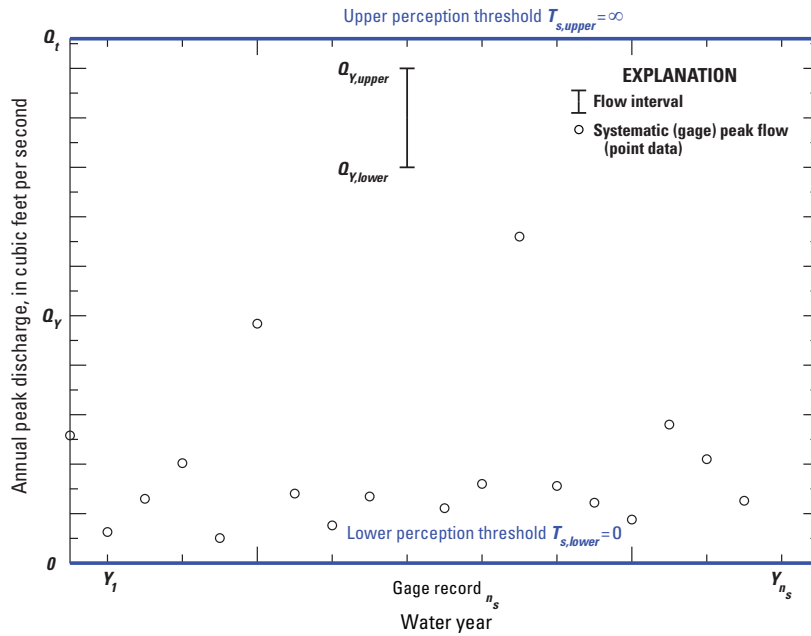


Figure 3–1. Graph showing typical flow intervals and perception thresholds for gaging stations. The perceptible range for the systematic (gage) period $T_{s,lower}, T_{s,upper} (0, \infty)$ is shown as blue lines.

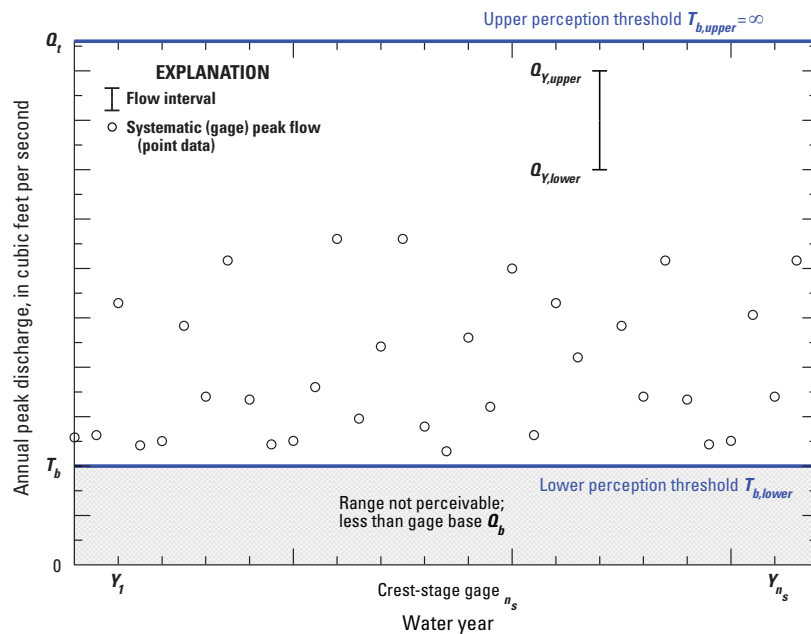


Figure 3–2. Graph showing typical flow intervals and perception thresholds for crest-stage gages. The perceptible range for the crest-stage gage period $T_{b,lower}, T_{b,upper} (T_b, \infty)$ is shown as blue lines.

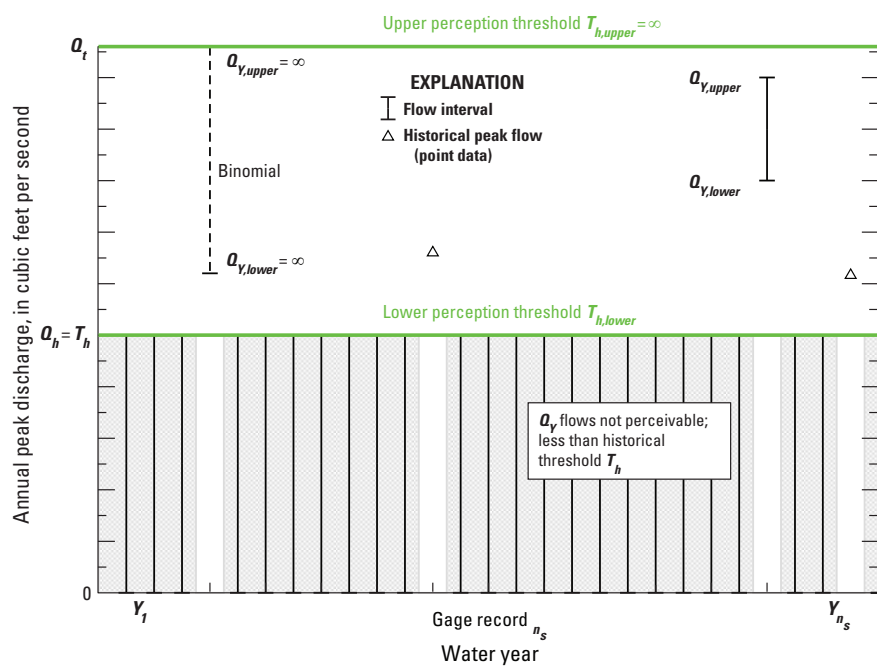


Figure 3–3. Graph showing typical flow intervals and perception thresholds for historical data. The perceptible range for the historical period $T_{h,lower}, T_{h,upper}$ (T_h, ∞) is shown as green lines.

Appendix 4. Initial Data Analysis

When conducting a flood frequency analysis, an initial step is to undertake basic analysis of the peak-flow time series to check for obvious errors and to check that the data conform to the assumptions used in the frequency analysis. One of the main assumptions in flood frequency analysis is that the data in the peak-flow time series are independent and identically distributed. Some tests that check that these assumptions are reasonable for a particular time series include tests for autocorrelation and nonstationarity. Visual inspection of the time series can also reveal issues that need to be addressed.

Visual Inspection—Plot the Data

Before any formal statistical tests are employed, a visual inspection of a plot of the peak-flow time series can be used to help identify any potential errors with the data. For example, any peaks that are orders of magnitude different from the others should be verified. Visual inspection of the time-series plot may also reveal obvious changes in the mean or standard deviation of the peak-flow data over time. For example, construction of a dam and reservoir may drastically alter peak-flow time series and the entire pre- and post-dam time series should not be used together for a peak-flow frequency analysis.

Autocorrelation

It is recommended that an annual flood series be examined for autocorrelation through the use of a correlogram ([Salas, 1993](#)). In an autocorrelated time series, the value in one time step is correlated with the value in a previous (and future) time step. Autocorrelated time series can also be said to exhibit persistence. Hydrologic time series will often exhibit long-term persistence. Note that this can affect trend testing, as discussed in the next section.

Trends and Shifts

The peak-flow frequency analysis methods described in this document are only applicable when the peak-flow data are believed to be part of the same underlying population. Changes in peak-flow generation processes can lead to gradual trends or abrupt shifts in the peak-flow time series. Statistical tests for trends and shifts can be useful for detecting such changes in the peak-flow time series. Depending on the likely causes and the magnitude of any detected changes, different treatments may be needed before Bulletin 17C methods can be applied. A particularly difficult case is when it is unknown whether the apparent trend will continue, level off, or reverse in the future. Possible approaches for dealing with such changes have been discussed in the research literature, but a consensus on best practices has not yet emerged. Consequently, substantial judgment must be exercised when trends are found.

Changes may occur gradually or abruptly and different tests are commonly used to test for the presence of either type of change. A visual inspection of a plot of the annual peak-flow time series should be the first step in assessing the time series. It is recommended that this be followed by trend tests to help assess whether changes over time may be important for the flood frequency analysis. This can be followed by a change point test for an abrupt change, if desired. The specific tests described below have been used frequently, but other tests may also be considered.

72 Guidelines for Determining Flood Flow Frequency—Bulletin 17C

Trend tests and change point analysis are most commonly done on the mean values of a time series, but tests for change in the variance of a time series can also be considered. Note that these tests can be sensitive to the start and end points used in the analysis. For example, if the period of record happens to either start or end with a large peak, there may be an apparent trend in the data. However, this apparent trend may simply be the result of the particular sample that was used. A slightly longer or shorter record would not show the same apparent trend. In other cases, the period of record may include only the drying or wetting phase of an oscillation with long periodicity. The apparent trend results from a finite record length, but in this case a much longer period of record is needed to fully understand the data.

Statistical Tests

A common test for trends in a time series is the Mann-Kendall test. This test uses Kendall's τ as the test statistic to measure the strength of the monotonic relationship between annual peak streamflow and the year in which it occurred. The Mann-Kendall test is nonparametric and does not require that the data conform to any specific statistical distribution. The statistic is calculated using the difference between concordant and discordant data pairs of the observed streamflow peaks with time, and not the actual magnitudes of the data values (Helsel and Hirsch, 2002). Positive values for τ indicate that occurrences of annual peak streamflows are increasing with time for the period of record, whereas negative values of τ indicate that annual peak streamflows are decreasing with time for the period of record.

As with other statistical tests, a p-value can be calculated for the test. Note that the p-values will be correct only when there is no serial correlation in the annual time series. This requirement can be problematic for hydrologic time series, which can exhibit short-term and long-term persistence (Cohn and Lins, 2005).

In addition to the statistical significance of a trend, the actual magnitude of the trend should be considered. The Theil slope (Helsel and Hirsch, 2002, p. 266) can be calculated in conjunction with Kendall's τ for this purpose. It is calculated as the median of all the slopes calculated by using all the possible pairs of peak-flow values and years, and is a nonparametric estimate of the slope.

In some situations, there may be an abrupt shift (McCabe and Wolock, 2002) or change in the time series, rather than a gradual trend. For example, there may be distinct periods, exhibiting different flood characteristics, before and after installation of flood-control structures. In other cases, the reason for the step change may not be as evident, but abrupt changes may still be found. Villarini and others (2009a), for example, found step changes that appeared to coincide with changes in the streamgage location. To refine the analysis, the test for a monotonic trend could be followed by a test for a step change. The Wilcoxon rank-sum test (also known as the Mann-Whitney test) or the Kolmogorov-Smirnov test are both nonparametric tests that can be used to test for differences between two samples, when there is a suitable hypothesis for separating the time series into two or more sections (Helsel and Hirsch, 2002). The potential step change should not be identified solely on the basis of visual inspection of the data, as this biases the test. The Pettitt test (Pettitt, 1979; Mallakpour and Villarini, 2016) and Lombard's Smooth Change Model (Lombard, 1987; Nayak and Villarini, 2016) have both been suggested as alternative tests for abrupt changes that do not require an analyst to predetermine where a likely change occurs (Villarini and others, 2009a; Quessy and others, 2011). Additional information on these tests can be found in Helsel and Hirsch (2002) and other statistical textbooks. Some information on changepoint tests is available in supplementary material on the Bulletin 17C website at <https://acwi.gov/hydrology/Frequency/b17c/>.

Example—Skokie River near Highland Park, Illinois

This example uses data from USGS gaging station 05535070, Skokie River near Highland Park, Illinois. Figure 4–1 shows a time-series plot of the Skokie River. It is a 21.1-square mile (mi^2) watershed that has

become more and more urbanized over time. The urbanized fraction was about 0.60 at the beginning of the period of record in 1967, and increased to about 0.90 by 2014 ([Over and others, 2016](#)). Visual inspection of the time series reveals an increasing trend over time.

The visual trend is confirmed with the Mann-Kendall test. The results from the test are as follows: $\tau = 0.321$, p-value = 0.00156, and Theil slope = 8.4 ft³/s per year. The annual peak flows at this station are not significantly autocorrelated, as shown in figure 4–2. This indicates that the estimated p-value is appropriate and is unaffected by autocorrelation.

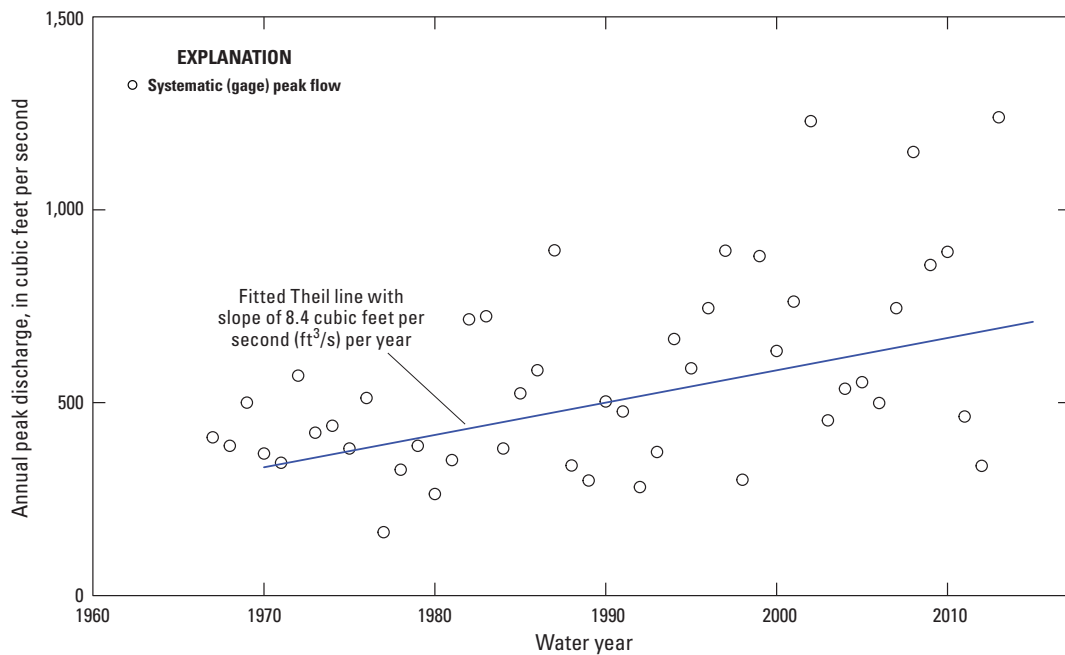


Figure 4–1. Graph showing U.S. Geological Survey station 05535070 Skokie River near Highland Park, Illinois, time-series plot. Annual peak discharges have increased at this streamgage because of urbanization. The line is the fitted Theil line with a slope of 8.4 cubic feet per second (ft³/s) per year.

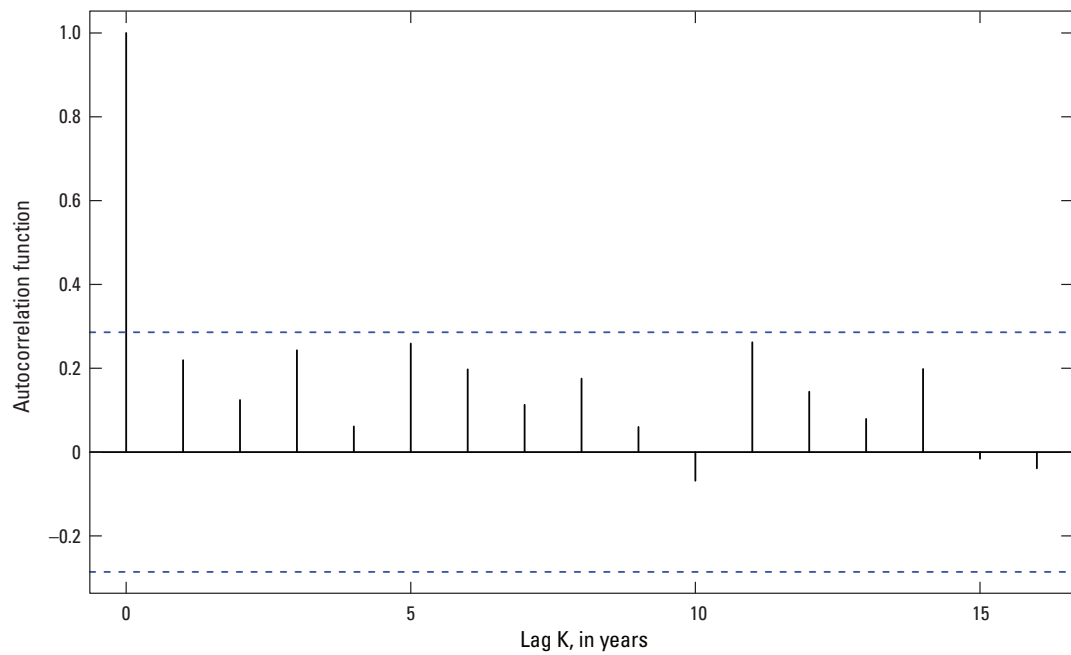


Figure 4–2. Graph showing U.S. Geological Survey station 05535070 Skokie River near Highland Park, Illinois, autocorrelation plot. The annual peaks do not exhibit any statistically significant autocorrelation for lag times between 1 and 15 years. The dashed lines are the thresholds for significant autocorrelation.

Appendix 5. Threshold-Exceedance Plotting Positions

This appendix provides an overview and equations for threshold-exceedance-based plotting positions. Table 5–1 provides plotting position parameters a and their motivation. A plotting parameter $a = 0$, corresponding to a Weibull formula and is recommended as a default value, consistent with current practice. Other plotting parameters, including 0.40 (Cunnane), 0.44 (Gringorten), and 0.50 (Hazen), are traditional choices that may also be considered. Some examples are shown in appendix 10.

Consider a historical flood record with an n_h -year historical period in addition to a complete n_s -year gaged flood record. Assume that during the total $n = (n_s + n_h)$ years of record, a total of k floods exceeded a perception threshold for historical floods (fig. 3). If the k values that exceeded the threshold are indexed by $i = 1, \dots, k$, reasonable plotting positions approximating the exceedance probabilities with the interval $(0, p_e)$ are

$$p_i = p_e \left(\frac{1 - a}{k + 1 - 2a} \right) = \frac{k}{n} \left(\frac{i - a}{k + 1 - 2a} \right) \quad (5-1)$$

where a is a value from table 5–1 and $p_e = k/n$ is the probability of exceeding a threshold. For $k \gg (1 - 2a)$, p_i is indistinguishable from $\frac{i - a}{n + 1 - 2a}$ for a single threshold. Hirsch (1987) notes that for the first k floods, equation 5–1 is identical to the Hazen formula with $a = 0.5$, and is very close to the Gringorten formula with $a = 0.44$. Reasonable choices for a generally make little difference to the resulting plotting positions.

The plotting positions for systematic record floods below the threshold must be adjusted to reflect the additional information provided by the historical flood record, if the historical flood data and the systematic record are to be analyzed jointly in a consistent and statistically efficient manner (Hirsch and Stedinger, 1987). In this case, let e_s be the number of gaged-record floods that exceeded the threshold and, hence, are counted among the k exceedances of that threshold. Plotting positions within $(p_e, 1)$ for the remaining $(n_s - e_s)$ below-threshold gaged-record floods are

$$p_r = p_e + (1 - p_e) \left(\frac{r - a}{n_s - e_s + 1 - 2a} \right) \quad (5-2)$$

for $r = 1$ through $n_s - e_s$, where a is again a value from table 5–1.

This approach directly generalizes to several thresholds. For the multiple exceedance threshold cases shown in figure 12, equation 5–1 can be generalized (Hirsch and Stedinger, 1987; Stedinger and others, 1988, 1993). The number of thresholds is defined as j ($j = 1, \dots, m$), where the thresholds Q_j ($j = 1, \dots, m$) are ordered (sorted) from largest to smallest such that $Q_1 > Q_2 > \dots > Q_m$. The probability of exceedance p_{e_j} for each threshold j is defined as

$$p_{e_j} = p_{e_{j-1}} + (1 - p_{e_{j-1}}) q_{e_j} \quad (5-3)$$

where q_{e_j} is the conditional probability that a flood falls between the j -th and $(j - 1)$ -th threshold. It is defined by

$$q_{e_j} = \frac{k_j}{n_j - \sum_{l=1}^{j-1} k_l} \quad (5-4)$$

76 Guidelines for Determining Flood Flow Frequency—Bulletin 17C

where k_j is the number of floods that exceed threshold j but not any higher thresholds ($j - 1$), and the denominator in equation 5–4 is the number of years (n_j) that threshold Q_j applies minus the sum of all floods k_l that exceed any higher ($j - 1, j - 2, \dots$) thresholds during period n_j . The above-threshold floods may be plotted by

$$p_i = p_{e_{j-1}} + (1 - p_{e_{j-1}}) q_{e_j} \left(\frac{i - a}{k_j + 1 - 2a} \right) \quad (5-5)$$

and the floods below all thresholds ($k_j + 1, \dots, g$) can be plotted using equation 5–2 with p_e equal to p_{e_j} .

Table 5-1. Typical plotting position parameter a values and their motivation
(Stedinger and others, 1993).

Method	a	Motivation
Weibull	0	Unbiased exceedance probabilities for all distributions
Cunnane	0.40	Approximately quantile-unbiased
Gringorten	0.44	Optimized for Gumbel distribution
Hazen	0.50	A traditional choice

Appendix 6. Potentially Influential Low Floods

This appendix provides a general introduction to potentially influential low floods (PILFs), and describes computation details for identifying PILFs—the Multiple Grubbs-Beck Test (MGBT). Some details on MGBT and its performance are documented in [Cohn and others \(2013\)](#), [Lamontagne and others \(2013\)](#), and [Lamontagne and others \(2016\)](#). Some examples of detecting PILFs with the MGBT are provided in appendix 10.

PILF Background and Philosophy

There are recognized problems with the Grubbs-Beck (GB) test ([Grubbs and Beck, 1972](#)) used in Bulletin 17B ([IACWD, 1982](#)) when there are multiple low outliers. This issue was discussed in the Bulletin 17B Frequently Asked Questions (FAQ), under the section “Low Outliers” written by Bill Kirby. Relevant portions of that FAQ are reproduced here, with **emphasis** on the important issues.

Bulletin 17B detects low outliers by means of a statistical criterion (the GB test) rather than by consideration of the influence of low-lying data points on the fit of the frequency curve. The test is based on the standardized distances, $(x_i - \hat{\mu})/\hat{\sigma}$, between the lowest observations and the mean of the dataset. **The test is easily defeated by occurrence of multiple low outliers, which exert a large distorting influence on the fitted frequency curve, but also increase the standard deviation, $\hat{\sigma}$, thereby making the standardized distance too small to trigger the Grubbs-Beck test.**

The FAQ also provides further background, and a hydrological basis to deviate from the GB test as follows, with **emphasis** on the relevant text.

Obviously, the intention is to allow as many low outliers to be designated as necessary to achieve a good fit to the part of the dataset that contains the significant flood and near-flood events. Equally obviously, the intention is that the GB result be used unless the resulting poor fit gives compelling justification for not doing so. There is no universal method that can be followed blindly to achieve a good fit. The sensitivity analysis alluded to in Bulletin 17B is **based on the engineering-hydrologic-common-sense proposition that the smallest observations in the dataset do not convey meaningful or valid information about the magnitude of significant flooding, although they do convey valid information about the frequency of significant flooding. Therefore, if the upper tail of the frequency curve is sensitive to the numerical values of the smallest observations, then that sensitivity is a spurious artifact based on the mathematical form of the assumed, but in fact unknown, flood distribution, and has no hydrologic validity.**

Others have noted this hydrologic phenomenon. A key observation is from [Klemeš \(1986, p. 183S\)](#), reproduced as follows: “For it is by no means hydrologically obvious why the regime of the highest floods should be affected by the regime of flows in years when no floods occur, why the probability of a severe storm hitting this basin should depend on the accumulation of snow in the few driest winters, why the return period of a given heavy rain should be by an order of magnitude different depending, say, on slight temperature fluctuations during the melting seasons of a couple of years (p. 183S).”

[Klemeš \(2000, p. 229\)](#) also described this hydrological problem in the context of frequency distributions, as follows, with **emphasis** on the relevant text.

“... It is ironic that the only clue the FA (Frequency Analysis) theory inadvertently takes from hydrology is the wrong one. It derives the “distributional assumptions” [i.e., the general shape of F(X)] from a “probability plot” such as Fig. 1(b) whose shape is dominated by the small and medium observations. This shape is generally convex on the Gaussian plot, because hydrological phenomena like precipitation, runoff, snow cover,

78 Guidelines for Determining Flood Flow Frequency—Bulletin 17C

etc., have a zero lower bound, which “bends” the lower tail of the plot towards a horizontal asymptote. As a result, all the “standard” distribution models are convex on Gaussian frequency scale; they all are models with positive skewness. **Hence, it is the physical regime prevailing in the formation of the lower tail that determines the shape of the extrapolated upper tail; observations that are hydrologically least relevant to the high extremes and to the safety of facilities affected by them—have the greatest influence on their estimated “probabilities”! . . .**

These observations, as well as the data issues described in the section [Zero Flows and Potentially Influential Low Floods](#), are handled with the MGBT.

Computational Details for Identifying PILFs with MGBT

The purpose of using the MGBT is to identify PILFs. PILFs are small observations (or zero flows) that potentially have a large influence on the fitted frequency curves. When datasets are negatively skewed, the smallest observations can be very influential in determining the estimated skewness coefficient and the estimated 1 percent AEP flood. The new MGBT is a statistically appropriate generalization of the GB test that is sensitive to the possibility that several of the smallest observations are “unusual,” or are potentially very influential. The MGBT also correctly evaluates cases where one or more observations are zero, or are below a recording threshold (partial record sites). Thus, it provides a consistent, objective, and statistically defensible algorithm that considers whether a range of the smallest observations should be classified as PILFs for a wide range of situations that are observed in practice (see, for example, cases in [Lamontagne and others \(2012\)](#), [Paretti and others \(2014a\)](#), and examples in appendix 10).

To provide an objective criteria for multiple low outlier identification, MGBT employs the actual distribution of the k -th largest observation in a sample of n independent normal variates, where the probability $p_{[k:n]}$ that the k -th largest observation in a normal sample of size n might have appeared to be smaller than the value observed ([Cohn and others, 2013](#)). If $p_{[k:n]}$ is small, then the k -th observation is unusually small.

To test null hypothesis H_0 , we consider whether $\{X_{[1:n]}, X_{[2:n]}, \dots, X_{[n:n]}\}$ are consistent with a normal distribution and the other observations in the sample by examining the statistic

$$\tilde{\omega} \equiv \frac{X_{[k:n]} - \hat{\mu}_k}{\hat{\sigma}_k} \quad (6-1)$$

where $X_{[k:n]}$ denotes the k -th smallest order statistic in the sample, and

$$\hat{\mu}_k = \frac{1}{n-k} \sum_{j=k+1}^n X_{[j:n]} \quad (6-2)$$

$$\hat{\sigma}_k^2 = \frac{1}{n-k-1} \sum_{j=k+1}^n (X_{[j:n]} - \hat{\mu}_k)^2. \quad (6-3)$$

The partial mean ($\hat{\mu}_k$) and partial variance ($\hat{\sigma}_k^2$) are computed based on all observations larger than $X_{[k:n]}$ to avoid swamping (specifying too many outliers). Each observation $X_{[k:n]}$ is tested sequentially. These larger observations greater than X_k are not suspected of being low outliers, thus $\hat{\mu}_k$ and $\hat{\sigma}_k^2$ are assumed to correspond to the population of interest. From $\tilde{\omega}$, we calculate the p-value: the probability given H_0 of obtaining a value of $\tilde{\omega}_{[k:n]}$ as small or smaller than that observed in the sample. The p-value of interest is given by

$$p_k[\eta] \equiv P [\tilde{\omega}_{[k:n]} < \eta]. \quad (6-4)$$

Substituting the definition of $\tilde{\omega}_{[k:n]}$ from equation 6–1 and rearranging the terms yields (Cohn and others, 2013)

$$p_k[\eta] = P \left[\left(\frac{Z_{[k:n]} - \hat{\mu}_{Z,k}}{\hat{\sigma}_{Z,k}} \right) < \eta \right] \quad (6-5)$$

where $Z_{[k:n]}$ is the k -th order statistic in a standard normal sample of size n , and $\hat{\mu}_{Z,k}, \hat{\sigma}_{Z,k}$ are the partial mean and standard deviation of the normal sample. If that p-value is small (for example, less than $\alpha = 10$ percent), then the k smallest observations are declared PILFs, such as those shown in figure 11. The PILF threshold X_l that is used in EMA is set to the $(k + 1)$ -th value.

The MGBT for identifying PILFs has two steps. The input data are base-10 logarithms X_j of annual peak flows from the systematic (gaging) record (n_s), with flow values exactly known as point observations ($Q_{Y,lower} = Q_{Y,upper} = Q_Y$). Flows are ranked from smallest to largest, as noted in the section [Zero Flows and Identifying Potentially Influential Low Floods](#).

1. Starting at the median and sweeping **outward** towards the smallest observation, each observation $X_{[k:n]}$ is tested and is identified as an outlier if $p(k;n) \leq \alpha_{out}$. If the k -th largest observation is identified as a low outlier, the outward sweep stops and the k -th and all smaller observations (that is, for all $j \leq k$) are also identified as low outliers.
2. An **inward** sweep starts at the smallest observation $X_{[1:n]}$ and moves towards the median, where the j -th observation is identified as an outlier if $p(k;n) \leq \alpha_{in}$. If an observation $m = 1, 2, \dots, n/2$ fails to be identified as an outlier by the inward sweep, the inward sweep stops.

The number of PILFs identified by the procedure is then the larger of k and $m - 1$.

The algorithm has two parameters: an **outward sweep** significance level α_{out} , and an **inward sweep** significance level α_{in} . The recommended values used in MGBT are $\alpha_{out} = 0.005$ (0.5 percent) and $\alpha_{in} = 0.10$ (10 percent). These values were determined through extensive testing and evaluation by the HFAWG through careful examination of 82 sites (Cohn and others, [in press](#)), testing and performance of alternatives (Lamontagne and others, 2013), and further investigations (Lamontagne and others, 2016).

The **outward** sweep seeks to determine if there is some break in the lower half of the data that would suggest the sample is best treated as if it had a number of low outliers. The **inward** sweep using a less severe significance level, $p(k; n) \leq 10$ percent, mimics Bulletin 17B's willingness to identify one or more of the smallest observations as low outliers so that the analysis is more robust. Bulletin 17B also used a 10 percent significance test with its single GB threshold. However, a critical difference is that the MGBT **inward** sweep uses the $p(k; n)$ function, which correctly describes whether the k -th largest observation in a normal sample of n variates is unusual.

For example, if a record has five zero flows, then the smallest nonzero flow is considered to be the sixth smallest observation in the record. This correctly reflects the fact that the flood record included five smaller values. The GB test in Bulletin 17B includes no mechanism for correcting its threshold when testing the smallest nonzero flood value in a record containing zeros, or below-threshold discharges at sites with crest-stage gages. This is particularly problematic because sites with zero flows are very likely to include one or more very small or near-zero flood values, which should legitimately be identified as low outliers were a statistically appropriate threshold employed. The MGBT solves this problem. Finally, computer programs (see the section [Software and Examples](#)) are used to perform the MGBT and report critical values and PILFs.

Appendix 7. Expected Moments Algorithm (EMA)

This appendix describes features of EMA, including some computational details, a generalized expected moments algorithm, and uncertainty of EMA moments, and confidence intervals with EMA.

EMA Computational Details

The EMA moments for the general situation with a historical flood perception threshold X_h and a PILF threshold X_l are as follows:

$$\hat{\mu}_{i+1} = \frac{\sum X_s^> + \sum X_l^> + \sum X_h^> + n_l^< E[X_l^<] + n_h^< E[X_h^<]}{n_s + n_h} \quad (7-1)$$

$$\begin{aligned} \hat{\sigma}_{i+1}^2 = \frac{c_2}{n} & \left[\sum(X_s^> - \hat{\mu}_i)^2 + \sum(X_l^> - \hat{\mu}_i)^2 + \sum(X_h^> - \hat{\mu}_i)^2 \right. \\ & \left. + n_l^< E[(X_l^< - \hat{\mu}_i)^2] + n_h^< E[(X_h^< - \hat{\mu}_i)^2] \right] \end{aligned} \quad (7-2)$$

$$\begin{aligned} \hat{\gamma}_{i+1} = \frac{c_3}{n\hat{\sigma}_{i+1}^3} & \left[\sum(X_s^> - \hat{\mu}_i)^3 + \sum(X_l^> - \hat{\mu}_i)^3 \right. \\ & + \sum(X_h^> - \hat{\mu}_i)^3 + n_l^< E[(X_l^< - \hat{\mu}_i)^3] \\ & \left. + n_h^< E[(X_h^< - \hat{\mu}_i)^3] \right] \end{aligned} \quad (7-3)$$

where c_2 and c_3 are bias correction factors, defined as

$$c_2 = \frac{n_s + n_h^>}{n_s + n_h^> - 1} \quad (7-4)$$

$$c_3 = \frac{(n_s + n_h^>)^2}{(n_s + n_h^> - 1)(n_s + n_h^> - 2)} \quad (7-5)$$

and recalling $n_s + n_h = n$.

The expression $E[X_h^<]$ is the expected value of an observation known to have a value less than the historical threshold X_h , and is a conditional expectation given that $X < X_h$, and is evaluated with

$$E[X|X \leq X_h; \hat{\tau}, \hat{\alpha}, \hat{\beta}] = \hat{\tau} + \hat{\beta} \frac{\Gamma\left(\frac{X_h - \hat{\tau}}{\hat{\beta}}, \hat{\alpha} + 1\right)}{\Gamma\left(\frac{X_h - \hat{\tau}}{\hat{\beta}}, \hat{\alpha}\right)} \quad (7-6)$$

where $\Gamma(y, \alpha)$ is the incomplete gamma function

$$\Gamma(y, \alpha) = \int_0^y t^{\alpha-1} \exp(-t) dt. \quad (7-7)$$

The expectation for higher order moments is

$$\begin{aligned} & E[(X - \hat{\mu})^p | X \leq X_h; \hat{\tau}, \hat{\alpha}, \hat{\beta}] \\ &= \sum_{j=0}^p \binom{p}{j} \hat{\beta}^j (\hat{\tau} - \hat{\mu})^{p-j} \left[\frac{\Gamma\left(\frac{X_h - \hat{\tau}}{\hat{\beta}}, \hat{\alpha} + j\right)}{\Gamma\left(\frac{X_h - \hat{\tau}}{\hat{\beta}}, \hat{\alpha}\right)} \right] \end{aligned} \quad (7-8)$$

where p is the central moment index ($p = 2, 3$). The conditional expectation for PILFs with $X < X_l$ and threshold X_l are similar to equations 7-6 and 7-8.

The EMA moments shown in equations 7-1 through 7-3, and expected values shown in equations 7-6 and 7-8, utilize observations whose magnitudes are exactly known, where $X_{lower} = X_{upper}$. In the cases where flow magnitudes are described by intervals or binomial observations, these equations are modified to account for logarithms of flow intervals ($X_{Y,lower}, X_{Y,upper}$) and are presented in equation 7-9. Information from broken, incomplete, and discontinued records, crest-stage gages, and multiple thresholds (for example, fig. 12) is easily represented by including additional expected value terms in the moments for each year Y or period where the flow interval or perception threshold varies.

The EMA employs the peak-flow intervals (Q_{lower}, Q_{upper}) to estimate the moments of the LP-III distribution. Using base-10 logarithms of flows, where $X_{lower} = \log_{10}(Q_{lower})$ and $X_{upper} = \log_{10}(Q_{upper})$, interval and binomial censored data are employed by replacing equation 7-8 with the following (Cohn and others, 1997):

$$\begin{aligned} & E[(X - \hat{\mu})^p | X_{lower} \leq X \leq X_{upper}; \hat{\tau}, \hat{\alpha}, \hat{\beta}] \\ &= \sum_{j=0}^p \binom{p}{j} \hat{\beta}^j (\hat{\tau} - \hat{\mu})^{p-j} \times \\ & \left[\frac{\Gamma\left(\frac{X_{upper} - \hat{\tau}}{\hat{\beta}}, \hat{\alpha} + j\right) - \Gamma\left(\frac{X_{lower} - \hat{\tau}}{\hat{\beta}}, \hat{\alpha} + j\right)}{\Gamma\left(\frac{X_{upper} - \hat{\tau}}{\hat{\beta}}, \hat{\alpha}\right) - \Gamma\left(\frac{X_{lower} - \hat{\tau}}{\hat{\beta}}, \hat{\alpha}\right)} \right]. \end{aligned} \quad (7-9)$$

When information from a regional skew coefficient G is available, it is included directly in the EMA, ensuring that the adjusted mean and standard deviation fit the data. Equation 7-3 for the skew coefficient $\hat{\gamma}_{i+1}$ is modified to include G , as

$$\begin{aligned} \hat{\gamma}_{i+1} = \frac{1}{(n + n_G)\hat{\sigma}_{i+1}^3} & \left[c_3 \left\{ \sum(X_s^> - \hat{\mu}_i)^3 + \sum(X_l^> - \hat{\mu}_i)^3 \right. \right. \\ & + \sum(X_h^> - \hat{\mu}_i)^3 + n_l^< E[(X_l^< - \hat{\mu}_i)^3] \\ & \left. \left. + n_h^< E[(X_h^< - \hat{\mu}_i)^3] \right\} + n_G G \hat{\sigma}_{i+1}^3 \right] \end{aligned} \quad (7-10)$$

where n_G is the additional years of record assigned to the regional skew G (Griffis and others, 2004). A skew constraint is imposed on each EMA iteration so that $\hat{\gamma}_{i+1} > -1.4$, as it is unlikely that the population skew would be less than -1.4 .

82 Guidelines for Determining Flood Flow Frequency—Bulletin 17C

A general listing of computations for flood flow frequency using EMA, which are implemented in software (see the section [Software and Examples](#)), is as follows:

1. Check for low outliers with MGBT. If low outliers are detected, recode flows as censored data with an interval ($Q_{Y,lower} = 0, Q_{Y,upper} = Q_{lower}$). Adjust perception thresholds accordingly: ($T_{Y,lower} = Q_{lower}, T_{Y,upper} = \infty$).
2. Organize all flow intervals and perception thresholds for estimating parameters and confidence intervals.
3. Begin iterative fitting of the LP-III distribution using EMA with all data, including regional skew information. For each iteration, ensure that the weighted skew coefficient $\tilde{G} \geq -1.41$ and the largest observation is within the fitted support of the distribution (for skews < 0).
 - (a) Fit the LP-III with EMA, using at-site data, to estimate the at-site skew;
 - (b) Estimate the at-site skew coefficient MSE with EMA;
 - (c) Estimate a weighted skew coefficient;
 - (d) Fit the LP-III with EMA using a weighted skew coefficient; and
 - (e) Test for convergence of EMA moments. If not converged, return to 3a.
4. Estimate quantile variances and compute confidence intervals based on the fitted LP-III model, including at-site and regional skew uncertainty.

The Generalized Expected Moments Algorithm

This section presents parameterizations of the P-III distribution and a generalized Expected Moments Algorithm. The notation and terms are utilized to explain uncertainty of EMA moments and confidence intervals. Bold terms, such as \mathbf{M} and $\boldsymbol{\theta}$, are used to indicate vectors or matrices. Carets (^) represent a sample estimate and tildes (~) indicate noncentral moments (on scalars) or estimators (on vectors).

The P-III distribution is typically characterized by three parameters that correspond to location $\{\tau\}$, scale $\{\beta\}$, and shape $\{\alpha\}$, where the vector $\boldsymbol{\theta} = \{\tau, \alpha, \beta\}$. The P-III distribution is also characterized by noncentral moments $\boldsymbol{\mu} = \{\tilde{\mu}_1, \tilde{\mu}_2, \tilde{\mu}_3\}$ (about zero) for algebraic tractability, and central moments $\mathbf{M} = \{M, S, G\} = \{\mu, \sigma, \gamma\}$ for simplicity of explanation.

Central moments are defined as

$$\begin{aligned} \mathbf{M} &= \begin{bmatrix} M \\ S \\ G \end{bmatrix} \equiv \begin{bmatrix} E[X] \\ \sqrt{E[(X - M)^2]} \\ E[(X - M)^3]/S^3 \end{bmatrix} \equiv \begin{bmatrix} \tilde{\mu}_1 \\ \sqrt{\tilde{\mu}_2 - \tilde{\mu}_1^2} \\ \frac{\tilde{\mu}_3 - 3\tilde{\mu}_2\tilde{\mu}_1 + 2\tilde{\mu}_1^3}{\sqrt{\tilde{\mu}_2 - \tilde{\mu}_1^2}} \end{bmatrix} \\ &\equiv \begin{bmatrix} \tau + \alpha\beta \\ \sqrt{\alpha\beta^2} \\ \text{sign}(\beta)2/\sqrt{\alpha} \end{bmatrix}. \end{aligned} \quad (7-11)$$

Noncentral moments are

$$\begin{aligned}\tilde{\boldsymbol{\mu}} &\equiv \begin{bmatrix} \tilde{\mu}_1 \\ \tilde{\mu}_2 \\ \tilde{\mu}_3 \end{bmatrix} \equiv \begin{bmatrix} E_{\theta}[X] \\ E_{\theta}[X^2] \\ E_{\theta}[X^3] \end{bmatrix} \equiv \begin{bmatrix} M \\ S^2 + M^2 \\ S^3 G + 3S^2 M + M^3 \end{bmatrix} \\ &\equiv \begin{bmatrix} \alpha\beta + \tau \\ \alpha(1+\alpha)\beta^2 + 2\alpha\beta\tau + \tau^2 \\ \alpha(1+\alpha)(2+\alpha)\beta^3 + 3\alpha(1+\alpha)\beta^2\tau + 3\alpha\beta\tau^2 + \tau^3 \end{bmatrix}. \quad (7-12)\end{aligned}$$

The P-III distribution parameters are

$$\boldsymbol{\theta} = \begin{bmatrix} \alpha \\ \beta \\ \tau \end{bmatrix} = \begin{bmatrix} 4/G^2 \\ SG/2 \\ M - 2S/G \end{bmatrix} \begin{bmatrix} \frac{4(\tilde{\mu}_2 - \tilde{\mu}_1^2)^3}{(\tilde{\mu}_3 - 3\tilde{\mu}_2\tilde{\mu}_1 + 2\tilde{\mu}_1^3)^2} \\ \frac{\tilde{\mu}_3 - 3\tilde{\mu}_2\tilde{\mu}_1 + 2\tilde{\mu}_1^3}{2(\tilde{\mu}_2 - \tilde{\mu}_1^2)} \\ \frac{\tilde{\mu}_3\tilde{\mu}_1 - 2\tilde{\mu}_2^2 + \tilde{\mu}_2\tilde{\mu}_1^2}{\tilde{\mu}_3 - 3\tilde{\mu}_2\tilde{\mu}_1 + 2\tilde{\mu}_1^3} \end{bmatrix}. \quad (7-13)$$

Here, $E[\cdot]$ denotes the expectation operator. The formulas in equations 7-11, 7-12 and 7-13 facilitate converting one parametrization to another. When using sample estimates, the conversion from noncentral moments $\hat{\boldsymbol{\mu}}$ to central moments \mathbf{M} needs to include bias-correction factors with

$$\hat{\mathbf{M}} = \begin{bmatrix} 1 & \frac{N}{N-1} & \frac{\sqrt{N(N-1)}}{(N-2)} \end{bmatrix} * (\hat{\boldsymbol{\mu}}) \quad (7-14)$$

where $*$ indicates matrix multiplication.

A generalized EMA employing central moments \mathbf{M} is as follows, where N is the total record length. For convenience in the equations, the terms are abbreviated as $X_{i,lower} = X_{i,l}$ and $X_{i,upper} = X_{i,u}$.

1. Initialize

- (a) Set $\hat{\mathbf{M}}_0 = \{0, 1, 0\}$
- (b) Define $\epsilon > 0$ as a satisfactory level of convergence.

A typical value for ϵ is 10^{-10} .

2. Iterate: for $j = 1, 2, \dots$

- (a) Update expected moments

$$\hat{\mathbf{M}}_j = \begin{bmatrix} M_j \\ S_j^2 \\ G_j \end{bmatrix} = \begin{bmatrix} \frac{1}{N} \sum_{i=1}^N E_{\tilde{\mathbf{M}}_{j-1}}[X_i | X_{i,1} \leq X_i < X_{i,u}] \\ \frac{1}{N-1} \sum_{i=1}^N E_{\tilde{\mathbf{M}}_{j-1}}[(X_i - M_j)^2 | X_{i,1} \leq X_i < X_{i,u}] \\ \frac{N}{S^3(N-1)(N-2)} \sum_{i=1}^N E_{\tilde{\mathbf{M}}_{j-1}}[(X_i - M_j)^3 | X_{i,1} \leq X_i < X_{i,u}] \end{bmatrix} \quad (7-15)$$

where

$$E_{\tilde{\mathbf{M}}_{j-1}}[(X_i - M_j)^k | X_{i,1} \leq X_i < X_{i,u}] = \sum_{l=0}^k \binom{k}{l} E_{\tilde{\mathbf{M}}_{j-1}}[X_i^l | X_{i,1} \leq X_i < X_{i,u}] (-M_j)^{k-l}$$

(7-16)

and, if the upper and lower bounds on X_i are equal (for example, $X_{i,l} = X_{i,u}$, which means we know the exact value of X_i), then

$$E_{\tilde{\mathbf{M}}_{j-1}}[X_i^k | X_{i,l} \leq X_i < X_{i,u}] = X_{i,l}^k = X_{i,u}^k. \quad (7-17)$$

If $X_{i,l} < X_{i,u}$, then we have to evaluate the expectation

$$E_\theta[X^k | X_{i,l} \leq X < X_{i,u}] = \begin{cases} \sum_{j=0}^k \binom{k}{j} \beta^j \tau^{k-j} \left(\frac{\Gamma(\alpha+j, \frac{X_{i,u}-\tau}{\beta}, \frac{X_{i,l}-\tau}{\beta})}{\Gamma(\alpha, \frac{X_{i,u}-\tau}{\beta}, \frac{X_{i,l}-\tau}{\beta})} \right) & \beta < 0 \\ \sum_{j=0}^k \binom{k}{j} \beta^j \tau^{k-j} \left(\frac{\Gamma(\alpha+j, \frac{X_{i,l}-\tau}{\beta}, \frac{X_{i,u}-\tau}{\beta})}{\Gamma(\alpha, \frac{X_{i,l}-\tau}{\beta}, \frac{X_{i,u}-\tau}{\beta})} \right) & \beta > 0 \end{cases} \quad (7-18)$$

where θ is the P-III parameters corresponding to $\tilde{\mathbf{M}}_{j-1}$, and

$$\Gamma(\alpha, X_{i,l}, X_{i,u}) = \int_{\max(0, X_{i,l})}^{\max(0, X_{i,u})} t^{\alpha-1} \exp(-t) dt. \quad (7-19)$$

(b) If available, weight with regional skew. This can be done conceptually via:

$$\tilde{G}_j = \frac{\text{MSE}_G \times \hat{\gamma}_j + \text{MSE}_{\hat{\gamma}_j} \times G}{\text{MSE}_G + \text{MSE}_{\hat{\gamma}_j}} \quad (7-20)$$

and the number of years and censoring thresholds are used to estimate the MSEs, as in equation 7–10.

(c) Test for convergence. If $\|\hat{\mathbf{M}}_j - \hat{\mathbf{M}}_{j-1}\| < \epsilon$, return $\mathbf{M} = \hat{\mathbf{M}}_j$ as the EMA estimate. Otherwise, increment j and return to 2a.

Uncertainty of EMA Moments

Uncertainty of moments, specifically the at-site skew coefficient ($\hat{\gamma}$), are estimated with EMA. Details and equations are presented in appendix A1 of [Cohn and others \(2001\)](#) and by Cohn (written commun., 2015).

For cases where there is historical information, PILFs, a gage-base discharge, or some type of censored or interval data, EMA utilizes an approach to estimate $\text{MSE}_{\hat{\gamma}}$ that is based on all the data. This includes censored data, intervals, historical information, and PILFs, including the P-III distribution parameters, as they are used in estimating the moments with EMA. For convenience in the equations, the terms are abbreviated as $X_{i,lower} = X_{i,l}$ and $X_{i,upper} = X_{i,u}$. Conceptually, this is done as follows:

$$\text{MSE}_{\hat{\gamma}} \approx \text{Var}(\hat{\gamma}) \approx \text{Var}(\hat{m}_3) \approx \frac{1}{n} f(X_{i,l}, X_{i,u}, T_{i,l}, T_{i,u}, \hat{\theta}) \quad (7-21)$$

where $\text{MSE}_{\hat{\gamma}}$ is proportional to the variance (Var) of the skew ($\hat{\gamma}$), is proportional to the variance of the third noncentral moment $\text{Var}(\hat{m}_3)$, is a function (f) of the observations (including censored data), and P-III parameters $\hat{\theta}$. In this case, n is the total record length (for example, $n = n_s + n_h = N$), including any historical period, PILFs, and censored and interval data.

As presented in appendix A1 of [Cohn and others \(2001\)](#), EMA estimates the variance of the each of the

noncentral moments $\{\hat{\mu} = [\hat{\mu}_1, \hat{\mu}_2, \hat{\mu}_3]\}$, where $\{\hat{\mu} = \hat{\mathbf{M}} = [m_1, m_2, m_3]\}$ as outlined in Cohn and others (2001). The noncentral moment \hat{m}_3 (moment computed around zero) is used to estimate $MSE_{\hat{\gamma}}$. Key equations from Cohn and others (2001, appendix A1) are presented below.

The EMA estimates noncentral moments $\hat{\mathbf{M}} = [\hat{m}_1, \hat{m}_2, \hat{m}_3]$ that directly take into account censored data through

$$\hat{\mathbf{M}} = (1/n) \sum_{i=1}^n \chi(\psi(X_i), \hat{\mathbf{M}}) \mathcal{I}[\psi(X_i)] \quad (7-22)$$

where

$$\mathcal{I}[X] \equiv \begin{bmatrix} \mathcal{I}(X < a) \\ \mathcal{I}(a \leq X \leq b) \\ \mathcal{I}(X > b) \end{bmatrix} \quad (7-23)$$

$$\mathcal{I}(\text{condition}) \equiv \begin{cases} 1 & \text{condition = true} \\ 0 & \text{otherwise} \end{cases} \quad (7-24)$$

and

$$\chi(\psi(X), \mathbf{M}) = \begin{bmatrix} E_{\theta[\mathbf{M}]}[X|X < a] & X_i & E_{\theta[\mathbf{M}]}[X|X > b] \\ E_{\theta[\mathbf{M}]}[X^2|X < a] & X_i^2 & E_{\theta[\mathbf{M}]}[X^2|X > b] \\ E_{\theta[\mathbf{M}]}[X^3|X < a] & X_i^3 & E_{\theta[\mathbf{M}]}[X^3|X > b] \end{bmatrix}. \quad (7-25)$$

The function $\mathcal{I}[X]$ defines the censored data category for the flow logarithms X . The following three categories are used: “less,” where X is less than the “perception threshold” a ; “between,” where X is within the closed interval $[a, b]$; or “greater” if X is known to exceed some “perception threshold” b (table 7–1). These threshold categories $[a, b]$ correspond to those described in the section Data Representation Using Flow Intervals and Perception Thresholds, where “between” is the “interval” category and “greater” is the “binomial” category. The “less than” category covers unobserved historical floods, flows less than a gage base, or low outliers. The magnitude of X is known if X is within $[a, b]$. Only a threshold on X can be identified if $X < a$ or $X > b$. The number of observations in each of these categories is a random variable, denoted n_l, n_b , and n_g , respectively. Because each X must fall into one of the three categories, the total sample size n is constant, where $n = n_l + n_b + n_g$.

The $MSE_{\hat{\gamma}}$ can be estimated by taking the variance of equation 7–22, as in equation 7–26. The formula for the asymptotic variance of the EMA moments estimator, denoted $\tilde{\Sigma}_{\hat{\mu}}$, is derived in Cohn and others (2001, appendix A1). It is obtained by linearizing the expectations in equation 7–22 and solving for \mathbf{M} in terms of the

Table 7–1. Expected Moments Algorithm censored-data threshold categories.

Value of X_i	Category	$(T_{i,l}, T_{i,u})$
$x < a$	l	$(-\infty, a)$
$a \leq X \leq b$	b	(X, X)
$x > b$	g	(b, ∞)

86 Guidelines for Determining Flood Flow Frequency—Bulletin 17C

sample X_i values. The estimator $\tilde{\Sigma}_{\hat{\mu}}$ is then expressed as a function of the population parameters, the record lengths, and the censoring thresholds. It can be used as an **estimator** of the variance-covariance matrix given estimated parameters ($\hat{\Sigma}_{\hat{M}}$):

$$\text{Var } \hat{M} = \text{Var} \begin{bmatrix} \hat{m}_1 \\ \hat{m}_2 \\ \hat{m}_3 \end{bmatrix} \approx \tilde{\Sigma}_{\hat{\mu}} \approx \hat{\Sigma}_{\hat{M}}. \quad (7-26)$$

The variance of \hat{M} is (Cohn and others, 2001, eq. 55):

$$\tilde{\Sigma}_{\hat{\mu}} = \frac{1}{n^2} \mathbf{A} (\text{Var}[\mathbf{B}] + \text{Var}[\mathbf{C}]) \mathbf{A}' \quad (7-27)$$

where

$$\begin{aligned} \mathbf{B} &= \boldsymbol{\mu}_X \mathbf{n} \\ \mathbf{C} &= \sum_{i=1}^{\mu_{n_b}} (\mathbf{X}_i - \boldsymbol{\mu}_{X_b}) \\ \mathbf{D} &= \frac{\mu_{n_l} \mathbf{J}_l + \mu_{N_g} \mathbf{J}_g}{n} \\ \mathbf{A} &= (\mathbf{I} - \mathbf{D})^{-1} \end{aligned} \quad (7-28)$$

and $\boldsymbol{\mu}_X$ is the vector of expected values for noncentral moments given parameters, value of X (Cohn and others, 2001, eq. 50–51), and $()^{-1}$ represents matrix inversion. The variance of \mathbf{B} is given by

$$\text{Var}[\mathbf{B}] = \boldsymbol{\mu}_X \text{Var}[\mathbf{n}] \boldsymbol{\mu}_X'. \quad (7-29)$$

The large-sample variance of \mathbf{C} is the expected value of the number of terms multiplied by the variance of each term:

$$\text{Var}[\mathbf{C}] = \mu_{n_B} \begin{bmatrix} V_{1,1} & V_{1,2} & V_{1,3} \\ V_{2,1} & V_{2,2} & V_{2,3} \\ V_{3,1} & V_{3,2} & V_{3,3} \end{bmatrix}. \quad (7-30)$$

The MSE of the EMA at-site skewness coefficient is estimated using a first-order approximation (Cohn and others, 2001, eq. 55), reproduced above as equation 7-27, with \hat{m}_3 as the noncentral moment of interest.

Confidence Intervals with EMA

A simple formula for a confidence interval on a flood quantile \hat{X}_q is (Stedinger and others, 1993; Cohn and others, 2001):

$$\hat{X}_q \pm z_{1-\alpha/2} \sqrt{\text{Var}(\hat{X}_q)} \quad (7-31)$$

where q is the quantile of interest (such as $q = 0.99$), $z_{1-\alpha/2}$ is the $(1 - \alpha)/2$ quantile of the standard Normal distribution, α is the confidence level and

$$\sqrt{\text{Var}(\hat{X}_q)} = \hat{\sigma}_{\hat{X}_q} \quad (7-32)$$

is the estimated standard error of the flood quantile. Typically, the confidence level $\alpha = 0.05$, resulting in a 90-percent confidence interval (5-percent and 95-percent confidence limits).

Confidence intervals for flood quantiles (\hat{X}_p) are estimated with EMA. [Cohn and others \(2001\)](#) derive EMA confidence intervals in detail and provide key equations. Cohn (written commun., 2015) improved the EMA confidence intervals for skews $|\hat{\gamma}| > 0.5$.

Confidence intervals are estimated using

$$\left(\hat{X}_p + \frac{\hat{\sigma}_{\hat{X}_p} T_{\nu, (1-\epsilon)/2}}{1 - \kappa T_{\nu, (1-\epsilon)/2}}, \hat{X}_p + \frac{\hat{\sigma}_{\hat{X}_p} T_{\nu, (1+\epsilon)/2}}{1 - \kappa T_{\nu, (1+\epsilon)/2}} \right) \quad (7-33)$$

where T_ν is a Student's T variate ([Abramowitz and Stegun, 1964](#)), ϵ is the confidence level, $\hat{\sigma}_{\hat{X}_p}$ is the standard deviation of the quantile \hat{X}_p , and

$$\kappa \equiv \frac{\text{Cov}[\hat{X}_p, \hat{\sigma}_{\hat{X}_p}]}{\hat{\sigma}_{\hat{X}_p}^2} \quad (7-34)$$

is a function of the sample size and the censoring threshold (and, to some extent, of α). Estimators for $\text{Cov}[\hat{X}_p, \hat{\sigma}_{\hat{X}_p}]$ and $\hat{\sigma}_{\hat{X}_p}^2$ are available from [Cohn and others \(2001, eq. 70\)](#).

The asymptotic variance of \hat{X}_p can be obtained from a first-order expansion of \hat{X}_p as a function of \mathbf{M} :

$$\hat{X}_p \approx X_p + \mathbf{J}_{\hat{X}_p}(\mathbf{M} - \boldsymbol{\mu}_{\mathbf{M}}) \quad (7-35)$$

where

$$\mathbf{J}_{\hat{X}_p} = \begin{bmatrix} \frac{\partial \hat{X}_p}{\partial \hat{m}_1} & \frac{\partial \hat{X}_p}{\partial \hat{m}_2} & \frac{\partial \hat{X}_p}{\partial \hat{m}_3} \end{bmatrix}. \quad (7-36)$$

The Jacobian can be evaluated by first computing derivatives with respect to $\{\alpha, \beta, \tau\}$ and then applying the chain rule.

The variance of \hat{X}_p can be approximated by

$$\tilde{\sigma}_{\hat{X}_p}^2 \approx \mathbf{J}_{\hat{X}_p} \cdot \tilde{\Sigma}_{\hat{\mu}} \cdot \mathbf{J}_{\hat{X}_p}' \quad (7-37)$$

where the linearized standard deviation, $\tilde{\sigma}_{\hat{X}_p}$, is defined as $\sqrt{\tilde{\sigma}_{\hat{X}_p}^2}$. Cohn (written commun., 2015) provided improved estimates of $\text{Var}[\hat{X}_p]$ using inverse quadrature.

Appendix 8. Record Extension with Nearby Sites

This appendix describes the background and computational details for transfer of information from a long-record nearby site to a site of concern that has a relatively shorter record. The transfer is based upon the observed correlation between the base-10 logarithms of the annual maximum series available at the two sites. This is an attractive method to transfer information from a long-record site to the site of interest while honoring the potentially influential low flood (PILF) criterion and the relative information provided by historical information and regional skewness estimators. An example illustrates the method.

Formally, such a method based upon the cross correlation between flood peaks at a short- and long-record site is called record augmentation (see [Glossary](#) for definitions). However, because the Bulletin 17C algorithm uses a PILF threshold to restrict the frequency analysis to floods greater than the PILF threshold, a simple record augmentation procedure that ignores that restriction would not be appropriate. The supplemental information provided by the record augmentation analysis is represented as an extension of the original flood record. The additional length of record is selected to approximate the “effective record length” of the additional information for the variance developed for the flood frequency analysis at the short-record site. The PILF threshold can then be applied to this extended record to allow for a consistent analysis of flood peaks that are greater than that threshold.

Record augmentation is attractive when two conditions are met. First, the record available at the site of interest is relatively short. And, there is a nearby longer record site whose flood series is highly correlated with the flood series at the short-record site. Then the longer record can be used to effectively extend the record at the short-record site employing the cross-correlation between floods at the two sites. The recommendation is that record augmentation be considered whenever the cross-correlation $\rho > 0.80$ and the short-record site is less than 20 years. It may be useful even when the short-record site exceeds 20 years. In any case, a minimum of 10 years concurrent years of record are needed at the two sites considered. [Matalas and Jacobs \(1964\)](#) and [Vogel and Stedinger \(1985\)](#) discuss the record augmentation procedures, and provide more complex criteria for when the cross-correlation between the two flood series and the concurrent record length are insufficient for the procedures to result in a gain in the mean and variance at the short-record site. The larger the cross correlation the better.

Record Augmentation of the Mean and Variance

[Matalas and Jacobs \(1964\)](#) developed an approach for obtaining unbiased estimates of the mean and variance of the lengthened time series (observed plus extended record) based upon ordinary least squares (OLS) regression. This approach is the basis of the “Two Station Comparison” method that is described in Bulletin 17B ([IACWD, 1982](#), appendix 7). Using the methods of moments recommended in Bulletin 17B, improved estimates of the mean and variance (standard deviation) can be computed based upon the Matalas-Jacobs procedure and then used in the computations. [Moran \(1974\)](#) considered use of more than one explanatory variable—a potentially useful extension of the concept. Because Bulletin 17C introduces the PILF criteria with EMA, integration of regional skewness information, and potentially historical information and other data, adopting information provided by record augmentation is not as straightforward. That will be accomplished with an extended systematic record that represents the additional information provided by correlation with the long-record site. The extended systematic record is introduced into the EMA computations, and then is subject to the PILF criteria.

Let the base-10 logarithms of floods $y = \log_{10}(Q_y)$ at the short-record site of interest be denoted y_i , and logarithms of floods $x = \log_{10}(Q_x)$ at the long-record site be denoted x_i . Furthermore let n_1 be the length of the short record, so that the series is y_i , for $i = 1, \dots, n_1$. Let n_2 be the additional years of record at the x -site, so that series can be written x_i , for $i = 1, \dots, (n_1 + n_2)$. For convenience, the presentation assumes that the n_1 concurrent observations between the two sites y and x correspond to the first n_1 observations. This need not be the case nor do the concurrent values need to be consecutive. Here the x series should be from a hydrologically-relevant site with similar climatic and watershed characteristics.

Definitions employed in the presentation include these following sample means and variances:

$$\bar{y}_1 = \frac{1}{n_1} \sum_{i=1}^{n_1} y_i, \quad (8-1)$$

$$\bar{x}_1 = \frac{1}{n_1} \sum_{i=1}^{n_1} x_i, \quad (8-2)$$

$$\bar{x}_2 = \frac{1}{n_2} \sum_{i=n_1+1}^{n_1+n_2} x_i, \quad (8-3)$$

$$s_{y_1}^2 = \frac{1}{n_1 - 1} \sum_{i=1}^{n_1} (y_i - \bar{y}_1)^2, \quad (8-4)$$

$$s_{x_1}^2 = \frac{1}{n_1 - 1} \sum_{i=1}^{n_1} (x_i - \bar{x}_1)^2, \quad (8-5)$$

and

$$s_{x_2}^2 = \frac{1}{n_2 - 1} \sum_{i=n_1+1}^{n_1+n_2} (x_i - \bar{x}_2)^2. \quad (8-6)$$

With these definitions, the Matalas-Jacobs estimators are ([Matalas and Jacobs, 1964](#); [Vogel and Stedinger, 1985](#)):

$$\hat{\mu}_y = \bar{y}_1 + \frac{n_2}{n_1 + n_2} \hat{\beta} (\bar{x}_2 - \bar{x}_1) \quad (8-7)$$

and

$$\begin{aligned} \hat{\sigma}_y^2 &= \frac{1}{n_1 + n_2 - 1} \left[(n_1 - 1)s_{y_1}^2 + (n_2 - 1)\hat{\beta}^2 s_{x_2}^2 + (n_2 - 1)\alpha^2(1 - \hat{\rho}^2)s_{y_1}^2 \right. \\ &\quad \left. + \frac{n_1 n_2}{(n_1 + n_2)} \hat{\beta}^2 (\bar{x}_2 - \bar{x}_1)^2 \right] \end{aligned} \quad (8-8)$$

90 Guidelines for Determining Flood Flow Frequency—Bulletin 17C

where

$$\hat{\rho} = \hat{\beta} \frac{s_{x_1}}{s_{y_1}} \quad (8-9)$$

$$\hat{\beta} = \frac{\sum_{i=1}^{n_1} (x_i - \bar{x}_1)(y_i - \bar{y}_1)}{\sum_{i=1}^{n_1} (x_i - \bar{x}_1)^2} \quad (8-10)$$

and

$$\alpha^2 = \frac{n_2(n_1 - 4)(n_1 - 1)}{(n_2 - 1)(n_1 - 3)(n_1 - 2)}. \quad (8-11)$$

It is important to understand the precision of the Matalas-Jacobs estimators of the mean and variance of flood peaks at the short-record site. Using the definitions introduced above, the variance, $\text{Var}(\cdot)$, of the estimated mean at the y -site is

$$\text{Var}(\hat{\mu}_y) = \frac{\sigma_y^2}{n_1} \left[1 - \frac{n_2}{n_1 + n_2} \left(\rho^2 - \frac{1 - \rho^2}{n_1 - 3} \right) \right] \quad (8-12)$$

whereas the variance of the variance of floods at the y -site is

$$\text{Var}(\hat{\sigma}_y^2) = \frac{2\sigma_y^4}{n_1 - 1} + \frac{n_2\sigma_y^4}{(n_1 + n_2 - 1)^2(n_1 - 3)} (A\rho^4 + B\rho^2 + C) \quad (8-13)$$

where

$$A = \frac{(n_2 + 2)(n_1 - 6)(n_1 - 8)}{(n_1 - 5)} + (n_1 - 4) \left(\frac{n_1 n_2 (n_1 - 4)}{(n_1 - 3)(n_1 - 2)} - \frac{2n_2(n_1 - 4)}{(n_1 - 3)} - 4 \right) \quad (8-14)$$

$$B = \frac{6(n_2 + 2)(n_1 - 6)}{(n_1 - 5)} + 2(n_1^2 - n_1 - 14) \\ + (n_1 - 4) \left(\frac{2n_2(n_1 - 5)}{(n_1 - 3)} - 2(n_1 + 3) - \frac{2n_1 n_2 (n_1 - 4)}{(n_1 - 3)(n_1 - 2)} \right) \quad (8-15)$$

$$C = 2(n_1 + 1) + \frac{3(n_2 + 2)}{(n_1 - 5)} - \frac{(n_1 + 1)(2n_1 + n_2 - 2)(n_1 - 3)}{(n_1 - 1)} \\ + (n_1 - 4) \left(\frac{2n_2}{(n_1 - 3)} + 2(n_1 + 1) + \frac{n_1 n_2 (n_1 - 4)}{(n_1 - 3)(n_1 - 2)} \right) \quad (8-16)$$

and these correspond to equations in [Matalas and Jacobs \(1964\)](#), [IACWD \(1982, appendix 7\)](#), and [Vogel and Stedinger \(1985\)](#).

If the improvement in the precision of the estimate of the y -mean is described by an increase in the effective record length n_e , then n_e would be defined by the equation

$$\text{Var}(\hat{\mu}_y) = \frac{\sigma_y^2}{(n_e + n_1)} \quad (8-17)$$

where σ_y^2 is the true variance of the y -series. Because $\text{Var}(\hat{\mu}_y)$ in equation 8–12 is proportional to σ_y^2 , the variance of the y series cancels out in the computation of n_e . Thus the total effective record length in terms of the estimated mean is

$$n_e + n_1 = \frac{n_1}{\left[1 - \frac{n_2}{n_1+n_2} \left(\rho^2 - \frac{1-\rho^2}{n_1-3}\right)\right]} \quad (8-18)$$

and corresponds to equation 7-7 in IACWD (1982, appendix 7).

In terms of the computation of flood quantiles, the estimator of the variance is much more important than the estimator of the mean. As a result, in the use of the Matalas-Jacobs estimators for flood frequency analysis, the effective increase in the record length in terms of the precision of the variance is the critical issue. Using equations 8–13 through 8–16, the needed relationship for the total effective record length for the estimated variance is

$$(n_e + n_1) = \frac{2}{\frac{2}{n_1-1} + \frac{n_2}{(n_1+n_2-1)^2(n_1-3)}(A\rho^4 + B\rho^2 + C)} + 1. \quad (8-19)$$

Use of the Matalas-Jacobs estimators is appropriate when they result in a substantial improvement in both the mean and variance estimators of flood peaks at the short-record y site, corresponding to an n_e of 4 or 5 or more. This is typically the case when $\hat{\rho} > 0.80$ (Vogel and Stedinger, 1985). The above equations were developed under the assumption that the logarithms of concurrent flow observations at the short-record site y_i and long-record site x_i have a joint normal probability distribution with a skewness of zero. When this assumption is seriously violated, the above equations are not exact and this technique should be used with caution.

Record Extension with MOVE

Having computed the improved Matalas-Jacobs estimators of the mean and variance for the y -site, and effective records $n_1 + n_e$ corresponding to the improvement in the variance estimator (eq. 8–19), the next step is to generate n_e additional observations to be added to the y -record to introduce this additional information into the frequency analysis. This is done employing the Maintenance of Variance Extension (MOVE) idea described by Hirsch (1982). As implied by the name, these techniques were developed to maintain the variance of a generated y -series when it was extended using a supplemental longer series, denoted here as x . As suggested by Vogel and Stedinger (1985), one can be careful in how model parameters are selected so that the original and extended values have exactly the mean and variance that a hydrologist specifies. In our case, the original n_1 observations represent themselves, and the additional n_e values represent the information provided by the additional observations in the x -series, given the less than perfect cross-correlation between the two series. It should be clear that the procedure adds just n_e observations to the original y series and those n_e observations have the values needed to transfer information about the mean and variance at the y -site.

A linear regression model is used to extend the record at the short site y_i by n_e (Vogel and Stedinger, 1985):

$$\hat{y}_i = a + b(x_i - \bar{x}_e) \quad \text{for } i = n_1 + 1, \dots, n_1 + n_e \quad (8-20)$$

where \bar{x}_e is the mean of the n_e x -series values from the non-overlapping period used to extend the y series. That is, given

$$\bar{x}_e = \frac{1}{n_e} \sum_{i=n_1+1}^{n_1+n_e} x_i \quad (8-21)$$

92 Guidelines for Determining Flood Flow Frequency—Bulletin 17C

and

$$s_{xe}^2 = \frac{1}{n_e - 1} \sum_{i=n_1+1}^{n_1+n_e} (x_i - \bar{x}_e)^2. \quad (8-22)$$

The intercept a to use to generate n_e new values is computed as

$$a = \frac{(n_1 + n_e)\hat{\mu}_y - n_1\bar{y}_1}{n_e} \quad (8-23)$$

with the slope ($b > 0$) estimated from

$$b^2 = \frac{(n_1 + n_e - 1)\hat{\sigma}_y^2 - (n_1 - 1)s_{y1}^2 - n_1(\bar{y}_1 - \hat{\mu}_y)^2 - n_e(a - \hat{\mu}_y)^2}{(n_e - 1)s_{xe}^2}. \quad (8-24)$$

Should b^2 be less than zero, it would appear that a useful extension with this method is not possible.

Summary of Procedure

The steps for record augmentation of the mean and variance at the short-record site and constructing a record extension with n_e observations to EMA are as follows:

1. Select a hydrologically relevant longer record site nearby to extend the short-record site of interest. The cross correlation between the two sites is critical and should be as large as possible. A time series plot of the two series may reveal if the transfer of information using the two sites is reasonable. Does the longer record appear to provide a longer view of what hydrologic events were observed in the shorter record?
2. Investigate the statistical properties and regression relationship between the short- and long-record sites using base-10 logarithms of the flood flows. If the correlation coefficient estimated with equation 8-9 exceeds a critical value ($\hat{\rho} > 0.80$), record extension may be suitable. Otherwise, it may be advisable to use the short record with a weighted skew estimate for frequency analysis, or other techniques such as quantile regression for the site of interest. Here the threshold for extension is given in terms of the true cross correlation between the series. In practice, a hydrologist must use the computed sample correlation or a regional estimator.
3. Estimate the sample statistics for the concurrent n_1 records using equations 8-1 through 8-6, and then the mean and variance estimators for the y -site based upon the complete record available at the long-record site ($n_1 + n_2$) using equations 8-7 and 8-8.
4. Estimate the total effective record length $n_1 + n_e$ using equation 8-19; n_e is the number of observations that need to be added to the y -series.
5. Estimate the extension parameters (eqs. 8-23 and 8-24). Use the model (eq. 8-20) to generate the additional n_e flow values to extend the record for the short site, with the most recent n_e observations from the n_2 non-concurrent record. Check to make sure the extension is reasonable. As an example, if a short extension of 10 years included the first or second largest floods in the much longer x -series, that short extension may misrepresent the likely skewness coefficient for the short-record site. In such cases the n_e x -observations used to generate the extension might be selected to be a sequence of years that generated a more typical skewness coefficient (considering the different n_e extensions that could be made) for the extended $n_1 + n_e$ record.

6. A frequency analysis can then be performed using this extended record flow series $n_1 + n_e$.

This procedure was recently developed to focus on n_e years. Additional work may be needed to select the n_e years. As noted above and in [Matalas and Jacobs \(1964\)](#), the basic model assumption of joint normality with a skewness equal to zero between the two sites needs to be reviewed.

An example is provided in the next section. Supplemental material to perform these calculations and this example is available at <https://acwi.gov/hydrology/Frequency/b17c/>.

MOVE Example—Suwanee Creek at Suwanee, Georgia

An example of record extension using MOVE is given for Suwanee Creek at Suwanee, Georgia (USGS station 02334885), where the drainage area is 47.0 square miles (mi^2). The watershed is located in north-central Georgia as shown in figure 8–1. There are 20 years of record at station 02334885 from 1985 to 2004, which is relatively short, as shown in figure 8–2. The analysis of the 20 years of record for Suwanee Creek provided low estimates of the flood discharges such as the 0.01 AEP flood compared to other long-term stations in the region. There is a nearby gaging station on the Etowah River at Canton, Georgia (USGS station 02392000), which has 113 years of record from 1892 to 2004 and a drainage area of 613 mi^2 . The annual peak data for the Etowah River were used to extend the record for Suwanee Creek by 13 additional years to obtain flood estimates such as the 0.01 AEP flood.

The concurrent annual peak data available at the Etowah River and Suwanee Creek through 2004 are listed in table 8–1.

For 8 of the 20 years of record, the annual maximum peak flow occurred on the same flood event for Suwanee Creek and the Etowah River. However, for 12 of the 20 years of concurrent record, the annual peak

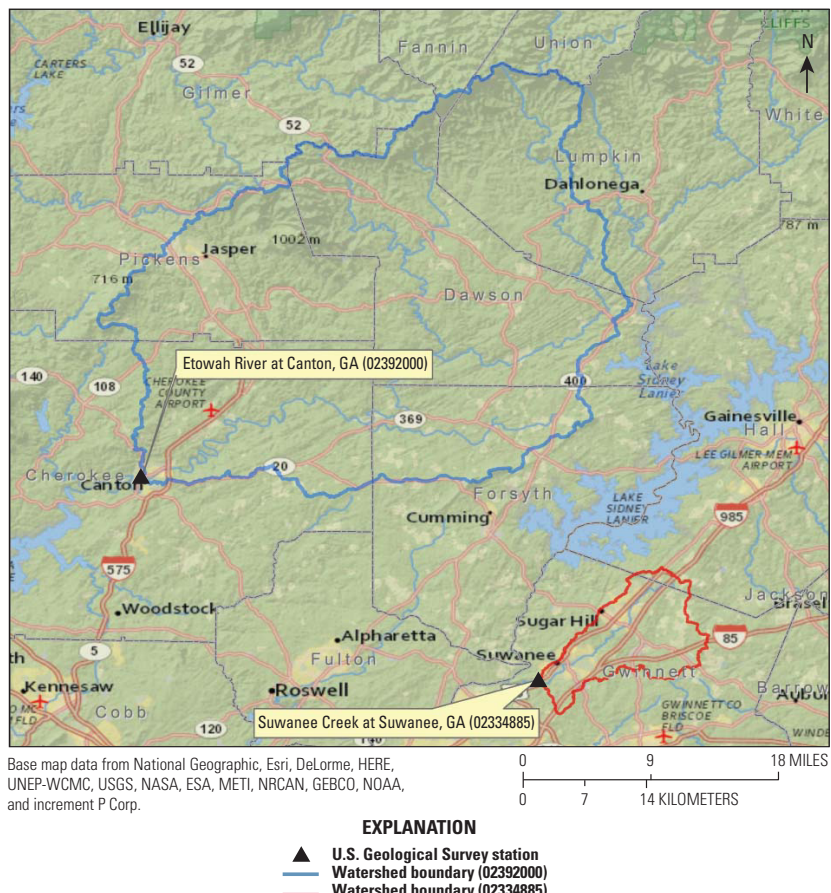


Figure 8–1. Map showing locations of Suwanee Creek at Suwanee, Georgia, U.S. Geological Survey station 02334885, and Etowah River at Canton, Georgia, U.S. Geological Survey station 02392000.

Table 8–1. Summary of concurrent observed annual peak data for the Etowah River and Suwanee Creek from 1985 to 2004.

[ft³/s, cubic feet per second]

Water year	Etowah River annual peak streamflow (ft ³ /s)	Suwanee Creek annual peak streamflow (ft ³ /s)
1985	5,030	1,440
1986	3,090	386
1987	12,200	2,150
1988	9,340	948
1989	9,080	1,220
1990	27,100	3,760
1991	5,940	1,320
1992	7,660	696
1993	10,900	2,540
1994	9,420	1,190
1995	10,500	2,650
1996	19,500	4,350
1997	11,300	2,360
1998	15,000	2,900
1999	5,530	816
2000	8,900	862
2001	9,270	2,090
2002	7,100	1,260
2003	13,600	2,940
2004	15,300	3,270

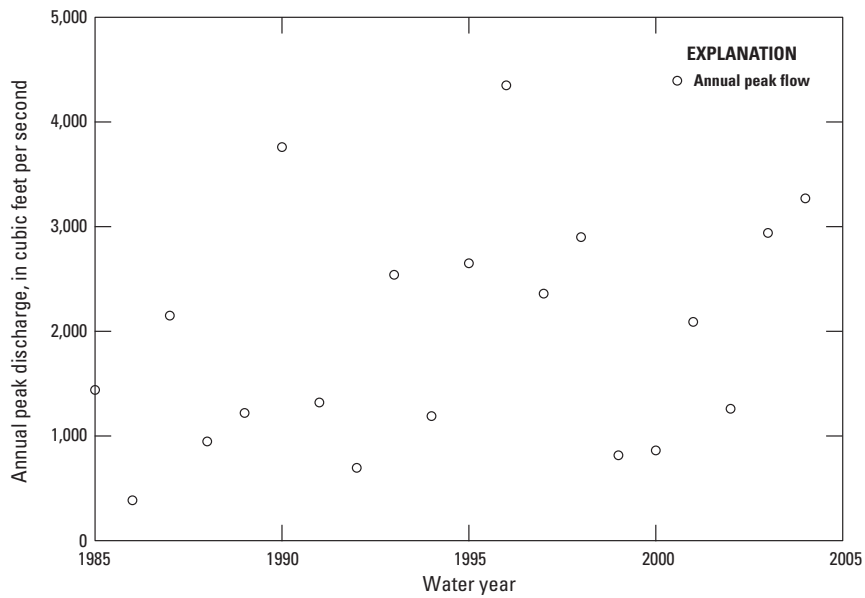


Figure 8–2. Graph showing annual peak flows for Suwanee Creek, U.S. Geological Survey station 02334885, the short record station, from 1985 to 2004.

flows corresponded to different flood events. For the purposes of record extension, concurrent flood peaks are those that occurred in the same water year, not on the same flood event.

The annual peak flows for the Etowah River at Canton, Georgia, the long-record station, are plotted in figure 8–3 for 1892 to 2004. As shown in figure 8–3, there were several large floods that were recorded on the Etowah River prior to 1985 when systematic data collection began at Suwanee Creek. The period of systematic record at Suwanee Creek for 1985 to 2004 does not include several large floods that occurred in 1892, 1916, and 1919 at the nearby Etowah River gaging station. These large floods, as well as information provided by other events in the 1892 to 1984 period, can be used through record augmentation to improve the mean and variance and extend the flood record at Suwanee Creek.

The 20 years of concurrent record for Suwanee Creek and the Etowah River are plotted in figure 8–4 on a log-log scale. As shown in figure 8–4, the logarithms of the annual peak flows define a linear relation with a R^2 value of 0.7258. The correlation coefficient is 0.8519, which is higher than the critical value ($\hat{\rho} > 0.80$) for both the mean and variance. This suggests that the mean and standard deviation from the extended record will be improved by use of a longer record. Even though the Etowah River is much larger than Suwanee Creek, there is a strong correlation in annual peak flows that facilitates record extension. The linear relation shown in figure 8–4 is the ordinary least squares regression line computed using the logarithms of the data.

The 20 years of record at Suwanee Creek from 1985 to 2004 provides low estimates of the flood discharges, like the 0.01 annual exceedance probability discharge because major floods that occurred prior to systematic data collection are not considered in the frequency analysis. The period 1985 to 2004 was a relatively dry period as compared to the period prior to 1985, as can be observed from the long-term Etowah River record shown in figure 8–3.

The flood records for Suwanee Creek were extended using record augmentation of the mean and variance and MOVE, based on the annual peak-flow data for the Etowah River from 1892 to 1984 and overlapping period from 1985 to 2004. As shown in figure 8–4, there is a strong linear relation between the logarithms

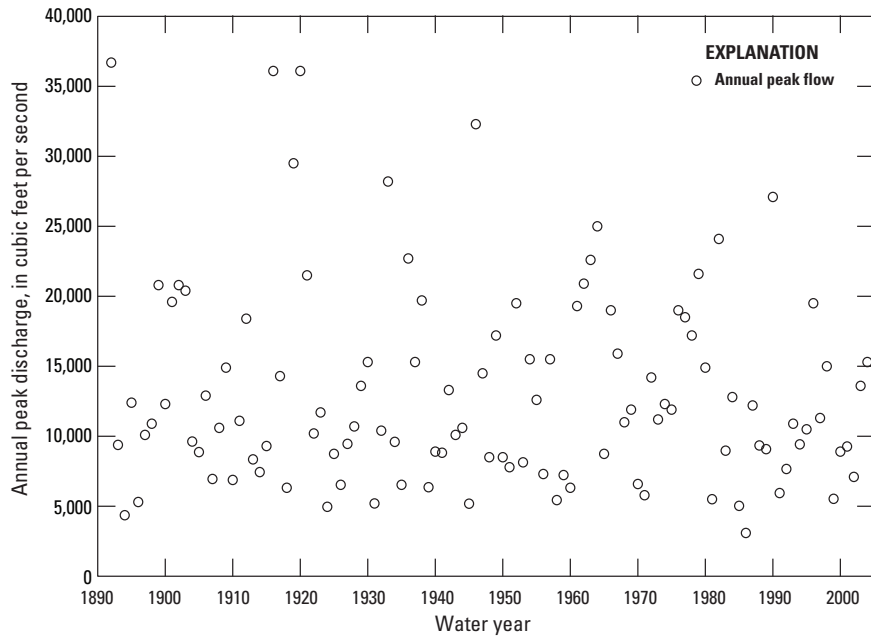


Figure 8–3. Graph showing annual peak flows for the Etowah River, U.S. Geological Survey station 02392000, the long record station, from 1892 to 2004.

of the annual peak flows. The estimated correlation coefficient for the overlapping 1985 to 2004 period is 0.8519. The sample statistics for the gages are

y_i = logarithmic discharge for Suwanee Creek for year i ,

x_i = logarithmic discharge for Etowah River for year i ,

n_1 = concurrent or overlapping period of record, 20 years (1985 to 2004),

n_2 = non-concurrent period of record, 93 years (1892 to 1984),

\bar{y}_1 = logarithmic mean for Suwanee Creek for concurrent period = 3.215 log units,

\bar{x}_1 = logarithmic mean for Etowah River for concurrent period = 3.984 log units,

\bar{x}_2 = logarithmic mean for Etowah River for non-concurrent period = 4.079 log units,

s_{y1} = logarithmic standard deviation for Suwanee Creek for concurrent period = 0.279 log units,

s_{x1} = logarithmic standard deviation for Etowah River for concurrent period = 0.214 log units, and

s_{x2} = logarithmic standard deviation for Etowah River for non-concurrent period = 0.219 log units.

Finally, using equation 8–19, the estimated extended record length n_e is 13 years.

The extended n_e years of record y_i for Suwanee Creek were estimated using the most recent non-overlapping 13 years from 1972 to 1984. Using the Matalas-Jacobs equations 8–7 through 8–11, the augmented mean and variance are $\mu_y = 3.3024$ and $\sigma_y^2 = 0.08105$. Solving equations 8–20 through 8–24, the MOVE equation in logarithmic linear form that is used to generate n_e flows is

$$y_i = 3.4364 + 1.4416 (x_i - 4.1414) \quad (8-25)$$

where x_i are the base-10 logarithms of the Etowah River flows for the period 1972 to 1984 and

$$Q_i = 10^{y_i} \quad (8-26)$$

98 Guidelines for Determining Flood Flow Frequency—Bulletin 17C

where Q_i are the extended discharges in ft^3/s for Suwanee Creek. Equation 8–26 was used to estimate annual peak flows for Suwanee Creek for the period 1972 to 1984, thereby extending the record an additional 13 years with data from the Etowah River. Extended flow estimates for Suwanee Creek are listed in table 8–2. Original flow estimates from the long-record site (Etowah River) are listed in table 8–3.

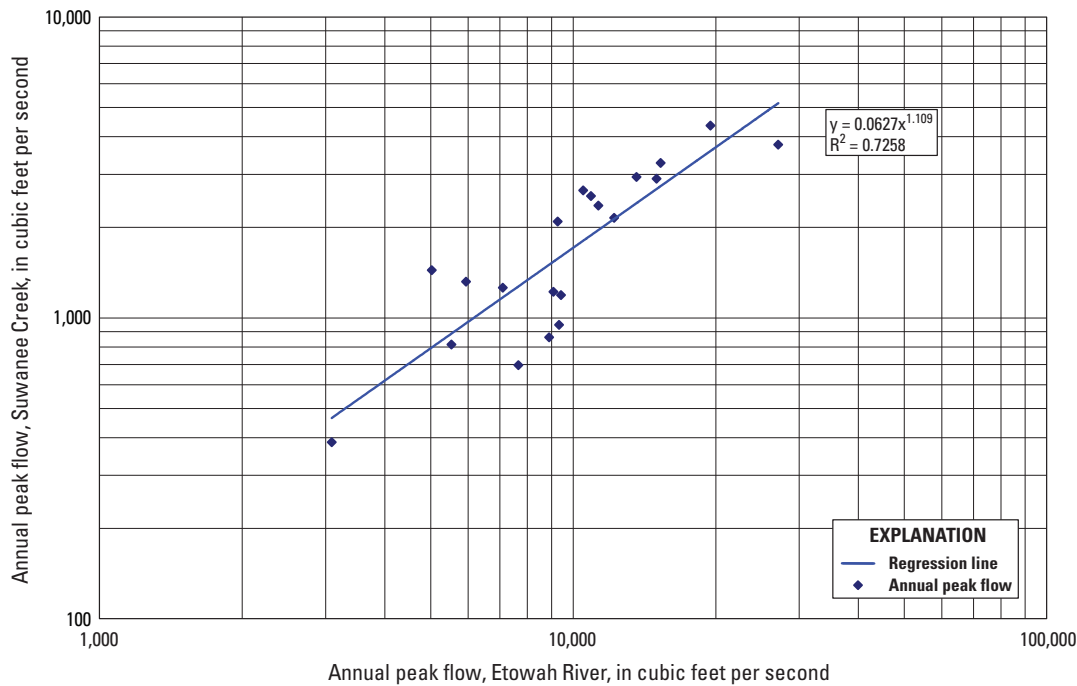


Figure 8–4. Graph of 20 concurrent years of record for Suwanee Creek and the Etowah River for the period 1985 to 2004 with the ordinary least squares regression line.

Table 8–2. MOVE extended record for 13 years (1972 to 1984) for Suwanee Creek at Suwanee, Georgia (station 02334885).

[ft³/s, cubic feet per second]

Water year	Annual peak streamflow (ft ³ /s)
1972	2,830
1973	2,010
1974	2,300
1975	2,200
1976	4,310
1977	4,150
1978	3,730
1979	5,180
1980	3,040
1981	722
1982	6,070
1983	1,460
1984	2,440

Table 8–3. Flood records for 93 years (1892 to 1984) for the Etowah River at Canton, Georgia (station 02335000).[ft³/s, cubic feet per second]

Water year	Annual peak streamflow (ft ³ /s)	Water year	Annual peak streamflow (ft ³ /s)	Water year	Annual peak streamflow (ft ³ /s)
1892	36,700	1923	11,700	1954	15,500
1893	9,380	1924	4,960	1955	12,600
1894	4,360	1925	8,740	1956	7,300
1895	12,400	1926	6,530	1957	15,500
1896	5,300	1927	9,460	1958	5,440
1897	10,100	1928	10,700	1959	7,230
1898	10,900	1929	13,600	1960	6,320
1899	20,800	1930	15,300	1961	19,300
1900	12,300	1931	5,200	1962	20,900
1901	19,600	1932	10,400	1963	22,600
1902	20,800	1933	28,200	1964	25,000
1903	20,400	1934	9,600	1965	8,740
1904	9,620	1935	6,530	1966	19,000
1905	8,870	1936	22,700	1967	15,900
1906	12,900	1937	15,300	1968	11,000
1907	6,950	1938	19,700	1969	11,900
1908	10,600	1939	6,360	1970	6,590
1909	14,900	1940	8,900	1971	5,790
1910	6,880	1941	8,820	1972	14,200
1911	11,100	1942	13,300	1973	11,200
1912	18,400	1943	10,100	1974	12,300
1913	8,350	1944	10,600	1975	11,900
1914	7,440	1945	5,180	1976	19,000
1915	9,300	1946	32,300	1977	18,500
1916	36,100	1947	14,500	1978	17,200
1917	14,300	1948	8,500	1979	21,600
1918	6,320	1949	17,200	1980	14,900
1919	29,500	1950	8,500	1981	5,500
1920	36,100	1951	7,790	1982	24,100
1921	21,500	1952	19,500	1983	8,970
1922	10,200	1953	8,140	1984	12,800

Appendix 9. Weighting of Independent Estimates

The uncertainty of peak-flow statistics, such as the one-percent annual exceedance probability (AEP) flow at a streamgage (the site), can be reduced by combining the at-site estimate with an independent regional estimate to obtain a weighted estimate of the flow statistic at the site. The analysis assumes that the two estimators are independent, unbiased, and that their estimates of the variances are reliable and consistent. A common use of this approach is to combine at-site flood frequency analysis estimates of flood quantiles with flood quantile estimates obtained by regional regression. In that case, methods developed by Federal agencies allow computation of weighted estimates using this method. In other cases, independent flood quantile estimates might be available based upon precipitation estimates with rainfall-runoff models. Alternative weighting procedures are evaluated by Griffis and Stedinger (2007a).

The following procedure is suggested for adjusting flow frequency estimates based upon short records (typically less than 20 years) to reflect flood experience in nearby hydrologically similar watersheds, as described in the section [Comparisons of Frequency Curves](#). The method is based upon the assumption that the estimates are independent, which for practical purposes is true in most situations. If the at-site estimate is used to develop the quantile regression model, quantile weighting is inappropriate as the estimates are not independent. Prior to weighting and combining estimates, the quantiles and variances of the estimates need to be evaluated.

Weighting Method

As stated in the section [Flood Distribution](#), the Pearson Type III distribution with log transformation of the peak-flow data should be the base method for the analysis of annual series data. Thus, the peak-flow statistic Q_i (such as the 0.01 AEP) is transformed using base-10 logarithms:

$$X_i = \log_{10}(Q_i) \quad (9-1)$$

where Q_i is the estimated peak-flow statistic at site i , and X_i is the log-transformed variable. All subsequent operations are performed on the transformed variable X_i . The weighted estimate is calculated using variances as

$$X_{weighted,i} = \frac{X_{site,i} \times V_{reg,i} + X_{reg,i} \times V_{site,i}}{V_{site,i} + V_{reg,i}} \quad (9-2)$$

where all X and V variables are in \log_{10} units, $X_{weighted,i}$ is the weighted estimate for site i , $X_{site,i}$ is the at-site estimate at site i , $X_{reg,i}$ is the regional estimate at site i , $V_{site,i}$ is the variance of the at-site estimate at site i , and $V_{reg,i}$ is the variance of the regional estimate at site i .

As described in appendix 7, the Expected Moments Algorithm (EMA) provides a direct fit of the log-Pearson Type III distribution, which includes an estimate of the variance $V_{site,i}$ corresponding to each computed AEP.

For independent $X_{site,i}$ and $X_{reg,i}$, the variance of the weighted estimate for site i is calculated (with all V variables in \log_{10} units) as

$$V_{weighted,i} = \frac{V_{site,i} \times V_{reg,i}}{V_{site,i} + V_{reg,i}}. \quad (9-3)$$

102 Guidelines for Determining Flood Flow Frequency—Bulletin 17C

Confidence intervals on the weighted estimated can also be calculated. For example, upper and lower 95 percent confidence limits on the weighted quantile estimate are calculated as

$$95\%_{-}CI_i = \left[10^{(X_{weighted,i} - 1.96\sqrt{V_{weighted,i}})}, 10^{(X_{weighted,i} + 1.96\sqrt{V_{weighted,i}})} \right], \quad (9-4)$$

and note that $X_{weighted,i}$, $V_{weighted,i}$, and CI_i must be calculated separately for each site i for each AEP of interest.

Example

A flood frequency analysis at a basin (site i) using the EMA produces an estimate of 861 ft³/s for the 0.01 AEP with a log space variance $V_{site} = 0.0281$. Based on hydrologically similar nearby basins, an independent regional estimate of the 0.01 AEP is 718 ft³/s with a log space variance $V_{reg} = 0.085$. By substituting these values into the above equations, the following weighted estimates are obtained. Using equation 9–1, the log transformed flow values are computed as

$$\begin{aligned} X_{site} &= \log_{10}(861) = 2.94 \\ X_{reg} &= \log_{10}(718) = 2.86. \end{aligned}$$

Using equation 9–2, the weighted log transformed flow is computed as

$$X_{weighted} = \frac{2.94 \times 0.085 + 2.86 \times 0.028}{0.028 + 0.085} = 2.92$$

and the peak flow $Q_{weighted}$ is

$$Q_{weighted} = 10^{2.92} = 832 \text{ ft}^3/\text{s}.$$

Using equation 9–3, the variance of the weighted log transformed flow is computed as:

$$V_{weighted} = \frac{0.028 \times 0.085}{0.028 + 0.085} = 0.021.$$

Using equation 9–4, a 95-percent confidence interval on the weighted estimate is computed as

$$\begin{aligned} 95\%_{-}CI_i &= \left[10^{(2.92 - 1.96\sqrt{0.021})}, 10^{(2.92 + 1.96\sqrt{0.021})} \right] \\ &= [432 \text{ ft}^3/\text{s}, 1,600 \text{ ft}^3/\text{s}]. \end{aligned}$$

Appendix 10. Examples

Flood Frequency Steps and Examples

The main steps to perform a flood frequency analysis using these Guidelines and some representative flood frequency examples are presented in this appendix. The main emphasis is on the data, flow intervals, and threshold inputs to EMA to illustrate applications. Steps to perform a flood frequency analysis at a gaged site are as follows:

1. Define the purpose of the flood frequency study and quantiles of interest (for example, Q_{50} or Q_{100});
2. Obtain peak-flow data at the gaged site, including any historical, paleoflood, and botanical data, regional skew estimates, and other precipitation, climate, and regional information as described in appendix 3. Perform field studies to collect additional extreme flood, historical, and paleoflood data as needed for the quantiles of interest;
3. Estimate perception thresholds and flow intervals with guidance in appendix 3;
4. Conduct exploratory data analysis as described in appendix 4 and evaluate data;
5. For short-record sites ($n < 20$), consider performing record extension as described in appendix 8;
6. Estimate flood frequency with EMA using the estimated at-site record and regional skew with recommended software listed at <https://acwi.gov/hydrology/Frequency/b17c/>; and
7. Consider performing quantile weighting described in appendix 9, in particular for short-record sites ($n < 20$) or to combine estimates from rainfall-runoff models, depending on the study purpose and quantiles of interest.

The following flood frequency examples illustrate application of the techniques recommended in these Guidelines. Annual flood peak data for seven stations have been selected to illustrate fitting the log-Pearson Type III distribution when one or more of the following are present in a peak flood record at a gage site:

1. Systematic record;
2. Potentially Influential Low Floods (PILFs);
3. Broken record;
4. Historical data;
5. Crest-stage gage censored data;
6. Historic data and PILFs; and
7. Paleoflood data.

104 Guidelines for Determining Flood Flow Frequency—Bulletin 17C

The gaging stations and types of data used in each example are listed in table 10–1. The USGS *PeakFQ* program (section [Software and Examples](#)) is used for most of the examples shown here; *PeakfqSA* is used for the historical and paleoflood examples. Input and output files from USGS *PeakFQ* software used to compute the examples, as well as example files for the U.S. Army Corps of Engineers HEC-SSP software, are available on the HFAWG web page at <https://acwi.gov/hydrology/Frequency/b17c/>.

These examples are meant to illustrate the main concepts presented in these Guidelines. They are not meant to be all inclusive, and are to be used for example purposes only. The examples are provided with sufficient documentation such that results are reproducible based on the input data shown. Given a single input dataset, two users will obtain the same answer. Different answers by users may be possible with different interpretations of the data and inputs. The input and output results shown are not intended to be used for making floodplain-management decisions at specific locations.

Table 10–1. Summary of flood frequency examples.

[PILF, potentially influential low flood]

Example no.	Example type	USGS station no.	Station name	Systematic	Historical	Broken	Censored	PILF
1	Systematic	01134500	Moose River at Victory, Vermont	X				
2	PILF	11274500	Orestimba Creek near Newman, California	X				X
3	Broken record	01614000	Back Creek near Jones Springs, West Virginia	X		X		
4	Historical data	07099500	Arkansas River at Pueblo, Colorado	X	X	X	X	
5	Crest stage (censored)	05489490	Bear Creek at Ottumwa, Iowa	X				X
6	Historic data + PILFs	09480000	Santa Cruz River at Lochiel, Arizona	X	X			X
7	Paleoflood data	11446500	American River at Fair Oaks, California	X	X	X	X	

It is important to note that for the purposes of flood frequency analysis, water years are used in these examples to define the years in which annual peak flows occur. A water year is defined as the 12-month period from October 1 to September 30. The water year is designated by the calendar year in which it ends and which includes 9 of the 12 months.

Weighted skew was only used in example 1: Systematic data; it was not used in examples 2–7. In order to clearly illustrate how the EMA and MGBT screening for PILFs are used in flood frequency analysis, only the at-site skew at each station was used.

Systematic Record Example—Moose River at Victory, Vermont

This example illustrates the use of EMA and the MGBT to perform a flood frequency analysis on a gage site with a record composed of systematic annual flood peaks.

For this example, USGS station 01134500 Moose River at Victory, Vermont, is used. The Moose River is located in the northeastern part of the State and flows mostly from north to south through hilly terrain. The Moose River basin is approximately 75 square miles (mi^2) of nearly all forest (Olson and Veilleux, 2014). Historically, the watershed was an important logging area and some logging still continues today. Attempts at farming in the basin have generally failed because of the presence of shallow rocky soil. There are a small number of villages in the basin, but overall it is sparsely populated with only a few miles of paved roadway. There is also a large bog approximately one third of a mile upstream from the gage. The bog is part of the 5,000-acre Victory Basin Wildlife management area. Whereas there is no streamflow regulation in the basin, the bog attenuates peaks in the basin.

USGS station 01134500 has an annual peak record consisting of 68 peaks, beginning in 1947 and ending in 2014. The annual peaks are listed in table 10–2 and can be downloaded from USGS NWIS at https://nwis.waterdata.usgs.gov/nwis/peak/?site_no=01134500&agency_cd=USGS.

EMA Representation of Peak Flow Data for Flood Frequency Analysis

As described in the [Data Representation Using Flow Intervals and Perception Thresholds](#) section, when using EMA the annual peak flow for every water year during the historical period is described by a flow interval ($(Q_{Y,\text{lower}}, Q_{Y,\text{upper}})$) for each water year Y . For peaks whose values are known and are not censored, the flow interval can be described as ($Q_{Y,\text{lower}} = Q_Y, Q_{Y,\text{upper}} = Q_Y$). For example, as shown in table 10–2, the peak for the 1947 water year is recorded as 2,080 ft^3/s . This peak is known and is not censored, thus the flow interval for the 1947 water year is ($Q_{1947,\text{lower}} = 2,080, Q_{1947,\text{upper}} = 2,080$). In this example, the flow values are known for all the years where the gage was in operation. Table 10–3 contains the EMA flow intervals for each water year in the record for station 01134500.

As described in the [Data Representation Using Flow Intervals and Perception Thresholds](#) section, EMA distinguishes among sampling properties by employing perception thresholds denoted ($T_{Y,\text{lower}}, T_{Y,\text{upper}}$) for each year Y , which reflect the range of flows that would have been measured or recorded had they occurred. Perception thresholds describe the range of measurable potential discharges and are independent of the actual peak discharges that have occurred. The lower bound, $T_{Y,\text{lower}}$, represents the smallest peak flow that would result in a recorded flow in water year Y . For most peaks at most gages, $T_{Y,\text{upper}}$ is assumed to be infinite, as bigger floods that might exceed the measurement capability of the streamgage are determined through study of high-water marks and other physical evidence of the flood. For periods of continuous, full-range peak-flow record, the perception threshold is represented by ($T_{Y,\text{lower}} = 0, T_{Y,\text{upper}} = \infty$), where $T_{Y,\text{lower}} = 0$ is the gage-base discharge. Table 10–4 contains the EMA perception thresholds for each water year in the record for USGS station 01134500.

The annual peaks, as well as their corresponding EMA flow intervals and perception thresholds, can be displayed graphically. Figure 10–1 contains a graphical representation of the recorded annual peaks, EMA flow intervals, and EMA perception thresholds. This graph of the data is simple for USGS station 01134500, as each year in the record has a recorded peak and the perception threshold for the entire period of record spans from ($T_{Y,\text{lower}} = 0, T_{Y,\text{upper}} = \infty$), thus indicating that all peaks were able to be recorded.

Table 10–2. U.S. Geological Survey station 01134500 Moose River at Victory, Vermont, annual peak-flow record consisting of 68 peaks from 1947 to 2014. This table contains the date of the annual peak recorded at the station, the water year of the annual peak, and the corresponding annual peak in cubic feet per second (ft^3/s).

[--, no entry or not available]

Date of peak streamflow	Water year	Annual peak streamflow (ft^3/s)	Date of peak streamflow	Water year	Annual peak streamflow (ft^3/s)	Date of peak streamflow	Water year	Annual peak streamflow (ft^3/s)
1947-04-13	1947	2,080	1970-04-25	1970	3,010	1993-04-17	1993	1,900
1948-03-28	1948	1,670	1971-05-04	1971	1,490	1994-04-17	1994	2,760
1949-03-28	1949	1,480	1972-05-05	1972	2,920	1995-08-06	1995	4,536
1950-04-21	1950	2,940	1973-07-01	1973	4,940	1996-04-24	1996	2,160
1950-12-05	1951	1,560	1973-12-22	1974	2,550	1996-12-02	1997	1,860
1952-06-02	1952	2,380	1975-04-20	1975	1,250	1998-03-31	1998	2,680
1953-03-27	1953	2,720	1976-04-02	1976	2,670	1999-09-18	1999	1,540
1954-04-23	1954	2,860	1977-03-31	1977	2,020	2000-05-11	2000	2,110
1955-04-15	1955	2,620	1978-05-10	1978	1,460	2001-04-25	2001	2,950
1956-04-30	1956	1,710	1979-03-26	1979	1,620	2002-04-14	2002	2,410
1957-04-22	1957	1,370	1980-04-10	1980	1,460	2003-03-30	2003	2,230
1957-12-21	1958	2,180	1981-02-21	1981	1,570	2003-10-28	2004	1,980
1959-04-04	1959	1,160	1982-04-18	1982	2,890	2005-04-04	2005	1,610
1959-11-29	1960	2,780	1983-05-04	1983	1,840	2005-10-17	2006	2,640
1961-04-24	1961	1,580	1984-05-31	1984	2,950	2007-04-24	2007	1,930
1962-04-08	1962	2,110	1985-04-17	1985	1,380	2008-04-20	2008	1,940
1963-04-22	1963	2,160	1986-03-31	1986	2,350	2009-04-04	2009	1,810
1964-04-15	1964	2,750	1987-03-31	1987	4,180	2010-03-24	2010	1,900
1965-06-14	1965	1,190	1988-04-06	1988	1,700	2010-10-01	2011	3,140
1966-03-26	1966	1,560	1989-04-06	1989	2,200	2012-03-20	2012	1,370
1967-04-03	1967	1,800	1990-03-18	1990	3,430	2013-04-20	2013	2,180
1968-03-24	1968	1,600	1990-12-24	1991	2,270	2014-04-16	2014	4,250
1969-04-29	1969	2,400	1992-04-23	1992	2,180	--	--	--

Table 10–3. U.S. Geological Survey station 01134500 Moose River at Victory, Vermont, Expected Moments Algorithm flow intervals for the systematic period from 1947 to 2014. This table contains the water year of the annual peak and the corresponding flow interval defined by lower bound, $Q_{Y,lower}$, and upper bound, $Q_{Y,upper}$, in cubic feet per second for each water year Y .

[--, no entry or not available]

Water year	$Q_{Y,lower}$	$Q_{Y,upper}$	Comments	Water year	$Q_{Y,lower}$	$Q_{Y,upper}$	Comments
1947	2,080	2,080	--	1981	1,570	1,570	--
1948	1,670	1,670	--	1982	2,890	2,890	--
1949	1,480	1,480	--	1983	1,840	1,840	--
1950	2,940	2,940	--	1984	2,950	2,950	--
1951	1,560	1,560	--	1985	1,380	1,380	--
1952	2,380	2,380	--	1986	2,350	2,350	--
1953	2,720	2,720	--	1987	4,180	4,180	--
1954	2,860	2,860	--	1988	1,700	1,700	--
1955	2,620	2,620	--	1989	2,200	2,200	--
1956	1,710	1,710	--	1990	3,430	3,430	--
1957	1,370	1,370	--	1991	2,270	2,270	--
1958	2,180	2,180	--	1992	2,180	2,180	--
1959	1,160	1,160	--	1993	1,900	1,900	--
1960	2,780	2,780	--	1994	2,760	2,760	--
1961	1,580	1,580	--	1995	4,536	4,536	--
1962	2,110	2,110	--	1996	2,160	2,160	--
1963	2,160	2,160	--	1997	1,860	1,860	--
1964	2,750	2,750	--	1998	2,680	2,680	--
1965	1,190	1,190	--	1999	1,540	1,540	--
1966	1,560	1,560	--	2000	2,110	2,110	--
1967	1,800	1,800	--	2001	2,950	2,950	--
1968	1,600	1,600	--	2002	2,410	2,410	--
1969	2,400	2,400	--	2003	2,230	2,230	--
1970	3,010	3,010	--	2004	1,980	1,980	--
1971	1,490	1,490	--	2005	1,610	1,610	--
1972	2,920	2,920	--	2006	2,640	2,640	--
1973	4,940	4,940	--	2007	1,930	1,930	--
1974	2,550	2,550	--	2008	1,940	1,940	--
1975	1,250	1,250	--	2009	1,810	1,810	--
1976	2,670	2,670	--	2010	1,900	1,900	--
1977	2,020	2,020	--	2011	3,140	3,140	--
1978	1,460	1,460	--	2012	1,370	1,370	--
1979	1,620	1,620	--	2013	2,180	2,180	--
1980	1,460	1,460	--	2014	4,250	4,250	--

Table 10–4. U.S. Geological Survey station 01134500 Moose River at Victory, Vermont, Expected Moments Algorithm (EMA) perception thresholds for the systematic period from 1947 to 2014. This table contains the water year ranges to which each perception threshold (in cubic feet per second) applies; $T_{Y,lower}$, the lower bound of the perception threshold for water year Y ; $T_{Y,upper}$, the upper bound of the perception threshold for water year Y ; and a comment describing the threshold.

Start year	End year	EMA perception threshold		Comment
		$T_{Y,lower}$	$T_{Y,upper}$	
1947	2014	0	Infinity	Continuous systematic record.

Results from Flood Frequency Analysis

A flood frequency analysis at USGS station 01134500 was performed using the EMA flow intervals and perception thresholds as shown in tables 10–3 and 10–4. The output from an at-site flood frequency analysis using EMA with the Multiple Grubbs-Beck Test (MGBT) to screen for potentially influential low floods (PILFs) is shown below. Note that for the analysis described below, weighted skew was used. As described in the section [Estimating Regional Skew](#), an improved estimate of skew can be computed by weighting the station skew with a regional skew (see the section [Weighted Skew Coefficient Estimator](#) for details). The regional skew used for this station is 0.44 with a corresponding standard error of 0.28 (MSE = 0.078) ([Olson and Veilleux, 2014](#)). The at-site skew estimate is 0.397 with a MSE = 0.10. The estimated peak flow for selected

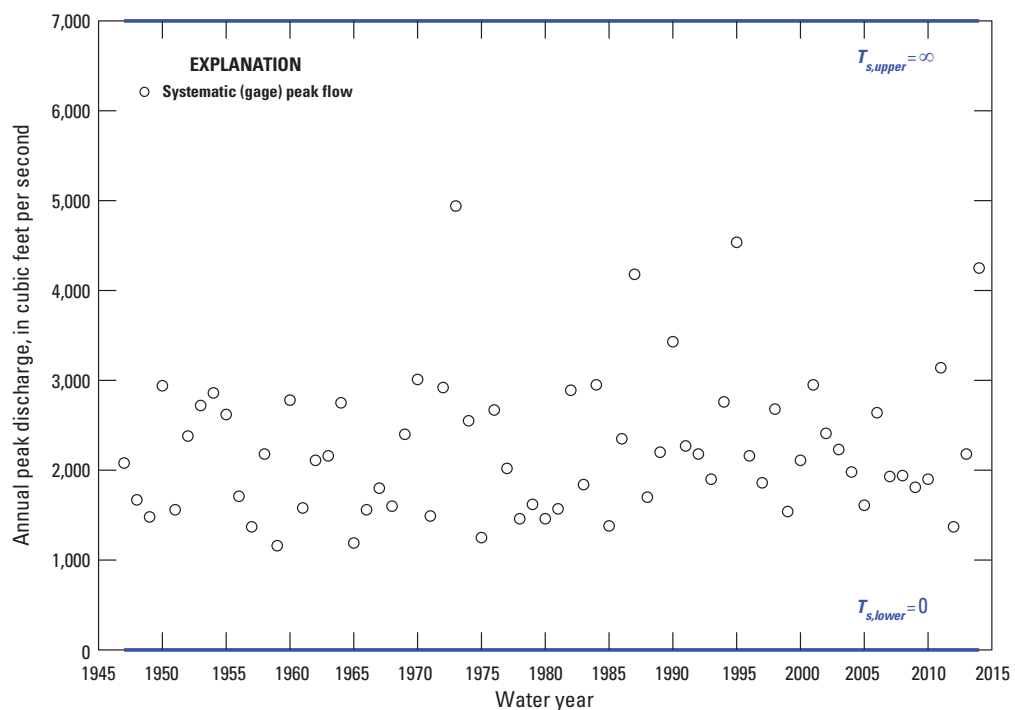


Figure 10–1. Graph showing U.S. Geological Survey station 01134500 Moose River at Victory, Vermont, annual peak-flow time series consisting of 68 peaks from 1947 to 2014. Open circles represent recorded systematic peaks. The perceptible range for the systematic (gage) period $T_{s,lower}, T_{s,upper}$ ($0, \infty$) is shown as blue lines.

annual exceedance probabilities can be found in table 10–5, whereas the fitted frequency curve is displayed in figure 10–2. The final estimated moments were 3.3286 (mean), 0.1403 (standard deviation), and 0.421 (weighted skew).

The results of the above analysis were generated using weighted skew. In order to demonstrate the potential impact of the weighted skew on a flood frequency analysis, here we present the results for the same analysis using solely the station skew and compare the results to those previously obtained using the weighted skew. As shown in figure 10–3, the confidence intervals when using only the station skew are wider for the smaller exceedance probabilities as compared to those in figure 10–2 when the weighted skew is used. It is important to note that this is just one example of the effect of weighted skew on a flood frequency analysis. The impact could be more significant or less significant than shown above, depending on the peak-flow data at the station, as well as the value of the station's corresponding regional skew and the accuracy of that regional skew.

The fitted frequency curve computed using EMA with MGBT is displayed in red in figure 10–2. Because the annual peak-flow record contains only systematic peaks with no historic information, no censored peaks, and no PILFs identified by the MGBT, the fitted frequency curve using these flood frequency Guidelines is the same as that from Bulletin 17B.

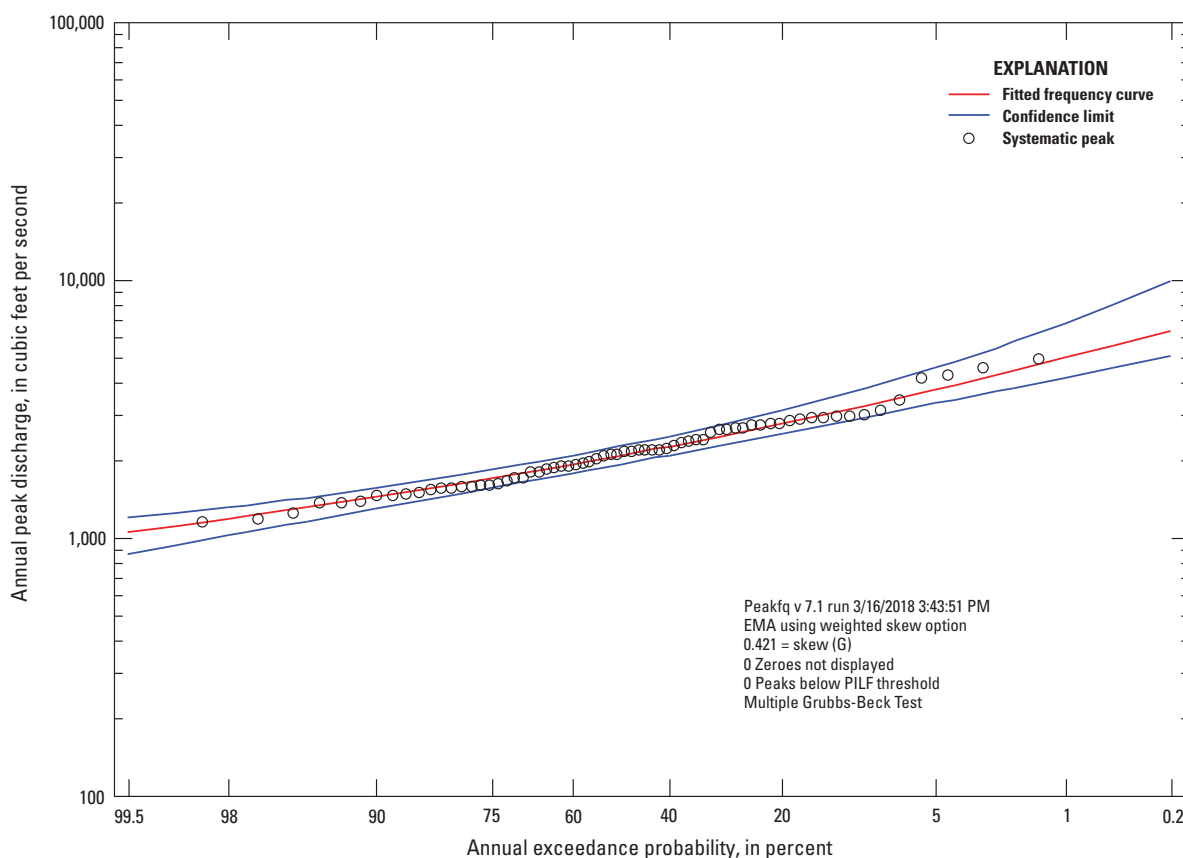


Figure 10–2. Graph showing annual exceedance probability plot for U.S. Geological Survey station 01134500 Moose River at Victory, Vermont, based on flood frequency analysis using Expected Moments Algorithm (EMA) with Multiple Grubbs-Beck Test and weighted skew. The red line is the fitted log-Pearson Type III frequency curve, the blue lines are the upper and lower confidence limits, and the black circles are the systematic peaks. PILF, potentially influential low flood.

Table 10–5. Peak-flow quantiles in cubic feet per second for U.S. Geological Survey station 01134500 based on flood frequency analysis using Expected Moments Algorithm (EMA) with Multiple Grubbs-Beck Test; variance of estimate shown in log space.

[%, percent; ft³/s, cubic feet per second]

Annual exceedance probability	EMA estimate (ft ³ /s)	Variance of estimate	Lower 2.5% confidence limit (ft ³ /s)	Upper 97.5% confidence limit (ft ³ /s)
0.100	3,261	0.0007	2,933	3,826
0.040	3,911	0.0014	3,426	5,038
0.020	4,422	0.0021	3,782	6,234
0.010	4,957	0.0031	4,131	7,735
0.005	5,519	0.0043	4,476	9,616
0.002	6,313	0.0064	4,929	12,850

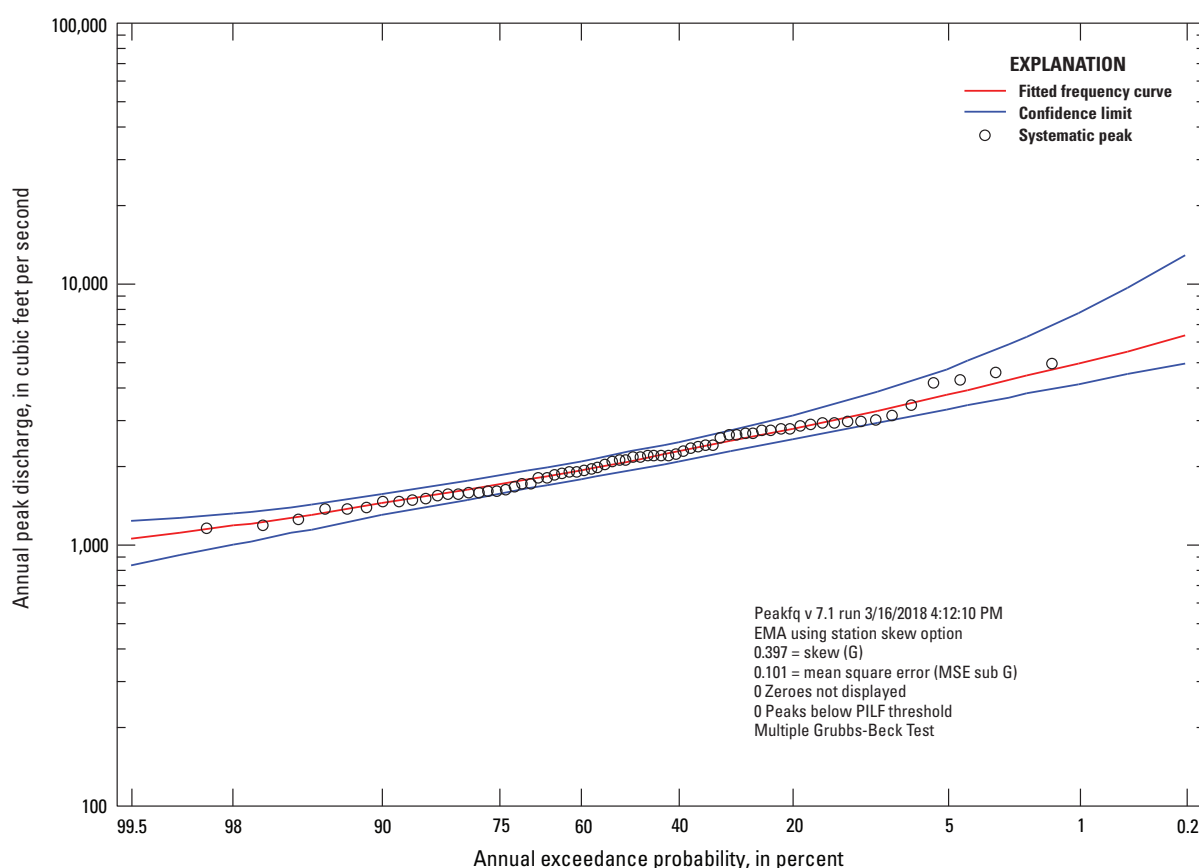


Figure 10–3. Graph showing annual exceedance probability plot for U.S. Geological Survey station 01134500 Moose River at Victory, Vermont, based on flood frequency analysis using Expected Moments Algorithm (EMA) with Multiple Grubbs-Beck Test and station skew only. The red line is the fitted log-Pearson Type III frequency curve, the blue lines are the upper and lower confidence limits, and the black circles are the systematic peaks. PILF, potentially influential low flood.

PILF Example—Orestimba Creek near Newman, California

This example demonstrates how the Expected Moments Algorithm (EMA) and the Multiple Grubbs-Beck Test (MGBT) can be used to perform a flood frequency analysis on a gage site with a record composed of systematic annual flood peaks when potentially influential low floods (PILFs) are present.

For this example, USGS station 11274500 Orestimba Creek near Newman, California, is used (Parrett and others, 2011; Gotvald and others, 2012). Orestimba Creek is a tributary to the San Joaquin River, whose 134-mi² drainage area lies on the eastern slope of the Diablo Range section of the Coast Range Mountains of California (U.S. Army Corps of Engineers, 2008). The drainage basin has an average basin elevation of 1,551 feet with peak flows usually occurring in late winter. Orestimba Creek is one of the few tributaries in the area to maintain a definite stream channel from the foothills to the San Joaquin River (U.S. Army Corps of Engineers, 2008). Some additional details about this station are in Gotvald and others (2012).

USGS station 11274500 has an annual peak record consisting of 82 peaks beginning in 1932 and ending in 2013. The annual peaks are listed in table 10–6 (downloaded from USGS NWIS: https://nwis.waterdata.usgs.gov/nwis/peak/?site_no=11274500&agency_cd=USGS) and shown in figure 10–4. Of the 82 annual peaks, there are 12 years for which the annual peak is 0 ft³/s.

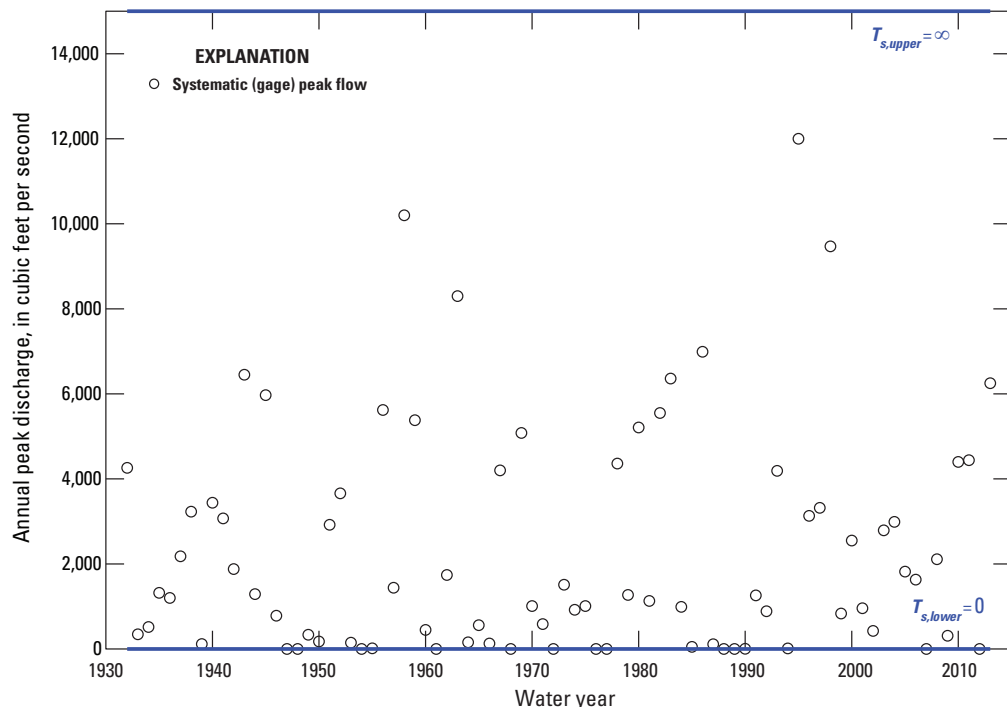


Figure 10–4. Graph showing U.S. Geological Survey station 11274500 Orestimba Creek near Newman, California, annual peak-flow time series consisting of 82 peaks from 1932 to 2013. Open circles represent recorded systematic peaks. The perceptible range for the systematic (gage) periods $T_{s,lower}$, $T_{s,upper}$ ($0, \infty$) is shown as blue lines.

Table 10–6. U.S. Geological Survey station 11274500 Orestimba Creek near Newman, California, annual peak-flow record consisting of 82 peaks from 1932 to 2013. This table contains the date of the annual peak recorded at the station, the water year of the annual peak, and the corresponding annual peak in cubic feet per second (ft^3/s).

[--, no entry or not available]

Date of peak streamflow	Water year	Annual peak streamflow (ft^3/s)	Date of peak streamflow	Water year	Annual peak streamflow (ft^3/s)	Date of peak streamflow	Water year	Annual peak streamflow (ft^3/s)
1932-02-08	1932	4,260	1960-02-10	1960	448	1988-00-00	1988	0
1933-01-29	1933	345	1961-00-00	1961	0	1989-00-00	1989	0
1934-01-01	1934	516	1962-02-15	1962	1,740	1990-05-28	1990	4
1935-04-08	1935	1,320	1963-02-01	1963	8,300	1991-03-24	1991	1,260
1936-02-13	1936	1,200	1964-01-22	1964	156	1992-02-15	1992	888
1937-02-13	1937	2,180	1965-01-06	1965	560	1993-01-13	1993	4,190
1938-02-11	1938	3,230	1965-12-30	1966	128	1994-02-20	1994	12
1939-03-09	1939	115	1967-01-24	1967	4,200	1995-03-10	1995	12,000
1940-02-27	1940	3,440	1968-00-00	1968	0	1996-02-19	1996	3,130
1941-04-04	1941	3,070	1969-01-25	1969	5,080	1997-01-23	1997	3,320
1942-01-24	1942	1,880	1970-03-01	1970	1,010	1998-02-03	1998	9,470
1943-01-21	1943	6,450	1970-12-21	1971	584	1999-02-09	1999	833
1944-02-29	1944	1,290	1972-00-00	1972	0	2000-02-14	2000	2,550
1945-02-02	1945	5,970	1973-02-11	1973	1,510	2001-03-05	2001	958
1945-12-25	1946	782	1974-03-03	1974	922	2002-01-03	2002	425
1947-00-00	1947	0	1975-03-08	1975	1,010	2002-12-16	2003	2,790
1948-00-00	1948	0	1976-00-00	1976	0	2004-02-25	2004	2,990
1949-03-12	1949	335	1977-00-00	1977	0	2005-02-16	2005	1,820
1950-02-05	1950	175	1978-01-17	1978	4,360	2006-01-02	2006	1,630
1950-12-03	1951	2,920	1979-02-21	1979	1,270	2007-00-00	2007	0
1952-01-12	1952	3,660	1980-02-16	1980	5,210	2008-01-25	2008	2,110
1952-12-07	1953	147	1981-01-29	1981	1,130	2009-02-17	2009	310
1954-00-00	1954	0	1982-01-05	1982	5,550	2010-01-20	2010	4,400
1955-01-19	1955	16	1983-01-24	1983	6,360	2011-03-24	2011	4,440
1955-12-23	1956	5,620	1983-12-25	1984	991	2012-00-00	2012	0
1957-02-24	1957	1,440	1985-02-09	1985	50	2012-12-24	2013	6,250
1958-04-02	1958	10,200	1986-02-19	1986	6,990	--	--	--
1959-02-16	1959	5,380	1987-03-06	1987	112	--	--	--

EMA Representation of Peak Flow Data for Flood Frequency Analysis

As described in the [Data Representation Using Flow Intervals and Perception Thresholds](#) section, when using EMA the annual peak flow for every water year during the historical period is described by a flow interval ($Q_{Y,lower}, Q_{Y,upper}$) for each water year Y . For peaks whose values are known and are not censored, the flow interval can be described as ($Q_{Y,lower} = Q_Y, Q_{Y,upper} = Q_Y$). For example, as shown in table 10–6, the peak for the 1932 water year is recorded as 4,260 ft³/s. This peak is known and is not censored, thus the flow interval for the 1932 water year is ($Q_{1932,lower} = 4,260, Q_{1932,upper} = 4,260$). Table 10–7 contains the EMA flow intervals for each water year in the record for station 11274500.

As described in the [Data Representation Using Flow Intervals and Perception Thresholds](#) section, EMA distinguishes among sampling properties by employing perception thresholds denoted ($T_{Y,lower}, T_{Y,upper}$) for each year Y , which reflect the range of flows that would have been measured or recorded had they occurred. Perception thresholds describe the range of measurable potential discharges and are independent of the actual peak discharges that have occurred. The lower bound, $T_{Y,lower}$, represents the smallest peak flow that would result in a recorded flow in water year Y . For most peaks at most gages, $T_{Y,upper}$ is assumed to be infinite, as bigger floods that might exceed the measurement capability of the streamgage are determined through study of high-water marks and other physical evidence of the flood. For periods of continuous, full-range peak-flow record, the perception threshold is represented by ($T_{Y,lower} = 0, T_{Y,upper} = \infty$), where $T_{Y,lower} = 0$ is the gage-base discharge. Table 10–8 contains the EMA perception thresholds for each water year in the record for USGS station 11274500.

Results from Flood Frequency Analysis

A flood frequency analysis at USGS station 11274500 was performed using the EMA flow intervals and perception thresholds as shown in tables 10–7 and 10–8. The output from an at-site flood frequency analysis using EMA with the Multiple Grubbs-Beck test to screen for PILFs is shown below. Note that station skew was used, thus allowing the focus to be on the at-site data. The fitted frequency curve is displayed in figure 10–5 with estimates provided in table 10–9. The final estimated moments were 3.0227 (mean), 0.6821 (standard deviation), and –0.929 (station skew).

As shown in figure 10–5, the PILF threshold T_{PILF} established by the MGBT is 782 ft³/s, with a significance level equal to 0.0007. Thus, all 30 annual peaks (including 12 zeros) less than 782 ft³/s are censored and re-coded in the framework of EMA with flow intervals of ($Q_{Y,lower} = 0, Q_{Y,upper} = 782$). The MGBT threshold also has the effect of adjusting the lower bound of the perception threshold. Thus for the entire historical period from 1932 to 2013, the perception threshold based on T_{PILF} is ($T_{Y,lower} = 782, T_{Y,upper} = \infty$). As shown in figure 10–5, by censoring the 30 smallest peaks in the record, the smallest annual exceedance probability peaks are well fit by the frequency curve (red line).

114 Guidelines for Determining Flood Flow Frequency—Bulletin 17C

Table 10-7. U.S. Geological Survey station 11274500 Orestimba Creek near Newman, California, Expected Moments Algorithm flow intervals for the systematic period from 1932 to 2013. This table contains the water year of the annual peak and the corresponding flow interval defined by lower bound, $Q_{Y,lower}$, and upper bound, $Q_{Y,upper}$, in cubic feet per second for each water year Y .

[--, no entry or not available]

Water year	$Q_{Y,lower}$	$Q_{Y,upper}$	Comments	Water year	$Q_{Y,lower}$	$Q_{Y,upper}$	Comments
1932	4,260	4,260	--	1973	1,510	1,510	--
1933	345	345	--	1974	922	922	--
1934	516	516	--	1975	1,010	1,010	--
1935	1,320	1,320	--	1976	0	0	Zero flow.
1936	1,200	1,200	--	1977	0	0	Zero flow.
1937	2,180	2,180	--	1978	4,360	4,360	--
1938	3,230	3,230	--	1979	1,270	1,270	--
1939	115	115	--	1980	5,210	5,210	--
1940	3,440	3,440	--	1981	1,130	1,130	--
1941	3,070	3,070	--	1982	5,550	5,550	--
1942	1,880	1,880	--	1983	6,360	6,360	--
1943	6,450	6,450	--	1984	991	991	--
1944	1,290	1,290	--	1985	50	50	--
1945	5,970	5,970	--	1986	6,990	6,990	--
1946	782	782	--	1987	112	112	--
1947	0	0	Zero flow.	1988	0	0	Zero flow.
1948	0	0	Zero flow.	1989	0	0	Zero flow.
1949	335	335	--	1990	4	4	--
1950	175	175	--	1991	1,260	1,260	--
1951	2,920	2,920	--	1992	888	888	--
1952	3,660	3,660	--	1993	4,190	4,190	--
1953	147	147	--	1994	12	12	--
1954	0	0	Zero flow.	1995	12,000	12,000	--
1955	16	16	--	1996	3,130	3,130	--
1956	5,620	5,620	--	1997	3,320	3,320	--
1957	1,440	1,440	--	1998	9,470	9,470	--
1958	10,200	10,200	--	1999	833	833	--
1959	5,380	5,380	--	2000	2,550	2,550	--
1960	448	448	--	2001	958	958	--
1961	0	0	Zero flow.	2002	425	425	--
1962	1,740	1,740	--	2003	2,790	2,790	--
1963	8,300	8,300	--	2004	2,990	2,990	--
1964	156	156	--	2005	1,820	1,820	--
1965	560	560	--	2006	1,630	1,630	--
1966	128	128	--	2007	0	0	Zero flow.
1967	4,200	4,200	--	2008	2,110	2,110	--
1968	0	0	Zero flow.	2009	310	310	--
1969	5,080	5,080	--	2010	4,400	4,400	--
1970	1,010	1,010	--	2011	4,440	4,440	--
1971	584	584	--	2012	0	0	Zero flow.
1972	0	0	Zero flow.	2013	6,250	6,250	--

Table 10–8. U.S. Geological Survey station 11274500 Orestimba Creek near Newman, California, Expected Moments Algorithm (EMA) perception thresholds for the period from 1932 to 2013. This table contains the water year ranges to which each perception threshold (in cubic feet per second) applies; $T_{Y,lower}$ the lower bound of the perception threshold for water year Y , $T_{Y,upper}$, the upper bound of the perception threshold for water year Y ; and a comment describing the threshold.

Start year	End year	EMA perception threshold		Comment
		$T_{Y,lower}$	$T_{Y,upper}$	
1932	2013	0	Infinity	Continuous systematic record.

Table 10–9. Peak-flow quantiles in cubic feet per second for U.S. Geological Survey station 11274500 Orestimba Creek near Newman, California, based on flood frequency analysis using Expected Moments Algorithm (EMA) with Multiple Grubbs-Beck Test; variance of estimate shown in log space.

[%, percent; ft³/s, cubic feet per second]

Annual exceedance probability	EMA estimate (ft ³ /s)	Variance of estimate	Lower 2.5% confidence limit (ft ³ /s)	Upper 97.5% confidence limit (ft ³ /s)
0.500	1,339	0.0078	620.6	1,840
0.200	4,026	0.0045	2,965	5,595
0.100	6,328	0.0049	4,686	9,394
0.040	9,426	0.0061	6,944	16,110
0.020	11,690	0.0073	8,489	21,920
0.010	13,820	0.0088	9,813	27,730
0.005	15,800	0.0106	10,910	33,500
0.002	18,150	0.0135	12,040	41,610

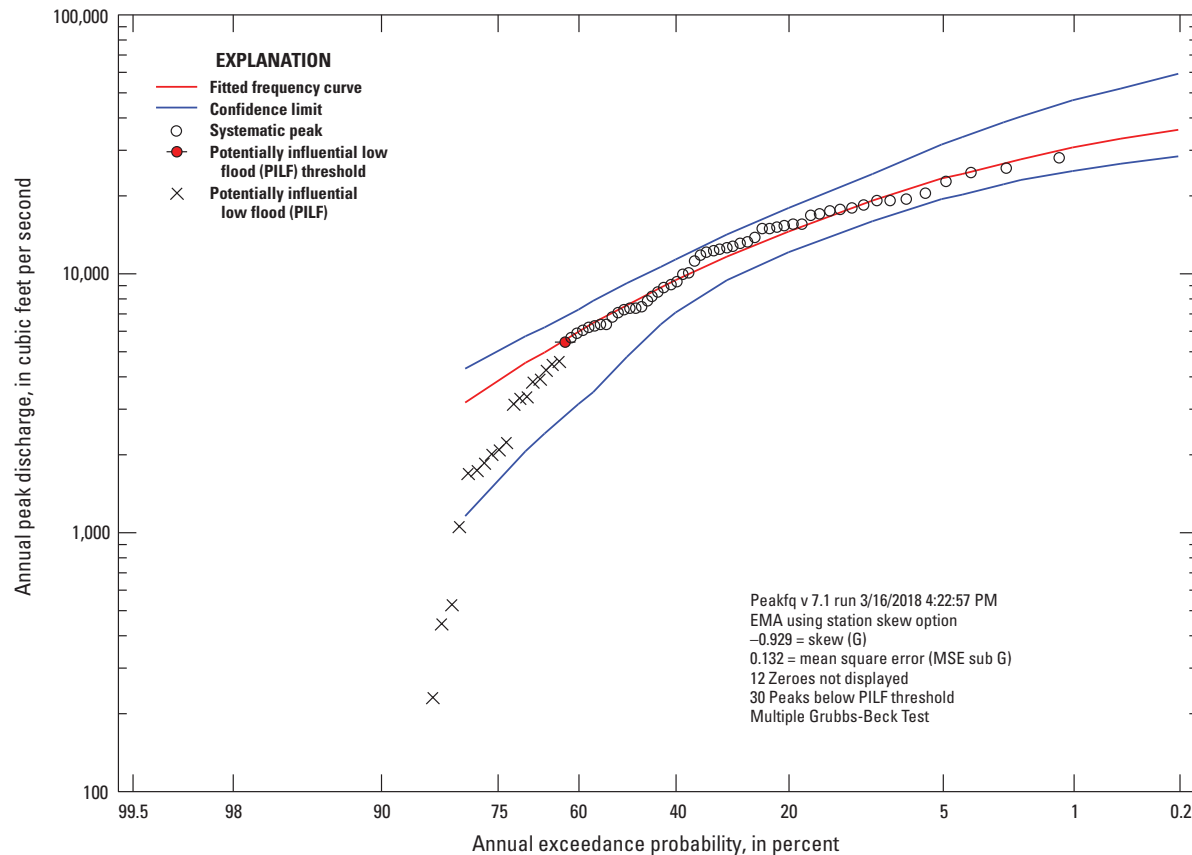


Figure 10–5. Graph showing annual exceedance probability plot for U.S. Geological Survey station 11274500 Orestimba Creek near Newman, California, based on flood frequency analysis using Expected Moments Algorithm (EMA) with Multiple Grubbs-Beck Test (MGBT). The red line is the fitted log-Pearson Type III frequency curve, the blue lines are the upper and lower confidence limits, the black circles are the systematic peaks, the solid red circle with a line through it is the potentially influential low flood (PILF) threshold as identified by the MGBT, and the black x's are the PILFs identified by the MGBT.

Broken Record Example—Back Creek near Jones Springs, West Virginia

This example illustrates the use of the Expected Moments Algorithm (EMA) for a broken record, as described in the section [Broken, Incomplete, and Discontinued Records](#). For this example, USGS station 01614000 Back Creek near Jones Springs, West Virginia, is used. Back Creek is a tributary to the Potomac River; the 235-mi² watershed lies within the Valley and Ridge province in West Virginia ([Wiley and Atkins, 2010](#)).

USGS station 01614000 has an annual peak record consisting of 56 peaks, beginning in 1929 and ending in 2012. There are three “broken record” periods where the station was discontinued: 1932 to 1937, 1976 to 1991, and 1999 to 2003. Thus, there are 28 years of missing data at this station during the period 1929 to 2012. There is a historic flood that occurred outside the period of gaging record on March 17, 1936. This flood is noted in the USGS Annual Water Data Report for this station, available in the peak-flow file, and there is historical information available for this large flood ([Grover, 1937](#)). The annual peaks are listed in table 10–10 and shown in figure 10–6. Of the 56 annual peaks, the October 1942 flood slightly exceeds the March 1936 historic flood peak. Based on the historical flood information in [Grover \(1937\)](#) for the 1936 flood, and the large regional floods and historical floods described by [Wiley and Atkins \(2010\)](#) in West Virginia for the period 1888 to 1996, information from the March 1936 flood is used as a perception threshold to represent the 28 years of missing information.

EMA Representation of Peak Flow Data for Flood Frequency Analysis

As described in the [Data Representation Using Flow Intervals and Perception Thresholds](#) section, when using EMA, the annual peak flow for every water year during the historical period is described by a flow interval ($Q_{Y,lower}, Q_{Y,upper}$) for each water year Y . For peaks whose values are known and are not censored, the flow interval can be described as ($Q_{Y,lower} = Q_Y, Q_{Y,upper} = Q_Y$). In this example, the flow values are known for all the years where the station was in operation. Table 10–11 contains the EMA flow intervals for each water year in the record for station 01614000. Missing years are described by perception thresholds.

As described in the [Data Representation Using Flow Intervals and Perception Thresholds](#) section, EMA distinguishes among sampling properties by employing perception thresholds denoted ($T_{Y,lower}, T_{Y,upper}$) for each year Y , which reflect the range of flows that would have been measured or recorded had they occurred. Perception thresholds describe the range of measurable potential discharges and are independent of the actual peak discharges that have occurred. The lower bound, $T_{Y,lower}$, represents the smallest peak flow that would result in a recorded flow in water year Y . For most peaks at most gages, $T_{Y,upper}$ is assumed to be infinite, as bigger floods that might exceed the measurement capability of the streamgage are determined through study of high-water marks and other physical evidence of the flood. For periods of continuous, full-range peak-flow record, the perception threshold is represented by ($T_{Y,lower} = 0, T_{Y,upper} = \infty$), where $T_{Y,lower} = 0$ is the gage-base discharge. In this example, there are missing years that are described by the 1936 historical flood magnitude. Based on the March 1936 large historical flood ([Grover, 1937](#)) and the regional historical flood information available for the largest floods in West Virginia ([Wiley and Atkins, 2010](#)), it is known that floods at this location would have been estimated (or recorded), had they exceeded approximately 21,000 ft³/s. Table 10–12 contains the EMA perception thresholds for each water year in the record, including missing periods, for USGS station 01614000.

Results from Flood Frequency Analysis

A flood frequency analysis at USGS station 01614000 was performed using the EMA flow intervals and perception thresholds as shown in tables 10–11 and 10–12. The output from an at-site flood frequency analysis

using EMA with the Multiple Grubbs-Beck Test (MGBT) to screen for potentially influential low floods (PILFs) is shown below. Note that station skew was used, thus allowing the focus to be on the at-site data. The fitted frequency curve is displayed in figure 10–7 with estimates provided in table 10–13. The final estimated moments were 3.7598 (mean), 0.2434 (standard deviation), and 0.144 (station skew).

As shown in figure 10–7, there are two floods that exceed the historical threshold ($21,000 \text{ ft}^3/\text{s}$): the March 1936 flood and the October 1942 flood. Using the MGBT, two PILFs were identified, with a threshold equal to $2,000 \text{ ft}^3/\text{s}$ and a significance level equal to 0.0881. Two annual peaks less than $2,000 \text{ ft}^3/\text{s}$ are censored and re-coded in the framework of EMA with flow intervals of ($Q_{Y,lower} = 0, Q_{Y,upper} = 2,000$). The MGBT threshold also has the effect of adjusting the lower bound of the perception threshold. Thus for the entire historical period from 1929 to 2012, with the exception of the missing years, the perception threshold is ($T_{Y,lower} = 2,000, T_{Y,upper} = \infty$). For the broken-record years covered by historical information, the lower threshold $T_{Y,lower} = 21,000$ (table 10–12). As shown in figure 10–7, by censoring the one smallest peak in the record, the remaining smallest annual exceedance probability peaks and the largest floods are well fit by the frequency curve (red line).

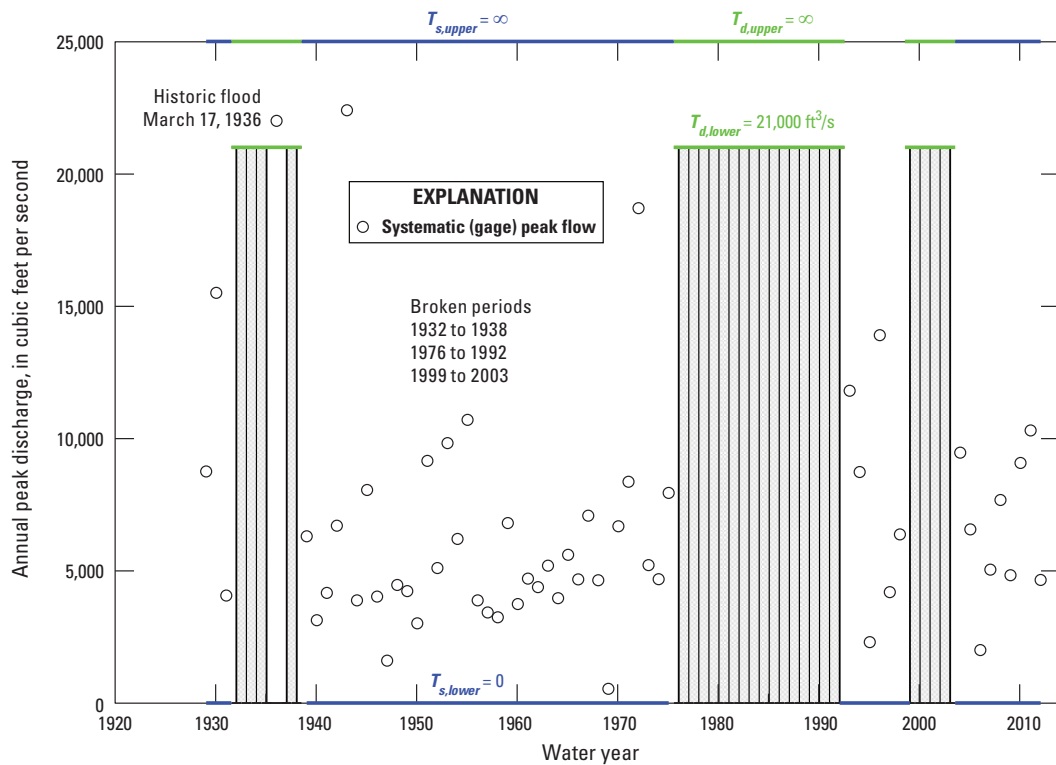


Figure 10–6. Graph showing U.S. Geological Survey station 01614000 Back Creek near Jones Springs, West Virginia, annual peak-flow time series consisting of 56 peaks from 1929 to 2012. Flood intervals are shown as black vertical bars with caps that represent lower and upper flow estimates. The gray shaded areas represent floods of unknown magnitude less than the perception threshold $T_{d,lower}$ during the broken record periods. The green lines represent the range in which floods would have been measured or recorded for the broken record periods 1932 to 1938, 1976 to 1992, and 1999 to 2003, with lower and upper perception thresholds $T_{d,lower}$ ($21,000 \text{ cubic feet per second } [\text{ft}^3/\text{s}]$) and $T_{d,upper}$ estimated from the March 1936 historic flood. The perceptible range for the systematic (gage) periods $T_{s,lower}, T_{s,upper} (0, \infty)$ is shown as blue lines.

Table 10–10. U.S. Geological Survey station 01614000 Back Creek near Jones Springs, West Virginia, annual peak-flow record consisting of 56 peaks from 1929 to 2012, including the 1936 historical flood. This table contains the date of the annual peak recorded at the station, the water year of the annual peak, and the corresponding annual peak in cubic feet per second (ft³/s). Horizontal lines indicate broken-record years.

[--, no entry or not available]

Date of peak streamflow	Water year	Annual peak streamflow (ft ³ /s)	Date of peak streamflow	Water year	Annual peak streamflow (ft ³ /s)	Date of peak streamflow	Water year	Annual peak streamflow (ft ³ /s)
1929-04-17	1929	8,750	1954-03-02	1954	6,200	1972-12-09	1973	5,210
1929-10-23	1930	15,500	1955-08-19	1955	10,700	1973-12-27	1974	4,680
1931-05-08	1931	4,060	1956-03-15	1956	3,880	1975-03-20	1975	7,940
1936-03-17	1936	22,000	1957-02-10	1957	3,420	1993-03-05	1993	11,800
1939-02-04	1939	6,300	1958-03-27	1958	3,240	1994-05-08	1994	8,730
1940-04-20	1940	3,130	1959-06-03	1959	6,800	1995-01-16	1995	2,300
1941-04-06	1941	4,160	1960-05-09	1960	3,740	1996-01-19	1996	13,900
1942-05-22	1942	6,700	1961-02-19	1961	4,700	1996-11-09	1997	4,190
1942-10-15	1943	22,400	1962-03-22	1962	4,380	1998-03-21	1998	6,370
1944-03-24	1944	3,880	1963-03-20	1963	5,190	2004-09-29	2004	9,460
1945-09-18	1945	8,050	1964-01-10	1964	3,960	2005-03-29	2005	6,560
1946-06-03	1946	4,020	1965-03-06	1965	5,600	2005-11-30	2006	2,000
1947-03-15	1947	1,600	1966-09-21	1966	4,670	2007-04-16	2007	5,040
1948-04-14	1948	4,460	1967-03-08	1967	7,080	2008-04-21	2008	7,670
1948-12-31	1949	4,230	1968-03-17	1968	4,640	2009-05-05	2009	4,830
1950-02-02	1950	3,010	1969-02-02	1969	536	2010-03-14	2010	9,070
1950-12-05	1951	9,150	1970-07-10	1970	6,680	2011-04-17	2011	10,300
1952-04-28	1952	5,100	1970-11-13	1971	8,360	2012-03-01	2012	4,650
1952-11-22	1953	9,820	1972-06-22	1972	18,700	--	--	--

Table 10–11. U.S. Geological Survey station 01614000 Back Creek near Jones Springs, West Virginia, Expected Moments Algorithm flow intervals for the systematic period from 1929 to 2012. This table contains the water year of the annual peak and the corresponding flow interval defined by lower bound, $Q_{Y,lower}$, and upper bound, $Q_{Y,upper}$, in cubic feet per second for each water year Y . Horizontal lines indicate broken-record years.

[--, no entry or not available]

Water year	$Q_{Y,lower}$	$Q_{Y,upper}$	Comments	Water year	$Q_{Y,lower}$	$Q_{Y,upper}$	Comments
1929	8,750	8,750	--	1963	5,190	5,190	--
1930	15,500	15,500	--	1964	3,960	3,960	--
1931	4,060	4,060	--	1965	5,600	5,600	--
1936	22,000	22,000	Historic flood.	1966	4,670	4,670	--
1939	6,300	6,300	--	1967	7,080	7,080	--
1940	3,130	3,130	--	1968	4,640	4,640	--
1941	4,160	4,160	--	1969	536	536	--
1942	6,700	6,700	--	1970	6,680	6,680	--
1943	22,400	22,400	--	1971	8,360	8,360	--
1944	3,880	3,880	--	1972	18,700	18,700	--
1945	8,050	8,050	--	1973	5,210	5,210	--
1946	4,020	4,020	--	1974	4,680	4,680	--
1947	1,600	1,600	--	1975	7,940	7,940	--
1948	4,460	4,460	--	1993	11,800	11,800	--
1949	4,230	4,230	--	1994	8,730	8,730	--
1950	3,010	3,010	--	1995	2,300	2,300	--
1951	9,150	9,150	--	1996	13,900	13,900	--
1952	5,100	5,100	--	1997	4,190	4,190	--
1953	9,820	9,820	--	1998	6,370	6,370	--
1954	6,200	6,200	--	2004	9,460	9,460	--
1955	10,700	10,700	--	2005	6,560	6,560	--
1956	3,880	3,880	--	2006	2,000	2,000	--
1957	3,420	3,420	--	2007	5,040	5,040	--
1958	3,240	3,240	--	2008	7,670	7,670	--
1959	6,800	6,800	--	2009	4,830	4,830	--
1960	3,740	3,740	--	2010	9,070	9,070	--
1961	4,700	4,700	--	2011	10,300	10,300	--
1962	4,380	4,380	--	2012	4,650	4,650	--

Table 10–12. U.S. Geological Survey station 01614000 Back Creek near Jones Springs, West Virginia, Expected Moments Algorithm (EMA) perception thresholds for the systematic period from 1929 to 2012. This table contains the water year ranges to which each perception threshold (in cubic feet per second) applies; $T_{Y,lower}$, the lower bound of the perception threshold for water year Y ; $T_{Y,upper}$, the upper bound of the perception threshold for water year Y ; and a comment describing the threshold.

Start year	End year	EMA perception threshold		Comment
		$T_{Y,lower}$	$T_{Y,upper}$	
1929	1931	0	Infinity	Continuous systematic record.
1932	1938	21,000	Infinity	Missing record with historical information.
1939	1975	0	Infinity	Continuous systematic record.
1976	1992	21,000	Infinity	Missing record with historical information.
1993	1998	0	Infinity	Continuous systematic record.
1999	2003	21,000	Infinity	Missing record with historical information.
2004	2012	0	Infinity	Continuous systematic record.

Table 10–13. Peak-flow quantiles in cubic feet per second for U.S. Geological Survey station 01614000 Back Creek near Jones Springs, West Virginia, based on flood frequency analysis using Expected Moments Algorithm (EMA) with Multiple Grubbs-Beck Test; variance of estimate shown in log space.

[%, percent; ft³/s, cubic feet per second]

Annual exceedance probability	EMA estimate (ft ³ /s)	Variance of estimate	Lower 2.5% confidence limit (ft ³ /s)	Upper 97.5% confidence limit (ft ³ /s)
0.500	5,675	0.0013	4,819	6,676
0.200	9,179	0.0015	7,745	11,040
0.100	11,890	0.0019	9,879	14,880
0.040	15,770	0.0031	12,690	21,900
0.020	18,980	0.0045	14,820	29,440
0.010	22,480	0.0065	16,950	39,610
0.005	26,290	0.0090	19,060	53,190
0.002	31,860	0.0133	21,840	78,210

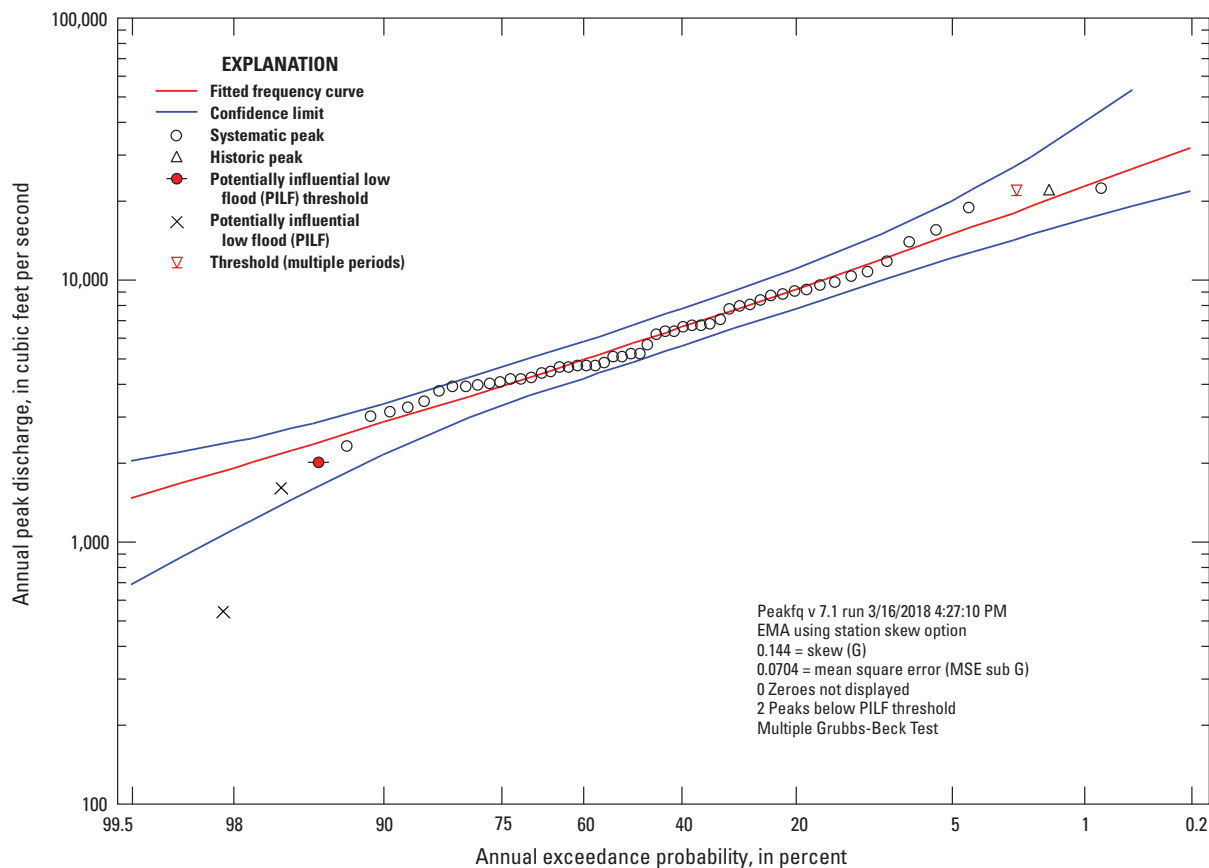


Figure 10–7. Graph showing annual exceedance probability plot for U.S. Geological Survey station 01614000 Back Creek near Jones Springs, West Virginia, based on flood frequency analysis using Expected Moments Algorithm (EMA) with Multiple Grubbs-Beck Test (MGBT). The red line is the fitted log-Pearson Type III frequency curve, the blue lines are the upper and lower confidence limits, the black circles are the systematic peaks, the solid red circle with a line through it is the potentially influential low flood (PILF) threshold as identified by the MGBT, and the black x's are the PILFs identified by the MGBT. The red triangle with the horizontal line represents the lower limit of the historical perception threshold (21,000 cubic feet per second).

Historical Record Example—Arkansas River at Pueblo, Colorado

This example illustrates the use of EMA for a historical record with several large floods (described in the section [Historical Flood Information](#)) and paleoflood information. The Arkansas River at Pueblo Dam near Pueblo, Colorado, is presented to illustrate the use of EMA with extensive historical information, paleoflood information, and the ability to place the record June 1921 flood in longer time context. The largest historic floods are described as interval data, and multiple thresholds are needed to effectively extend the discontinued streamgaging record after the dam was built. Paleoflood data are also included for this Reclamation dam safety application. Details of this example are presented in [England and others \(2006\)](#) and [England and others \(2010\)](#). Peak discharge probability estimates were made at four paleoflood sites on the Arkansas River at Pueblo State Park, Parkdale, at Loma Linda and at Adobe Park. We focus on the Pueblo State Park site flood frequency in this example; flood frequency results for other locations, as well as regional frequency results are presented in [England and others \(2006\)](#).

For this example, peak discharge estimates on the Arkansas River at Pueblo State Park are combined from USGS gaging stations at Portland (07097000) (years 1975 to 1976), near Portland (07099200) (1974), and near Pueblo (07099500) (years 1864 to 1973), and are used with Pueblo reservoir records (years 1977 to 2004) in order to gain a complete record of all large floods that exceeded approximately 10,000 ft³/s for the period of record. Some of these data, particularly the historical flood estimates, were obtained from USGS Water-Supply Papers, Colorado Division of Water Resources Records, historical accounts of the June 1921 flood, and other sources. As such, they do not directly correspond to peak flows in the USGS NWIS database. These gaging stations were previously documented and analyzed by [England and others \(2006\)](#); see also [England and others \(2010\)](#).

The annual peaks are listed in table 10–14 and shown in figure 10–8. Of the 85 annual peaks, including historical information, the June 3, 1921, peak ([Follansbee and Jones, 1922](#); [Munn and Savage, 1922](#)) is the largest. The total combined gage record length, excluding historical data, is 110 years (1895 to 2004) (fig. 10–8). The largest peak discharge estimates from these gages were unaffected by upstream regulation. Reviews of available historical information ([Follansbee and Jones, 1922](#); [Munn and Savage, 1922](#); [Follansbee and Sawyer, 1948](#)) indicated there was historical flood information at the site for frequency analysis. The historical record was estimated to begin in 1859, resulting in a 146-year period (1859 to 2004). Three historical floods were included: June 1864, July 1893, and May 1894. The magnitudes of these floods were large relative to the floods in the gaging record; estimates within a range were based on [Follansbee and Sawyer \(1948\)](#) and included in the flood frequency analysis. These estimates have relatively large uncertainties as compared to the smaller floods in the gage record. A paleohydrologic bound of about 840 years (before water year 2004) was estimated at this site for inclusion in the flood frequency curve. The estimate is based on three soils pits, two radiocarbon ages, and hydraulic modeling of a 7,500-foot reach ([England and others, 2006](#)). No estimates of individual paleofloods were made at this site, due to the relatively wide channel geometry and the lack of apparent stratigraphic evidence of large paleofloods during the limited field study ([England and others, 2010](#)). Peak discharge, historical flood, and nonexceedance-bound data synthesis for flood frequency show that these historical floods are the largest in the record, and combined with the paleoflood data, result in a substantially longer time series (fig. 10–8).

EMA Representation of Peak Flow Data for Flood Frequency Analysis

As described in the [Data Representation Using Flow Intervals and Perception Thresholds](#) section, when using EMA the annual peak flow for every water year during the historical period is described by a flow interval ($Q_{Y,lower}$, $Q_{Y,upper}$) for each water year Y . For peaks whose values are known and are not censored, the flow interval can be described as ($Q_{Y,lower} = Q_Y$, $Q_{Y,upper} = Q_Y$). In this example, the flow values are

Table 10–14. U.S. Geological Survey station 07099500 (and others) Arkansas River annual peak-flow record consisting of 85 peaks from 1864 to 1976. This table contains the water year of the annual peak and the corresponding annual peak in cubic feet per second (ft^3/s). Horizontal lines indicate broken-record years.

[--, no entry or not available]

Water year	Annual peak streamflow (ft^3/s)	Water year	Annual peak streamflow (ft^3/s)	Water year	Annual peak streamflow (ft^3/s)
1864	>41,000	1921	>80,000	1950	8,700
1893	>20,000	1922	8,850	1951	9,300
1894	>35,000	1923	25,600	1952	4,740
1895	6,100	1924	6,510	1953	6,770
1896	16,500	1925	4,930	1954	10,200
1897	4,300	1926	4,520	1955	11,100
1898	7,500	1927	12,400	1956	8,010
1899	8,800	1928	7,800	1957	9,070
1900	7,600	1929	10,500	1958	4,540
1901	11,100	1930	6,050	1959	2,820
1902	30,000	1931	3,560	1960	5,260
1903	10,500	1932	4,380	1961	5,760
1904	8,500	1933	8,630	1962	3,540
1905	8,000	1934	2,580	1963	8,360
1906	11,000	1935	9,880	1964	2,840
1907	6,600	1936	11,200	1965	23,500
1908	7,600	1937	9,300	1966	10,600
1909	5,800	1938	11,200	1967	5,870
1910	8,400	1939	2,910	1968	5,190
1911	3,700	1940	3,860	1969	6,620
1912	10,500	1941	7,560	1970	6,300
1913	7,800	1942	10,300	1971	3,360
1914	7,500	1943	3,320	1972	3,360
1915	17,000	1944	5,980	1973	6,760
1916	8,900	1945	9,290	1974	5,440
1917	6,800	1946	7,050	1975	10,200
1918	9,600	1947	7,280	1976	12,800
1919	6,300	1948	10,900	--	--
1920	8,500	1949	12,800	--	--

known for all the years where the gage was in operation. Table 10–15 contains the EMA flow intervals for each water year in the record for USGS station 07099500. The historical period is described by a perception threshold, as is the period after the gage was discontinued (1977 to 2004).

As described in the [Data Representation Using Flow Intervals and Perception Thresholds](#) section, EMA distinguishes among sampling properties by employing perception thresholds denoted ($T_{Y,lower}$, $T_{Y,upper}$) for each year Y , which reflect the range of flows that would have been measured or recorded had they occurred. Perception thresholds describe the range of measurable potential discharges and are independent of the actual peak discharges that have occurred. The lower bound, $T_{Y,lower}$, represents the smallest peak flow that would result in a recorded flow in water year Y . For most peaks at most gages, $T_{Y,upper}$ is assumed to be infinite, as bigger floods that might exceed the measurement capability of the streamgage are determined through study of highwater marks and other physical evidence of the flood. For periods of continuous, full-range peak flow record, the perception threshold is represented by ($T_{Y,lower} = 0$, $T_{Y,upper} = \infty$), where $T_{Y,lower} = 0$ is the gage-base discharge. Based on the historical floods and reservoir records, it is known that floods at this location would have been estimated (or recorded), had they exceeded approximately 20,000 ft³/s. Table 10–16 contains the EMA perception thresholds for each water year in the record, including the historical and paleo-flood period, for station 07099500.

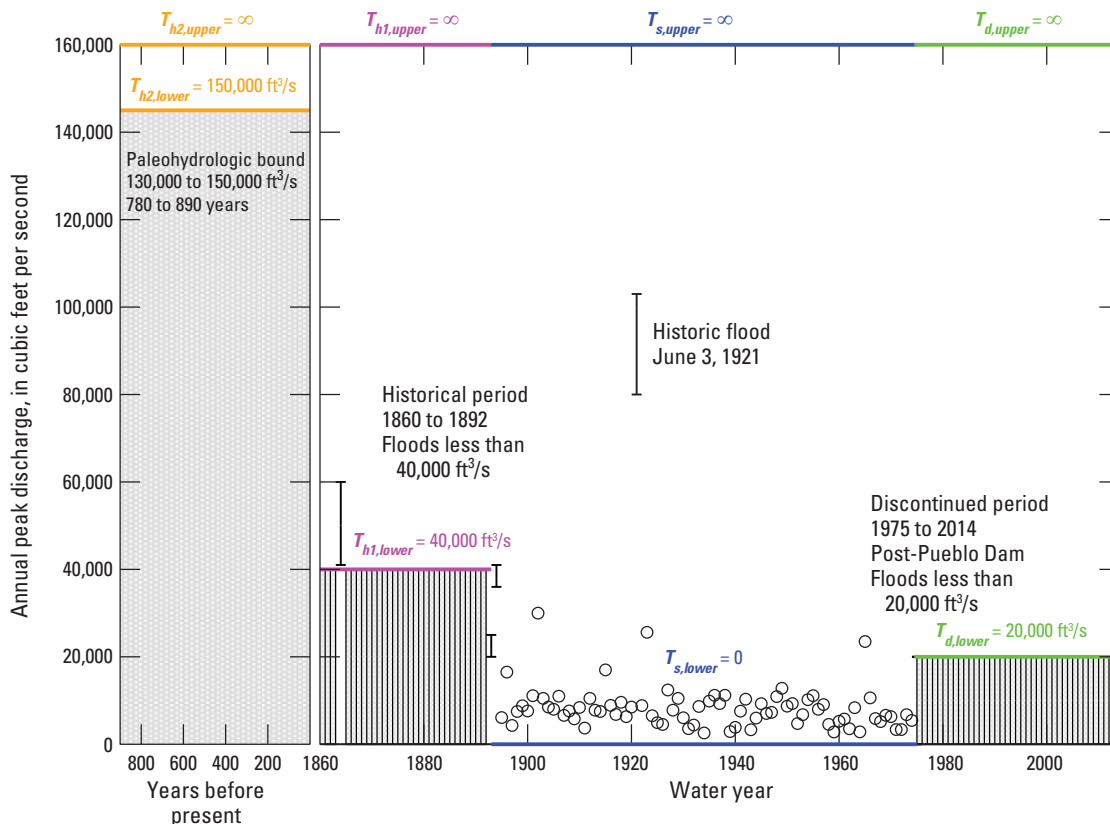


Figure 10–8. Graph showing peak discharge, historical and paleoflood estimates, Arkansas River at Pueblo State Park. A scale break is used to separate the gage and historical data from the longer paleoflood record. Flood intervals are shown as black vertical bars with caps that represent lower and upper flow estimates, including unobserved estimates in the historical period and historical floods in 1864, 1893, 1894 and 1921. The gray shaded areas represents floods of unknown magnitude less than the perception thresholds for the paleoflood period $T_{h2,lower}$, the historical period $T_{h1,lower}$, and the discontinued period $T_{d,lower}$. Perception threshold ranges in cubic feet per second (ft³/s) are shown as orange lines for the paleoflood period, magenta lines for the historical period, blue lines for the systematic period, and green lines for the discontinued period.

126 Guidelines for Determining Flood Flow Frequency—Bulletin 17C

Table 10-15. Arkansas River at Pueblo EMA flow intervals for the period from 1864 to 1976. Horizontal lines indicate broken-record years.

[--, no entry or not available]

Water year	Q _{y,lower}	Q _{y,upper}	Comments	Water year	Q _{y,lower}	Q _{y,upper}	Comments
1864	41,000	60,000	Historical flood.	1935	9,880	9,880	--
1893	20,000	25,000	Historical flood.	1936	11,200	11,200	--
1894	35,000	40,000	Historical flood.	1937	9,300	9,300	--
1895	6,100	6,100	--	1938	11,200	11,200	--
1896	16,500	16,500	--	1939	2,910	2,910	--
1897	4,300	4,300	--	1940	3,860	3,860	--
1898	7,500	7,500	--	1941	7,560	7,560	--
1899	8,800	8,800	--	1942	10,300	10,300	--
1900	7,600	7,600	--	1943	3,320	3,320	--
1901	11,100	11,100	--	1944	5,980	5,980	--
1902	30,000	30,000	--	1945	9,290	9,290	--
1903	10,500	10,500	--	1946	7,050	7,050	--
1904	8,500	8,500	--	1947	7,280	7,280	--
1905	8,000	8,000	--	1948	10,900	10,900	--
1906	11,000	11,000	--	1949	12,800	12,800	--
1907	6,600	6,600	--	1950	8,700	8,700	--
1908	7,600	7,600	--	1951	9,300	9,300	--
1909	5,800	5,800	--	1952	4,740	4,740	--
1910	8,400	8,400	--	1953	6,770	6,770	--
1911	3,700	3,700	--	1954	10,200	10,200	--
1912	10,500	10,500	--	1955	11,100	11,100	--
1913	7,800	7,800	--	1956	8,010	8,010	--
1914	7,500	7,500	--	1957	9,070	9,070	--
1915	17,000	17,000	--	1958	4,540	4,540	--
1916	8,900	8,900	--	1959	2,820	2,820	--
1917	6,800	6,800	--	1960	5,260	5,260	--
1918	9,600	9,600	--	1961	5,760	5,760	--
1919	6,300	6,300	--	1962	3,540	3,540	--
1920	8,500	8,500	--	1963	8,360	8,360	--
1921	80,000	103,000	Historical flood.	1,964	2,840	2,840	--
1922	8,850	8,850	--	1965	23,500	23,500	--
1923	25,600	25,600	--	1966	10,600	10,600	--
1924	6,510	6,510	--	1967	5,870	5,870	--
1925	4,930	4,930	--	1968	5,190	5,190	--
1926	4,520	4,520	--	1969	6,620	6,620	--
1927	12,400	12,400	--	1970	6,300	6,300	--
1928	7,800	7,800	--	1971	3,360	3,360	--
1929	10,500	10,500	--	1972	3,360	3,360	--
1930	6,050	6,050	--	1973	6,760	6,760	--
1931	3,560	3,560	--	1974	5,440	5,440	--
1932	4,380	4,380	--	1975	10,200	10,200	--
1933	8,630	8,630	--	1976	12,800	12,800	--
1934	2,580	2,580	--	--	--	--	--

Table 10–16. U.S. Geological Survey station 07099500 (and others) Arkansas River Expected Moments Algorithm (EMA) perception thresholds for the paleoflood, historical, and systematic period from 1165 to 2004. This table contains the water year ranges to which each perception threshold (in cubic feet per second) applies; $T_{Y,\text{lower}}$, the lower bound of the perception threshold for water year Y ; $T_{Y,\text{upper}}$, the upper bound of the perception threshold for water year Y ; and a comment describing the threshold.

Start year	End year	EMA perception threshold		Comment
		$T_{Y,\text{lower}}$	$T_{Y,\text{upper}}$	
1165	1858	150,000	Infinity	Paleoflood nonexceedance bound.
1859	1892	40,000	Infinity	1864 Historical information.
1893	1894	19,900	Infinity	1893 Historical information.
1895	1976	0	Infinity	Continuous systematic record.
1977	2004	20,000	Infinity	Post-reservoir bound.

Results from Flood Frequency Analysis

A flood frequency analysis for the Arkansas River at Pueblo was performed using the EMA flow intervals and perception thresholds as shown in tables 10–15 and 10–16. The output from an at-site flood frequency analysis using EMA with the Multiple Grubbs-Beck Test (MGBT) is shown below; no potentially influential low floods (PILFs) were identified. Note that station skew was used, thus allowing the focus to be on the at-site data. The fitted frequency curve is displayed in figure 10–9 with estimates provided in table 10–17. The flood frequency results (fig. 10–9) indicate the LP-III model fits the bulk of the data well, including most of the large floods, but underfits the largest flood (June 1921) because of the paleoflood data influence. The paleoflood nonexceedance-bound data at Pueblo State Park increases the peak discharge record length substantially to about 840 years, and has an effect on the upper end of the extrapolated frequency curve principally by reducing the skewness coefficient. One can observe the large positive skew and relatively steep transition between snowmelt-dominant floods to rainfall-dominant floods greater than about 10,000 ft³/s. These large rainfall floods are responsible for the shape of the upper portion of the frequency curve. The AEP of the largest flood on record (June 1921) is about 1 in 270 from the exceedance-based plotting position, and about 1 in 1,600 from the LP-III model.

Table 10–17. Peak-flow quantiles in cubic feet per second for U.S. Geological Survey station 07099500 (and others) Arkansas River based on flood frequency analysis using Expected Moments Algorithm (EMA) with Multiple Grubbs-Beck Test; variance of estimate shown in log space.

[%, percent; ft³/s, cubic feet per second]

Annual exceedance probability	EMA estimate (ft ³ /s)	Variance of estimate	Lower 2.5% confidence limit (ft ³ /s)	Upper 97.5% confidence limit (ft ³ /s)
0.500	7,100	0.000960	6,300	8,000
0.200	11,900	0.001280	10,400	13,700
0.100	16,400	0.001650	14,100	19,300
0.040	23,800	0.002900	19,600	29,600
0.020	31,000	0.004630	24,300	40,900
0.010	39,800	0.007170	29,500	56,800
0.005	50,600	0.010610	35,600	79,400
0.002	68,800	0.016660	44,800	124,100
0.001	86,300	0.022430	53,000	174,400
0.0001	177,300	0.049590	88,700	545,300

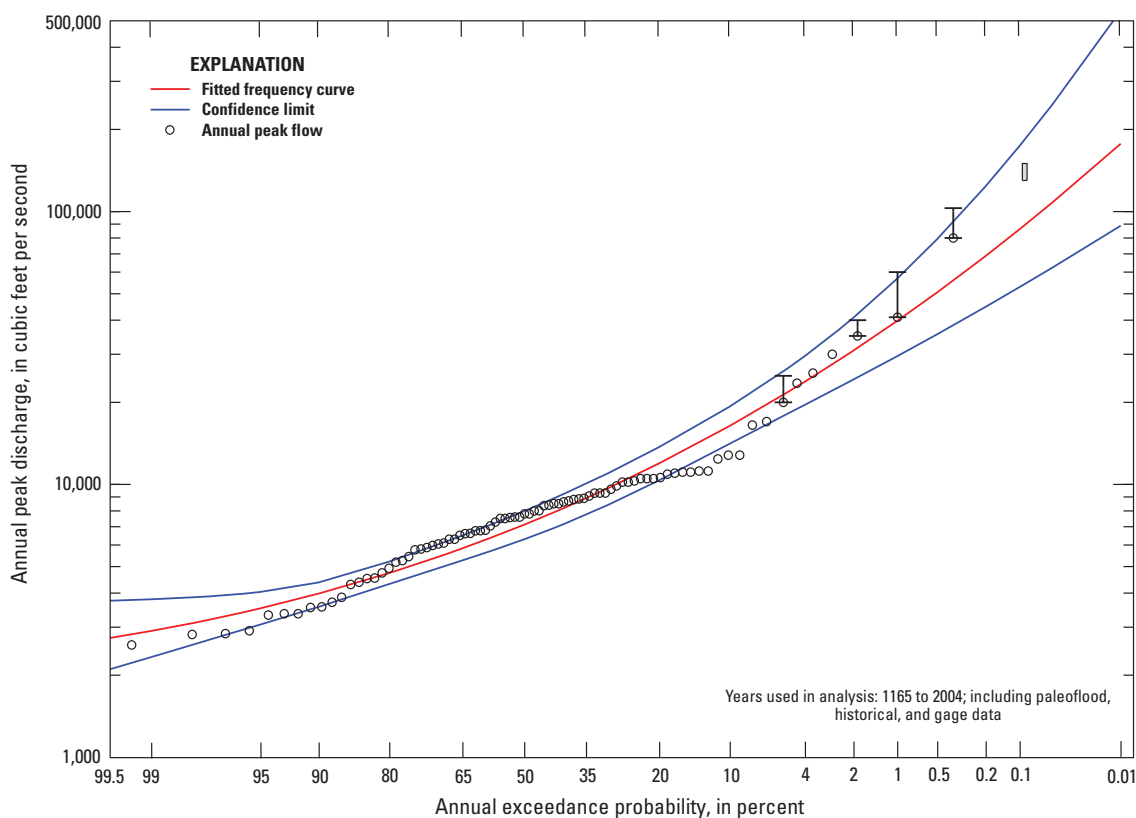


Figure 10–9. Graph showing the peak discharge frequency curve, Arkansas River at Pueblo State Park, including gage, historical, and paleoflood data. The red line is the fitted log-Pearson Type III frequency curve and the blue lines are the upper and lower confidence limits. Peak discharge estimates from the gage are shown as open circles; vertical bars represent estimated data uncertainty for some of the largest floods. Paleoflood nonexceedance bound shown as a gray box.

Crest Stage Gage Example—Bear Creek at Ottumwa, Iowa

This example demonstrates how the Expected Moments Algorithm (EMA) and Multiple Grubbs-Beck Test (MGBT) can be used to correctly perform a flood frequency analysis when censored data are present with variable perception thresholds from a crest stage gage.

A crest-stage gage (CSG) is a simple, reliable device used to obtain the elevation of the flood peak of a stream. Most commonly, a CSG consists of a vertical metal pipe containing a wood or aluminum staff held in a fixed position with relation to a datum reference. At the bottom of the pipe is a perforated cap containing granulated cork. When the water in the stream reaches and exceeds the height of the bottom cap (commonly referred to as the gage base), water is able to enter the pipe. As the water rises up the pipe, the cork floats on the water's surface and as the water reaches its peak and starts to recede, the cork adheres to the staff, thereby retaining the crest stage of the flood (Sauer and Turnipseed, 2010). Thus, CSGs provide a censored record of peak flows, as no annual peak flow that results in a flood stage below the bottom cap of the pipe will be recorded. This example demonstrates how the EMA with the MGBT for potentially influential low floods (PILFs) can correctly represent these censored annual peak records from CSGs in a flood frequency analysis.

For this example, USGS station 05489490 Bear Creek at Ottumwa, Iowa, is used. This station is a CSG and has a drainage area of 22.9 mi². It is located in southeast Iowa in the Southern Iowa Drift Plain land-form region, which is characterized by rolling hills and deeply carved stream channels (Prior, 1991). The stream banks and channel bed are composed of sand, silt, and clay materials that are prone to shifting from hydrologic events. The flood plain areas contain a combination of wooded areas, pasture, and row-crop fields.

USGS station 05489490 has an annual peak record consisting of 49 peaks, beginning in 1965 and ending in 2014 (Eash and others, 2013, table 1). The annual peaks are listed in table 10–18 (downloaded from USGS NWIS: https://nwis.waterdata.usgs.gov/nwis/peak/?site_no=05489490&agency_cd=USGS) and shown in figure 10–10.

EMA Representation of Peak Flow Data for Flood Frequency Analysis

As described in the [Data Representation Using Flow Intervals and Perception Thresholds](#) section, when using EMA, the annual peak flow for every water year during the historical period is described by a flow interval ($Q_{Y,lower}$, $Q_{Y,upper}$) for each water year Y . For peaks whose values are known and are not censored, the flow interval can be described as ($Q_{Y,lower} = Q_Y$, $Q_{Y,upper} = Q_Y$). For example, as shown in table 10–18, the peak for the 1965 water year is recorded as 4,000 ft³/s. This peak is known and is not censored, thus the flow interval for the 1965 water years is ($Q_{1965,lower} = 4,000$, $Q_{1965,upper} = 4,000$).

As shown in table 10–18, there are six censored peaks occurring in 1966, 1971, 1975, 1988, 1997, and 2006. Five of these water years (1966, 1971, 1975, 1997, and 2006) have censored peaks because of the stage of the annual peak not reaching the gage base of the CSG. These peak can be described by flow intervals in which $Q_{Y,lower} = 0$ and $Q_{Y,upper} = \text{CSG gage base}$. Similarly, the annual peak in water year 1988 is censored; however, in this case, the censoring is because of issues related to backwater. The CSG recorded an annual peak of 899 ft³/s, but it is known that the peak was affected by backwater because of ice causing the recorded peak to be larger than the actual peak. Thus, since there is no further information pertaining to the 1988 peak, it can be represented as a flow interval in which $Q_{1988,lower} = 0$ and $Q_{1988,upper} = 899$ ft³/s. Table 10–19 contains the EMA flow intervals for each water year in the record for station 05489490.

As described in the [Data Representation Using Flow Intervals and Perception Thresholds](#) section, EMA distinguishes among sampling properties by employing perception thresholds denoted ($T_{Y,lower}$, $T_{Y,upper}$) for each year Y , which reflect the range of flows that would have been measured or recorded had they occurred. Perception thresholds describe the range of measurable potential discharges and are independent of the actual peak discharges that have occurred. The lower bound, $T_{Y,lower}$, represents the smallest peak flow that would

Table 10–18. U.S. Geological Survey station 05489490 Bear Creek at Ottumwa, Iowa, annual peak-flow record consisting of 49 peaks from 1965 to 2014. This table contains the date of the annual peak recorded at the station, the water year of the annual peak, and the corresponding annual peak in cubic feet per second (ft³/s).

[<, less than; --, no entry or not available]

Date of peak streamflow	Water year	Annual peak streamflow (ft ³ /s)	Date of peak streamflow	Water year	Annual peak streamflow (ft ³ /s)	Date of peak streamflow	Water year	Annual peak streamflow (ft ³ /s)
1965-09-21	1965	4,000	1982-07-03	1982	4,030	1998-10-05	1999	2,840
1966-00-00	1966	< 1,180	1982-10-08	1983	2,180	2000-06-23	2000	3,520
1967-06-09	1967	2,880	1984-06-08	1984	1,780	2001-05-15	2001	2,430
1967-10-15	1968	1,310	1985-03-04	1985	1,610	2002-05-11	2002	2,670
1968-10-15	1969	1,420	1986-09-19	1986	1,910	2003-06-26	2003	560
1970-06-24	1970	3,130	1987-05-31	1987	990	2004-08-27	2004	3,000
1971-00-00	1971	< 1,180	1988-02-20	1988	< 899	2005-04-12	2005	859
1972-05-08	1972	1,620	1989-09-09	1989	1,820	2006-00-00	2006	< 710
1973-01-19	1973	1,570	1990-05-25	1990	3,120	2007-08-23	2007	2,390
1974-05-19	1974	2,060	1991-04-18	1991	1,850	2008-05-11	2008	3,160
1975-00-00	1975	< 705	1992-09-15	1992	1,840	2009-08-27	2009	2,520
1976-04-24	1976	3,340	1993-05-07	1993	2,410	2010-08-09	2010	3,750
1977-08-07	1977	3,530	1994-06-23	1994	1,400	2011-06-14	2011	2,600
1978-07-21	1978	2,010	1995-04-11	1995	1,560	2012-04-14	2012	1,450
1979-03-29	1979	1,830	1996-05-28	1996	3,130	2013-05-28	2013	3,850
1980-08-17	1980	2,240	1997-00-00	1997	< 714	2014-09-10	2014	1,200
1981-07-04	1981	2,770	1998-06-18	1998	1,940	--	--	--

Table 10–19. U.S. Geological Survey station 05489490 Bear Creek at Ottumwa, Iowa, Expected Moments Algorithm flow intervals for the systematic period from 1965 to 2014. This table contains the water year of the annual peak and the corresponding flow interval defined by lower bound, $Q_{Y,lower}$, and upper bound, $Q_{Y,upper}$, in cubic feet per second for each water year Y . [<<, less than; --, no entry or not available]

Water year	$Q_{Y,lower}$	$Q_{Y,upper}$	Comments	Water year	$Q_{Y,lower}$	$Q_{Y,upper}$	Comments
1965	4,000	4,000	--	1990	3,120	3,120	--
1966	0	1,180	Peak < gage base.	1991	1,850	1,850	--
1967	2,880	2,880	--	1992	1,840	1,840	--
1968	1,310	1,310	--	1993	2,410	2,410	--
1969	1,420	1,420	--	1994	1,400	1,400	--
1970	3,130	3,130	--	1995	1,560	1,560	--
1971	0	1,180	Peak < gage base.	1996	3,130	3,130	--
1972	1,620	1,620	--	1997	0	714	Peak < gage base.
1973	1,570	1,570	--	1998	1,940	1,940	--
1974	2,060	2,060	--	1999	2,840	2,840	--
1975	0	705	Peak < gage base.	2000	3,520	3,520	--
1976	3,340	3,340	--	2001	2,430	2,430	--
1977	3,530	3,530	--	2002	2,670	2,670	--
1978	2,010	2,010	--	2003	560	560	--
1979	1,830	1,830	--	2004	3,000	3,000	--
1980	2,240	2,240	--	2005	859	859	--
1981	2,770	2,770	--	2006	0	710	Peak < gage base.
1982	4,030	4,030	--	2007	2,390	2,390	--
1983	2,180	2,180	--	2008	3,160	3,160	--
1984	1,780	1,780	--	2009	2,520	2,520	--
1985	1,610	1,610	--	2010	3,750	3,750	--
1986	1,910	1,910	--	2011	2,600	2,600	--
1987	990	990	--	2012	1,450	1450	--
1988	0	899	Peak affected by backwater.	2013	3,850	3,850	--
1989	1,820	1,820	--	2014	1,200	1,200	--

result in a recorded flow in water year Y . Thus, for a CSG, $T_{Y,lower}$ can be adjusted to accommodate a changing gage-base discharge. Table 10–20 contains the EMA perception thresholds for each water year in the record for station 05489490.

The annual peaks, as well as their corresponding EMA flow intervals and perception thresholds, can be displayed graphically. Figure 10–10 shows a representation of the recorded annual peaks, EMA flow intervals, and EMA perception thresholds. The flow intervals whose lower bound is equal to the upper bound are represented by black circles, whereas the black vertical bars represent the interval flood estimates for those peaks that were not able to be recorded as they were below gage base. The solid-colored blocks represent the many perception thresholds applied to the record. The colored areas represent flows that would be unable to be recorded as they are smaller than the lower bound of the perception threshold $T_{Y,lower}$. The white space above the colored areas represents flow ranges for which annual peaks were able to be recorded had they occurred. For example, in figure 10–10, the left-most cyan-colored block represents a perception threshold from 1965 to 1972 where $T_{Y,lower} = 1,180 \text{ ft}^3/\text{s}$, $T_{Y,upper} = \infty$. The cyan-colored block spans from 0 ft^3/s to 1,180 ft^3/s , signifying that no annual peak less than 1,180 ft^3/s could be measured during the time period from 1965 to 1972.

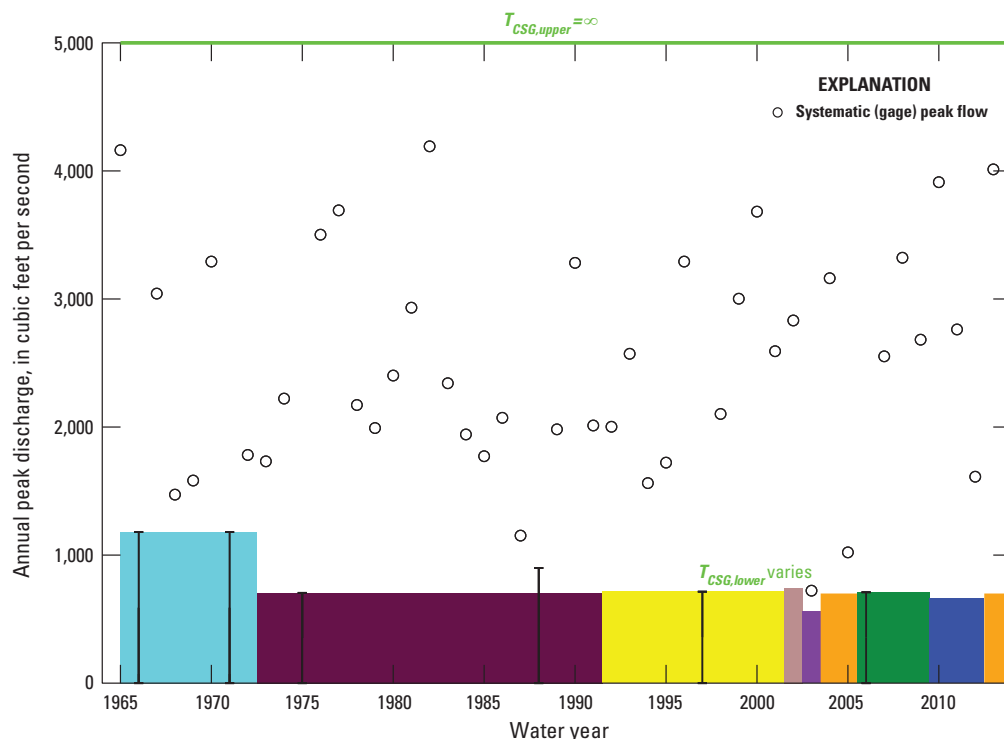


Figure 10–10. Graph showing U.S. Geological Survey station 05489490 Bear Creek at Ottumwa, Iowa, annual peak-flow time series consisting of 49 peaks from 1965 to 2014. The black open circles are the systematic peaks, the black vertical bars with caps represent the interval flood estimates, and the solid rectangular blocks are the lower perception thresholds $T_{CSG,lower}$ that vary. The upper perception threshold $T_{CSG,upper}$ is shown as a green line.

Table 10–20. U.S. Geological Survey station 05489490 Bear Creek at Ottumwa, Iowa, Expected Moments Algorithm (EMA) perception thresholds for the systematic period from 1965 to 2014. This table contains the water year ranges to which each perception threshold (in cubic feet per second) applies; $T_{Y,lower}$, the lower bound of the perception threshold for water year Y ; $T_{Y,upper}$, the upper bound of the perception threshold for water year Y ; and a comment describing the threshold.

[CSG, crest-stage gage; HWM, high-water mark]

Start year	End year	EMA perception threshold		Comment
		$T_{Y,lower}$	$T_{Y,upper}$	
1965	1972	1,180	Infinity	Initial gage base of CSG = 1,180 ft ³ /s.
1973	1991	705	Infinity	Gage base lowered.
1992	2001	714	Infinity	Gage base raised as a result of spring thaw.
2002	2002	743	Infinity	Gage base raised as a result of spring thaw.
2003	2003	560	Infinity	Gage base lowered as a result of routine site visit (HWM).
2004	2005	700	Infinity	Gage base raised as a result of spring thaw.
2006	2009	710	Infinity	Gage base raised as a result of spring thaw.
2010	2012	661	Infinity	Gage base lowered as a result of spring thaw.
2013	2014	700	Infinity	Gage base raised as a result of spring thaw.

Results from Flood Frequency Analysis

A flood frequency analysis at USGS station 05489490 was performed using the EMA flow intervals and perception thresholds as shown in tables 10–19 and 10–20. The output from an at-site flood frequency analysis using EMA with the MGBT to screen for PILFs is shown below. Note that station skew was used, thus allowing the focus to be on the at-site data. The fitted frequency curve is displayed in figure 10–11 with estimates provided in table 10–21. The final estimated moments were 3.2787 (mean), 0.2331 (standard deviation), and 0.925 (station skew).

Table 10–21. Peak-flow quantiles in cubic feet per second for U.S. Geological Survey station 05489490 Bear Creek at Ottumwa, Iowa, based on flood frequency analysis using Expected Moments Algorithm (EMA) with Multiple Grubbs-Beck Test; variance of estimate shown in log space.

[%, percent; ft³/s, cubic feet per second]

Annual exceedance probability	EMA estimate (ft ³ /s)	Variance of estimate	Lower 2.5% confidence limit (ft ³ /s)	Upper 97.5% confidence limit (ft ³ /s)
0.500	2,061	0.0012	1,702	2,406
0.200	3,004	0.0009	2,611	3,444
0.100	3,507	0.0008	3,080	4,064
0.040	4,021	0.0010	3,543	4,856
0.020	4,329	0.0013	3,779	5,454
0.010	4,586	0.0018	3,942	6,074
0.005	4,802	0.0024	4,057	6,746
0.002	5,036	0.0033	4,160	7,750

As shown in the example above, EMA correctly represents the censored annual peak data through the use of flow intervals and perception thresholds. The EMA flow intervals provide a straightforward approach to appropriately represent the censored flows, while the perception thresholds accommodate the changing gage base. Special thanks to Jon Nania and David Eash of the USGS Iowa Water Science Center for providing data and insight relating to USGS station 05489490 Bear Creek at Ottumwa, Iowa.

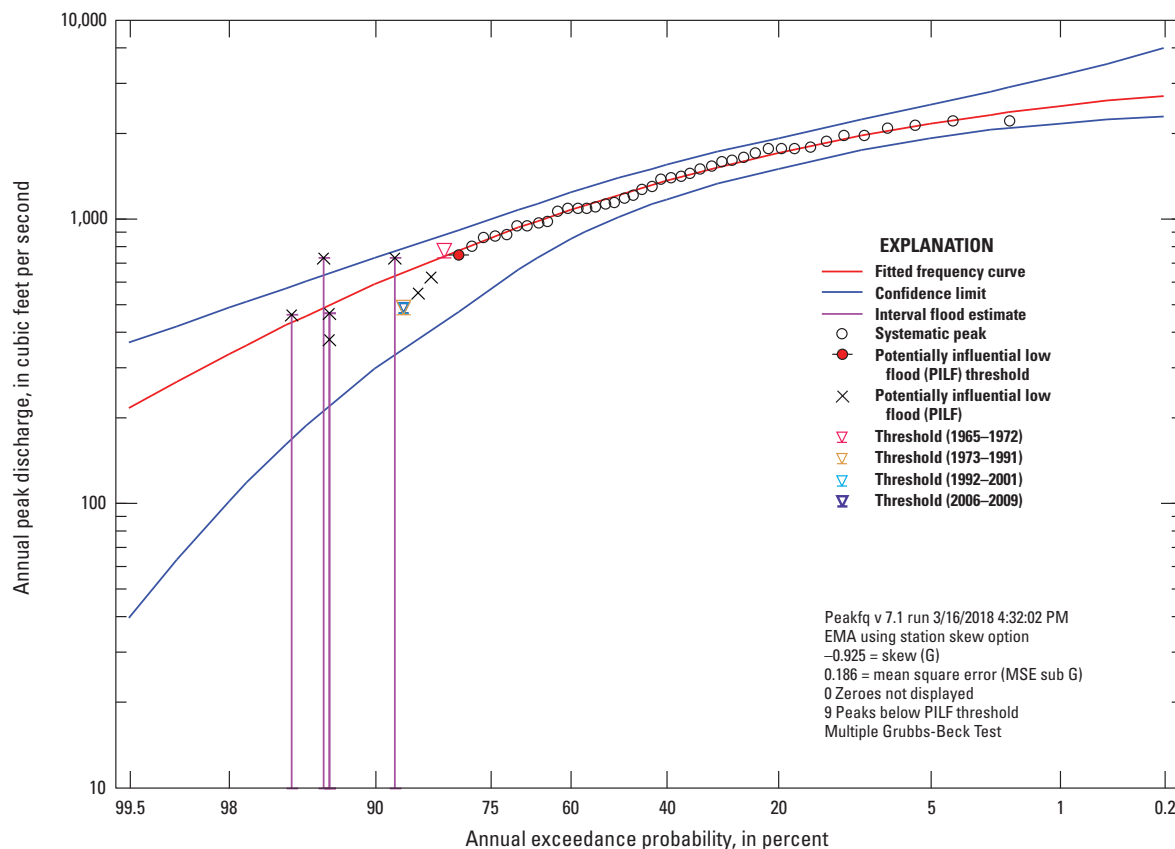


Figure 10–11. Graph showing annual exceedance probability plot for U.S. Geological Survey station 05489490 Bear Creek at Ottumwa, Iowa, based on flood frequency analysis using Expected Moments Algorithm (EMA) with Multiple Grubbs-Beck Test (MGBT). The red line is the fitted log-Pearson Type III frequency curve, the blue lines are the upper and lower confidence limits, the black circles are the systematic peaks, the purple lines represent the interval flood estimates, the solid red circle with a line through it is the potentially influential low flood (PILF) threshold as identified by the MGBT, and the black x's are the PILFs identified by the MGBT.

Historical and PILF Example—Santa Cruz River near Lochiel, Arizona

This example illustrates the use of the Expected Moments Algorithm (EMA) for a historical record with one large flood (described in the section [Historical Flood Information](#)) and a number of potentially influential low floods (PILFs) (described in section [Zero Flows and Potentially Influential Low Floods](#)).

For this example, USGS station 09480000 Santa Cruz River near Lochiel, Arizona, is used. The Santa Cruz River is a tributary to the Gila River; the 82.2-mi² watershed lies within the Basin and Range province in Arizona ([Paretti and others, 2014a](#)). This gaging station was previously analyzed by [Cohn and others \(in press\)](#) and [Paretti and others \(2014a, fig. 21\)](#).

Station 09480000 has an annual peak record consisting of 65 peaks, beginning in 1949 and ending in 2013. There is a historic flood that occurred within the period of gaging record on October 9, 1977. This flood is noted in the USGS Annual Water Data Report for this gage, available in the peak-flow file, and there is historical information available for this large flood ([Aldridge and Eychaner, 1984](#)) that indicates this flood is the largest since 1927. The annual peaks are listed in table 10–22 and shown in figure 10–12. Of the 65 annual peaks, the August 15, 1984 flood is equal to the October 1977 historic flood peak. Based on the historical flood information in [Aldridge and Eychaner \(1984\)](#) for the 1977 flood, information from the October 1977 flood is used as a perception threshold to represent the 22 years of missing information from 1927 to 1948.

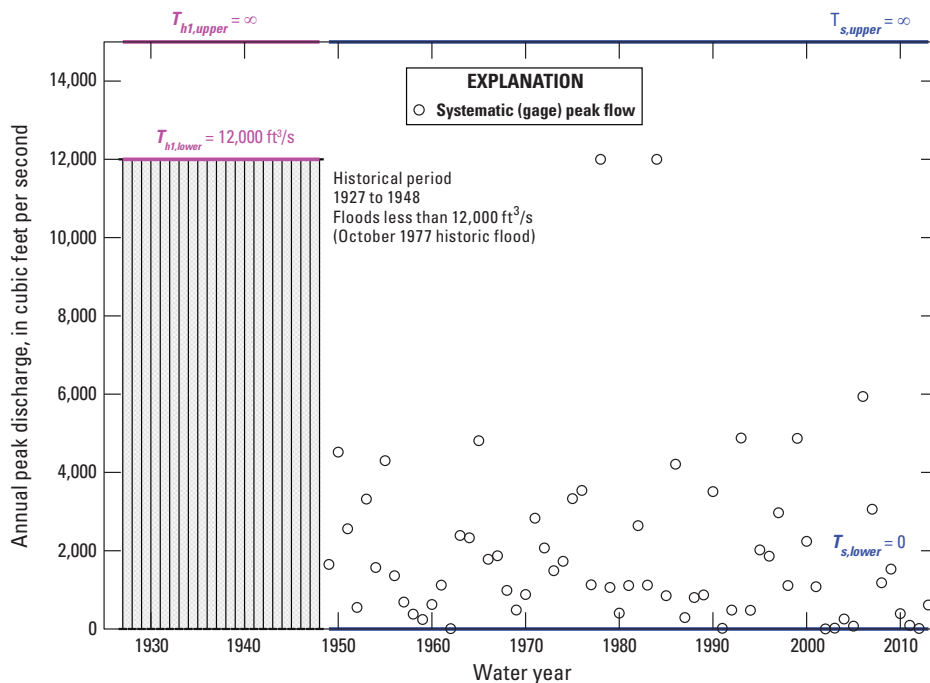


Figure 10–12. Graph showing U.S. Geological Survey station 09480000 Santa Cruz River near Lochiel, Arizona, annual peak-flow time series consisting of 65 peaks from 1949 to 2013. The historical period is shown as a gray shaded area, with a perception threshold (12,000 cubic feet per second [ft^3/s]) estimated from the October 1977 historic flood. Perception threshold ranges are shown as magenta lines for the historical period and blue lines for the systematic period.

Table 10–22. U.S. Geological Survey station 09480000 Santa Cruz River near Lochiel, Arizona, annual peak-flow record consisting of 65 peaks from 1949 to 2013. This table contains the date of the annual peak recorded at the station, the water year of the annual peak, and the corresponding annual peak in cubic feet per second (ft^3/s).

[--, no entry or not available]

Date of peak streamflow	Water year	Annual peak streamflow (ft^3/s)	Date of peak streamflow	Water year	Annual peak streamflow (ft^3/s)	Date of peak streamflow	Water year	Annual peak streamflow (ft^3/s)
1949-09-13	1949	1,650	1971-08-10	1971	2,830	1993-01-18	1993	4,880
1950-07-30	1950	4,520	1972-07-16	1972	2,070	1994-08-30	1994	478
1951-08-02	1951	2,560	1973-06-30	1973	1,490	1995-07-12	1995	2,020
1952-08-16	1952	550	1974-08-04	1974	1,730	1996-07-10	1996	1,860
1953-07-14	1953	3,320	1975-07-22	1975	3,330	1997-09-11	1997	2,970
1954-07-22	1954	1,570	1976-07-22	1976	3,540	1998-07-07	1998	1,110
1955-08-06	1955	4,300	1977-09-05	1977	1,130	1999-07-28	1999	4,870
1956-07-17	1956	1,360	1977-10-09	1978	12,000	2000-08-06	2000	2,240
1957-08-09	1957	688	1979-01-25	1979	1,060	2000-10-22	2001	1,080
1958-08-07	1958	380	1980-06-30	1980	406	2002-03-04	2002	1.5
1959-08-14	1959	243	1981-07-15	1981	1,110	2003-08-14	2003	22
1960-07-30	1960	625	1982-08-11	1982	2,640	2004-08-05	2004	256
1961-08-08	1961	1,120	1983-03-04	1983	1,120	2005-08-23	2005	73
1962-07-29	1962	7.6	1984-08-15	1984	12,000	2006-08-08	2006	5,940
1963-08-25	1963	2,390	1985-07-19	1985	850	2007-07-19	2007	3,060
1964-09-09	1964	2,330	1986-08-29	1986	4,210	2008-07-23	2008	1,180
1965-09-12	1965	4,810	1987-08-10	1987	291	2009-07-20	2009	1,530
1966-08-18	1966	1,780	1988-08-23	1988	804	2010-07-31	2010	392
1967-08-03	1967	1,870	1989-08-04	1989	871	2011-08-13	2011	95
1967-12-20	1968	986	1990-07-17	1990	3,510	2012-07-28	2012	12
1969-08-05	1969	484	1991-07-26	1991	17	2013-09-08	2013	612
1970-08-03	1970	880	1992-08-01	1992	483	--	--	--

EMA Representation of Peak Flow Data for Flood Frequency Analysis

As described in the [Data Representation Using Flow Intervals and Perception Thresholds](#) section, when using EMA, the annual peak flow for every water year during the historical period is described by a flow interval ($Q_{Y,lower}$, $Q_{Y,upper}$) for each water year Y . For peaks whose values are known and are not censored, the flow interval can be described as ($Q_{Y,lower} = Q_Y$, $Q_{Y,upper} = Q_Y$). In this example, the flow values are known for all the years where the station was in operation. Table 10–23 contains the EMA flow intervals for each water year in the record for station 09480000. The historical period is described by a perception threshold.

As described in the [Data Representation Using Flow Intervals and Perception Thresholds](#) section, EMA distinguishes among sampling properties by employing perception thresholds denoted ($T_{Y,lower}$, $T_{Y,upper}$) for each year Y , which reflect the range of flows that would have been measured or recorded had they occurred. Perception thresholds describe the range of measurable potential discharges and are independent of the actual peak discharges that have occurred. The lower bound, $T_{Y,lower}$, represents the smallest peak flow that would result in a recorded flow in water year Y . For most peaks at most gages, $T_{Y,upper}$ is assumed to be infinite, as bigger floods that might exceed the measurement capability of the streamgage are determined through study of high-water marks and other physical evidence of the flood. For periods of continuous, full-range peak-flow record, the perception threshold is represented by ($T_{Y,lower} = 0$, $T_{Y,upper} = \infty$), where $T_{Y,lower} = 0$ is the gage-base discharge. Based on the October 1977 large historical flood ([Aldridge and Eychaner, 1984](#)), it is known that floods at this location would have been estimated (or recorded) had they exceeded approximately 12,000 ft³/s. Table 10–24 contains the EMA perception thresholds for each water year in the record, including the historical period, for station 09480000.

Results from Flood Frequency Analysis

A flood frequency analysis at USGS station 09480000 was performed using the EMA flow intervals and perception thresholds as shown in tables 10–23 and 10–24. The output from an at-site flood frequency analysis using EMA with the Multiple Grubbs-Beck Test (MGBT) to screen for PILFs is shown below. Note that station skew was used, thus allowing the focus to be on the at-site data. The fitted frequency curve is displayed in figure 10–13 with estimates provided in table 10–25. The final estimated moments were 3.0691 (mean), 0.4898 (standard deviation), and –0.462 (station skew).

As shown in figure 10–13, there are two floods that exceed the historical threshold (12,000 ft³/s): the October 1977 flood and the August 1984 flood. Using MGBT, ten PILFs were identified, with a threshold equal to 380 ft³/s and a significance level equal to 0.0228. Thus, all 10 annual peaks less than 380 ft³/s are censored and recoded in the framework of EMA with flow intervals of ($Q_{Y,lower} = 0$, $Q_{Y,upper} = 380$). The MGBT threshold also has the effect of adjusting the lower bound of the perception threshold. Thus, for the systematic period from 1949 to 2013, the perception threshold is ($T_{Y,lower} = 380$, $T_{Y,upper} = \infty$). For the historical information, the lower threshold is $T_{Y,lower} = 12,000$ (table 10–24). As shown in figure 10–13, by censoring the eight smallest peaks in the record, the remaining smallest annual exceedance probability peaks and the largest floods are well fit by the frequency curve (red line).

Table 10–23. U.S. Geological Survey station 09480000 Santa Cruz River near Lochiel, Arizona, Expected Moments Algorithm flow intervals for the systematic period from 1949 to 2013. This table contains the water year of the annual peak and the corresponding flow interval defined by lower bound, $Q_{Y,lower}$, and upper bound, $Q_{Y,upper}$, in cubic feet per second for each water year Y .

[--, no entry or not available]

Water year	$Q_{Y,lower}$	$Q_{Y,upper}$	Comments	Water year	$Q_{Y,lower}$	$Q_{Y,upper}$	Comments
1949	1,650	1,650	--	1982	2,640	2,640	--
1950	4,520	4,520	--	1983	1,120	1,120	--
1951	2,560	2,560	--	1984	12,000	12,000	--
1952	550	550	--	1985	850	850	--
1953	3,320	3,320	--	1986	4,210	4,210	--
1954	1,570	1,570	--	1987	291	291	--
1955	4,300	4,300	--	1988	804	804	--
1956	1,360	1,360	--	1989	871	871	--
1957	688	688	--	1990	3,510	3,510	--
1958	380	380	--	1991	17	17	--
1959	243	243	--	1992	483	483	--
1960	625	625	--	1993	4,880	4,880	--
1961	1,120	1,120	--	1994	478	478	--
1962	7.6	7.6	--	1995	2,020	2,020	--
1963	2,390	2,390	--	1996	1,860	1,860	--
1964	2,330	2,330	--	1997	2,970	2,970	--
1965	4,810	4,810	--	1998	1,110	1,110	--
1966	1,780	1,780	--	1999	4,870	4,870	--
1967	1,870	1,870	--	2000	2,240	2,240	--
1968	986	986	--	2001	1,080	1,080	--
1969	484	484	--	2002	1.5	1.5	--
1970	880	880	--	2003	22	22	--
1971	2,830	2,830	--	2004	256	256	--
1972	2,070	2,070	--	2005	73	73	--
1973	1,490	1,490	--	2006	5,940	5,940	--
1974	1,730	1,730	--	2007	3,060	3,060	--
1975	3,330	3,330	--	2008	1,180	1,180	--
1976	3,540	3,540	--	2009	1,530	1,530	--
1977	1,130	1,130	--	2010	392	392	--
1978	12,000	12,000	Historic flood.	2011	95	95	--
1979	1,060	1,060	--	2012	12	12	--
1980	406	406	--	2013	612	612	--
1981	1,110	1,110	--	--	--	--	--

Table 10–24. U.S. Geological Survey station 09480000 Santa Cruz River near Lochiel, Arizona, Expected Moments Algorithm (EMA) perception thresholds for the historical and systematic period from 1927 to 2013. This table contains the water year ranges to which each perception threshold (in cubic feet per second) applies; $T_{Y,lower}$ the lower bound of the perception threshold for water year Y ; $T_{Y,upper}$, the upper bound of the perception threshold for water year Y ; and a comment describing the threshold.

Start year	End year	EMA perception threshold		Comment
		$T_{Y,lower}$	$T_{Y,upper}$	
1927	1948	12,000	Infinity	Historical information.
1949	2013	0	Infinity	Continuous systematic record.

Table 10–25. Peak-flow quantiles in cubic feet per second for U.S. Geological Survey station 09480000 Santa Cruz River near Lochiel, Arizona, based on flood frequency analysis using Expected Moments Algorithm (EMA) with Multiple Grubbs-Beck Test; variance of estimate shown in log space.

[%, percent; ft³/s, cubic feet per second]

Annual exceedance probability	EMA estimate (ft ³ /s)	Variance of estimate	Lower 2.5% confidence limit (ft ³ /s)	Upper 97.5% confidence limit (ft ³ /s)
0.500	1,279	0.0042	936.1	1,719
0.200	3,079	0.0040	2,314	4,138
0.100	4,652	0.0042	3,481	6,394
0.040	6,982	0.0056	5,119	10,460
0.020	8,914	0.0076	6,337	14,780
0.010	10,970	0.0105	7,474	20,570
0.005	13,150	0.0144	8,509	28,280
0.002	16,170	0.0211	9,719	42,560

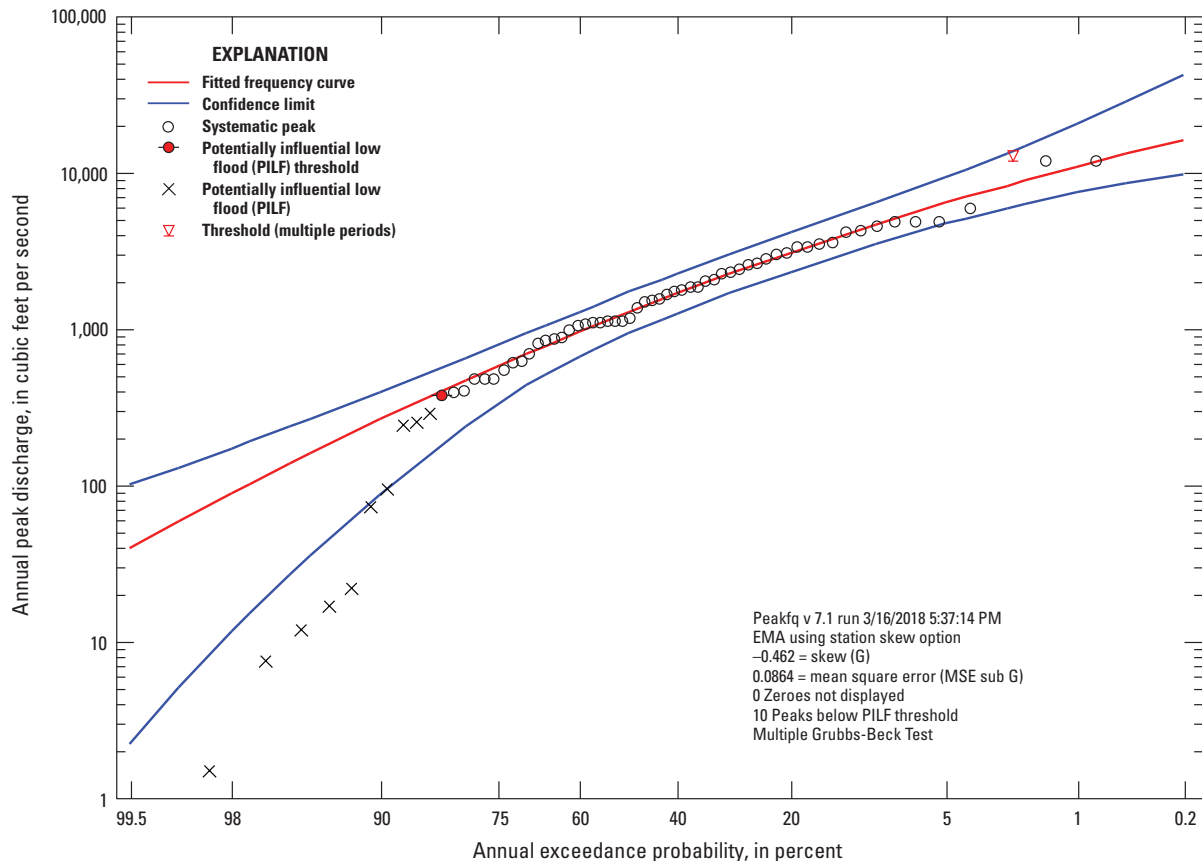


Figure 10–13. Graph showing annual exceedance probability plot for U.S. Geological Survey station 09480000 Santa Cruz River near Lochiel, Arizona, based on flood frequency analysis using Expected Moments Algorithm (EMA) with Multiple Grubbs-Beck Test (MGBT). The red line is the fitted log-Pearson Type III frequency curve, the blue lines are the upper and lower confidence limits, the black circles are the systematic peaks, the solid red circle with a line through it is the potentially influential low flood (PILF) threshold as identified by the MGBT, and the black x's are the PILFs identified by the MGBT. The red triangle with the horizontal line represents the lower limit of the historical perception threshold (12,000 cubic feet per second).

Paleoflood Record Example—American River at Fair Oaks, California

This example illustrates the use of the Expected Moments Algorithm (EMA) for a historical record with several large floods (described in the section [Historical Flood Information](#)) and detailed paleoflood data (described in the section [Paleoflood and Botanical Information](#)), utilizing multiple censoring and interval data for Reclamation's Folsom Dam ([Bureau of Reclamation, 2002](#)). For this example, USGS station 11446500 American River at Fair Oaks, California, is used, with additional data from the historical and paleoflood record, interpretations from USACE and Reclamation data and investigations, and other historical sources. In 1986 and 1997, floods on the American River and in central California heightened concerns about the hydrologic risk at Folsom Dam. In part, these concerns led to two National Research Council panels to evaluate American River flood hazards ([National Research Council, 1995, 1999](#)). These panels reviewed flood control and floodplain-management issues, focusing on estimating floods with AEPs greater than 0.005 (1 in 200), specifically 1 in 100 (0.01). For dam safety, the primary concern is floods with very small AEPs generally in the range of 0.001 to 0.0001 (1 in 1,000 to 1 in 10,000). For this example, these estimates are made using gage, historical, and paleoflood data. This example illustrates the use of a very long paleoflood record with large floods outside the gaging period, historical information, multiple thresholds, and interval observations. This example is meant to be illustrative and is not intended to be used for making floodplain-management decisions along the American River.

[Bureau of Reclamation \(2002\)](#) conducted a paleoflood and flood frequency study to investigate these issues. The primary objective of the study was to develop an estimate of peak discharge frequency of the American River at Folsom Dam in the above annual probability range. The peak discharge frequency information was subsequently combined with historical hydrographs to develop probabilistic hydrographs based on paleoflood information. Paleoflood information for the [Bureau of Reclamation \(2002\)](#) study was based on geomorphic, stratigraphic, and geochronologic information collected from four sites in the American River basin: (1) South Fork American River near Kyburz, (2) South Fork American River near Lotus, (3) North Fork of the American River at Ponderosa Bridge, and (4) lower American River near Fair Oaks. Two main types of paleoflood data were collected from the four sites to evaluate the flood hazard for Folsom Dam: (1) paleoflood magnitude and age estimates for the South Fork near Kyburz and Lotus, and the lower American River, and (2) a single paleohydrologic bound for the North Fork. Stratigraphic information from 14 sites provides evidence for late Holocene paleofloods that are preserved at or above the peak stage of the largest historical floods. The age of these paleofloods is constrained by 38 radiocarbon ages, published archaeological age correlations, and published obsidian hydration age estimates.

For this example, peak-flow data from the lower American River at Fair Oaks, California (station 11446500) are used and modified based on additional information from USGS Water-Supply Papers, USACE records, Bureau of Reclamation records and investigations, and other historical information. As such, they do not directly correspond to peak flows in the USGS NWIS database. There are 77 peaks beginning in 1905 and ending in 1997, with several missing years or years of low floods (1910, 1912 to 1913, 1918, 1929, 1977). Large historical floods occurred in 1997, 1986, and 1862, and are described in [National Research Council \(1999\)](#) and [Bureau of Reclamation \(2002\)](#). The paleoflood period covers the past 2,000 years, from year 1 to 1847, the historical period begins in 1848, and the gaging period begins in 1905. The annual peaks, historical floods, and paleofloods are listed in table 10–26 and shown in figure 10–14. Perception thresholds are estimated based on the March 1907 flood, the January 1862 flood, and paleofloods.

EMA Representation of Peak Flow Data for Flood Frequency Analysis

As described in the [Data Representation Using Flow Intervals and Perception Thresholds](#) section, when using EMA, the annual peak flow for every water year during the historical period is described by a flow

Table 10–26. U.S. Geological Survey station 11446500 American River at Fair Oaks annual peak-flow record consisting of 77 peaks from 1905 to 1997, with historical floods and paleofloods. This table contains the water year of the annual peak and the corresponding annual peak in cubic feet per second (ft³/s). Horizontal lines indicate broken-record years.

[>, greater than; --, no entry or not available]

Water year	Annual peak streamflow (ft ³ /s)	Water year	Annual peak streamflow (ft ³ /s)	Water year	Annual peak streamflow (ft ³ /s)
650	>600,000	1933	16,500	1961	8,000
1437	>400,000	1934	22,600	1962	40,000
1574	>400,000	1935	60,900	1963	240,000
1711	>400,000	1936	58,300	1964	24,000
1862	>262,000	1937	33,000	1965	260,000
1905	24,200	1938	114,000	1966	6,500
1906	59,700	1939	10,900	1967	46,000
1907	156,000	1940	89,200	1968	30,000
1908	10,300	1941	38,800	1969	120,000
1909	119,000	1942	83,200	1970	122,000
1911	81,300	1943	152,000	1971	48,000
1914	74,100	1944	20,100	1972	12,000
1915	47,900	1945	94,400	1973	69,000
1916	40,700	1946	42,200	1974	55,000
1917	42,300	1947	27,900	1975	46,000
1919	67,500	1948	21,000	1976	15,000
1920	20,100	1949	37,500	1978	40,000
1921	39,200	1950	34,400	1979	33,000
1922	31,600	1951	180,000	1980	175,000
1923	39,000	1952	37,200	1981	20,000
1924	14,000	1953	49,700	1982	152,000
1925	99,500	1954	42,600	1983	93,000
1926	27,400	1955	10,800	1984	88,000
1927	67,700	1956	219,000	1985	17,000
1928	163,000	1957	42,000	1986	259,000
1930	24,400	1958	54,000	1997	298,000
1931	9,900	1959	20,000	--	--
1932	21,100	1960	75,000	--	--

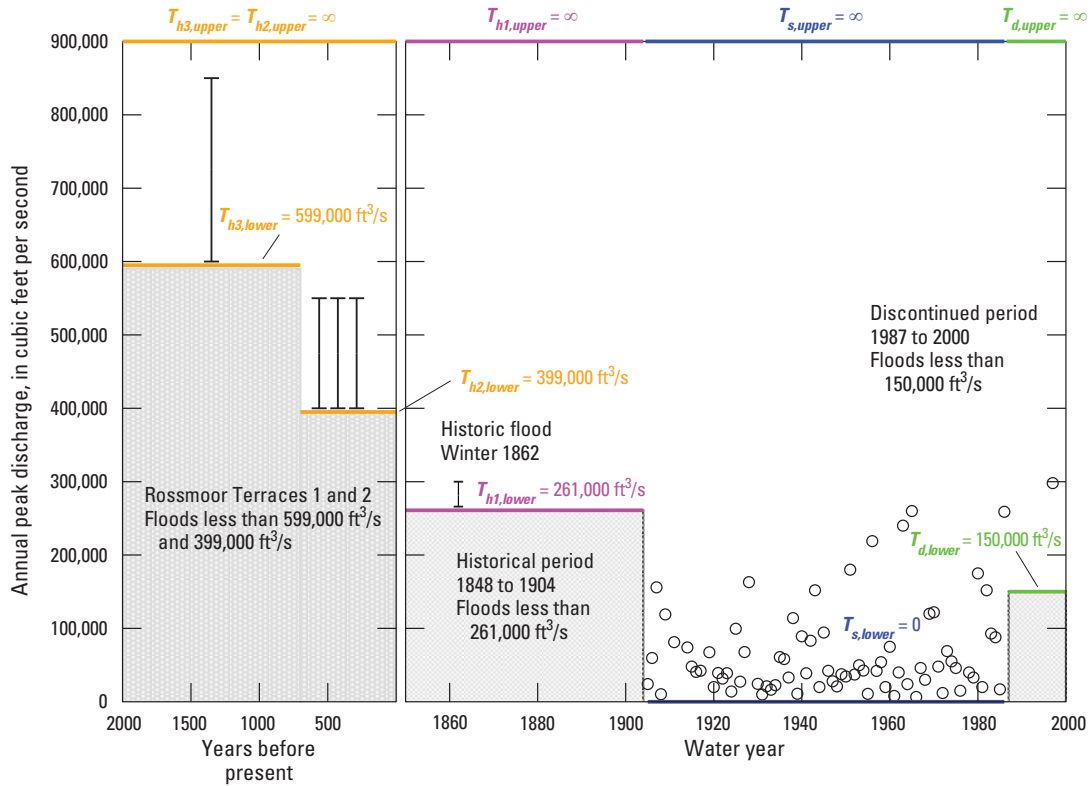


Figure 10–14. Graph showing approximate unregulated peak discharge and paleoflood estimates, with historical and paleoflood exceedance thresholds, American River at Fair Oaks. A scale break is used to separate the gaging station data from the much longer paleoflood record. Flood intervals for large floods in the paleoflood and historical period are shown as black vertical bars with caps that represent lower and upper flow estimates. The gray shaded areas represents floods of unknown magnitude less than the perception thresholds for the paleoflood periods $T_{h3,lower}$, $T_{h2,lower}$, the historical period $T_{h1,lower}$, and the discontinued period $T_{d,lower}$. Perception threshold ranges in cubic feet per second (ft^3/s) are shown as orange lines for the paleoflood period, magenta lines for the historical period, blue lines for the systematic period, and green lines for the discontinued period. Mean values of paleofloods threshold age data are plotted for simplicity.

interval ($(Q_{Y,lower}, Q_{Y,upper})$ for each water year Y . For peaks whose values are known and are not censored, the flow interval can be described as ($Q_{Y,lower} = Q_Y, Q_{Y,upper} = Q_Y$). In this example, the flow values are known for all the years where the station was in operation. Table 10–27 contains the EMA flow intervals for each water year in the record for station 11446500. The historical and paleoflood periods are described by perception thresholds.

As described in the [Data Representation Using Flow Intervals and Perception Thresholds](#) section, EMA distinguishes among sampling properties by employing perception thresholds denoted ($T_{Y,lower}, T_{Y,upper}$) for each year Y , which reflect the range of flows that would have been measured or recorded had they occurred. Perception thresholds describe the range of measurable potential discharges and are independent of the actual peak discharges that have occurred. The lower bound, $T_{Y,lower}$, represents the smallest peak flow that would result in a recorded flow in water year Y . For most peaks at most gages, $T_{Y,upper}$, is assumed to be infinite, as bigger floods that might exceed the measurement capability of the streamgage are determined through study of highwater marks and other physical evidence of the flood. For periods of continuous, full-range peak flow record, the perception threshold is represented by ($T_{Y,lower} = 0, T_{Y,upper} = \infty$), where $T_{Y,lower} = 0$ is the gage-base discharge. Based on the March 1907 large historical flood ([Bureau of Reclamation, 2002](#)), it is

Table 10–27. U.S. Geological Survey station 11446500 American River at Fair Oaks Expected Moments Algorithm flow intervals for the historical and systematic period from 650 to 1997. Horizontal lines indicate broken-record years.

[--, no entry or not available]

Water year	$Q_{Y,\text{lower}}$	$Q_{Y,\text{upper}}$	Comments	Water year	$Q_{Y,\text{lower}}$	$Q_{Y,\text{upper}}$	Comments
650	600,000	850,000	Paleoflood.	1946	42,200	42,200	--
1437	400,000	550,000	Paleoflood.	1947	27,900	27,900	--
1574	400,000	550,000	Paleoflood.	1948	21,000	21,000	--
1711	400,000	550,000	Paleoflood.	1949	37,500	37,500	--
1862	262,000	300,000	Historical flood.	1950	34,400	34,400	--
1905	24,200	24,200	--	1951	180,000	180,000	--
1906	59,700	59,700	--	1952	37,200	37,200	--
1907	156,000	156,000	--	1953	49,700	49,700	--
1908	10,300	10,300	--	1954	42,600	42,600	--
1909	119,000	119,000	--	1955	10,800	10,800	--
1911	81,300	81,300	--	1956	219,000	219,000	--
1914	74,100	74,100	--	1957	42,000	42,000	--
1915	47,900	47,900	--	1958	54,000	54,000	--
1916	40,700	40,700	--	1959	20,000	20,000	--
1917	42,300	42,300	--	1960	75,000	75,000	--
1919	67,500	67,500	--	1961	8,000	8,000	--
1920	20,100	20,100	--	1962	40,000	40,000	--
1921	39,200	39,200	--	1963	240,000	240,000	--
1922	31,600	31,600	--	1964	24,000	24,000	--
1923	39,000	39,000	--	1965	260,000	260,000	--
1924	14,000	14,000	--	1966	6,500	6,500	--
1925	99,500	99,500	--	1967	46,000	46,000	--
1926	27,400	27,400	--	1968	30,000	30,000	--
1927	67,700	67,700	--	1969	120,000	120,000	--
1928	163,000	163,000	--	1970	122,000	122,000	--
1930	24,400	24,400	--	1971	48,000	48,000	--
1931	9,900	9,900	--	1972	12,000	12,000	--
1932	21,100	21,100	--	1973	69,000	69,000	--
1933	16,500	16,500	--	1974	55,000	55,000	--
1934	22,600	22,600	--	1975	46,000	46,000	--
1935	60,900	60,900	--	1976	15,000	15,000	--
1936	58,300	58,300	--	1978	40,000	40,000	--
1937	33,000	33,000	--	1979	33,000	33,000	--
1938	114,000	114,000	--	1980	175,000	175,000	--
1939	10,900	10,900	--	1981	20,000	20,000	--
1940	89,200	89,200	--	1982	152,000	152,000	--
1941	38,800	38,800	--	1983	93,000	93,000	--
1942	83,200	83,200	--	1984	88,000	88,000	--
1943	152,000	152,000	--	1985	17,000	17,000	--
1944	20,100	20,100	--	1986	259,000	259,000	--
1945	94,400	94,400	--	1997	298,000	298,000	--

Table 10–28. U.S. Geological Survey station 11446500 American River at Fair Oaks Expected Moments Algorithm (EMA) perception thresholds for the paleoflood, historical, and systematic period from 1 to 2000. This table contains the water year ranges to which each perception threshold (in cubic feet per second) applies; $T_{Y,lower}$ the lower bound of the perception threshold for water year Y ; $T_{Y,upper}$, the upper bound of the perception threshold for water year Y ; and a comment describing the threshold.

Start year	End year	EMA perception threshold		Comment
		$T_{Y,lower}$	$T_{Y,upper}$	
1	1301	599,000	Infinity	Lower Rossmoor terrace 1.
1302	1847	399,000	Infinity	Lower Rossmoor terrace 2.
1848	1904	261,000	Infinity	1862 historical threshold.
1905	1909	0	Infinity	Gage record.
1910	1910	150,000	Infinity	March 1907 low floods and missing.
1911	1911	0	Infinity	Gage record.
1912	1913	150,000	Infinity	March 1907 low floods and missing.
1914	1917	0	Infinity	Gage record.
1918	1918	150,000	Infinity	March 1907 low floods and missing.
1919	1928	0	Infinity	Gage record.
1929	1929	150,000	Infinity	March 1907 low floods and missing.
1930	1976	0	Infinity	Gage record.
1977	1977	150,000	Infinity	March 1907 low floods and missing.
1978	1986	0	Infinity	Gage record.
1987	1996	150,000	Infinity	March 1907 low floods and missing.
1997	1997	0	Infinity	Gage record.
1998	2000	150,000	Infinity	March 1907 low floods and missing.

known that floods at this location would have been estimated (or recorded), had they exceeded approximately 150,000 ft³/s. Table 10–28 contains the EMA perception thresholds for each water year in the record, including the historical period, for station 11446500.

Results from Flood Frequency Analysis

A flood frequency analysis at USGS station 11446500 was performed using the EMA flow intervals and perception thresholds as shown in tables 10–27 and 10–28. The output from an at-site flood frequency analysis using EMA with the Multiple Grubbs-Beck Test (MGBT) to screen for potentially influential low floods (PILFs) is shown below. Note that station skew was used, thus allowing the focus to be on the at-site data. The fitted frequency curve is displayed in figure 10–15 with estimates provided in table 10–30. Peak discharge estimates for the interval floods are shown in the figure with estimated uncertainty. Peak discharge probabilities are estimated using Cunnane plotting positions with the threshold-exceedance formula that includes paleoflood data. The results indicate that the LP-III model provides an adequate fit to the gage and paleoflood data.

Table 10–29. U.S. Geological Survey station 11446500 American River at Fair Oaks Expected Moments Algorithm (EMA) perception thresholds for the paleoflood, historical, and systematic period from 1 to 2000. This table contains the water year ranges to which each perception threshold (in cubic feet per second) applies; $T_{Y,lower}$ the lower bound of the perception threshold for water year Y ; $T_{Y,upper}$, the upper bound of the perception threshold for water year Y ; and a comment describing the threshold.

Start year	End year	EMA perception threshold		Comment
		$T_{Y,lower}$	$T_{Y,upper}$	
1	1301	599,000	Infinity	Lower Rossmoor terrace 1.
1302	1847	399,000	Infinity	Lower Rossmoor terrace 2.
1848	1904	261,000	Infinity	1862 historical threshold.
1905	1909	0	Infinity	Gage record.
1910	1910	150,000	Infinity	March 1907 low floods and missing.
1911	1911	0	Infinity	Gage record.
1912	1913	150,000	Infinity	March 1907 low floods and missing.
1914	1917	0	Infinity	Gage record.
1918	1918	150,000	Infinity	March 1907 low floods and missing.
1919	1928	0	Infinity	Gage record.
1929	1929	150,000	Infinity	March 1907 low floods and missing.
1930	1976	0	Infinity	Gage record.
1977	1977	150,000	Infinity	March 1907 low floods and missing.
1978	1986	0	Infinity	Gage record.
1987	1996	150,000	Infinity	March 1907 low floods and missing.
1997	1997	0	Infinity	Gage record.
1998	2000	150,000	Infinity	March 1907 low floods and missing.

Table 10–30. Peak-flow quantiles in cubic feet per second for U.S. Geological Survey station 11446500 American River at Fair Oaks based on flood frequency analysis using Expected Moments Algorithm (EMA) with Multiple Grubbs-Beck Test; variance of estimate shown in log space.

[%, percent; ft³/s, cubic feet per second]

Annual exceedance probability	EMA estimate (ft ³ /s)	Variance of estimate	Lower 2.5% confidence limit (ft ³ /s)	Upper 97.5% confidence limit (ft ³ /s)
0.500	45,700	0.001890	38,600	53,700
0.200	93,800	0.001730	79,800	109,600
0.100	135,500	0.001590	115,800	157,000
0.040	199,400	0.001460	170,700	228,300
0.020	255,000	0.001450	217,500	291,100
0.010	317,500	0.001570	268,800	364,500
0.005	387,300	0.001830	324,600	451,400
0.002	491,600	0.002440	404,700	591,900
0.001	580,200	0.003110	469,300	720,800
0.0001	941,200	0.006810	702,800	1,325,300

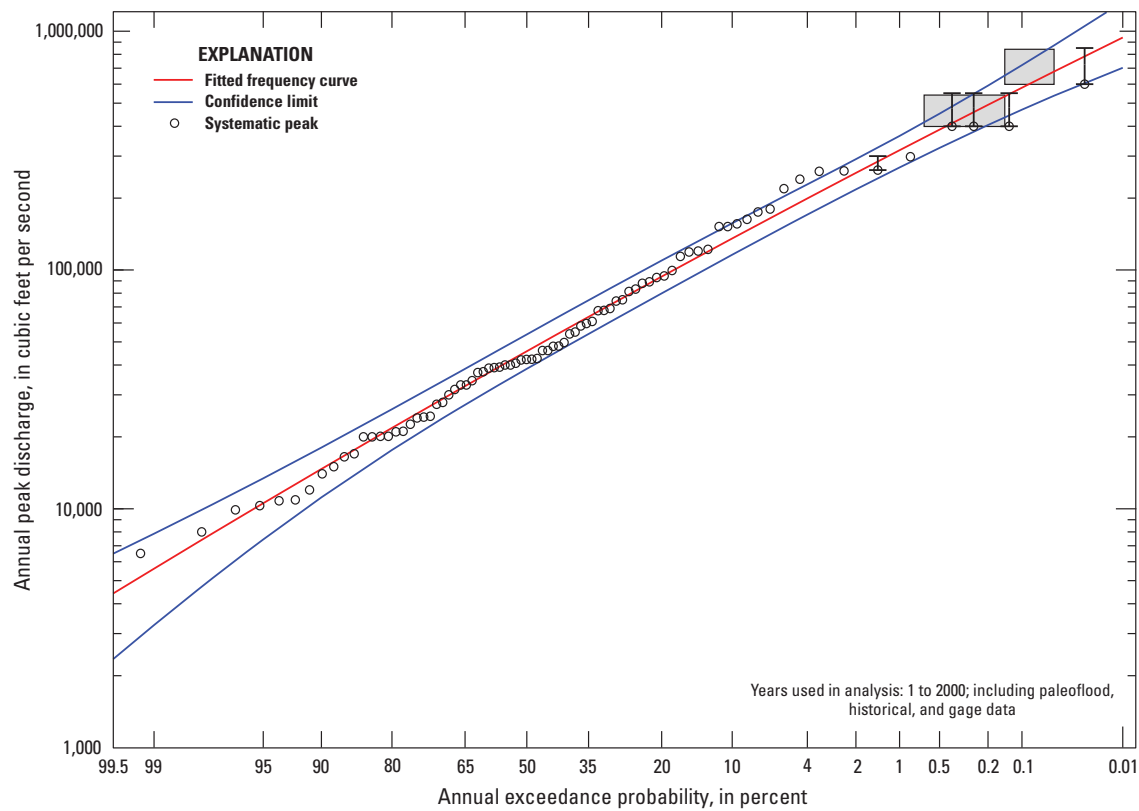


Figure 10–15. Graph showing approximate unregulated peak discharge frequency curve, American River at Fair Oaks, including gage, historical, and paleoflood data. The red line is the fitted log-Pearson Type III frequency curve and the blue lines are the upper and lower confidence limits. Peak discharge estimates from the gage are shown as open circles; vertical bars represent estimated data uncertainty for some of the largest floods. Paleoflood nonexceedance bounds shown as gray boxes.

This page intentionally left blank.

This page intentionally left blank.

Publishing support provided by the U.S. Geological Survey
Science Publishing Network, Reston Publishing Service Center

For information concerning this publication, please contact:

Chief, Analysis and Prediction Branch
Integrated Modeling and Prediction Division
Water Mission Area
U.S. Geological Survey
12201 Sunrise Valley Drive, Mail Stop 415
Reston, VA 20192
<https://water.usgs.gov/>

ISBN 978-1-4113-4223-1



ISSN 2328-7047 (print)
ISSN 2328-7055 (online)
<https://doi.org/10.3133/tm4B5>